IMPACT OF GANGLIOSIDE-MIMICKING BACTERIA ON HOST AUTOIMMUNITY AND MICROBIAL COMPETITION

by

ROBERT T. PATRY

(Under the Direction of Christine M. Szymanski)

ABSTRACT

Guillain-Barré Syndrome (GBS) is the leading cause of paralysis since the near eradication of polio, resulting from an autoimmune reaction where self-reactive antibodies are directed against gangliosides on the body's own nerve cells. By mimicking GM1 gangliosides using its lipooligosaccharide (LOS) structures, *Campylobacter jejuni* is known to trigger GBS. The LOS structures also provide receptors for bacterially produced AB_5 toxins, resulting in growth inhibition that is related to an increase in cell permeability. This selection pressure prompts *C. jejuni* LOS phase-variation and likely contributes to competition between gut pathogens. Through investigating this phenomenon, additional GM1-mimicking bacteria were detected in the chicken cecum by fluorescence microscopy and decreases in the Firmicutes phylum were observed after feeding AB_5 toxins to chickens. From this we concluded that AB_5 toxins may have a broader role in competition with the gut microbiota beyond *C. jejuni*. We also hypothesized that a consistent presence of GM1-mimicking gut microbes could influence the type of immune response directed against *C. jejuni* infections; especially if individuals are exposed to ganglioside-mimicking bacteria early in life during immune development. By screening 154 infant *C. jejuni* fecal

isolates from endemic nations, we showed that this exposure does indeed occur. Experiments with human macrophage THP-1 cells showed that training with low doses of ganglioside-mimicking bacteria reduces the release of pro-inflammatory cytokines upon subsequent challenge with *C. jejuni* that display GBS antigens. In our attempts to identify commensal ganglioside-mimicking bacteria, we isolated three *Enterococcus* species from the chicken gut and determined that they produce glycoproteins reactive with α-GM1 antibodies. The full genomes of these isolates were sequenced and two of their glycoproteomes were analyzed. This revealed numerous glycosylated proteins in each species including several which contain HexNAc-Hex modifications possibly involved in asialo-GM1 ganglioside-mimicry. The discovery of these glycoproteins suggests a general O-linked protein-glycosylation system in the *Enterococcus* genus and identifies a new protein glycosylation system in Gram-positive bacteria. Overall, this project has shed new light on the complexity of ganglioside-mimicking bacteria and their interactions with competing organisms as well as the host.

INDEX WORDS: Guillain-Barré Syndrome, autoimmunity, ganglioside-mimicry, *Campylobacter jejuni*, AB_5 toxin, oral tolerance, protein glycosylation, *Enterococcus*

IMPACT OF GANGLIOSIDE-MIMICKING BACTERIA ON HOST AUTOIMMUNITY AND MICROBIAL COMPETITION

by

ROBERT T. PATRY

BSc, The University of Alberta, Canada, 2014

A Dissertation Submitted to the Graduate Faculty of The University of Georgia in Partial Fulfillment of the Requirements for the Degree

DOCTOR OF PHILOSOPHY

ATHENS, GEORGIA

2020

IMPACT OF GANGLIOSIDE-MIMICKING BACTERIA ON HOST AUTOIMMUNITY AND MICROBIAL COMPETITION

by

ROBERT T. PATRY

Major Professor:	Christine M. Szymanski
Committee:	Eric T. Harvill
	Michael Pierce
	Eric V. Stabb

Electronic Version Approved:

Ron Walcott
Interim Dean of the Graduate School
The University of Georgia
May 2020

DEDICATION

I dedicate this dissertation to the ones in my life who have helped me through trying times and encouraged me in my passion for science. First, I have an immensely close family that has never wavered in their support, even when I decided to move all the way across the continent. My parents Martha and Don along with my siblings Chris and Katherine have been a continuing source of strength throughout my life. I would also like to thank my siblings' spouses Char and John along with my more recently added family members, my god-daughter Hazel, nephew Jacob and niece Danica. I am so grateful to have all of you in my life. I would also like to thank my extended family and all the friends from Edmonton for relationships that haven't changed since I left. A special thanks also goes to my friends here in Georgia for making me feel at home so far from home, especially my roommate Cody, always making it easier to forget about stressful situations and have fun. I would also like to thank Christine as well as her husband Todd and son Ryan, who really took me under their wing when we first moved to Georgia. My first time living away from home proved difficult for me and they have treated me like family which was an immense help to my well-being through this experience. Lastly but most importantly, I want to thank my girlfriend Kendra, who's kindness and love over the last 10 years have gotten me through my most difficult moments. Without her encouragement and support, including moving over 4000 km to join me through this journey, I wouldn't have made it here.

ACKNOWLEDGEMENTS

Beginning with grade school, I have been blessed to be taught by many brilliant and inspiring teachers, who sparked my love for learning and science. I was first inspired to pursue a career in science by Ashley Davey (now Hughes) who was an amazing mentor and made me excited about research. She graciously included me in her work at a time when I was certainly more of a burden than a help. Dr. Denise Hemmings, my first lab supervisor, got my feet wet in science and gave me a great experience along with Dr. Randi Gombos and Dr. Daniel Kerage. Dr. Brian Lanoil was the professor who ignited my interest in Microbiology and turned my attention to the Szymanski lab. During my PhD I have had several great mentors, starting with my supervisor Dr. Christine Szymanski. I can't express the tremendous amount of inspiration and support that she has given me through this experience both scientifically and personally. Also, Jessica Sacher, Harald Nothaft and Cory Wenzel, who have generously given so much of their time to answering my questions and showing me techniques. During my move and stay in Georgia my fellow graduate students almost became family, so special thanks go to Cody, Clay, Silke, Justin, Jolene and Bibi in addition to the many other friends I made in the Microbiology department and CCRC. I would like to thank Jennifer Walker for her efforts in nurturing my love for teaching and giving me opportunity to develop that skill. I would also like to thank my committee members Drs. Eric Harvill, Mike Pierce and Eric Stabb along with my many collaborators for their guidance and helpful contributions to my PhD project.

TABLE OF CONTENTS

Page

LIST OF TABLES

Page

LIST OF FIGURES

Page

CHAPTER 1

INTRODUCTION AND LITERATURE REVIEW

1. *Campylobacter jejuni* and ganglioside mimicry

1.1. History of *Campylobacter*

The genus *Campylobacter* is a group of bacteria belonging to the Epsilonproteobacteria class. *Campylobacter* species are Gram-negative and very motile owing to their spiral shape as well as bipolar flagella that allow them to spin and swim easily (1) (Figure 1.1). Though Theodor Escherich first observed this organism in 1886 from the stool of children who died of diarrheal disease, he was unable to culture it and did not draw a connection to the onset of the disease (1, 2). Unfortunately, this article was forgotten over many years and *Campylobacter* species were not tied to human disease until the 1970s (1). The first successful isolation of a *Campylobacter* species occurred in 1909 when McFadyean and Stockman isolated *Campylobacter fetus* (or *Vibrio fetus* as it was referred to at that time) from the fetal tissue of aborted sheep whose flock had an abortion rate of 33% (3, 4). The correlation between *Campylobacter* species and animal disease meant that most research regarding this group was done by veterinarians in animal systems at the time (3). This research led to the subsequent discovery of *Camplobacter jejuni* which in addition to causing abortions in sheep, also was shown to cause dysentery in calves and pigs (1). Due to overgrowth of common fecal bacteria in the routine isolation methods used by clinicians, *C. jejuni* was not successfully isolated from human feces until 1968 and the results were not published until 1972 (1). Using the aid of a veterinary college, the

bacterium was isolated from the blood and feces of a nurse who had been stricken with diarrhea in Belgium and since they did not observe any other enteric pathogens in the sample, it was concluded that *Campylobacter* was the root of her symptoms (5). Since then, much research has gone into the study of *Campylobacter* species, (most notably *C. jejuni*) as campylobacteriosis is now recognized as the most common cause of acute bacterial enteritis in the world (3).

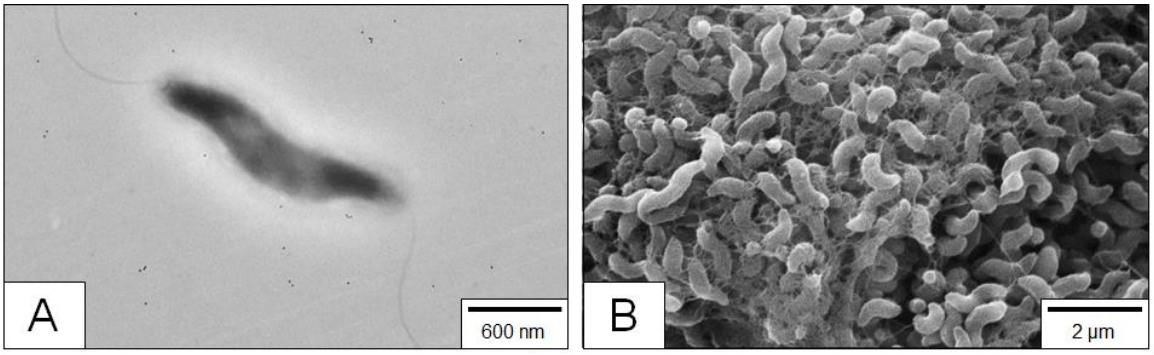

Figure 1.1. Electron micrographs of *Campylobacter jejuni*. Unpublished images of *C. jejuni* taken using transmission electron microscopy (A) and scanning electron microscopy (B) using methods described in (6).

1.2. Clinical information, prevalence and distribution of campylobacteriosis

Campylobacteriosis is most commonly contracted by the consumption of improperly cooked poultry meats or cross-contaminated products because Campylobacters are commensal in avian species (7). Examination of poultry products in Edmonton, Alberta for example, revealed the presence of *Campylobacter* in 62% of raw chicken legs (8). Major outbreaks of the disease have usually been associated with improperly pasteurized dairy products or inadequately treated water sources and have occurred all across the developed world (1, 9). In humans, the main symptoms of campylobacteriosis are fever

and abdominal pain which are mostly, but not always accompanied by diarrhea (10). In addition to these symptoms, patients commonly experience fever, headache, myalgia and blood in the feces (10). *Campylobacter* has also been associated with inflammatory bowel disease (11, 12) and in low and middle-income countries it has been shown to contribute to growth stunting in children (13-15). Though infection with *Campylobacter* can lead to more serious sequelae such as reactive arthritis, erythema nodosum and Guillain-Barré syndrome, fatalities are rare and often associated with other underlying conditions (16, 17). The Centers for Disease Control and Prevention (CDC) report the case fatality rate of *Campylobacter* to be 0.21% (18). In developed nations, campylobacteriosis is the number one cause of acute gastroenteritis, most frequently infecting children under four and young adults aged 15-44 years old (1). Though campylobacteriosis is thought to be vastly underreported, the CDC recently reported an incidence rate of 12.82/100 000 in the United States (18), also stating this year that it is the leading cause of bacterial foodborne diarrheal disease in the country (19). It is more difficult to gather information in developing nations due to a lack of surveillance programs; however, the World Health Organization has provided estimates in the past which suggest that children in developing nations are more frequently infected than those in developed nations (20). This makes sense due to reduced access to proper sanitation and hygiene in these regions. Interestingly, this difference between developed and developing countries holds true for children under the age of five, but is not the same for the general population, which is infected at similar rates in both (20). Young children are thought to be most affected because the older population is exposed to the bacteria early in life and the level of immunoglobulin A antibodies specific to *Campylobacter* species increases over time (21). Erythromycin is typically the drug of

choice for treatment since *Campylobacter* was shown to be susceptible early on and it is relatively inexpensive (22, 23). Alternative drugs that are commonly used include tetracycline, doxycycline and chloramphenicol (23). Fluoroquinolones have also been used in the past, however *Campylobacter*, in many areas of the world, have developed resistance in response to the previous use of fluoroquinolones use in raising poultry (1).

1.3. Pathogenesis and important virulence factors

1.3.1. Gastroenteritis

C. jejuni accounts for 90% of the infections that result in campylobacteriosis and as a result, has been the most studied of the *Campylobacter* species (24). The dose of *C. jejuni* needed for infection is less than 500 cells (25), often resulting in the onset of acute gastroenteritis with the possibility of various sequelae. After entering the body orally, *C. jejuni* makes its way to the small intestine first where it colonizes the host (26). It then moves to the colon where it causes the disease. Once colonization occurs, the pathogen attaches to intestinal epithelial cells using adhesins, flagella, outer membrane proteins and surface polysaccharides (27). It has been shown that mutants deficient in motility, protein glycosylation and capsular biosynthesis are deficient in their ability to both bind and invade the epithelium; therefore a functional flagellum and glycosylated surface structures are thought to be necessary for this initial stage of infection (28, 29). Following attachment to the epithelial membrane, *C. jejuni* uses both host microtubules and microfilaments to gain entry into the cell (30-32). The pathogen is then sequestered in a membrane-bound vacuole called the *C. jejuni* containing vacuole (CCV) which avoids delivery to the lysosomes and allows the organism to remain viable for up to 24 hours (33). In this vacuole, the pathogen continues to translocate across the cell and be exocytosed on the basal surface where it is

free to invade other epithelial cells (27). There is also evidence that *C. jejuni* can move paracellularly by disrupting tight junctions between cells (26). Throughout attachment and invasion of the epithelium, the bacteria release effector proteins which cause inflammation, cell death, aberrant water secretion/absorption and other harmful effects (27). The best studied *C. jejuni* effector is cytolethal distending toxin (CDT) released using outer membrane vesicles (34), which induces double strand breaks in host DNA, causing cell cycle arrest and apoptosis (27). CDT and the other effectors are thought to be the eventual cause of symptoms associated with campylobacteriosis.

1.3.2. Guillain-Barré Syndrome

Guillain-Barré Syndrome (GBS) is a severe post-infectious sequela caused by certain strains of *C. jejuni* and is the number one cause of paralysis in humans since the near eradication of poliomyelitis (35). The incidence of GBS is highly dependent on geographic location, but ranges from 0.4 to 3.25 per 100, 000 people (36). The onset of symptoms is rapid (usually within 1-2 weeks (36)), with paralysis spreading quickly to include the arms, legs and less commonly facial, bulbar and respiratory muscles (37). In addition to the high rate of mortality from complications of this disease (approximately 5%), patients are commonly in need of intensive care for months and left with weakness, sensory difficulties and pain symptoms that are never resolved (37). This disease is an acute inflammatory demyelinating neuropathy that has been increasing in incidence, being associated with recent outbreaks in North America (38) and Peru (39). It is identified by a symmetrical and progressive weakness along with a loss of normal tendon reflexes mainly in the extremities (40). This effect is thought to be due to an aberrant immune response of auto-reactive immunoglobulin G antibodies specific to ganglioside structures on nerve

cells (41). The antibodies gather at nodes of Ranvier where the concentration of gangliosides is the highest, and recruit the complement membrane attack complex which damages nerve fibers and causes interference of neural impulses (41). This was supported in a rabbit model where bovine brain gangliosides were introduced to the rabbits resulting in a similar paralysis to what is seen in humans (42) (Figure 1.2).

The mechanism that identifies auto-reactive antibodies as the major culprit in GBS is generally favored over alternative explanations due to the success of plasma exchange as a treatment. Microbial pathogens are an important factor in the development of GBS as antecedent infections occur prior to the disease in about two-thirds of cases (43). *C. jejuni* is the most common antecedent infection and was first reported as a possible cause of the disease in 1982, where a 45-year-old man developed GBS symptoms 2 weeks after having campylobacteriosis (44, 45) . Multiple case studies within the next few years then reported similar findings (45). Some estimates now claim that *C. jejuni* precedes GBS in up to 39% of patients (46). Around 60% of *C. jejuni* strains are capable of mimicking gangliosides using sugar structures on their lipooligosaccharides (LOS) (47-52); this will be discussed at more length later in this chapter. It is thought that *C. jejuni* ganglioside mimicry increases the likelihood of an autoimmune response and promotes the development of GBS. About 1/1000 patients infected with *C. jejuni* will subsequently develop GBS (53, 54). In support of this idea and related to the experiment mentioned earlier, rabbits immunized with ganglioside-mimicking LOS from *C. jejuni* developed GBS similar to those exposed to foreign gangliosides (42) (Figure 1.2). Given the severity of GBS and its potential for long term defects to normal function, it is not surprising that the fatalities associated with the disease are around 5%; however, this is mostly observed in severe cases or in the elderly

who often die following improvement in nerve function during the recovery phase (55). It is also imprtant to note that in developing nations, the reported mortality rates are significantly higher than those in the US, even though data in these countries is limited (56).

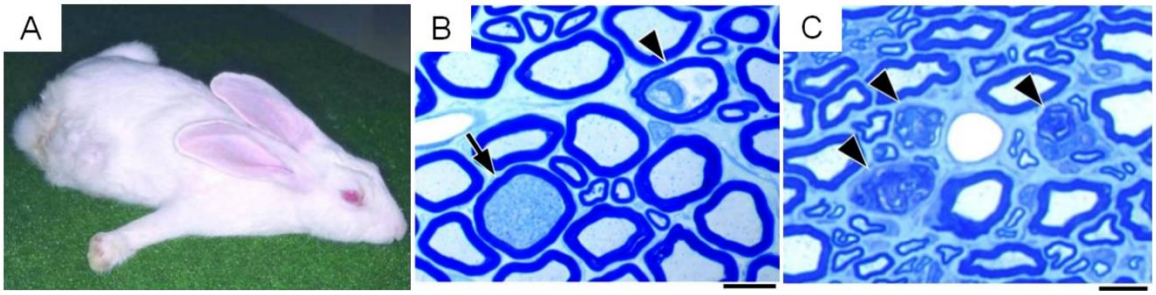

Figure 1.2. Guillain-Barré Syndrome displayed in a rabbit model. (A) Image depicting a rabbit experiencing flaccid limb weakness with legs splayed, limbs extended and head resting on the ground rather than sitting upright and hunched as would be normal. (B and C) Microcopy of toluidine blue stained cauda equina cross sections. Arrowheads show where macrophages have invaded nerve fibers, while the arrow shows the beginning of axonal degradation. These figures show the nerve cells' progression from (B): the initial stages of degradation to (C): full Wallerian-like degeneration (Scale bars = 10 µm). [1]

1.3. Glycosylation in *Campylobacter jejuni*

1.3.1. Protein glycosylation

The addition of sugar structures to peptides is a common and important modification used in all domains of life. In most cases, this is done by the covalent attachment of glycans to either the amide of asparagine residues (N-glycosylation) or the hydroxyl group of serine or threonine residues (O-glycosylation). In *C. jejuni* N-glycosylation, sugar monomers from nucleotide activated donors are assembled onto a lipid carrier attached to the cytoplasmic side of the inner membrane (57). Once a

[1] Reprinted with permission from Proceedings of the National Academy of Sciences of the United States of America, volume 10, Yuki N, Susuki K, Koga M, Nishimoto Y, Odaka M, Hirata K, Taguchi K, Miyatake T, Furukawa K, Kobata T, Yamada M, Carbohydrate mimicry between human ganglioside GM1 and Campylobacter jejuni lipooligosaccharide causes Guillain-Barré syndrome, pages 11404-11409. Copyright (2004) National Academy of Sciences, USA. The figure was changed by removing several panels to focus on the most pertinent images.

heptasaccharide has been formed on the carrier, the entire unit is flipped across the inner membrane and the oligosaccharide can be transferred by the oligosaccharyltransferase (PglB) to over 80 identified proteins with a particular target sequence (58, 59). The *N*-glycosylation system in *C. jejuni* was the first to be described in bacteria and as a result, it is now a model for the study of these modifications (60). Although not essential for the organism *in vitro*, the absence of *N*-glycosylation has a negative effect on its pathogenicity and ability to colonize in various hosts (28, 59, 61). This is owing to the observation that many proteins require glycosylation for proper complex formation and protection against proteolysis. Thus, the absence of this system results in decreased colonization, adherence and invasion, resistance to gut proteases, DNA uptake and avoidance of the host immune system, while also impacting nitrate reductase activity, chemotaxis, nutrient uptake and antimicrobial resistance (59). The *O*-glycosylation system in *C. jejuni* is used to solely modify flagellar subunits and is essential for the proper assembly of the flagella and thus motility (62). The system works through the activity of individual glycosyltransferases transferring sugar monomers from CMP activated donors onto the FlaA/FlaB flagellar subunits in the cytoplasm and then exporting those subunits through the flagellar apparatus to be added to the assembling flagellum (57). Due to its necessity in the assembly of the flagellum, O-glycosylation is also important in the pathogenicity as well as colonization ability of this organism (62). Loss of O-glycosylation causes an inability to agglutinate and significantly impacts the ability of *C. jejuni* to adhere to and invade host epithelial cells (29). The flagellum is not only important for motility, but also aids in biofilm formation, and secretion of effector molecules (62). *Campylobacter* species are among the few

bacteria capable of both N- and O-linked glycosylation, making protein glycosylation an important part of the biology of this organism (57).

1.3.2. Capsular Polysaccharides

Unlike some other common enteric pathogens, *Campylobacter* species are encased by a large capsule that is comprised of heterogeneous capsular polysaccharide (CPS) structures. Since the capsule is large and occasionally negatively charged, it provides a hydrated layer of protection for bacteria from desiccation (63). The capsule can also be quite long, and since it extends from the cell, it is often the first structural component of the bacterium to be recognized by the immune system; due to this fact, the capsule in bacteria is important to pathogenesis and variation of CPS molecules is helpful to evade immune detection (64). The CPS of *C. jejuni* strains is highly variable, which is why it is the major contributor to the Penner serotyping scheme for differentiation of these strains. The CPS can also undergo phase variation within a population to allow strains of *C. jejuni* to turn expression on and off, resulting in specific modifications to the structure (65). The components that are common among *C. jejuni* strains include unusually configured heptose sugars and O-methyl phosphoramidate residues (65). In addition to immune evasion, CPS is important to pathogenesis due to its contributions to biofilm formation and antibiotic resistance (66, 67). Specifically in *C. jejuni*, the role of CPS in pathogenesis is not fully understood; however, studies have suggested that mutants lacking the capsule are less invasive and colonization in chickens is greatly reduced (68). These structures are also important receptors involved in bacteriophage recognition (69-71), serum resistance (64, 72), vaccine development (65, 73) and other host immune factors (72, 74).

1.3.3. Lipooligosaccharides

Lipooligosaccharides (LOS) are another type of surface polysaccharides that impact the survivability of *C. jejuni*. One difference between LOS and CPS however is that LOS contain a unique lipid A portion that consists of six long chain fatty acids substituted onto a disaccharide (D-glucosamine and 2,3-diamino-2,3-dideoxy-D-glucose), which is linked to two 2-keto- 3-deoxyoctulosonic acid molecules (75). The long fatty acids of the lipid A anchor the LOS to the membrane making a strong attachment to the cell wall. Besides its function as an anchor, the lipid A also acts as an endotoxin, contributing to the inflammation associated with campylobacteriosis (76). Attached to the lipid A is the carbohydrate core, which is divided into two sections referred to as the inner and outer core. The inner core remains generally the same between different strains of *C. jejuni*, consisting of two heptoses and a glucose; however, strains do differ in the modification of one heptose, adding either a phosphate or phosphoethanolamine (77). The outer core of the LOS contain a series of hexasaccharides and *N*-acetylhexosamines, and differs significantly between strains of *C. jejuni* (77). Similar to CPS, it can also vary between individual colonies of the same strain due to phase variability in biosynthesis genes (78). Besides the endotoxin activity of lipid A, LOS is also involved in avoiding immune detection. *C. jejuni* can sialylate the outer core region of the LOS and make it resemble human antigens (79). This allows the organism to disguise itself to look like the host and prevent an adaptive immune response from being initiated. Among the best studied examples of this phenomenon is when *C. jejuni* cells use their LOS outer core to mimic mammalian gangliosides. This can cause an autoimmune response against nerve cells that display the antigen and is what links *C. jejuni* to GBS (77, 78) (Figure 1.3).

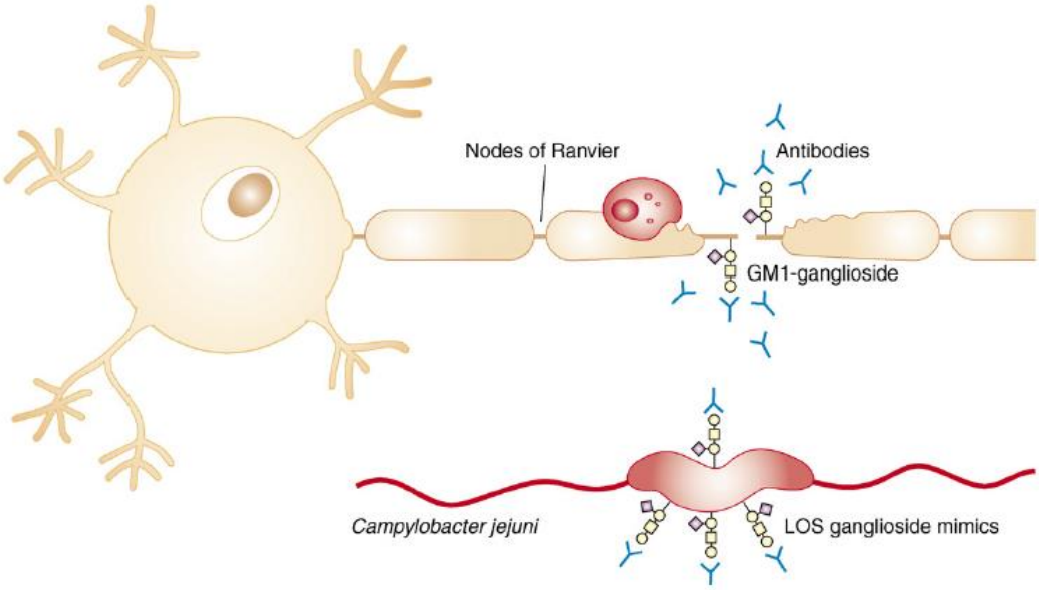

Figure 1.3. Mechanism of *Campylobacter jejuni*-induced Guillain-Barré Syndrome. [2]

1.4. Molecular mimicry of human gangliosides

1.4.1. Human gangliosides

Gangliosides are a type of glycolipid that contain at least one sialic acid as a part of their carbohydrate portion and are attached to ceramide lipids. These structures are particularly abundant in the nervous system and decorate the membrane of most nerve cells but can also be found in most other areas of the body. It has been suggested that gangliosides are important for many functions including cell-cell communication and adhesion, homeostasis, prevention of nerve cell degradation, and the transmission of neural impulses (80). Since human populations defective in the production of gangliosides are very rare, mouse experiments have been needed to elucidate the importance of different ganglioside structures in brain development (81). Mice incapable of producing the major brain gangliosides experienced detachment of myelin sheaths which led to axonal

[2] Reprinted from Trends in Microbiology, volume 16 (issue 9), Guerry P, Szymanski CM., Campylobacter sugars sticking out, pages 428-435. Copyright 2008, with permission from Elsevier.

degradation (82). These symptoms were even more severe in mice with little to no brain ganglioside production capability, resulting in death shortly after weaning (83). This effect arises because gangliosides are important receptors for myelin-associated glycoprotein which is crucial to axonal-myelin interactions and the proper functioning of myelinated axons (82-84). GM1 ganglioside was the first structure to be characterized and is the most studied ganglioside due to its prevalence and involvement with several different diseases (85). It has recently been examined as a therapy for the treatment of multiple neurodegenerative disorders such as Huntington's disease and Alzheimers, making it a current topic of discussion (86).

1.4.2. Variation in *C. jejuni* LOS and mimicry of gangliosides

As mentioned earlier, the LOS of *C. jejuni* is of particular interest to researchers mainly due to its involvement in GBS. Since many *C. jejuni* strains have the capacity to sialylate their LOS, there is a tremendous capability of these organisms to mimic the structure of human gangliosides (77, 79). As previously described, this can lead to recognition of the body's own nerve cells as foreign and the degradation of spinal nerve axons by immune effectors. The LOS biosynthesis loci among *C. jejuni* isolates are highly variable, leading to many differences in the outer core between serotypes (87). Together, the strains of *C. jejuni* are capable of mimicking GM1a, GM2, GM3, GD1a, GD1b, GD2, GD3, and GT1a gangliosides (77) (Figure 1.4). This includes most of the major gangliosides that can be found in the human body. GM1 ganglioside mimicry is of particular interest because it was the first ganglioside structure to be characterized and is among the most studied due to its close involvement in *C. jejuni*-induced GBS and with several diarrheal diseases (85). These studies include the recognition of *C. jejuni* LOS by

cholera toxin (CT) produced by *Vibrio cholerae* and heat-labile enterotoxin (LT) produced by enterotoxigenic *Escherichia coli* (88-90), which will be discussed at length later in this chapter. Phase-variation within the genetic loci also causes individual colonies within a *C. jejuni* population to display variable LOS ganglioside mimics, altering bacterial invasiveness *in vivo* (91, 92). To better explain this phenomenon and the variation between *C. jejuni* strains, three different strains will be used as models that show diversity in the species.

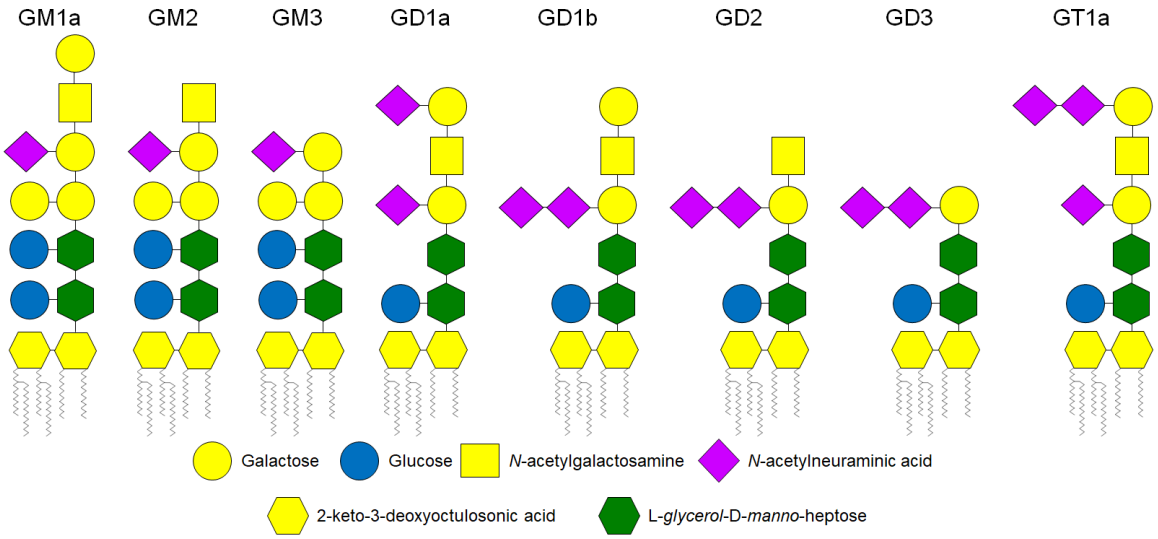

Figure 1.4. Structural representation of ganglioside-mimicking *C. jejuni* lipooligosaccharides.

1.4.3. *C. jejuni* HS:19 serostrain

The HS:19 serostrain of *C. jejuni* constitutively displays LOS mimics of the major gangliosides, making it particularly dangerous with regard to human disease. Due to this, it is no surprise that many studies have demonstrated an association between the HS:19 serotype and the development of GBS (93). The structure of the HS:19 outer core consists of both as a GM1 and GD1a ganglioside mimics (Figure 1.4) (77). There does not appear to be any phase variability in the LOS biosynthesis locus of this type strain (though other

HS:19 strains have been shown to contain homopolymeric G tracts capable of phase variation (94, 95)); the differences in structure of individual LOS molecules are thought to be from variable sialyltransferase activity (CstII) involved in the addition of N-acetylneuraminic acid (96). Due to this, the enzyme will either add one or two sialic acids to any given LOS molecule, resulting in a mixture of GM1 and GD1a ganglioside-mimicking LOS structures present on the surface of the cell (Figure 1.4).

1.4.4. *C. jejuni* NCTC 11168

The LOS of *C. jejuni* NCTC 11168 (serotype HS:2) differs from HS:19. It is also an isolate that produces ganglioside mimics constitutively, but HS:2 strains are not as frequently implicated in the development of GBS. This strain is also capable of mimicking GM1 ganglioside with its LOS outer core (Figure 1.4), in addition to mimicking GM2 ganglioside (Figure 1.4) based on phase-variation within the LOS biosynthesis locus (97). This strain contains a homopolymeric guanine tract (several consecutive guanine nucleotides capable of being miscopied during replication) within the gene encoding the galactosyl transferase (CgtB) adding the terminal galactose of the outer core LOS (97). The presence of this homopolymeric tract can cause an error during DNA replication when the strands do not pair properly. This results in the addition or deletion of a single nucleotide and a frameshift mutation the typically leads to premature stop codons and loss of enzyme function. Linton *et al.* 2000 discovered that if there are 8 consecutive Gs present in the homopolymeric tract of *cgtB*, the encoded enzyme is functional (97). However, if 9Gs are present, a premature stop codon results which truncates the protein and destroys enzyme function (97). Therefore, the status of the homopolymeric tract in this gene determines

whether the LOS produced by a single cell will mimic GM1 or GM2 ganglioside, creating a population that is a mixture of both mimics.

1.4.5. *C. jejuni* HS:3 serostrain

The HS:3 serostrain differs from the other two *C. jejuni* strains mentioned because it is unable to mimic any human gangliosides at all. This is because HS:3 cells are incapable of producing the sialic acids necessary for ganglioside mimicry (47). The LOS in HS:3 is very unusual compared to the other strains, containing quinovosamine (3-amino-3,6-dideoxy-D-glucose) and having no β-D-galactose residues that are capable of binding N-acetylneuraminic acid (77). The LOS of this strain better resembles certain strains of *C. coli* than *C. jejuni* due to the presence of the quinovosamine residue (98). As would be expected, this strain has never been implicated in the onset of GBS and is normally used as a negative control when investigating anti-ganglioside antibodies from patients to see if they are cross-reactive with *C. jejuni* (77).

1.4.6. Guillain-Barré Syndrome and other infectious agents

As mentioned previously, pathogens have an important association with GBS and *C. jejuni* is most commonly associated with the disease. *C. jejuni* is also the most well developed preceding infection considering that it meets the 4 criteria needed to conclude that a particular autoimmune disease is triggered by exposure to a molecular mimic (99). In making this conclusion, there must be an epidemiological correlation between the pathogen and the disease, T-cells or antibodies must be identified which bind to the target autoantigen, the mimic must be identified on the microbe and the disease must be reproduced in an animal model using this pathogen (99). While some other bacteria and viruses meet most of these criteria, none have had their molecular mimics as thoroughly

characterized as *C. jejuni*, making their connection to GBS less certain; however, there are a few infectious agents where the evidence of their involvement with GBS is very compelling. A close relative of *C. jejuni*, *Campylobacter coli* has been isolated in GBS patients with IgG titers against ganglioside structures and showed to bind CT by ELISA (100). The LOS from these isolates was able to induce an anti-asialo-GM1 response in rats (100). *Mycoplasma pneumoniae* is thought to precede approximately 5% of GBS cases (46) and there have been studies finding IgG antibodies directed against GM1, GD1b and asialo-GM1 gangliosides in those patients (101), but the carbohydrate structures present in this organism have not been well studied (46). Some *Brucella melitensis* have been shown to possess a GM1 ganglioside-mimicking lipopolysaccharide (LPS) that binds to CT and can cause anti-GM1 antibodies to be produced in immunized mice leading to flaccid limb weakness (102). There have also been multiple reports of *Haemophilus influenzae* associated with patients that had anti-GM1 antibodies (103, 104), however it is difficult to conclude much from this data considering that this bacteria is normally found in the respiratory tract of a majority of people. Some GBS patients associated with *H. influenzae* were also found to be seropositive for *C. jejuni* and their anti-ganglioside antibodies did not cross-react with *H. influenzae* (105). In addition to bacteria, there are multiple viruses linked with the development of GBS and production of anti-ganglioside antibodies, including cytomegalovirus (up to 22% of cases) (46, 106-108) and Epstein-Barr virus (up to 13% of cases) (46, 108-110). A more recent concern has been the correlation of GBS with Zika virus, which has been observed all over South America (111-116) and in French Polynesia (117) in the past few years. While all these infectious agents have been linked to GBS and some have evidence of ganglioside mimicry, it is important to include that these

pathogens may be contributing to the development of GBS in a manner that is unrelated to true ganglioside mimicry. For example, auto-reactive ganglioside antibodies have been detected in patients with Zika virus-induced GBS, these antibodies could not be linked to ganglioside mimicry (117, 118). The true mechanism behind Zika virus-related GBS is not fully understood, but researchers have suggested that the highly stimulated immune response accompanying Zika virus could lead to the autoimmune disease (119).

2. *Vibrio cholerae* and enterotoxigenic *E. coli*

2.1. *Vibrio cholerae*

2.1.1. Lifestyle of *Vibrio cholerae*.

Vibrio cholerae is a Gram-negative, curved rod-shaped bacterium with a single flagellum at one pole. It is widely spread through many water ecosystems due to its preference to grow in saline environments. In these ecosystems, *V. cholerae* survives by using chitinases to make the chitin of zooplankton and shellfish freely available as a carbon and nitrogen source (120). Chitin also triggers the organism to become naturally competent and capable of sharing traits through lateral gene transfer (121). Due to this, *V. cholerae* is normally found in association with zooplankton or shellfish such as copepods (122). The other part of the bacterial lifecycle occurs after its ingestion by various animals where it can persist and, in humans, can also cause cholera through virulence factors such as CT present in certain strains (122).

2.1.2. Clinical information regarding cholera.

Following infection with CT-producing *V. cholerae* strains, large amounts of water are secreted into the lumen of the intestine causing profuse diarrhea that resembles rice water. This appearance occurs because the fecal matter from the intestine is quickly

cleared, leaving mainly water and sloughed cells to constitute the diarrhea. When infected, water is lost at an incredible rate, causing severe dehydration and morbidity if patients are not properly rehydrated. The disease is most prevalent and deadly in children under 5 years old (123), but can also cause disease in adults, especially in areas where the population is naïve to the organism (124). Usually, rehydration with water, sodium and glucose is sufficient to prevent death, but in desperate cases, tetracyclines, fluoroquinolones and macrolides are also used to aid in treatment (125). These therapies are used sparingly due to the potential effects on resident human microbiota as well as the threat of antibiotic resistance; however, when the correct antibiotic is chosen (considering local resistance patterns), the disease duration and stool loss can be cut in half and duration of shedding reduced by several days (125). In some regions, treatment can be difficult to receive and mortality reaches over 10% while the afflicted patients wait for proper care (125). During the cholera epidemic in Haiti, the median time between patients starting to experience diarrheal symptoms and dying was only 12 hours, leaving little time to implement effective treatment measures (126). If left untreated, the mortality rate associated with the disease can reach over 70% (127). Cholera has an enormous capacity to spread through populations due to the amount of bacteria shed by infected individuals. *V. cholerae* is spread through oral ingestion of fecal matter, and although filtration through a sari cloth can reduce transmission by up to 50%, transfer between individuals is still common and has been observed within households (125). To enhance further its ability to spread, *V. cholerae* that are shed in the stool of infected humans are much more infectious than those from other sources; the infectious dose of human excreted *V. cholerae* is 10 to 100 times less than those contracted from water (128).

2.1.2. History of known cholera outbreaks.

The first known description of a disease resembling cholera was written in Sanskrit and originated in India around 500 BC (129). It is not fully known whether this description was of *V. cholerae,* but the disease is believed to have affected ancient humans, though the organism has likely changed considerably over time. European settlers in India recorded the presence of the disease near the beginning of the 16th century, but the modern written history began with the first pandemic which arose in the Ganges River Delta area of Bengal in 1817 (129). John Snow was the first to describe cholera as being communicable through infectious agents in drinking water during a cholera outbreak in London from 1849 to 1854 (130). *V. cholerae* was then isolated by Robert Koch in 1884 during the fifth pandemic in Egypt and subsequently deemed responsible for the disease (130). There are now over 200 serogroups of *V. cholerae* characterized by the O-antigen repeats on the LPS, but only the O1 and O139 serogroups have caused epidemics (131). The O1 serogroup is further separated into two distinct biotypes. The Classical biotype, which was responsible for the first six of seven recorded pandemics, is now considered extinct outside of the laboratory (129). The El Tor biotype first isolated in Egypt in 1905 proved to be much better suited to its environment, outcompeting the Classical efficiently in countries where both existed (129). In those areas, the displacement of the Classical biotype generally occurred within one year (129). The El Tor biotype is thought to be less virulent than Classical (132), but it is the cause of the quickly spreading seventh cholera pandemic which is still ongoing and very threatening. The O1 serogroup is also divided into two serotypes: Inaga and Ogawa (133). These two differ only in the *rfbT* gene which is required to change the O-antigen structure to the Ogawa serotype (133). The O139 serogroup was discovered more recently

when it caused a cholera epidemic in Asia in 1992 (134, 135). This serogroup is very similar to the O1 serogroup and differs solely with the O139 antigen replacing the O1 antigen through lateral gene transfer (125). Cholera causes epidemics and is endemic mostly in regions within Asia and Africa, but it also can cause outbreaks in other areas. Recently there has been a large outbreak in Haiti following an overwhelming earthquake that the nation experienced in 2010. This was surprising considering that cholera had not been observed in Haiti previously. This was the largest cholera epidemic in the past half century and had infected over 600,000 people, killing approximately 8000 (136). It serves as a good example that cholera is still a current and important issue. Due to a serious number of unreported cases of cholera, exact figures relating to the disease are difficult to obtain; however, the World Health Organization has estimated that 3-5 million people contract it annually (137).

2.2. *Vibrio cholerae* interaction with bacteriophage

2.2.1. Bacteriophages and their discovery involving *V. cholerae*

Bacteriophages, or phages for short, are microscopic virions that subsist by infecting bacteria and recruiting host machinery to ensure their replication. Though the debate is still ongoing whether phages can be termed as living organisms, they constitute the most abundant life-form on this planet with estimated 10^{30}-10^{32} total virions on earth (138). This means that phages outnumber bacteria ten-fold with estimates that half of the world's bacterial population are killed by phages every 48 hours (138, 139). All phages consist of chromosomal DNA or RNA that is packaged in a protein sheath called a capsid and attached to a tail structure also made up of phage proteins. There are two different lifecycles that the phage can undergo. In the lytic phase, the phage infects its host and

replicates rapidly using the host machinery. Then the bacteriophage use a variety of different strategies to lyse host cells and allow for their newly made virions to infect new bacteria (140). The lysogenic cycle allows the phage to incorporate their DNA into the host genome where it can lay dormant and be passed on through many generations, even causing alterations to the phenotype of the host bacterium through the expression of its genes. It is generally accepted that phages were first discovered by Felix d'Herelle and Frederick Twort in the early 20th century (141). However, there were a few studies prior to the discovery which suggested their existence (141). One of the researchers who made such a suggestion was Ernest Hankin in 1896, when he described the bactericidal effect of water in the Ganges toward the causative agent of cholera (141, 142). He noted that well water on the other hand had no negative effect on the bacterium and to the contrary was a good medium for growth, hinting that there was an antibacterial agent present in the Ganges River. Relating back to this initial finding, there have been numerous subsequent studies on phages that infect *V. cholerae* (vibriophages) and their role in its lifestyle. There are many different phages that influence *V. cholerae*, both in the lytic and lysogenic cycles. The lytic phages exist in a dynamic equilibrium with the strain of *V. cholerae* that they infect. As the amount of phages present in the water increases, the *V. cholerae* population decreases to a point where the phage experiences a decline due to a lack of hosts (143). This makes phages an important factor in outbreaks of cholera, contributing to the duration and severity of an epidemic (143). There are also many examples of lysogenic phages that have contributed genetic information to the genome of *V. cholerae* and have been heavily studied. The reason that there is so much interest in these phages is that they supply the bacterium with some of the major virulence factors required for its pathogenesis.

2.2.2. CTX bacteriophage

The CTX phage is the most well studied example of a lysogenic phage that aids in the pathogenicity of *V. cholerae* by integrating its genome into the host as a stable lysogen for many generations. It is best known for encoding CT, the primary causative agent of the disease cholera (144). CTX is a filamentous phage that is only able to infect *V. cholerae* displaying the toxin coregulated pilus (TCP) on their surface, given that this is its receptor (144) (Figure 1.5). The TCP is made up of individual TcpA subunits that are encoded by the *tcpA* gene. This gene is located on the TCP pathogenicity island which is 40kb long and flanked by *att*-like attachment sequences that are reminiscent of what is commonly seen in phage genes (145, 146). The phage needs this structure in order to bind to the bacterium and the shortage of non-O1/non-O139 strains carrying CT is thought to result from a lack of abundance of TCP genes in those groups (144). It has been previously thought that the genes required for the TCP may have also come from a filamentous lysogenic phage (VPI phage) (147). These claims have been subsequently shown to be incorrect and it is now thought that the TCP genes come from a satellite element given its different GC content from the rest of the genome (148). They were more likely packaged by a helper phage in error rather than constituting a viable phage genome of its own that was incorporated (148). Besides being important for bacteriophage infection, the TCP has also been shown to aid *V. cholerae* in its attachment to the intestinal epithelium and forms a protective layer to defend against some antibacterial compounds (149). This makes the TCP very important to *V. cholerae* pathogenesis in more ways than one. Once the CTX phage binds to the *V. cholerae* cell wall, it injects single-stranded DNA into the cytoplasm where it circularizes into a plasmid that can stay as it is, or become integrated at targeted

areas in the host genome (148) (Figure 1.5). The CTX phage genome is 6.9 kb in size and consists of two modules (148). The first is called the repeat sequence 2 module. It consists of three genes: *rstA* which aids in DNA replication, *rstB* helps with integration into the genome by stabilizing the DNA and *rstR* which is a repressor protein (148). The other module is called the core region and encodes proteins required for the structure and assembly of the phage in addition to the *ctxAB* genes for CT (144). Although the *ctxAB* genes are contained within the genome of the CTX phage, their GC content (38%) is different from the rest of the genome (40%), hinting that they were acquired from a prior unknown source (148). This phage does not have its own integrase gene so it needs to use the XerC and XerD host proteins, which allow for direct integration of the single-stranded DNA into the genome rather than converting to double-stranded first (144, 148). Like other filamentous phages, the CTX phage proliferates by being secreted from the cell without the need for lysis. Though in this case, the phage recruits host machinery to achieve this and is secreted by the type II secretion system of *V. cholerae* normally used to secrete proteases and chitinases among other proteins (150, 151). Coincidentally, this is the same machinery that is recruited for the secretion of CT (150). Though the CTX phage is the best-known lysogenic phage related to *V. cholerae* due to its importance in pathogenesis, there are many other filamentous phage that also contribute to the genome of this organism and play important roles of their own (148). Some of them are even necessary for proper integration and functioning of the CTX phage (148).

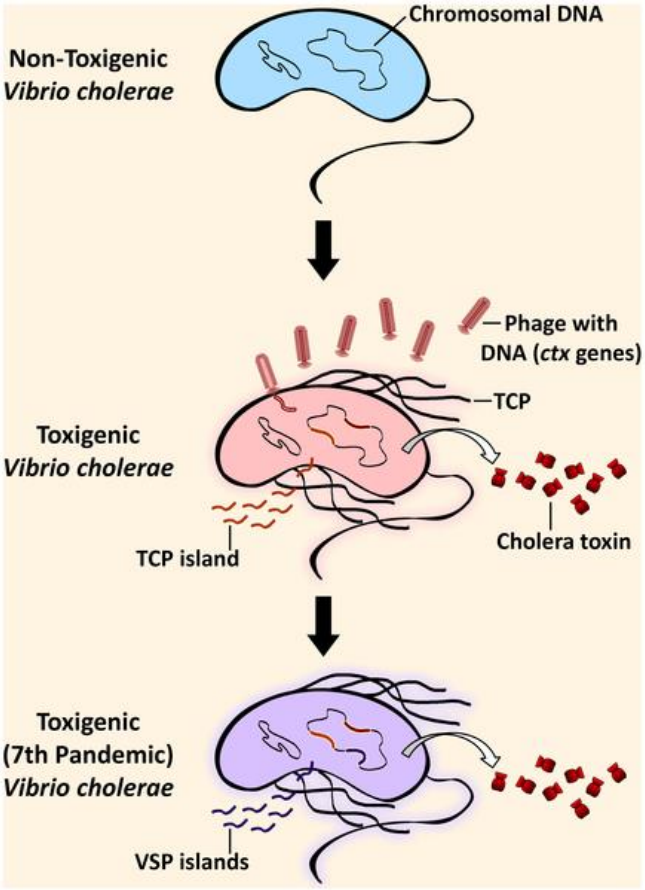

Figure 1.5. CTX bacteriophage and toxin coregulated pilus involvement in the evolution of the seventh pandemic *Vibrio cholerae*. In this figure, the CTX phage is shown attaching to *V. cholerae* strains that display the TCP, allowing them to insert their genetic information which contains the cholera toxin (ctx) genes. These strains are now toxigenic, able to produce cholera toxin and also spread the genes necessary for TCP by releasing the TCP pathogenicity island. *V. cholerae* strains responsible for the seventh cholera pandemic possess additional pathogenesis genes located on the *Vibrio* seventh pandemic (VSP) islands.[3]

2.3. Cholera toxin

2.3.1. Subunit structure and general function

Cholera toxin (CT) is a member of the AB_5 group of bacterial toxins. This group is related due to their common structure and pathway to enter host cells. Each member of this group has six different proteins which make up the holotoxin: there are the 5 B-subunits that function by binding to surface carbohydrate receptors of target cells and initiating entry and a single A-subunit that exerts the subsequent toxic effect which varies between toxins (152) (Figure 1.6). Besides CT, other notable and dangerous members of this group include

[3] Reprinted from PLOS Pathogens, volume 10, Orata F.D., Keim P.S., Boucher Y., The 2010 Cholera Outbreak in Haiti: How Science Solved a Controversy, page e1003967. Copyright 2014 Orata et al., this is an open-access article distributed under the terms of the Creative Commons Attribution License (https://creativecommons.org/licenses/by/4.0/legalcode).

pertussis toxin from *Bordetella pertussis* which causes whooping cough, heat-labile enterotoxins from enterotoxigenic *Escherichia coli* causing diarrhea and shiga toxin from enterohaemorrhagic *Escherichia coli* that causes dysentery (152). The B-subunits of CT (CTB) are each 11.6 kDa and they are arranged in a symmetrical and stable ring shaped pentamer that is referred to as choleragenoid in the absence of the A subunit (153, 154). Each of these subunits have binding capability, giving the toxin high avidity and affinity for its major receptor GM1 ganglioside (90). The A subunit of CT (CTA) is divided into two portions. The N-terminal chain is referred to as A1 (11 kDa) and it is responsible for the catalytic effect of the toxin (90). A1 is connected to the C-terminal A2 chain (18 kDa) by a disulfide bond and extensive non-covalent interactions (90, 155). The A2 chain inserts into the pore created by the choleragenoid and tethers the two subunits together non-covalently into the holotoxin (155).

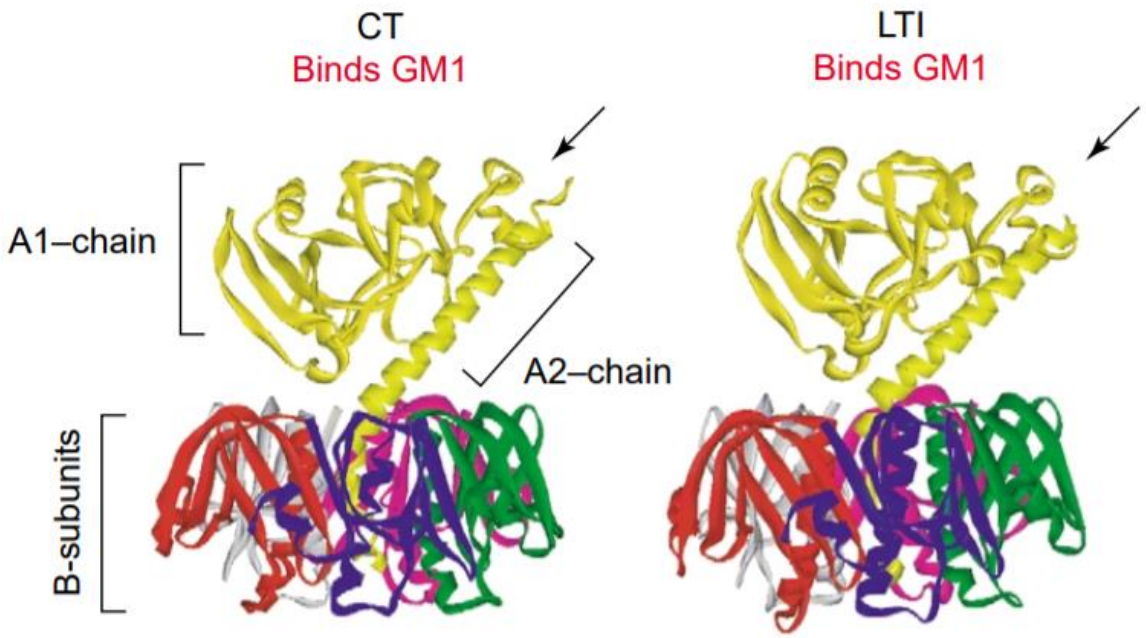

Figure 1.6. Crystal structures of two AB_5 toxins. Cholera toxin (CT) and heat-labile enterotoxin I (LTI) are represented, which both bind GM1 ganglioside as their primary receptor. Arrows indicate the proteolytic cleavage site which allows for the release of the A subunit once unfolding takes place in the endoplasmic reticulum. [4]

2.3.2. Mechanism of action

To best understand the way that *V. cholerae* causes cholera, it is important to understand the effect of CT on the intestinal epithelium and how this causes the disease. Once *V. cholerae* enters the oral cavity of the host, its first major obstacle is to make it past the gastric acids of the stomach (125). This kills a majority of the bacteria, but those that survive travel to the small intestine. As mentioned before, the TCP pilus is important for binding to intestinal epithelial cells and in conjunction with other adhesive molecules, allows for the cells to attach and establish colonization in the small intestine. Once this occurs, CT is secreted, and its mechanism of action is initiated. This is believed to begin

[4] Reprinted from Trends in Biochemical Sciences, volume 28, Lencer WI, Tsai B., The intracellular voyage of cholera toxin: going retro, pages 639-645, Copyright 2003, with permission from Elsevier. The figure was changed by removing parts of the figure to focus on the AB_5 toxins more pertinent to this dissertation.

through the binding of the toxin to GM1 gangliosides on the apical surface of the intestinal epithelial cells (156). The toxins are thought to gather in lipid raft domains present on the cell surface where gangliosides are most abundant (157, 158). Recent investigations have revealed that fucosylated glycoproteins are likely also a key factor in the function of CT as they have been shown to not only bind to the toxin (159-162), but this binding can result in internalization and intoxication of host cells (163, 164). Besides this point, CT is thought to bind to these receptors using its B-subunits, which causes its association into lipid rafts and the eventual entry of the toxin into the cell by both clathrin-dependent and independent mechanisms (155). From there, the toxin has been shown to travel in endosomes through the Golgi apparatus by retrograde transport and make its way to the endoplasmic reticulum (ER). This was a process that was first observed in regard to shiga toxin (165). CT contains a KDEL motif near the C-terminus of its A2 chain that aids in the efficiency of this process, though it is not essential (166, 167). It has also been suggested that the toxin can move directly through the entire cell via transcytosis, staying intact the entire journey to the basolateral surface where it can be released (168, 169). Both pathways seem to be dependent on the structure of the ceramide domain of the GM1 on the cell surface and retrograde transport requires the gangliosides to be in lipid rafts, so the process appears to be lipid-specific rather than protein-specific (168). CT enters the ER with both the A and B subunits attached and recruits host machinery to unfold and release the A1 chain of the A-subunit (155). The disulfide bond between the A1 and A2 portions of the A subunit is believed to be proteolytically cleaved as the toxin is secreted from *V. cholerae* and before it enters the host cell by serine proteases present in the lumen of the intestine (90) (Figure 1.6). This is thought to be important in exposing hydrophobic residues that are partially

hidden in the holotoxin and are needed for retrograde transport and unfolding in the ER (170, 171). Stable folding ensures that the A1-chain still remains firmly attached to the rest of the toxin until the protein is unfolded in the ER (166). The unfolded A1- chain is then translocated out of the ER by a mechanism that is currently unknown, and is believed to refold spontaneously and rapidly once it has been released by the host proteins of the ER (155, 172). This ability and the fact that the A1-chain has very few of the domains needed for polyubiquitination are likely the reasons that it is able to reach its targeted substrate in the cytoplasm (172). That target is the $G_{s\alpha}$ protein of adenylate cyclase (156). The A1-chain ADP-ribosylates this protein causing it to bind GTP and constitutively activate adenylate cyclase's ability to convert ATP to cyclic AMP (cAMP) (156, 173). This rise in cAMP leads to increased efflux of chloride ions into the intestinal lumen by the cystic fibrosis trans-membrane conductance regulator (CFTR) (173). An enormous amount of water enters the lumen of the intestine as a result, causing the rice-water diarrhea and severe dehydration that are hallmarks of the disease.

2.4. Enterotoxigenic *Escherichia coli* and heat-labile enterotoxin

2.4.1. *Escherichia coli* background

Escherichia coli is a facultative anaerobic, Gram-negative, rod-shaped member of the Gammaproteobacteria often possessing multiple flagella and/or pili. *E. coli* is best known for its importance as a model organism and its role in disease, but outside of the lab and hospital, they have a complex set of environmental niches and are a very diverse species. Importantly, they make up a significant portion of the gut microbiome in mammals and birds, and generally exist as a commensal organism without incident unless an individual is immunocompromised, or the protective barrier of the gut epithelium has been

damaged. Along with other members of the natural microbiota, they contribute to the prevention of pathogen colonization (174), produce vitamins K (175) and B12 (176) which can be used by the host and also consume oxygen that enters the gut, making the environment inhabitable for beneficial anaerobic bacteria (177). Those *E. coli* variants that are pathogenic however can be grouped into six pathogenic groups called pathotypes based on how they cause disease. These include: enteroaggregative (EAEC), enterohemmorhagic (EHEC), enteropathogenic (EPEC), enterotoxigenic (ETEC), enteroinvasive (EIEC) and diffusely adherent (DAEC) *E. coli* (178). This chapter will focus specifically on the enterotoxigenic *E. coli*.

2.1.4. Enterotoxigenic *Escherichia coli*

Enterotoxigenic *E. coli* are separated from the other pathotypes of pathogenic *E. coli* by their ability to cause disease in humans and animals through a specific set of colonization factors and enterotoxins. Fimbrial or fibrillar colonization factors which are antigenically diverse among strains of this group allow for the organism to colonize the gastrointestinal tract (178). Enterotoxins of two different groups are then released: the heat-labile (LT) and heat-stable (ST) enterotoxins. Individual strains within this group can produce one or both toxins. LT is closely related to CT both in structure and function having 80% amino acid sequence homology (156). It is an AB_5 toxin with pentameric binding B-subunits capable of binding to ganglioside receptors and an enzymatic A subunit that ADP-ribosylates G-proteins, resulting in irreversible activation of adenylate cyclase and consequently increased chloride ion secretion through the CFTR by the same mechanism as CT (156). Through sequence analysis, it has been suggested that CT and LT are evolutionarily linked and that *E. coli* acquired the LT genes via horizontal gene-transfer

from an ancestor shared with *V. cholerae* approximately 130 million years ago, before the two diverged as a species (179); it is important to note however, that the genes encoding for LT (*eltA* and *eltB*) are located on a plasmid in ETEC and not a lysogenic bacteriophage (156). There are two types of LT: LT-I (Figure 1.6) which is most closely associated with CT and human disease and binds to GM1 gangliosides and LT-II, subdivided into LT-IIa which binds GM1, GD1a and GD1b gangliosides, and LT-IIb which only binds GD1a ganglioside (180). It is also important to note that while LT-I and CT share many similarities, the binding specificity of CT is more specific for GM1 than that of LT-I. While LT-I still binds with highest affinity to GM1, it can also bind to other gangliosides, blood sugar antigens and even *E. coli* LPS (181). LT-I is the type referred to in this dissertation due to its high affinity for GM1 ganglioside and its proven ability to cause disease in humans. LT-II toxins are found in animals, however the connection between these toxins and disease is still not fully explored (180).

2.1.5 Enterotoxigenic *Escherichia coli* and traveler's diarrhea

Consistent with the similarity of LT to CT, infection with ETEC can result in watery diarrhea and vomiting which then leads to dehydration due to loss of fluids and electrolytes. It is difficult to estimate the impact of ETEC worldwide since reporting tends to be inconsistent, especially in low and middle income countries(182), however estimates suggest that ETEC causes 157, 000 deaths per year and that the majority are young children (182-184). In less serious cases, this organism is also known as one of the most common causes of traveler's diarrhea, which is a disease that affects an estimated 20-50% of people travelling internationally (185). The disease is normally self-limiting and generally can be treated with simple rehydration therapy; however, as a result of the wide-reaching impact

of this organism and its particular danger to children, it has become a major target for vaccine development (186).

3. AB_5 toxin binding to *Campylobacter* lipooligosaccharides

3.1. Cholera toxin and heat-labile enterotoxin affinity for various ganglioside structures

By surface plasmon resonance, researchers have been able to determine which of the gangliosides CT and the very closely related heat-labile enterotoxin I (LTI) bind the best (88, 89). Not surprisingly, these toxins prefer to bind their shared native receptor GM1 ganglioside with reported dissociation constant (KD) values as low as 4.61 x 10-12 M (88, 89). The binding affinity was much lower for GM1 gangliosides missing the sialic acid portion (asialo-GM1) which had KD values as high as 1.5 x 10-8 M (88, 89). The pattern of dissociation constants showed that the terminal galactose and neuraminic acid residues of the antigen were critical to CT's ability to bind (89). The toxin did show some tolerance to having a second neuraminic acid attached to the first as is the case of the GD1b ganglioside structure (89). A more recent study fragmented GM1 into its smaller components to determine which contributed most to the binding of the toxin, confirming the previous studies by reporting that the terminal galactose and sialic acid residues contribute 54% and 44% to the binding energy of the interaction respectively (187).

3.2. Beneficial uses of cholera toxin

Generally, CT is considered for the negative impact that it has relating to cholera and for the holotoxin, this characterization is quite accurate. However, since CTB in the choleragenoid form is missing the toxic component, it has been used in a variety of helpful capacities for microscopy and immunology. Given its high affinity for GM1 and the

abundance of this ganglioside on the surface of a variety of human cells, CTB is often used in conjunction with fluorescent protein linkers for labelling in fluorescence microscopy. It is able to retain its binding capability with different linkers attached, so it works well in experiments where multiple fluorescent agents are being used. And more recently, both LT and CT are becoming commonly used for their benefits as adjuvants in vaccines due to several structural and immunological qualities that they possess. Since these proteins are enterotoxins, they are very resistant to degradation by the proteases of the intestine, making them desirable in environments where other adjuvants could be destroyed (188). In addition to intestinal epithelial cells, GM1 is also present on M-cells and all antigen-presenting cells (188). This along with their ADP-ribosylation activity in some cases makes these toxins potent stimulators of the immune response in humans (188).

3.3 Cholera toxin's ability to bind *Campylobacter jejuni* lipooligosaccharides

Since *C. jejuni* is able to mimic the structure of GM1 ganglioside with its LOS, labeled CT was used by Linton et al. 2000 to identify the genes in *C. jejuni* 11168 that encoded enzymes responsible for ganglioside mimicry (97, 189). This is congruent with previous data revealing that the most important requirements of GM1 binding to CT were the terminal galactose and neuraminic acid residues (187). *C. jejuni* 11168 has the capability to display these features on its LOS, but as mentioned, the gene responsible for the addition of the terminal galactose is phase-variable in this strain. If we relate these results to the other two strains discussed earlier, it can be anticipated that individual cells of the HS:19 serostrain would all be capable of binding CT given that each of them have some GM1 mimicking LOS present on their surface. In contrast, the HS:3 serostrain should be incapable of binding CT because it lacks the genes required to produce the mimic. A

later study determined that GM1 mimics synthesized using *C. jejuni* enzymes had a similar binding affinity to CTB than bovine GM1 ganglioside (190). Interestingly, the authors also tested the ability of these synthesized mimics to bind to the LTI B-subunit and determined that the binding affinity was higher than that of the bovine ganglioside (190). These results suggest that these AB_5 type toxins show no preference for GM1 ganglioside over *C. jejuni* created mimics. This could indicate that the toxins have an alternative function that relates to their distinct ability to bind these bacterial LOS structures.

3.4. Coinfection of *C. jejuni, V. cholerae* and *E. coli*

Many areas of the developing world have individuals suffering from multiple enteric pathogens and the infections tend to be most prevalent and in infants and young children whose immune systems are naïve to the pathogens leaving them most vulnerable to infection. There have been several studies reporting that coinfection with multiple diarrheal pathogens is common for infants in these nations, also showing that infection with one type of proteobacteria such as *C. jejuni*, *V. cholerae* and *E. coli* can increase susceptibility to subsequent proteobacterial infection in what can be termed a proteobacterial bloom (183, 191-193) (Figure 1.7). There are have been multiple studies conducted specifically on infants and children in low- and middle-income countries such as the Malnutrition and Enteric Disease Study (MAL-ED) (13, 194) and Global Enteric Multicenter Study (GEMS) (184) aimed at understanding the increased susceptibility and impact associated with diarrheal diseases. As mentioned earlier, avian species are the native host of *C. jejuni* and most chickens are colonized with *C. jejuni. V. cholerae* and toxin-producing *Escherichia* species have also be found in chickens and have become a rising concern with antibiotic resistant strains being found in consumable product (195,

196). To the author's knowledge, there has not been a case-study describing a disease-state in chickens brought on by infection with *V. cholerae*; however, CT added to chick intestinal epithelial cells *in vitro* does causes an increase in cAMP production (197). Those areas where both *V. cholerae* and *C. jejuni* are endemic likely pose a co-colonization risk in chickens as well, though this has not yet been investigated.

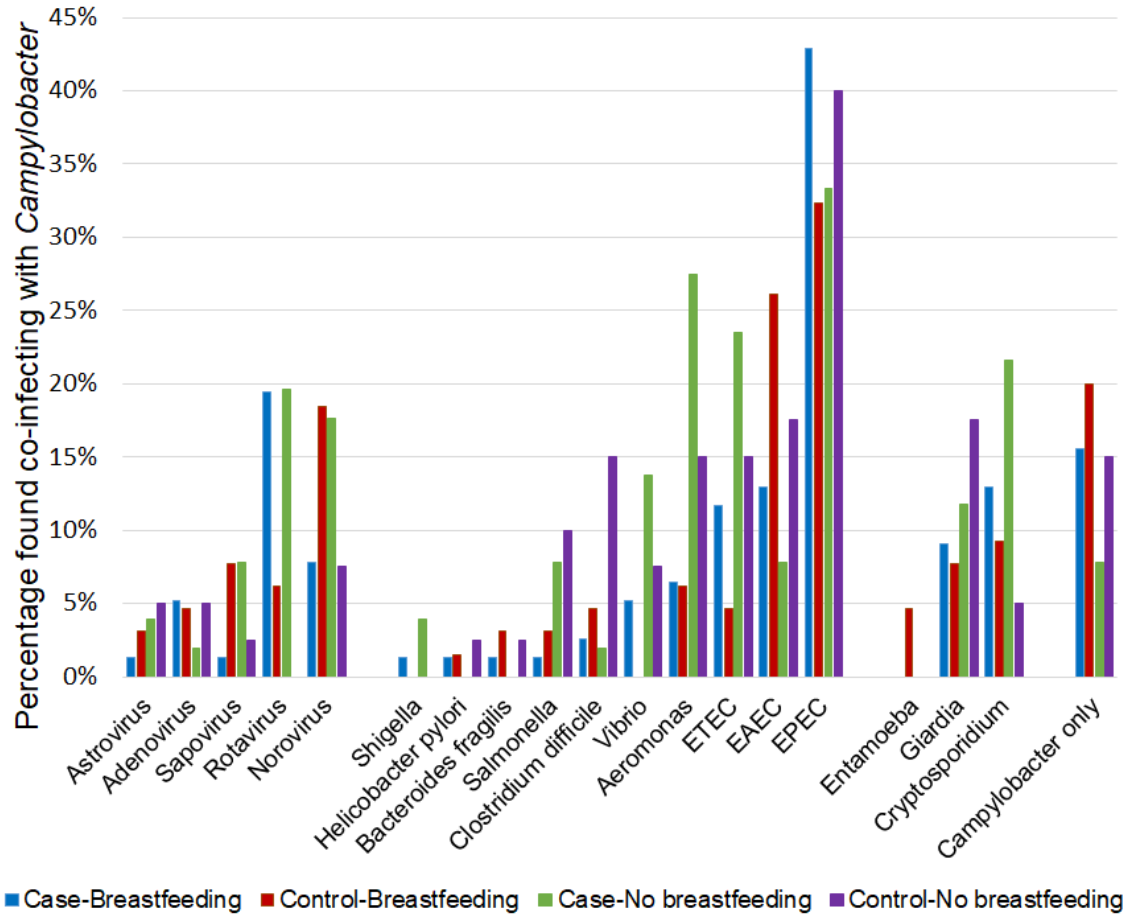

Figure 1.7. Co-infection rates of *Campylobacter* with other diarrheal pathogens from infants from the Global Enteric Multicenter Study. [5]

[5] Reprinted from mSphere, volume 5, Bian X., Garber J.M., Cooper K.K., Huynh S., Jones J., Mills M.K., Rafala D., Nasrin D., Kotloff K.L., Parker C.T., Tennant S.M., Miller W.G., Szymanski C.M., Campylobacter Abundance in Breastfed Infants and Identification of a New Species in the Global Enterics Multicenter Study, page e00735-19. Copyright 2020 Bian et al., this is an open-access article distributed under the terms of the Creative Commons Attribution License (https://creativecommons.org/licenses/by/4.0/legalcode).

4. *Enterococcus* species and glycosylation

4.1. *Enterococcus* background

The *Enterococcus* genus contains organisms that also colonize a wide range of hosts and environments including mammal, bird, reptile and insect guts, a wide range of food products, plants, soil and water (198-200). Of those found in humans, *Enterococcus faecalis* is the most common, followed by *E. faecium* and more rarely *E. avium, E. casseliflavus, E. durans, E. gallinarum, and E. raffinosus* (198). Most of these organisms exist as commensals of the gut microbiome, but they can also cause disease in humans. Enterococci are a large group in the Firmicutes phylum that consists of Gram-positive, facultative anaerobic, lactic acid bacteria. These organisms were previously classified as Group D Streptococci before being separated in 1984 based on DNA hybridization and 16S rRNA sequencing (201). Part of what distinguishes this genus from others is their ability to grow in a wide range of conditions. These include temperatures of 5-50˚C (202) (also able to survive 60˚C for 30 min (200)), pH between 4.6 and 9.9 (202), up to 40% (w/v) bile salts and 6.5% NaCl (199). They are also quite resistant to high metal concentration and desiccation (199). Enterococci are known for their ability to produce a variety of antimicrobial peptides called bacteriocins that can be released extracellularly to attack nearby related species by permeabilizing their cell membrane (199). Bacteriocins primarily target other Gram-positive bacteria such as *Listeria* and *Clostridium* species as well as *Staphylococcus aureus* (199). These peptides provide enterococci with a competitive advantage against other bacteria found in the host, allowing them to efficiently colonize and occasionally cause disease.

4.2. *Enterococcus* and human disease

Despite being a normal part of the human gut, Enterococci frequently cause infection when they gain access to privileged areas like the blood, urinary and bilary tracts, wounds, etc. (203). Enterococci are commonly reported as the second most common cause of wound and urinary tract infections and the third most common cause of bacteremia (199). They are thought to cause about 12% of hospital-acquired infections in the United States (199) and about 30% of the strains isolated from these infections are vancomycin resistant (204). Though the incidence of these hospital-acquired infections has been decreasing over the past few years, there were still 54, 500 reported cases in 2017 in the US resulting in 5, 400 deaths and a total cost of $539 million to the healthcare system (204). Therefore the CDC has declared vancomycin resistant enterococci a "serious threat" (204). *E. faecalis* is the species most commonly causing these infections, but *E. faecium* is more likely to be antibiotic resistant, with over 70% of the latter thought to be vancomycin resistant. *E. faecium* is also the most common cause of central-line associated bloodstream infections in the US (198, 204). Enterococci (mostly *E.* faecalis) are also commonly isolated from the root canal causing endodontic failure and periodontitis (199). Next to *E. faecalis* and *E. faecium*, *E. gallinarum* is the next most prevalent species in infection (about 2% of enterococcal infections) resulting in similar disease outcomes to the other *Enterococcus* species, but also being implicated in meningitis more in recent years due to hospital-acquired infections (205). This species has also been linked to systemic lupus erythematosus due to its ability to weaken tight junctions of the epithelium and translocate to systemic organs and drive autoimmune pathogenesis (206). *E. gallinarum* and *E. casseliflavus* are especially interesting due to their intrinsic resistance to vancomycin

through their natural genotype possessing the *vanC* gene (207). Non-*faecium*, Non-*faecalis* Vancomycin resistant *Enterococcus* infections are only reported in 1-2% of cases, but this is likely underestimated due to limits of detection (207). Though rarer, these other *Enterococcus* species have been associated with severe disease and cannot be overlooked.

4.3 Glycosylation in Gram-positive bacteria

4.3.1. Teichoic acids

Teichoic acids refer to a set of cell surface glycans that contain phosphodiester-linked polyol repeats (208). These glycans are present on the surfaces of Gram-positive bacteria and vary in structure across different species and within the same species (209). The term teichoic acid encompasses both the wall teichoic acids (WTA) which are covalently linked to the N-acetylmuramic acid (MurNAc) of the peptidoglycan and the lipoteichoic acids which are connected to the cell membrane directly via a glycolipid anchor. WTAs have two components, the linker portion which is highly conserved among different bacterial species, and a long polymer made up of phosphodiester-linked polyol repeating units (208). The conserved structure for the linker is typically an N-acetylmannosamine (ManNAc) linked (β1-4) to N-acetylglucosamine-1-phosphate (GlcNAc-1P) with a glycerol-3-phosphate attached to the ManNAc (208). The most well characterized repeat units consist of either ribitol-phosphate or glycerolphosphate, but there are examples of more complex sugar polymers (209). This structure is assembled onto an undecaprenyl-phosphate carrier on the cytoplasmic membrane before being translocated or flipped across the membrane by a largely unknown mechanism (208). The structure is then attached to a MurNAc residue in the peptidoglycan. In some Gram-positive bacteria, WTAs contribute up to 60% of the cell wall mass (210). LTAs are

typically more simplistic, made of a polyglycerol phosphate chain that is linked to a glycolipid anchor directly to the cell membrane (211). Polymerization of the chain occurs outside of the cell and the glycerol phosphate subunits come from the head group of the phosphatidyl glycerol located on the membrane lipids (211). These subunits are thought to be added to the distal end as the chain grows (211). Though there has been some debate in the past, more recent studies have conclusively shown that LTA can elicit the production of pro-inflammatory immune mediators, functioning in a similar way to the LPS endotoxins of Gram-negative bacteria (212). Teichoic acids are decorated with D-alanines and monosaccharides which can alter the surface charge of the bacterium among having other effects (210). These molecules to play a role not only in ion homeostasis, but also cell adhesion, biofilm formation and colonization (211, 213, 214). They impact pathogenesis by altering binding to host phagocytes, anti-microbial peptides and cationic antibiotics (208, 211). Also, in interacting with peptidoglycan machinery, they influence cell morphology and division (210, 211) as well as peptidoglycan autolytic enzyme localization (208).

4.3.2. Protein glycosylation

In comparison to eukaryotes, our view of protein glycosylation in bacteria is still relatively underdeveloped. This is especially the case considering that bacterial protein glycosylation systems already appear to be more complex than that of eukaryotes, with the potential to modify proteins in a wide variety of unique ways (215). In Gram-positive bacteria, the literature regarding protein glycosylation is far less expansive, suggesting that research into this area could be even more impactful. For instance, N-glycosylation of proteins has not been observed in Gram-positive bacteria thus far (216). However, there

are some examples of protein O-glycosylation in Gram-positive bacteria to be discussed. Starting with the first description of protein glycosylation in bacteria where researchers investigated the surface (S-) layer glycoproteins present in *Halobacterium salinarum* (217) and clostridial (218) species. These form crystalline arrays that encase the bacterium with glycan moieties extending from the cell surface and some Gram-positive organisms devote up to 20% of total protein synthesis to their production (219). S-layer glycosylation includes a wide variety of complex structures from many different bacteria (219). Gram-positive bacteria have been shown to possess O-mannosylated glycoproteins like those found in yeast and fungi (216). These are generally surface glycoproteins decorated with repeating mannose residues of 3 or less found in bacteria of the Actinomyces class (216). Similar to what is found in Gram-negative bacteria, several Gram-positives have been shown to glycosylate their flagella with O-glycans. Examples of this are *Clostridium botulinum* (220), *Clostridium difficile* (221), *Listeria monocytogenes* (222) and *Paenibacillus alvei* (223). O-glycosylation has also been observed in Gram-positive bacteria on a group of proteins called serine-rich repeat glycoproteins which include various surface adhesins (215). Examples of these proteins include: *Streptococcus gordonii* GspB (224) and *Staphylococcus aureus* SraP (225) used to bind human platelets leading to endocarditis (226, 227) and *Streptococcus pneumoniae* PsrP (228) which causes attachment to lung cells (229). The BclA spore surface proteins of *Bacillus anthracis* (230-232), *Bacillus cereus* (232) and *Clostridium difficile* (233) are also O-glycosylated. In addition to these pathogens, commensal Gram-positives have also been shown to O-glycosylate glycoproteins, though they are far-less investigated. Peptidoglycan restructuring enzymes in some *Lactobacillus* spp. are glycosylated with hexoses and N-

acetylhexosamines which improve enzyme stability and provide protection from proteases (215). In addition to wall and teichoic acids, Gram-positive bacteria also glycosylate a wide array of proteins.

4.3.3. Glycosylation in *Enterococcus*

As with most other bacteria, the full capacity of glycosylation pathways in enterococci is unknown. Most studies focus on the most common pathogens in the genus, *E. faecalis* and *E. faecium*. These organisms possess a peptidoglycan with a known structure (234) as well as wall teichoic acids and lipoteichoic acids that have several impacts on pathogenicity. For example, the WTA and LTA structures can influence complement (235) and antimicrobial peptide (236) resistance, host cytokine expression (237), biofilm formation (236) and adherence to host cells (238). There are very few enterococcal glycoproteins described in the literature and even those that have been discovered have not been studied thoroughly. It has been shown that *E. faecalis* has proteins that bind to several lectins (239), suggesting that they are glycoproteins, though these have not been further isolated and their glycans have not been characterized. Maky *et al.* also discovered a bacteriocin in *E. faecalis* F4-9 that is O-glycosylated with N-acetylglucosamine residues that are needed to maintain its antimicrobial impact (240). They also identified a gene that resembles a glycosyltransferase in the same gene cluster as the bacteriocin and termed it *enfC* (240). Though these studies represent a key beginning to the elucidation of protein glycosylation in enterococci, there is still much to be uncovered as there are likely more glycoproteins to be found. Further investigation of glycan structures in commensal gut bacteria like enterococci have important health

implications reaching beyond infectious disease. These organisms have a profound impact on host immune development and how the immune system responds to all oral antigens.

5. Oral tolerance and the microbiome

5.1. Bacteria and the gut-associated lymphoid tissue

The immune system surrounding the gut is unique compared to other areas of the human body given the broad array of antigens that we are exposed to. In addition to the foreign antigens that are introduced through food ingestion (>100g of foreign protein per day (241)), there is an enormous burden on this system to react differentially to the various bacteria that enter and occupy the space (up to 10^{12} bacteria per gram of contents in the colon (241)). There are over 100 trillion microbes present in the gut which in total possess 100 times more genes as the human genome (242). The gut-associated lymphoid tissue (GALT) is tasked with protecting an infection-prone area against dangerous pathogenic bacteria while also tolerating the presence of commensal organisms and food antigens. The induction of tolerance for these antigens is important in the GALT to prevent proinflammatory immune responses that result in inflammatory bowel diseases, allergies and other autoimmune diseases. Interestingly, the mechanisms of tolerance for food antigens and commensal microbes, while related, are different in that tolerance to microbes seems limited to the GALT, while food antigen tolerance has both a local and systemic impact on immune attenuation (241).

5.2. Immune cells involved in commensal bacterial tolerance

The importance of commensal bacteria in the stability of the immune system is evident in the immune systems of germ-free models. In the absence of commensal microbes, these animals show differences in cytokine production and immune cell quantity,

and develop defects in the Peyer's patches and spleen (243). Microbes release numerous peptides and molecules through their metabolism that induce tolerance to foreign antigens, and their presence is also thought to alter the composition of immune cells in the mucosa (244). Particularly, there are an abundance of CD4+ T-regulatory cells present in the intestinal mucosa that release IL-10 and TGF-β anti-inflammatory cytokines, promoting immune homeostasis (245). Also involved in this process are CD8+ and double negative T regulatory cells (244) as well as T helper (TH) 1 and TH-17 cells which show much decreased abundance in germ-free animals (246, 247). Antibiotic treatment has been shown not only to reduce the number of T regulatory cells in total, but also modify the antigens that are displayed on their T-cell receptors (248). Researchers were able to induce FoxP3+ anti-inflammatory T regulatory cells in germ-free animals by colonizing them with *Bacteroides fragilis* that secrete capsular polysaccharide A (249). It was further found that the CPS alone contributed to the prevention and even treatment of colitis in animals, further suggesting its involvement in tolerance development (249). Bacterial LPS added to the feed of germ-free mice also led to an increase in CD4+ and FoxP3+ T cells in mesenteric lymph nodes (250). In addition, the intestinal epithelial cells also play an important part in the tolerance of commensal bacteria. The expression of toll-like receptors (TLR) specific for bacteria is much greater on the basolateral surface of the cells as opposed to the apical surface where they encounter commensal bacteria and the activation of these receptors is also differential (251, 252). For example, the flagella of *E coli* on the apical side of the intestinal epithelium does not normally induce TLR 5, however, if pathogenic *Salmonella* invades the epithelium, it can trigger TLR 5 on the basolateral surface and induce an inflammatory response (253). TLR 2 and TLR 4, primarily targeting bacterial

peptidoglycan and LPS respectively, are particularly low on the apical surface of the epithelium (243). Besides TLRs, there are other receptors that are likely involved in this process by recognition of pathogen associated molecular patterns such as retinoic acid-inducible gene-I (RIG-I)-like, nucleotide-binding oligomerization domain (NOD)-like and DNA-sensing cytosolic receptors (243).

5.4. Commensal bacteria and autoimmune disease

Considering the impact that commensal bacteria have on immune tolerance, it could be surmised that they also may play a role in the development of autoimmune diseases. This link has been further confirmed by results seen in animal models of autoimmune disease. Non-obese diabetic mice are a common model used for the study of type-I diabetes. Normally, these mice are resistant to the disease, but when they are germ-free, they develop severe diabetes symptoms (254). Germ-free mice that are colonized early on to simulate a healthy human microbiome experience reduced rates and severity of diabetes (254). In the experimental autoimmune encephalomyelitis (EAE) model for multiple sclerosis, researchers fed the rats lactobacilli and observed a suppression of the disease symptoms (255). This is accompanied by differences in the microbiota, a decrease in pro-inflammatory cytokines and an increase in anti-inflammatory cytokines (256). Oral tolerance in this model was also stimulated by the addition of capsular polysaccharide A from *B. fragilis* (257). Taken together, these studies establish a noteworthy link between the tolerance attributed to the commensal microbiota and autoimmune disease development.

Research Aims

The existence of ganglioside-mimicking glycans in bacteria and their role in the development of GBS has been suggested and proven for decades (35, 52). However, while it is assumed that there are multiple bacteria with this ability, *C. jejuni* is the only species where the mimicking glycans have been fully characterized (77, 258) and where studies show robust evidence that the organism can cause GBS in animal models (41, 259-261). With all that is known regarding *C. jejuni* ganglioside mimicry and its impact on the host immune system, there are many details about the full influence of these structures that requires further investigation. The goals of the projects outlined in this dissertation follow a common theme as they are all aimed at better understanding ganglioside-mimicry in bacteria and how this impacts the host and the complex ecosystem contained within. The dissertation began with the knowledge that AB_5 toxins produced by other gut pathogens can bind the ganglioside mimics present on *C. jejuni* cells and we hypothesized that this interaction could have a negative impact on *C. jejuni* survival. While exploring this first question, it was discovered that there are commensal bacteria in the chicken gut that also mimic ganglioside structures and this led to additional project aims. These new goals included determining if other bacteria in the chicken gut could be impacted by AB_5 toxins, investigating the influence that these commensal bacteria may have in the development of GBS, and isolating these ganglioside-mimicking commensal bacteria to characterize the glycan component responsible for the mimicry. Taken together, these studies explore microbial ganglioside mimicry and its impact on competition within the gut and what impacts these mimics may have on autoimmunity and the development of GBS. The research objectives of the studies in this dissertation are listed below. Each sub-aim is

directed at topics which will be discussed at further length in subsequent chapters, consisting of manuscripts summarizing my work centering around these goals.

I) Determine the impact of AB_5 toxins on *C. jejuni* and other ganglioside-mimicking bacteria in the gut.

It is known that CT of *V. cholerae* and LTI of enterotoxigenic *E. coli* bind GM1 gangliosides with high affinity and this glycolipid has been regarded as the primary receptor that is used for cell entry and disease causation (156) (though recent studies have disputed this notion (159-164)). Additionally, since many isolates of *C. jejuni* express GM1 mimics on their LOS, CT and LT are also capable of binding to *C. jejuni* (97). However, the impact of this interaction on *C. jejuni* has not been investigated before. Furthermore, the study of ganglioside mimicry in bacteria has largely focused on pathogens to this point, neglecting exploration of these mimics on other bacteria found in the gut microbiome. These subjects are the topic surrounding the following sub-aims:

a) Confirm GM1 ganglioside-dependent binding of CT and LT to *C. jejuni* and examine any deleterious effects of this binding using growth assays and electron microscopy.
b) If deleterious effects are observed, determine if CT and LT can act as a selective pressure for phase-variable *C. jejuni* strains to favor non-GM1-mimicking LOS. This will be done by comparing LOS structures and phase-variable gene sequences between cells exposed to the toxins and those left untreated.
c) Determine if the deleterious effects observed are a consequence of increased membrane-permeability using an ethidium-bromide assay and also if the

presence of toxins decreases virulence in the *Galleria mellonella* wax-moth larva model.

d) By probing chicken cecal cross-sections with CT and GM1 ganglioside antibodies, examine whether there are additional commensal bacteria in the chicken that mimic GM1 gangliosides.

e) Feed chickens the toxins and examine the 16S rRNA gene sequence profile of the chicken cecal microbiome to determine if the toxins made a significant change in the microbial community.

II) Investigate how the presence of ganglioside-mimicking bacteria during immune development could tolerate the host to GBS antigens.

Oral tolerance to antigens is developed early in life and is greatly impacted by the microbes present in the microbiome (262-265). Those early residents help to train the immune system to tolerate the presence of common and harmless foreign antigens including commensal bacteria, while attacking harmful antigens expressed by pathogens (266). This delicate balance early in life has a proven impact on the development of some major autoimmune diseases later in life (262). GBS is primarily caused by antecedent infectious diseases, most commonly involving ganglioside-mimicking bacteria such as *C. jejuni* (46). To the author's knowledge, there have not been any publications specifically investigating the frequency of ganglioside-mimicking *Campylobacters* in young children during this early tolerance phase. Additionally, it is not known how the presence of low levels of ganglioside-mimicking bacteria (potentially introduced through diet) could impact subsequent responses against these antigens and susceptibility to GBS. These are the topics that will be examined by the following sub-aims:

a) Survey infant fecal *Campylobacter* isolates from the GEMS study for the ability to produce GM1 ganglioside mimics by isolating their LOS and using CT as a probe in far western blot experiments.

b) Develop an assay using the THP-1 monocytic cell line to investigate whether prior exposure to intact bacterial cells displaying GM1 ganglioside-mimics can tolerize the immune system to subsequent challenge with bacteria that display GBS antigens. This will be accomplished using ELISA assays to measure differences in pro-inflammatory cytokine production between macrophages that have been previously exposed to the antigen and those that are naïve to it.

c) If an effect is observed, explore what receptor is mediating tolerance induction using THP-1 knock-down mutants in TLR2 and TLR4 and compare cytokine production to wildtype THP-1 cells in the previously mentioned conditions.

d) Measure differences in the expression of A20 between the groups by western blot on whole-cell lysates of the THP-1 macrophages because A20 is a negative regulator which promotes endotoxin tolerance in macrophages.

III) Isolate ganglioside-mimicking bacteria from the chicken cecum and characterize their mimicking structures.

From our first study, we detected ganglioside-mimicking commensal bacteria in the examined chicken cecal samples. As mentioned previously, although other bacteria have been implicated in the development of GBS, very little research has gone into the characterization of ganglioside-mimics in these bacteria. Even less effort has gone into investigating ganglioside-mimicking commensal bacteria since this was not previously described. In order to expand the understanding of ganglioside-mimicry in commensal

bacteria and explore their role in autoimmunity, I needed to first isolate these bacteria and work to characterize the ganglioside mimics that they express.

a) Use pull-down and colony-lift experiments with anti-CT and anti-GM1 ganglioside antibodies to isolate ganglioside-mimicking commensal bacteria from chicken cecal samples.
b) Identify the genus and species of the bacteria that are isolated using 16S rRNA sequencing and MALDI-TOF mass spectrometry.
c) Use ganglioside antibodies to probe whole-cell lysates of the isolated bacteria to narrow down what structures could be displaying the ganglioside mimics and perform preliminary mass-spectrometry to confirm the presence of glycans.
d) Sequence the genomes of the isolates and perform glycoproteomics on isolated trypsin-digested peptides to determine which proteins are glycosylated and the type of protein glycosylation system used.
e) Isolate ganglioside-mimicking glycoproteins in large quantities for NMR experiments to determine the complete glycan structure and to use in future THP-1 macrophage assays.

CHAPTER 2

BACTERIAL AB_5 TOXINS INHIBIT THE GROWTH OF GUT BACTERIA BY TARGETING GANGLIOSIDE-LIKE GLYCOCONJUGATES[6]

[6] **Patry R. T.**, Stahl M., Perez-Munoz M.E., Nothaft H., Wenzel C.Q., Sacher J.C., Coros C., Walter J., Vallance B.A., Szymanski C.M. 2019. *Nature Communications* 10: 1390. Reprinted here with permission of publisher. https://creativecommons.org/licenses/by/4.0/legalcode.
Author contributions: RTP and CMS designed the study with insight from HN and JCS. RTP performed all transmission and scanning electron microscopy. RTP completed clearance assays of *C. jejuni* strains exposed to toxins. RTP isolated and analyzed lipooligosaccharides as well as genomic DNA from toxin-exposed cells. RTP and HN constructed *C. jejuni* 11168 mutants for use in cell permeability assays. RTP performed ethidium bromide cell permeability assays. *C. jejuni* virulence in *Galleria mellonella* was assayed by RTP. Chicken gavaging, handling and cecum preparation was done by CQW and HN. Fluorescence microscopy for chicken ceca and pull-down isolated bacteria was performed by MS and HN respectively. 16S rRNA metagenomic sequencing of chicken cecal samples was completed by CC. Analysis of metagenomic data was done by MEP. HN isolated bacteria from the chicken cecum. Paper was written by RTP and CMS with contributions from all other authors. CC, JW, BAV and CMS supervised the project.

Abstract

The AB_5 toxins cholera toxin (CT) from *Vibrio cholerae* and heat-labile enterotoxin (LT) from enterotoxigenic *Escherichia coli* are notorious for their roles in diarrheal disease, but their effect on other intestinal bacteria remains unexplored. Another foodborne pathogen, *Campylobacter jejuni*, can mimic the GM1 ganglioside receptor of CT and LT. Here we demonstrate that the toxin B-subunits (CTB and LTB) inhibit *C. jejuni* growth by binding to GM1-mimicking lipooligosaccharides and increasing permeability of the cell membrane. Furthermore, incubation of CTB or LTB with a *C. jejuni* isolate capable of altering its lipooligosaccharide structure selects for variants lacking the GM1 mimic. Examining the chicken GI tract with immunofluorescence microscopy demonstrates that GM1 reactive structures are abundant on epithelial cells and commensal bacteria, further emphasizing the relevance of this mimicry. Exposure of chickens to CTB or LTB causes shifts in the gut microbial composition, providing evidence for new toxin functions in bacterial gut competition.

Introduction

The gut microbiome is an exceedingly complex ecosystem where bacteria employ every tactic at their disposal to gain an advantage over competitors while avoiding clearance by the host. Among these strategies, bacteria display a diverse array of surface glycan structures (267) and mimic host glycans (268-271) to evade immune recognition. Given that these structures are prominently exposed, many animals have developed innate glycan-binding proteins, such as toll-like receptors or siglecs (272), to target non-self pathogen-associated molecular patterns and aid in immune clearance. There are also several glycan binding proteins such as galectins (273), intelectins (274) and resistin-like

molecule β (RELMβ)(275) that directly inhibit bacterial spread in the intestine. This study explores the ability of bacteria to use glycan binding proteins to target each other, contributing to competition between groups within the intestinal ecosystem.

Cholera toxin (CT) is produced by *Vibrio cholerae*, the causative agent of cholera, a devastating gastrointestinal disease currently endemic in 51 countries (276). The toxin is a member of the AB_5 group of bacterial toxins and consists of 5 B-subunits that specifically target cell surface glycan receptors and trigger entry into the host (152). AB_5 toxins also contain an enzymatic A-subunit responsible for the toxic effect observed. The A-subunit of CT ADP-ribosylates the Gsα protein of adenylate cyclase, causing it to bind GTP and constitutively stimulate conversion of ATP to cyclic AMP (cAMP) (156). This leads to increased efflux of ions into the intestinal lumen, resulting in the rice-water diarrhea and severe dehydration that are hallmarks of the disease (173). The B-subunits of CT (CTB) are arranged in a symmetrical, ring-shaped pentamer (153, 154). It was originally believed that CTB bound to GM1 gangliosides on the apical surface of intestinal epithelial cells to achieve entry (155). This hypothesis predominated in part due to CT's exceptionally high affinity for its receptor, with a reported dissociation constant of 0.73 nM (89). However, the dogma that binding to the intestinal epithelium is mediated through GM1 gangliosides has recently been disputed due to observations that these receptors are sparsely present in the human GI tract (163, 277). Further reports demonstrate that CT is capable of binding to fucosylated structures that serve as functional receptors for the toxin (163, 278, 279).

Heat-labile enterotoxin (LT) from enterotoxigenic *Escherichia coli* (ETEC) is another AB_5 toxin that shares a similar structure and function to CT. Both exhibit nM affinities for GM1 ganglioside receptors, though recent studies have identified other, albeit lower-affinity, receptors for these toxins. LT is capable of binding to blood group antigens, and both CT and LT were shown to bind several human milk oligosaccharides, notably those containing fucosylated residues (278). It has been shown that the fucose binding sites on these toxins are distinct from those binding GM1 gangliosides (278), leading us to question the role of the high affinity GM1 binding sites on these toxins. Notably, CT has been used as a reagent to assess GM1 ganglioside mimicry of another gastrointestinal pathogen, *Campylobacter jejuni* (97).

C. jejuni is a leading cause of gastroenteritis worldwide (1, 13). In addition, *C. jejuni* can cause the serious post-infectious sequelae Guillain-Barré Syndrome (GBS) through its ability to mimic human gangliosides with the lipooligosaccharide (LOS) structures displayed on its surface (79). Gangliosides are glycolipids containing sialic acid in their carbohydrate structure and are attached to ceramide lipids. These structures commonly decorate nerve cells but can also be found on other cells throughout the body. LOS is a shorter lipopolysaccharide (LPS) lacking the O-antigen and consists of a lipid A portion, which anchors it to the cell wall, as well as inner and outer core oligosaccharides. Among *C. jejuni* strains, the outer core structure exhibits considerable variation in the type and arrangement of the saccharides presented. Many *C. jejuni* strains sialylate their LOS, enabling them to mimic human gangliosides (79).

Approximately 60% of *C. jejuni* strains can mimic gangliosides (47), including GM1, GM2, GM3, GD1a, GD1b, GD2, GD3, and GT1a ganglioside types (77). This subset encompasses most of the major gangliosides found in the human body, and mimicry of these structures is believed to allow *C. jejuni* to escape immune detection by their hosts. GBS occurs when there is a breakdown in immune tolerance and the host generates α-ganglioside antibodies that not only attack the pathogen but subsequently recognize host nerve cells as foreign. This leads to degradation of spinal nerve axons and paralysis (41). GM1 gangliosides are the most common gangliosides mimicked by *C. jejuni* glycans (structures depicted in Figure 2.1), and CT has been used to probe for the expression of these structures on its surface (97).

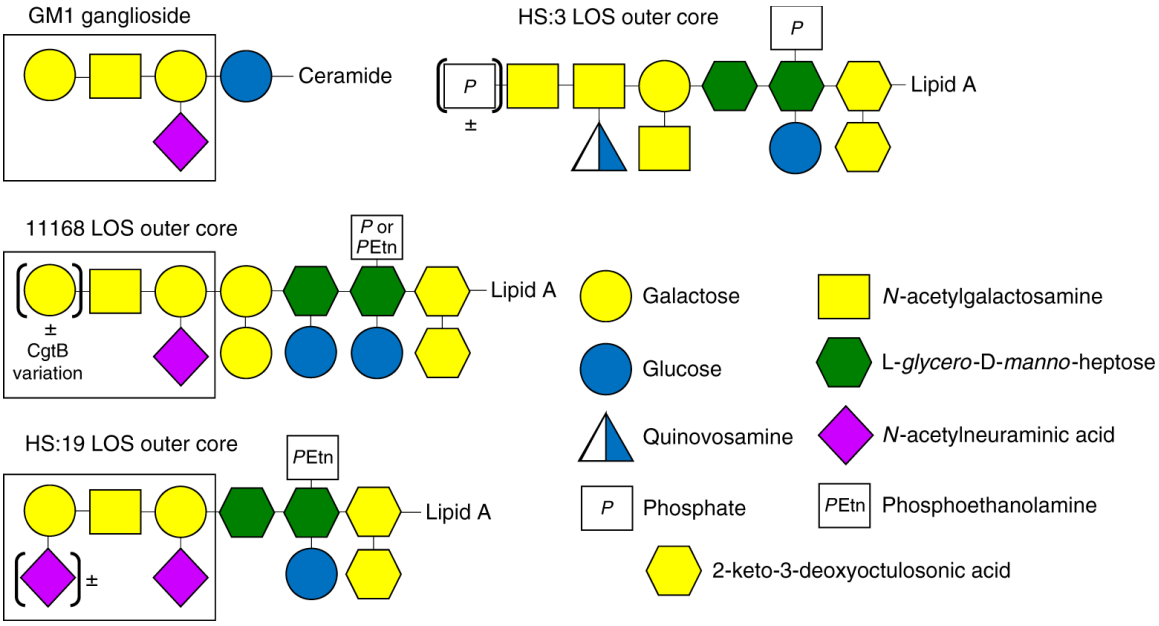

Figure 2.1. Structures of GM1 ganglioside and the outer LOS core of the wildtype *C. jejuni* strains used in this study. The portion of each receptor that is recognized by α-GM1 antibodies and cholera toxin is indicated by the box

The ability of CTB to bind *C. jejuni* is strain-dependent, due to variation in LOS structures resulting from differences in biosynthetic enzymes and/or variation in the expression of terminal sugar transferases (77). The heat-stable (HS) serostrain HS:19,

along with its serogroup members, have most commonly been isolated from GBS patients and express a heterogeneous LOS outer core displaying a mixture of GM1 and GD1a mimics (96). Conversely, the HS:3 serostrain is incapable of mimicking gangliosides since the strain lacks enzymes to synthesize the appropriate sugars (47). The 11168 strain of *C. jejuni* is capable of phase-varying its *cgtB* gene (cj1139c), which encodes the β 1–3 galactosyltransferase responsible for addition of a terminal galactose onto the LOS (97). This strain can vary its GM1 ganglioside mimics through slipped-strand mispairing in the poly-guanosine tract within *cgtB* (Figure 2.1) resulting in premature truncation of the transferase and loss of mimicry (97).

In this study, we demonstrate that CTB and LT increase cell membrane permeability and inhibit the growth of GM1-mimicking *C. jejuni* strains, presenting novel functions for these toxins. This effect is observed void of the toxic A subunit of each toxin and selects for *C. jejuni* variants not expressing GM1 mimicry. In addition, we identify another CT-binding bacterium in the chicken gut, *Enterococcus gallinarum/casseliflavus*, and provide evidence that oral administration of CTB and LT B-subunit (LTB) to chickens induces changes in the gut microbiome.

Results

Cholera toxin shows GM1-dependent binding to *C. jejuni*

A schematic of the LOS outer core structures of each strain used in this study is depicted in Figure 2.1, along with GM1 ganglioside for comparison. CTB binding to *C. jejuni* LOS was compared by transmission electron microscopy and immunogold labeling (Figure 2.2a–c). CTB binding was dependent on the presence of LOS-mimicking GM1 structures. *C. jejuni* HS:19 cells, which express GM1 mimics (96), showed toxin binding

(Figure 2.2a), whereas *C. jejuni* HS:3 cells unable to mimic GM1, showed no toxin binding (Figure 2.2c). *C. jejuni* 11168, which is known to display a mixed population of LOS variants(97), showed a mixed CTB binding phenotype (Figure 2.2b).

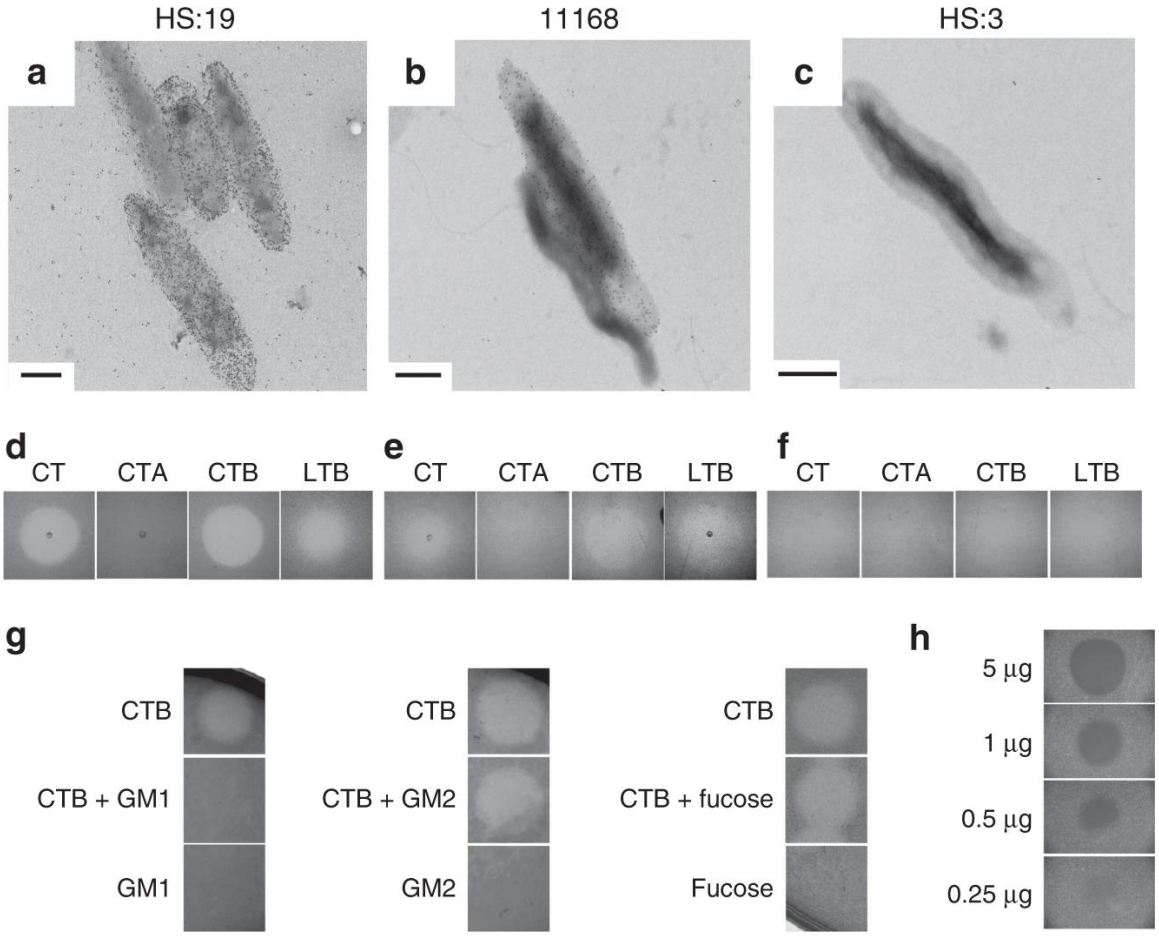

Figure 2.2. Cholera toxin B subunit (CTB) and heat-labile enterotoxin B subunit (LTB) bind and clear GM1 ganglioside-mimicking *C. jejuni* strains. a–f) Transmission electron micrographs depicting different *C. jejuni* strains bound by immunogold-labeled CTB (a–c, scale bars are 0.5 µm), accompanied by images of agar plates showing *C. jejuni* following exposure to 2 µL of either CT, CTB, CTA, or LTB (each at 1 mg mL-1) for 24 h while growing in soft agar (d–f). a, d) *C. jejuni* HS:19. b, e) *C. jejuni* 11168. c,f) *C. jejuni* HS:3. g) Competitive clearance assay where CTB was mixed 1:1 with indicated glycans prior to spotting onto growing *C. jejuni* HS:19. h) CTB spotted on *C. jejuni* HS:19 in various concentrations to determine the amount needed for clearance.

The B-subunits of CT and LT clear *C. jejuni* growth

CT, CTA, CTB and LTB were spotted on agar plates containing different *C. jejuni* strains to determine the effect of toxin binding on the growth of each strain. A zone of clearance was observed when CT, CTB, or LTB were spotted on *C. jejuni* HS:19 (Figure 2.2d). This phenotype was not observed for strain HS:3, which does not bind CT (Figure 2.2f), while the partial clearance observed for strain 11168 reflects the mixed binding phenotype (Figure 2.2e). The clearance caused by CTB suggests that the enzymatically active A-subunit known to be toxic to eukaryotic cells was not necessary to cause the clearance phenotype. LTB, the B-subunit of the related AB_5 toxin also showed similar clearance to that seen with CTB (Figure 2.2). When these same treatments were applied to *E. coli* CWG308 pGM1a/pCst, a strain engineered to display the GM1 ganglioside mimic on its LOS, no clearance was observed (Figure 2.8).

To confirm that the observed clearance was mediated through the GM1 ganglioside-binding domain of the toxin and not through the fucose-binding domain, CTB was mixed at a 1:1 ratio with GM1 ganglioside, GM2 ganglioside or fucose prior to spotting onto *C. jejuni* HS:19-containing plates (Figure 2.2g). The GM1 ganglioside competitively inhibited the clearance effect of CTB, while neither pre-incubation with GM2 or with fucose had an effect, indicating that the GM1 ganglioside-binding domain of the toxin is required for the clearing activity. The minimum amount of toxin required to see this effect was determined to be 0.25 μg (4.3 μM) by spotting various concentrations of CTB onto *C. jejuni* HS:19 and observing the extent of clearance in each zone (Figure 2.2h).

CTB mediated clearance is bacteriostatic

To better understand the clearance phenotype, scanning electron microscopy was used to examine the interface between the clearance/growth zone on *C. jejuni* HS:19 plates. Squares of agar were excised from either inside, outside, or directly on the edge of the clearance zones, to visualize the growth simultaneously (Figure 2.3a). When viewed at low magnification, regions outside of the CTB clearance zone showed growth in many discrete spheres, whereas these spheres were more sparsely distributed within the clearance zone (Figure 2.3b). This difference was also apparent at higher magnifications, where a drastic decrease in the number of *C. jejuni* cells inside the clearance zone was observed compared to outside (Figure 2.3c vs. 2.3e), but all showed normal cell morphologies (Figure 2.3d, f, Figure 2.9A and 2.9B). Addition of CTB to agar plates with already existing *C. jejuni* growth did not cause clearing (Figure 2.9D). These results support the hypothesis that toxin exposure leads to decreased *C. jejuni* growth in the observed zones of clearance.

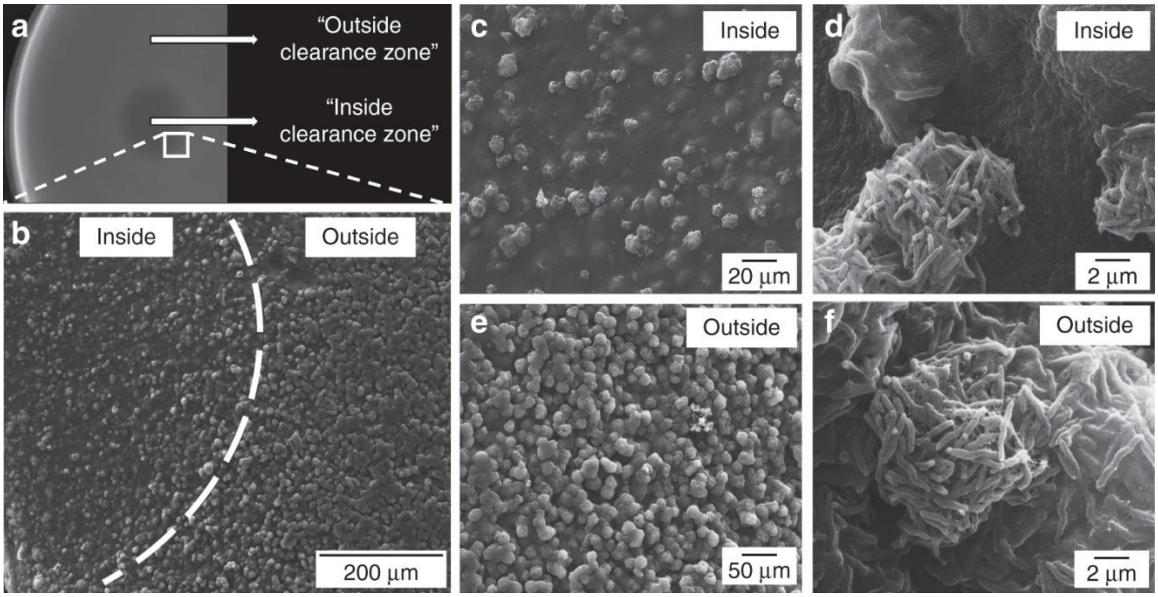

Figure 2.3. Scanning electron micrographs depicting *C. jejuni* HS:19 grown in NZCYM soft agar following exposure to cholera toxin B subunit (CTB). a Clearance zone 24 h after spotting CTB (the white square indicates the location of the excised agar slab). b A low magnification image highlighting the difference in surface structure of the agar slab between the exposed area (left side) and the unexposed area (right side). c, d Increasingly magnified images of the agar surface inside the zone of clearance. e, f Increasingly magnified images of the agar surface outside the zone of clearance. Images are representative of 3 replicate experiments.

Changes in LOS and *cgtB* suggest selection against mimic

To analyze whether cells exposed to CTB and LTB can alter their LOS structures and phase-vary GM1 ganglioside mimics, the LOS was isolated from *C. jejuni* 11168 cells inside and outside CTB and LTB clearance zones. LOS from each was compared using SDS-PAGE followed by silver staining to visualize molecular weight differences in the LOS (Figure 2.4a), and then by far western blotting with CTB to verify decreased LOS recognition by CTB (Figure 2.4b). The silver stained LOS from cells isolated from outside the zones showed a doublet (indicated by the arrow) and was reduced to a single lower molecular weight band for LOS isolated from cells inside the clearance zones (Figure 2.4a). The top band of the doublet (Figure 2.4a, lane 1) was presumed to represent the full length

LOS and the lower band to be lacking the terminal galactose residue. The LOS single band from cells inside the zones migrates similar to the lower of the two bands of the doublet from outside the clearance zone. To confirm this, a far western blot probed with CTB was done on the same samples and showed much greater CTB binding to LOS isolated from cells unexposed to CTB/LTB compared with those that had already been exposed (Figure 2.4b). The shift in mass and reduction in CTB binding observed in CTB/LTB-exposed cells suggests that exposure to the toxin provides a selective pressure against GM1 ganglioside mimicry in *C. jejuni*.

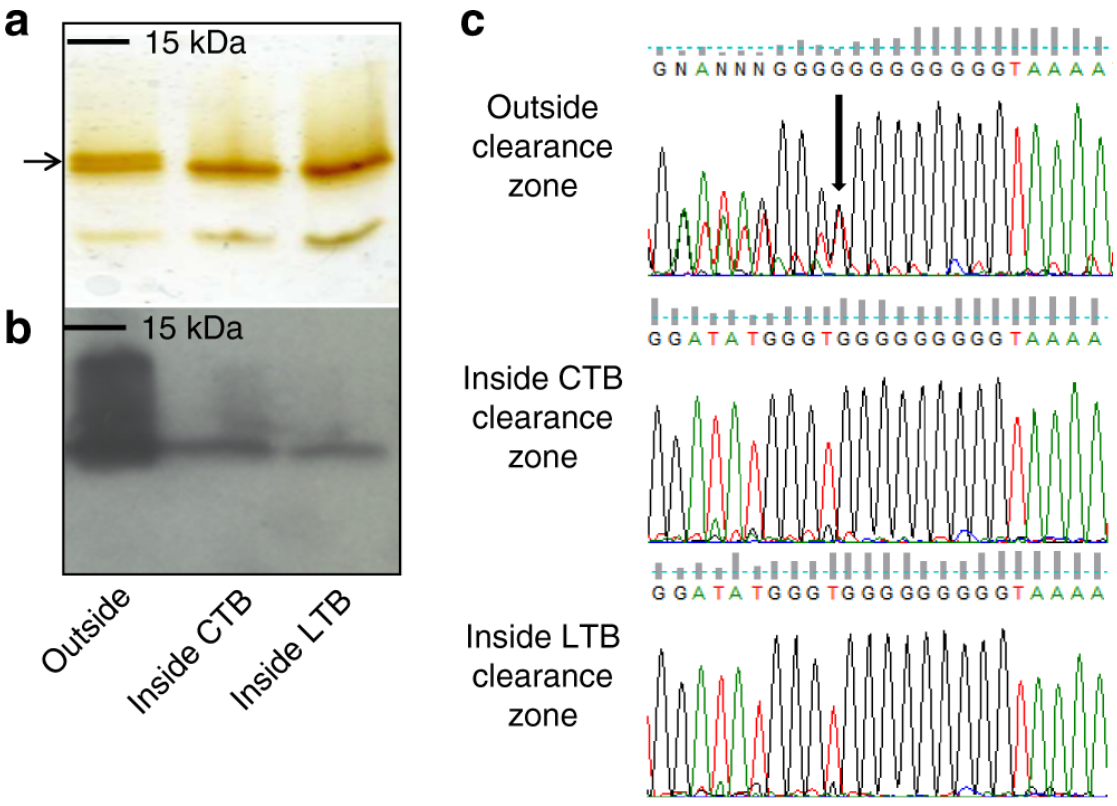

Figure 2.4. Exposure of *C. jejuni* 11168 cells to cholera toxin B subunit (CTB) led to changes in lipooligosaccharide (LOS) structure. This is shown by silver stain (a) and far western blot using CTB as a probe (b). CTB exposure also led to changes in the length of the poly-G tract in the *cgtB* gene, which is essential for GM1 ganglioside mimicry, leading to a frameshift mutation (c). The arrow in a marks the two bands associated with two distinct LOS structures in wildtype 11168 and the arrow in c marks the ninth G in the homopolymeric tract where heterogeneity is seen in the sequence. Source data are provided as a Source Data file.

To determine whether sequence variation in *cgtB* (necessary for addition of the terminal galactose in generating the GM1 mimic) led to the alteration in *C. jejuni* LOS following CTB or LTB exposure, DNA was isolated from *C. jejuni* 11168 cells inside and outside the same clearance zones. The *cgtB* gene was then PCR-amplified and sequenced from each sample. Interestingly, cells outside the zone of clearance displayed sequence heterogeneity at the homopolymeric G tract in *cgtB*, indicative of a population comprised of cells containing either 8 or 9 Gs in this region (Figure 2.4c). However, this heterogeneity was not present for cells obtained inside the zones of clearance, which consistently showed a sequence of 9 Gs. This shift from 8 to 9 Gs causes a frameshift during *cgtB* mRNA translation, which creates a premature stop codon resulting in a non-functional protein and abrogation of GM1 ganglioside mimicry (97). It is apparent from our data that *C. jejuni* 11168 cells inside CTB- and LTB-induced zones of clearance have "switched off" expression of *cgtB*, supporting the hypothesis that exposure to CTB or LTB constitutes a selective pressure against GM1 mimic expression.

Exposure to CTB increases cell permeability to EtBr

To determine if the inhibitory effect of CTB binding was due to a change in membrane permeability, accumulation of ethidium bromide (EtBr) inside the cells was measured by spectrophotometry. EtBr has been used previously to measure cell membrane permeability changes, as well as activity of multi-drug efflux pumps (280, 281). *C. jejuni* 11168 was used for this experiment along with several isogenic mutants (Table 1) including two abolishing GM1 mimicry (*cgtB* and *neuC1*) and one in the major efflux pump gene, *cmeA*. As seen in Figure 2.4, addition of CTB to the *C. jejuni* wildtype, capable of

mimicking GM1 gangliosides, resulted in an increased influx of EtBr unrelated to *C. jejuni* efflux pump activity. The relative fluorescence recorded 20 min after EtBr addition changed significantly when 11168 wildtype cells had been exposed to CTB ($n = 21$, $dF = 40$, $t = 4.3294$, $p = 9.74 \times 10{-}5$, t-test) and as well for *ΔcmeA* ($n = 12$, $dF = 22$, $t = 2.4580$, $p = 0.0223$, t-test); however, no difference was observed when the toxin could no longer bind in *ΔcgtB* ($n = 12$, $dF = 22$, $t = 0.9388$, $p = 0.3580$, t-test) and *ΔneuC1* ($n = 12$, $dF = 22$, $t = 1.4302$, $p = 0.1667$, t-test). Consistent with the spot assay, we did not see a change in EtBr uptake following CTB treatment of *E. coli* CWG308 pGM1a/pCst ($n = 6$, $dF = 10$, $t = 1.8869$, $p = 0.0885$, t-test) (Figure 2.8D). *E. coli* CWG308 wildtype showed a statistically significant increase in fluorescence after CTB exposure ($n = 9$, $dF = 16$, $t = 3.8268$, $p = 0.0015$, t-test), but this difference was small in comparison to that seen for *C. jejuni* 11168 and the significance may result more from low data variance (Figure 2.8D). Relative fluorescence measurements were taken every 2 min, but the trends remained relatively consistent throughout (Figure 2.10). These findings support that CTB causes an increase in membrane permeability upon binding to *C. jejuni* and is correlated with strains that show the clearance phenotype.

Table 2.1. Strains and mutants used in this study

Strain or Mutant	Description	Source
C. jejuni HS:19 serostrain	Human clinical isolate displaying both GM1 and GD1a ganglioside mimics	ATCC 43446[(282)]
C. jejuni HS:3 serostrain	Isolate incapable of mimicking mammalian gangliosides due to lack of sialic acid biosynthesis genes.	ATCC 43431[(282)]
C. jejuni 11168	Human clinical isolate displaying GM1 and GM2 gangliosides dependent on the phase-variable state of the *cgtB* gene.	(283)
C. jejuni 11168 Δ*cgtB::kan*^{R}	Kanamycin cassette knockout mutant in the cgtB gene incapable of adding terminal galactose to generate GM1 ganglioside mimic.	This study
C. jejuni 11168 *ΔcmeA::cm*^{R}	Chloramphenicol cassette knockout mutant in the *cmeA* gene creating a non-functional multi-drug efflux pump.	This study
C. jejuni 11168 *ΔneuC1::kan*^{R}	Kanamycin cassette knockout mutant in the *neuC1* gene incapable of creating N-acetylneuraminic acid to generate GM1 ganglioside mimic.	This study
E. coli CWG308	*waaO* mutant of *E. coli* R1 strain F470 with truncated LPS containing only the lipid A and inner core portions.	(284)
E. coli CWG308 pGM1a/pCst	A mutant made in *E. coli* CWG308 which harbors *C. jejuni cgtA*, *cgtB* and *cstII*, as well as *Neisseria lgtE* and *E. coli gne* on two separate plasmids, to display LOS GM1 ganglioside mimics.	(285)
Enterococcus gallinarum/casseliflavus	A GM1 ganglioside-mimicking bacterium isolated from the chicken cecum.	This study

CTB reduces *C. jejuni* virulence in *Galleria mellonella* model

The *G. mellonella* model is commonly used to assess *C. jejuni* virulence due to its susceptibility to *C. jejuni* infection and mortality phenotype in response to virulent strains (286). To test the potential impact of CTB on *C. jejuni* pathogenicity, ~ 1.0 × 109 colony forming units of *C. jejuni* HS:19 was introduced into the hind-leg of *G. melonella* to assess its virulence in the presence of CTB. When *C. jejuni* was incubated with CTB prior to

injection, a significant increase (n = 9, dF = 16, t = 4.3374, p = 0.0005, t-test) in larvae survival was observed after 5 days infection compared to HS:19 administered alone (Figure 2.5). This indicates that CTB binding to *C. jejuni* has a significant impact on its ability to infect and cause disease in a model host.

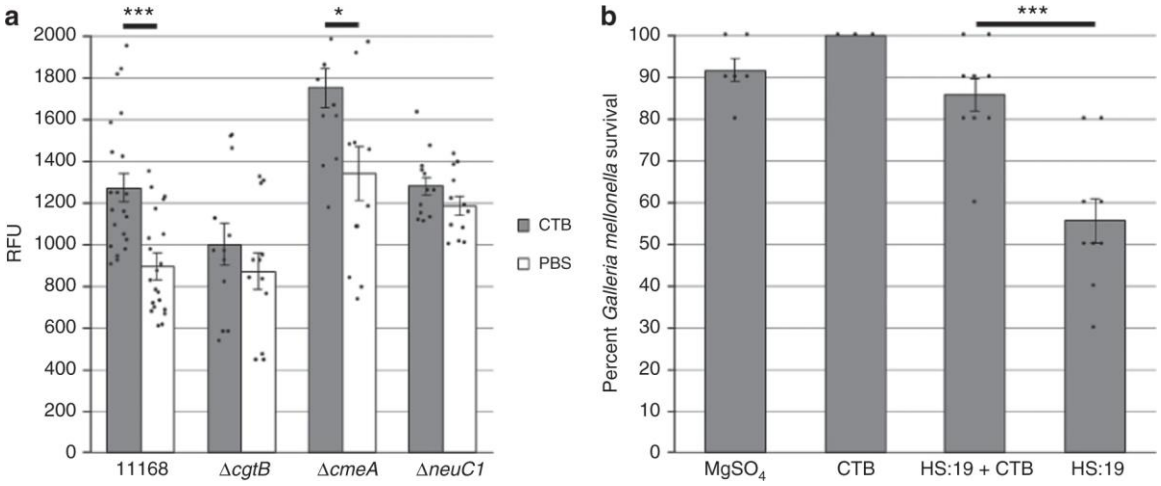

Figure 2.5. Cholera toxin B subunit (CTB) increases membrane permeability and reduces *C. jejuni* virulence in the *Galleria mellonella* model. a) *C. jejuni* 11168 wildtype (n = 21 per condition), *ΔcgtB* (n = 12 per condition), *ΔcmeA* (n = 12 per condition) and ΔneuC1 (n = 12 per condition) were incubated with ethidium bromide for 20 min following treatment with PBS (white) or CTB (gray) and the relative fluorescence when exposed to CTB was measured. b) *G. mellonella* larvae were inoculated with *C. jejuni* HS:19 alone (n = 9) or together with CTB (n = 9), MgSO4 buffer alone (n = 6), or $MgSO_4$ buffer together with CTB (n = 3), and larvae survival rates were determined after 5 days. Error bars represent the standard error within each group. ***p-value ≤ 0.001, *p-value ≤ 0.05 determined by two-tailed t-test. Source data are provided as a Source Data file.

CTB binds to mucins, epithelium and commensal bacteria

Chickens are a common host for *C. jejuni* so cloacal swabs were performed on 10% of chickens upon arrival to confirm that we received a Campylobacter-negative flock by plating onto Karmali selective agar. At the termination of the experiment, cecal contents from all birds were serially diluted and plated onto Karmali agar to confirm the chickens were not colonized with *C. jejuni*. To determine whether chicken intestinal epithelial cells or chicken gut bacteria other than *C. jejuni* display GM1 mimics or fucosylated structures

capable of CTB binding, chicken ceca and their contents were fixed, and cross-sections were paraffin-embedded and sectioned for analysis by immunofluorescent microscopy. Paraffin cross-sections were probed using either CTB or α-GM1 ganglioside antibodies. CTB bound strongly to the apical surface of the epithelium, to the mucus layer and to mucin-filled goblet cells (Figure 2.6a, c). A majority of the binding to mucus was negated by prior treatment of the slides with α1-2-fucosidase (Figure 2.6d), suggesting that this binding was mediated by the fucose binding site of CTB. CTB also bound to commensal bacteria present within the cecal lumen (Figure 2.6e). Similar to CTB, α-GM1 ganglioside antibodies labeled both the apical border of the epithelium, as well as many commensal bacteria within the cecal lumen (Figure 2.6b, f). However, unlike CTB, the α-GM1 ganglioside antibody did not bind the mucus or goblet cells (Figure 2.6a, b). This indicates that CTB may bind to the apical epithelium and to bacteria colonizing the chicken intestine via its GM1-binding site, since it shares specificity for these structures with αGM1 antibodies. In addition, our evidence suggests that CTB binds mucus and goblet cells via its fucose receptor, as binding to these components was abrogated by fucosidase treatment and since specificity for these components is not shared with α-GM1 antibodies.

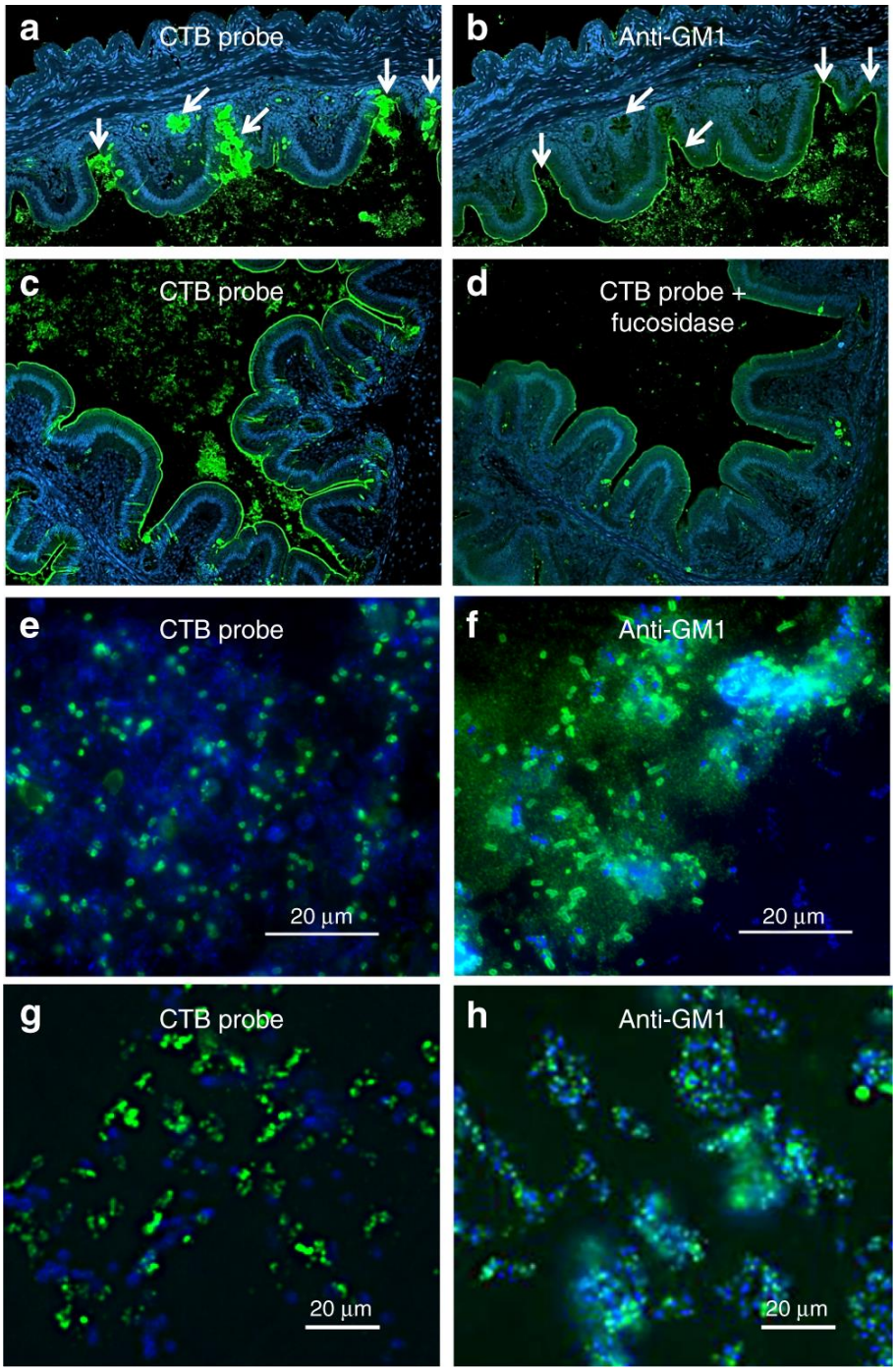

Figure 2.6. Cholera toxin (CT) binds to goblet cells, mucins and commensal bacteria in the chicken cecum. Fluorescence microscopy of sequentially cut chicken cecal cross-sections labeled with DAPI (blue) and either α-CT (green) (a, c–e, g) or α-GM1 ganglioside (green) (b, f, h). Images a–d were taken at ×200. Arrows in a, b indicate goblet cells and mucus. d Cells were treated with fucosidase prior to labeling. e, f) Magnified images to show bacterial binding. g) CTB (green) and DAPI (blue) labeling of bacteria isolated after CTB-protein G pulldown of bacteria isolated from the initial GM1-protein G pull-down.
h) Bacteria isolated after GM1 pulldown and labeled with DAPI (blue) and α-GM1 (green).

LTB administration to chickens shifts intestinal microbiota

Given the evidence that AB_5 toxins bind to a subset of bacteria present in the chicken intestine, we next examined if such toxins impact the composition of the chicken intestinal microbiota. We compared the 16S rRNA gene sequence profile of the cecal bacterial communities in chickens treated with LTB ($n = 9$) or with PBS ($n = 10$) as a control ($dF = 17$). We focused this experiment on LTB since enterotoxin producing E. coli strains have been reported in chickens (287, 288), and producing these toxins may be ecologically relevant. Administration of LTB causes shifts in the overall composition of the gut microbiome relative to PBS-treated chickens as shown by NMDS analysis of Bray Curtis dissimilarity ($p = 0.0120$ by Adonis PERMANOVA test) (Figure 2.7a). Although α-diversity is not affected, LTB significantly reduces β-diversity of the cecal bacterial community (Figure 2.7b), indicating that the toxin lowers inter-individuality of the gut microbiota. In terms of specific taxa, we found that LTB caused major shifts in the abundance of bacteria classified within the phyla Firmicutes ($p = 0.04$) and Bacteroidetes ($p = 0.04$) (Figure 2.7c, Table 2.2, statistical significance determined by two-tailed unpaired t-test with Welch's correction). Analysis of relative abundance at lower taxonomic levels shows that the majority of changes involve decreases in the families Ruminococcaceae ($p = 0.02$) and Lachnospiraceae ($p = 0.05$), as well as genera and OTUs within these families, while the genus *Bacteroides* was increased ($p = 0.04$) (Figure 2.7d, Table 2.2). These findings demonstrate that LTB has a major effect on the chicken gut microbiota.

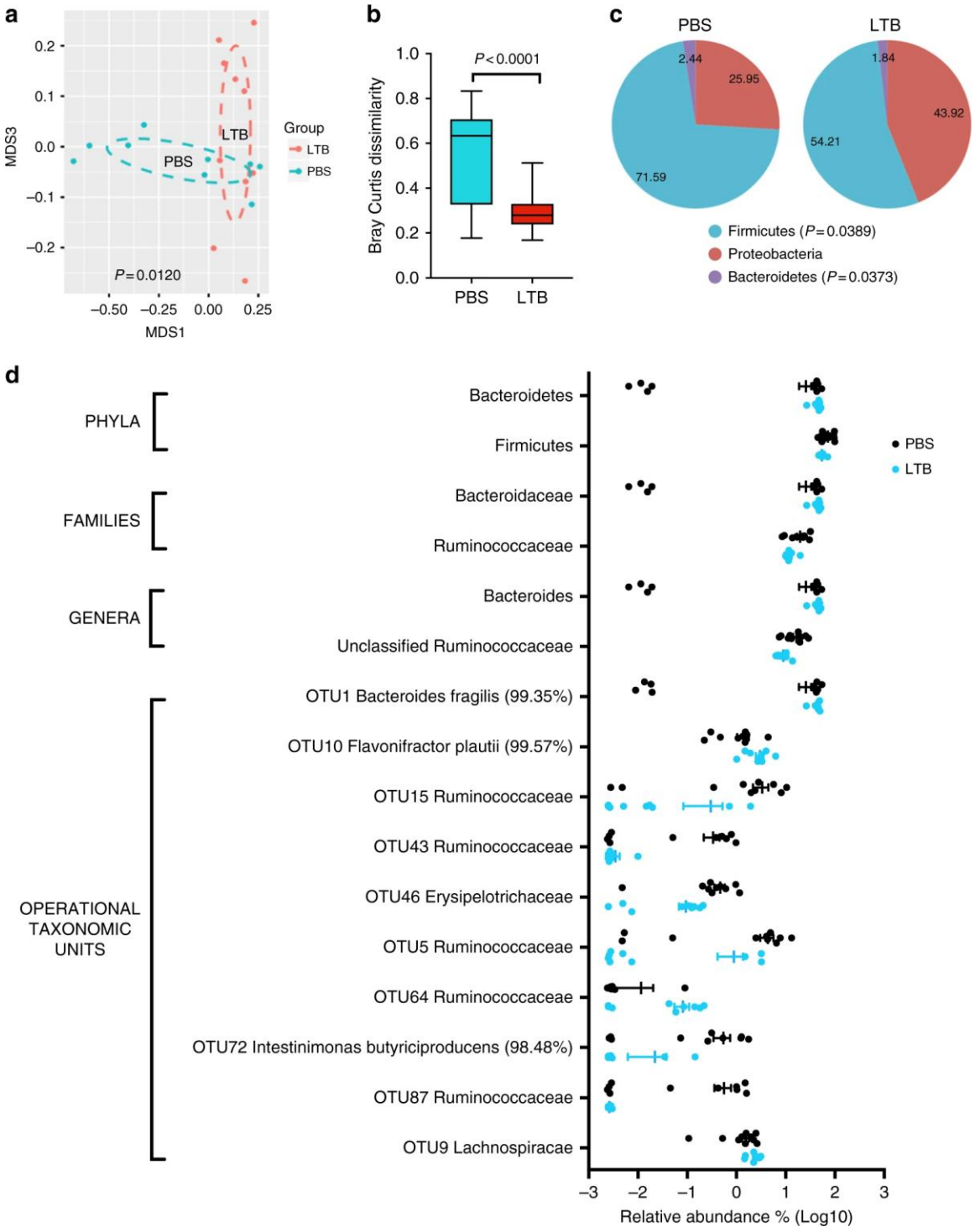

Figure 2.7. AB_5 toxins cause shifts in the gut microbiome of chickens by affecting diversity and composition. a) NMDS plot based on Bray Curtis distances show that introduction of heat-labile enterotoxin (LTB, n = 9) causes a significant shift ($p = 0.0120$, Adonis PERMANOVA test) in the gut microbiome of chickens relative to chickens treated with PBS (n = 10). b) Although α-diversity is not affected, LTB decreases β-diversity ($p < 0.0001$, two-tailed unpaired t-test with Welch's correction) indicating that the toxin

lowers inter-individuality of the gut microbiota. c) LTB decreases the relative abundance of Firmicutes ($p = 0.0389$) with parallel increases in Bacteroidetes ($p = 0.0373$). d) Significant changes in relative abundance (expressed as $\log_{10}$) at selected taxonomic level (see Table 2.2 for *p*-values and percentages of relative abundance). Whiskers in (b) represent minimum and maximum values. Lines and bars in (d) represent means and standard error of means. Source data are provided as a Source Data file.

Table 2.2. Relative abundance and *p*-values of statistically significant changes in taxa caused by administration of LTB.

Taxonomic Level	Name	PBS (%)	LTB (%)	*p*-value*
Phylum	Bacteroidetes	25.9458	43.9206	0.0373
Phylum	Firmicutes	71.5893	54.2123	0.0389
Family	Bacteroidaceae	25.9458	43.9206	0.0373
Family	Lachnospiraceae	42.8754	31.8613	0.0507
Family	Ruminococcaceae	19.529	12.2352	0.0197
Genus	*Bacteroides*	25.9458	43.9206	0.0373
Genus	unclassified_Ruminococcaceae	16.4285	8.9802	0.0096
OTU1	*Bacteroides fragilis* (99.35%)	25.7470	42.5499	0.0478
OTU10	*Flavonifractor plautii* (99.57%)	1.4066	3.0087	0.0214
OTU15	Ruminococcaceae	3.3204	0.3017	0.0247
OTU43	Ruminococcaceae	0.3348	0.0034	0.0168
OTU46	Erysipelotrichaceae	0.4693	0.0941	0.0064
OTU5	Ruminococcaceae	4.3303	0.8824	0.0302
OTU64	Ruminococcaceae	0.0116	0.0822	0.0198
OTU72	Intestinimonas Butyriciproducens_(98.48%)	0.5461	0.0219	0.0266
OTU87	Ruminococcaceae	0.5623	0.0026	0.0214
OTU9	Lachnospiraceae	1.5424	2.3670	0.0227

*Statistical significance obtained using two-tailed unpaired t-test with Welch's correction

To test if similar findings apply to CTB, we sequenced the gut microbiota of three birds receiving CTB and three with PBS. Although statistical significance could not be obtained, we observed similar trends to those obtained with LTB (Figure 2.11). Overall, our findings indicate that AB_5 toxins affect more than just *C. jejuni* in the chicken gut.

Isolation and identification of GM1-mimicking Firmicutes

Upon finding evidence to support other GM1-ganglioside mimicking bacteria in the chicken gut impacted by AB_5 toxins, α-GM1-protein G agarose was used to pull-down bacteria that display ganglioside mimics on their surface. Isolated bacteria were screened and one GM1-positive species, confirmed to bind α-GM1 and CTB by fluorescence microscopy, was further characterized. The isolate was identified as *Enterococcus gallinarum/casseliflavus*, a member of the Firmicutes phylum. Fluorescent microscopy of the isolated strain with α-GM1 ganglioside antibody showed two distinct populations with only a fraction of cells being bound by the GM1 antibody (Figure 2.6g). Further pull-downs with CTB in combination with α-CTB and protein G agarose intended to isolate the GM1-ganglioside mimicking variants (Figure 2.6h) followed by microscopic analyses after CTB-α-CTB surface staining resulted in a similar phenotype with only a fraction of bacteria being positive for CTB binding. This indicates that only a fraction of the culture expresses the potential GM1 mimics in vivo, reminiscent of potential phase-variation as observed in *C. jejuni* 11168.

Discussion

It has long been considered that the primary role of bacterial toxins is to target vertebrate hosts and cause disease (289). Another assumption, that has recently been disputed, is that GM1 gangliosides in the human gut are necessary for CT to induce disease in humans (163). However, since CT is capable of binding to *C. jejuni* GM1 ganglioside mimics (97), and the toxin genes are encoded by a *V. cholerae* bacteriophage (144), we thought it was possible for CT to possess an antibacterial function. *C. jejuni* is capable of mimicking various host gangliosides through variation of its LOS outer core, which allows

the organisms to evade host immune detection (91, 290). Furthermore, *C. jejuni* is an intestinal pathogen that occupies a niche shared with other enteric pathogens such as *V. cholerae*, suggesting the two organisms could compete for resources (290).

In endemic areas, *C. jejuni* is rarely the sole enteric pathogen infecting an individual, and the organism is routinely isolated from humans co-infected with *V. cholerae* and/or enterotoxigenic *E. coli* (291, 292). The latter produces LT, another AB_5 toxin with binding and enzymatic properties remarkably similar to CT (181). AB_5 toxin-producing bacteria have also been found in chickens, a common commensal host for *C. jejuni* (8, 195, 196, 287, 288). As a result, *C. jejuni* may come into contact with ganglioside-targeting, AB_5 toxin-producing bacteria in its natural environment. This study has demonstrated that CT and LT do in fact inhibit growth of GM1-mimicking *C. jejuni*. In addition, we have shown that when fed to chickens, LTB (and CTB) alter the microbial composition of the chicken intestinal tract, suggesting that these toxins and others like it may indeed play a role in inter-bacterial warfare.

After confirming that CT binding to *C. jejuni* was dependent on GM1 ganglioside mimicry and that this binding inhibited *C. jejuni* growth, we tested which component of the AB_5 toxins mediated the antibacterial activity. Interestingly, we found that the B-subunit was sufficient for the binding and growth clearance phenotype. This was unexpected, since the B-subunit of these toxins, while crucial for adhesion and internalization by eukaryotic cells, as well as for immune activation in humans and animals, is not toxic to eukaryotic tissues without the enzymatically active A-subunit (293). In contrast, the antibacterial effect we observed appears to be mediated through binding by the toxin. It is important to note however, that we have not excluded the possibility that the

A and B subunits could have a synergistic effect to cause increased clearance when the two are together in the holotoxin configuration.

The fact that the binding subunits of CTB and LTB alone are sufficient for clearance shows that the ADP-ribosylating action of the toxins is not necessary for the activity. The observations that this exposure does not alter individual cell morphology (Figure 2.9A-B) and that CTB does not clear *C. jejuni* if added after cells have grown (Figure 2.9) suggest that the observed effect is bacteriostatic as opposed to bactericidal. This is in contrast to lysis buffer, which causes visible clearing within minutes of spotting onto *C. jejuni* (Figure 2.9D). In *Cryptococcus neoformans*, growth inhibition has been observed as a result of antibodies directed against its capsular polysaccharide; the antibodies completely surround the cells and prevent it from dividing by encapsulating the organism (294). However, if our observed CTB-induced clearing occurred via the same mechanism, we would expect α-GM1 antibodies to reproduce the clearing effect, which we did not observe (Figure 2.9). Since the outer leaflet of the outer membrane acts as a permeability barrier, helping bacteria to regulate flow of harmful compounds, as well as beneficial nutrients (295), we postulated that disruption of this barrier may cause the bacteriostatic effect that we observe. Indeed, the results of our EtBr accumulation assay suggest that the mechanism is related to an increase in membrane permeability upon toxin binding. To determine if increased EtBr accumulation was an effect of the toxin blocking active efflux of EtBr, a mutant in the periplasmic component of the *Campylobacter* multidrug efflux pump, *cmeA* was inactivated. This mutant still showed an increase in EtBr permeability even in the absence of an active efflux pump, suggesting that CTB might act directly on the membrane. Interestingly, although CTB bound extensively to *E. coli* CWG

308 pGM1/pCst displaying GM1 ganglioside mimics on its LOS, none of the toxin subunits or the CT holotoxin were able to clear this engineered strain (Figure 2.8) and the EtBr accumulation assay showed no effect of CTB on membrane permeability. This could be due to inherent differences between these bacteria in their membrane architecture.

C. jejuni is known to stochastically vary expression of its surface structures through changes in the homopolymeric nucleotide tract length within specific genes resulting in frequent frameshifts and premature stop codons during replication. This effectively leads to "on/off-switching" of genes containing these tracts, many of which are involved in surface glycan biosynthesis and transfer affording *C. jejuni* the ability to rapidly shift the composition and diversity of surface structures in that community. Alterations in these structures has been shown to reduce the susceptibility of *C. jejuni* to serum, bacteriophages48 and anti-microbial peptides (91, 290). As well, even small changes in LOS have been shown to have a profound effect on *C. jejuni* invasiveness (91). By encoding a polyguanosine tract in the *cgtB* gene, strain *C. jejuni* 11168 varies the expression of the galactosyltransferase responsible for addition of the LOS terminal galactose. Those cells expressing "off-switched" *cgtB* will thus present the GM2 ganglioside epitope as opposed to that of GM1. This study demonstrates that LOS from CTB-exposed cells is substantially reduced in CTB binding, and that these cells display off-switched *cgtB* expression at the poly-G tract. Together these results indicate that CTB and LTB select against GM1 epitope expression by *C. jejuni*. Interestingly, we also found that pre-incubation with CTB for less than two cell divisions was sufficient to decrease the virulence of *C. jejuni* in a *G. mellonella* model. This not only suggests that expression of the GM1 ganglioside in wax moth larvae is important for virulence, but also shows that

CTB binding to *C. jejuni* has consequences on the biology of the organism that extend beyond growth inhibition *in vitro*.

Since our studies demonstrated that there is an abundance of ganglioside structures in the chicken intestine, it was unexpected, but reasonable to find many ganglioside-mimicking bacteria existing in this environment. Investigation of chicken cecal cross-sections identified bacteria that were readily labeled by both CTB and by α-GM1 antibodies, indicating the presence of other ganglioside receptors and possibly fucosylated structures. Additionally, the CTB bound abundantly to the mucus and goblet cells, which were not bound by α-GM1 antibody. This binding was largely abrogated by the addition of an α1-2-fucosidase to cross-sections prior to fluorescence detection, indicating that CTB binding to these structures was mediated through its fucose-binding domain. In support of this hypothesis, fucose is known to be abundant in mucins and in goblet cells producing mucin (296). Remarkably, both CTB and the α-GM1 antibodies also bound extensively to bacteria in the intestinal lumen, suggesting that there are other bacteria present in the chicken gut that display antigens resembling GM1 gangliosides. Ganglioside mimicry is a phenomenon thought to be rare in bacteria, and as described earlier, can lead to autoimmune disease in humans. Therefore, the observation that other ganglioside-mimicking bacteria are prevalent in food animals warrants further investigation into their identity and into the nature of the glycoconjugates they display.

Given the broad distribution of GM1 ganglioside-mimicking bacteria among the gut microbiota of chickens, we hypothesized that the administration of AB_5 toxins would alter the microbial composition. The most striking impact we observed was the decrease in microbes in the Firmicutes phylum, which represents a major component of the chicken

gut microbiome. We were also able to isolate a member of the Firmicutes, *E. gallinarum/casseliflavus*, from the chicken gut based on its ability to mimic GM1-ganglioside. Interestingly, *E. gallinarum* has recently been associated with another autoimmune disease, systemic lupus erythematosus (206). Other researchers have also observed gut microbiome changes following *V. cholerae* infection (297, 298). Hsiao et al. showed that *V. cholerae* infection correlated to an unhealthy microbiome, leading to long-lasting effects on gut microbial composition even after the infection had subsided (297, 298) while Monira *et al.* linked *V. cholerae* infection to increases in Proteobacteria and decreases in other phyla, including Firmicutes (298). In the published studies, it is not possible to distinguish between direct toxin effects on the gut microbiota vs consequences of the pathological process; however, the sole administration of the toxin B-subunits used in our studies does not induce pathology (293), suggesting that these AB_5 toxins could directly provide a competitive advantage for those that produce them through growth inhibition or simply reduced colonization. It may be particularly important for AB_5 toxin-producers to target ganglioside-mimicking bacteria due to the fitness that mimicry imparts in dealing with host defenses (91, 290). This would make AB_5 toxins particularly useful tools in the microbiome and supports the notion that these toxins did not only (or primarily) evolve to target the host, but instead increase competitiveness of the producers as colonizers of the gastrointestinal tract.

The evidence that other gut bacteria have the capacity to mimic GM1 gangliosides and that AB_5 toxins may influence these species has other implications for human health. As mentioned above, ganglioside mimicry is closely linked to the development of GBS, but not all persons infected with GM1-mimicking *C. jejuni* develop the disease. It is

possible that other ganglioside-mimicking bacteria could be present in our gut or appear transiently through ingestion of poultry products and could impact individual disease susceptibility by either immune tolerizing or training. Further studies into the extent to which other bacteria presenting these antigens contribute to the manifestation of GBS are warranted. It is also relevant that CTB is currently administered as part of an increasing number of health-promoting strategies including use in the oral cholera vaccine, as a toxoid adjuvant (with unexpected cross-reactivity to the *C. jejuni* major outer membrane protein (299)), and recently as an anti-inflammatory agent for treatment of diseases such as diabetes mellitus and atherosclerosis (300). Taken together, our studies identify a new role for AB_5 toxins and may explain why some organisms have developed mechanisms to vary their ganglioside mimics. We demonstrate that the chicken gut is rich in ganglioside structures derived from the host and the resident microbiota may impact both bacterial competition and human health.

Methods

Bacterial strains and growth conditions

The *C. jejuni* strains used in this study were grown on NZCYM agar (Difco) under microaerobic conditions (85% N2, 10% CO2 and 5% O2) at 37 °C. The *E. coli* strains were grown on LB agar under atmospheric conditions at 37 °C. Mutant strains were grown in media supplemented with ampicillin (50 μg mL^{-1}) and/or kanamycin (25 μg mL^{-1}). Table 2.1 lists the bacterial strains used in this study along with their sources.

To create the C. jejuni 11168 *ΔcgtB* mutant, primers cgtB-mut-F-XhoI and cgtB-mut-R-SacI (Table 2.3) were used to PCR-amplify the *cgtB* gene from *C. jejuni* 11168. The fragment was then ligated into pGEM®-T Easy Vector (Promega) and primers InvPCR-

cgtB-F-BamHI and InvPCR-cgtB-R-BamHI (Table 2.3) were used to perform inverse PCR to introduce a BamHI site into *cgtB*. The kanamycin cassette was isolated from the pMW2 plasmid by BamHI digest and inserted into *cgtB*. In the case of the *ΔneuC1* mutant, primers neuC1F15 and neuC1R984 (Table 2.3) were used to amplify the gene out of *C. jejuni* 11168. The PCR product was ligated into pPCR-Script Amp and a kanamycin resistance cassette from pILL600 was inserted into the NdeI restriction site present within the gene. Next, for both mutants, *C. jejuni* 11168 cells were grown on kanamycin (50 μg mL^{-1}) selective agar. The resulting colonies were evaluated for insertion of the kanamycin cassette by PCR and sequencing. For the *ΔcmeA* mutant, plasmid pET22b Cf-CmeA55 was linearized using SpeI and blunt-ended with T4 DNA polymerase. The cat cassette was obtained from plasmid pRY109 after SmaI digestion. After ligation, the correct orientation of the cassette in *cmeA* was confirmed by sequencing of candidate plasmids with primers CmeA-F and CmeA-R (Table 2.3). These primers were then used to amplify *cmeA*::cat by PCR. The purified PCR product was used to transform strain 11168 by natural transformation. Cm^R clones were analyzed by PCR for the correct insertion of the cassette into the chromosome with CmeA-os-R and CmeA-os-F (Table 2.3). Absence of CmeA in the mutant was also confirmed by western blotting with CmeA-specific antibodies.

Immunogold labeling and transmission electron microscopy

Following growth of *C. jejuni* or *E. coli* overnight, cells were harvested in NZCYM or LB broth, respectively, and their optical density at 600 nm (OD_{600}) was adjusted to 0.5 for *C. jejuni* or 1.0 for *E. coli*. Then, 2 μL of CTB (1 mg mL−1, Sigma) was added to 2 mL of each cell suspension. The suspensions were incubated under normal growth conditions for each organism for 1 h and then centrifuged at 6,000 × g for 4 min Cell pellets were

washed and resuspended in PBS. Immunogold labeling and transmission electron microscopy were carried out as described in previous reports with minor modifications (301, 302). Briefly, Formvar-coated copper grid was floated on top of the cell suspension for 1 h. Grids were then floated on blocking solution (PBS with 5% bovine serum albumin) for 1 h to block, followed by 1:50 rabbit α-CT antibodies (Fitzgerald Industries International) (in blocking solution) for 1 h, and goat α-rabbit IgG conjugated to 10-nm gold particles (BB International, diluted 1:50 in blocking solution) for 2 h, washing 3 times in blocking solution after each step. The grids were then examined by transmission electron microscopy (Philips Morgagni 268; FEI Company) and images were taken using a charge-coupled camera and controller (Gatan) and processed using DigitalMicrograph (Gatan).

Bacterial clearance assay

The effect of the holotoxins and toxin subunits on bacterial growth was examined by spotting CT, CTA, CTB or LTB onto cell-containing double layer agar plates prepared using the standard overlay agar method commonly used in bacteriophage plaque assays (69). *C. jejuni* HS:19, 11168, and HS:3 strains or *E. coli* CWG 308 and CWG308 pGM1a/pCst were grown overnight and harvested in NZCYM or LB broth and adjusted to an OD_{600} of 0.1. Then, 200 µL of this suspension was mixed with 5 mL of 0.6% molten NZCYM or LB agar and poured onto a previously solidified and pre-warmed NZCYM or LB agar plate containing 1.5% agar. The molten agar layer was allowed to solidify at RT for 15 min and then 2–5 µL of toxin (1 mg mL^{-1}), or toxin mixed 1:1 with competitive binding glycan (both at 1 mg mL^{-1}) in the case of competitive inhibition assays, was spotted onto the agar surface. For the concentration determination assay, CTB was diluted with Milli-Q H2O to contain 5, 1, 0.5, or 0.25 µg in 5 µL spotted onto *C. jejuni* HS:19.

These plates were incubated agar-side-down for 18–24 h under normal growth conditions as described above and imaged using a GO21 camera connected to an Olympus SZX16 stereoscope.

Scanning electron microscopy

Following a clearance assay with CTB on *C. jejuni* HS:19 as described above, agar squares were excised from inside, outside or at the interface of the clearance zones and prepared using the following established protocol (301). The squares were excised using a scalpel and trimmed to leave only the top layer of agar (about 2 mm) and then incubated in scanning electron microscopy (SEM) fixative (2.5% glutaraldehyde; 2% paraformaldehyde in 0.1 M phosphate buffer) overnight at 4 °C. Excised squares were then washed in 0.1 M phosphate buffer three times for 10 min and dehydrated using a series of 15 min washes: 50% ethanol, 70% ethanol, 90% ethanol, 100% ethanol, ethanol: hexamethyldisilazane (HMDS) 75:25, ethanol:HMDS 50:50, ethanol:HMDS 25:75 and 100% HMDS. After leaving HMDS to evaporate overnight, the excised squares were mounted onto SEM stubs and sputter-coated with the Hummer sputtering system (Anatech Ltd.). The squares were then imaged using the Phillips/FEI (XL30) scanning electron microscope (Philips/FEI) with an electron beam energy of 20 kV.

Isolation of *C. jejuni* LOS from clearance zones

Following a clearance assay with CTB or LTB, sections of agar were excised using a scalpel from either inside or outside the observed clearance zone, and the agar sections were incubated for 15 min at RT to elute the embedded cells. The eluate was then transferred to a new tube and centrifuged at 6000 × g for 4 min to collect the cells. The pellet was resuspended in 100 µL of PBS, spread onto NZCYM plates and incubated under

microaerobic conditions at 37 °C overnight. The cells were then harvested in 500 µL PBS, centrifuged at 18,300 × g for 90 s and resuspended in 50 µL sample buffer (100 mM Tris-Cl (pH 8.0), 2% β-mercaptoethanol, 4% SDS, 0.2% bromophenol blue, 0.2% xylene cyanol, 20% glycerol). This mixture was boiled for 10 min at 95 °C and cooled to RT before adding 47.5 µL additional sample buffer with 2.5 µL proteinase K (20 mg mL^{-1}) and incubating overnight at 37 °C. The following day, the proteinase K was inactivated by heating to 65 °C for 1 h and the samples were either loaded directly onto an SDS-PAGE gel or stored at −20 °C.

Silver staining of LOS

After isolation of LOS, the samples were separated by SDS-PAGE using 15% SDS-PAGE. The gel was then silver-stained according to the method described by Tsai and Frasch (1982) with a few modifications (303). The separated gels were immediately immersed in fixing solution (55% Milli-Q H_2O, 40% ethanol, 5% acetic acid) and incubated for at least 1.5 h. The gels were then rinsed 4 times and washed twice for 5 min in Milli-Q H_2O before being placed in oxidizing solution (fixing solution with 0.7% periodic acid) for 10 min After rinsing 4 times and washing twice for 5 min in Milli-Q H_2O, the gels were immersed in pre-stain solution (18.67 mM NaOH, 1.3% NH_4OH in Milli-Q H_2O) for 10 min, then stained with staining solution (pre-stain solution with 39.2 mM silver nitrate). Following 4 rinses and 2 washes for 10 min in Milli-Q H_2O, development was done using the BioRad Silver Stain Developer as directed and development was stopped by adding stopping solution (5% acetic acid in Milli-Q H_2O).

Far western blot of LOS and *cgtB* sequencing

After isolation of the LOS as described above, the samples were separated by SDS-PAGE and the gel was transferred to a PVDF membrane overnight at 30 V at 4 °C. The membrane was then blocked with 5% skim milk/PBST for 1 h, probed with CTB (1:100,000) for 1 h, washed 3 × 10 min in PBST, probed with rabbit α-CT antibodies (1:6,500) for 1 h, washed 3 × 10 min PBST, and probed with goat α-rabbit-HRP antibodies (1:20,000) for 1 h. The membrane was developed using a chemiluminescent substrate mix (Western LightningTM Plus-ECL from PerkinElmer) and images were captured using X-ray development film (Kodak).

Cells were isolated from inside and outside the clearance zones of agar using the same method as was described for the isolation of LOS. For DNA isolation, once the isolated *C. jejuni* 11168 cells were grown on NZCYM, cells were resuspended in 500 µL of TE Buffer (10 mM Tris- HCL pH 8.0, 0.1 mM EDTA in Milli-Q H_2O) and centrifuged at 18,300 × g for 2 min. The pellet was resuspended in 0.2 mL Buffer TE and genomic DNA was isolated using the Genomic DNA Purification Kit (Fermentas) according to manufacturer's instructions. The *cgtB* gene was amplified using Vent polymerase (NEB) and the primers described by Linton *et al*. (97): DL39 and DL41 (Table 2.3). The resulting solution was purified using the GeneJETTM Gel Purification Kit (Fermentas) as instructed by the manufacturer. The purified PCR product was then sequenced using the reverse primer 1139R (Table 2.3) with sequencing services offered by the Molecular Biology Service Unit at the University of Alberta.

Ethidium bromide accumulation assay

The ethidium bromide (EtBr) accumulation assay was performed using the following established protocol (280). *C. jejuni* 11168 wildtype, *ΔcgtB, ΔcmeA, ΔneuC1* cells, as well as *E. coli* CWG 308 and pGM1/pCst were harvested from agar plates in PBS and adjusted to OD600 = 0.2. The cells were then incubated with CTB (50 μg mL^{-1}) for 30 min at 37 °C before adding EtBr to a final concentration of 1.875 μg mL^{-1}. The accumulation of EtBr was measured by relative fluorescence every 2 min over a total of 20 min using the Bio Tek Synergy H1 plate reader with an excitation wavelength of 530 nm and emission wavelength of 600 nm. This experiment included 7 biological replicates for 11168 wildtype, 4 for *ΔcgtB, ΔcmeA and ΔneuC1,* and 3 for both of the *E. coli* strains. Each biological replicate included 3 technical replicates.

***Galleria mellonella* infection assay**

The *Galleria mellonella* wax moth model was used as a model to assess *C. jejuni* virulence similar to what has previously been done (304). *C. jejuni* HS:19 was suspended in 10 mM $MgSO_4$ solution to an OD600 = 1.0 (~1.0 × 109). The cell suspensions were then mixed with either $MgSO_4$, or CTB to a final concentration of 50 μg mL^{-1}, and incubated for 4 h at 37 °C. Following this incubation, cell counts were verified by serial dilution plating and 5 μL of suspension or control $MgSO_4$ was injected into the hind leg of the wax moth larvae (Backwater Reptiles Inc.). The larvae were incubated at 37 °C for 5 days before counting the proportion of dead and alive moths. The *G. mellonella* incubation time coincides with growth curves established to determine time needed for *C. jejuni* HS:19 to cause mortality. This experiment included 3 biological replicates for both HS:19 and

HS:19 + CTB, 2 for $MgSO_4$ and 1 for CTB. Each biological replicate included 3 technical replicates.

Chicken studies

Commercial broiler chickens (Ross 308, Avigen) were obtained on the day of hatch from Lilydale, Edmonton. Upon arrival, birds were divided into groups with up to 9 chickens each. The birds were orally gavaged with PBS, PBS + CTB, or PBS + LTB initially on day 30, then again 8 h and 12 h later using 100 μg of toxin per 300 μL gavage. The birds were then euthanized on day 31 and both ceca were removed and processed immediately. All animal studies were carried out in accordance with the protocol approved by the Animal Care and Use Committee at the University of Alberta, protocol number AUP00003.

Fluorescence microscopy

Intact chicken ceca were soaked in fresh Carnoy's fixative (60% ethanol, 30% chloroform, 10% glacial acetic acid) for 2 h and then moved to 100% ethanol. They were then cut into appropriate sized cross-sections with a scalpel, anchored in tissue cassettes and stored in 70% ethanol prior to embedding. Paraffin embedding involved sequential ethanol dehydration steps: 1 h in 70% ethanol, 1 h in 90% ethanol, 1.5 h in 100% ethanol, 1.5 h in 100% ethanol, 1.25 h in ethanol:toluene (1:1), followed by 2 × 0.5 h in 100% toluene. The specimen was then put in two wax treatments for 2 h each and embedded the following morning in paraffin.

Immunofluorescent staining of the paraffin-embedded sections was conducted using the following established protocols (305). Tissue sections were deparaffinized using 5 min washes in xylene (4×), 100% ethanol (2×), 95% ethanol, 70% ethanol and dH_2O.

Antigen retrieval was performed by steaming slides for 30 min in sodium citrate buffer (10 mM Sodium Citrate, 0.05% Tween 20, pH 6.0). Slides were blocked for 1 h using blocking buffer (PBS containing: 0.2% Triton X-100, 0.05% Tween, 1% bovine serum albumin, 5% donkey serum). Where indicated, slides were treated with α1-2-fucosidase (NEB, P0724S) following antigen retrieval in sodium citrate buffer, but prior to blocking with donkey serum buffer. Slides were treated for 1 h, with 1 µl (20 units) of α1-2-fucosidase in 10 µl of 1× Glycobuffer (supplied by the manufacturer), at 37 °C, followed by a PBS wash. Each slide was then treated with CTB (1 mM, Sigma, Cat. No. C9903) for 1 h, followed by either α-CTB antibody (1:100) or α-GM1 antibody (1:100, Abcam) for 1 h. Slides were visualized using Alexa Fluor 488-conjugated donkey α-rabbit IgG (1:1000, Invitrogen). The tissues were mounted using ProLong Gold antifade reagent containing DAPI (Invitrogen). The stained slides were viewed using a Zeiss AxioImager Z1, and photographed using an AxioCam HRm camera with AxioVision software.

Whole cell surface staining of GM1 pull-down candidates was performed as follows: isolated bacteria were harvested from their respective growth media and adjusted to OD600 = 1.0. Cells from 100 µl were pelleted by centrifugation (1 min, 13,000 rpm), suspended in 1 ml blocking solution (PBS, 5% skim milk) and incubated on ice for 30 min Cells were subsequently probed with either α-GM1 (1:1000 in PBS; Abcam, Cat. No. 23943) or CTB (1 mM) in combination with α-CTB (1:1000 in PBS; Biorad, Cat. No. 2060–0020) and Alexa Flour-488 conjugated α-rabbit antiserum (1:500 in PBS; Invitrogen, Cat # A-11008). Each incubation was done on ice for 20–30 min and three washes with 1 ml PBS were performed in between antibody incubations. Cells were counterstained with

DAPI (1 $\mu g\, mL^{-1}$), mounted on glass slides and analyzed on a DeltaVision fluorescent microscope equipped with a sCMOS camera.

16S rRNA sequence analysis of chicken ceca

DNA isolation and 16S rRNA tag sequence analysis of bacterial DNA isolated from chicken cecal samples was performed using the following established protocol (306). DNA was amplified using the 926F and 1392R universal primers (Table 2.3) that target the V6 to V8 region of the 16S ribosomal RNA gene. The PCR conditions used are described in 16S Metagenomic Sequencing Library Preparation (Illumina®, San Diego, CA). Sequencing of the 16S rRNA gene was completed with an Illumina MiSeq Sequencer using MiSeq Reagent kit V3 (Illumina). Reads were trimmed to 290 bp with the FASTX-Toolkit (http://hannonlab.cshl.edu/fastx_toolkit/), and paired-end reads were merged with the merge-illumina-pairs application (https://github.com/meren/illumina-utils/). Sequences between 440 and 470 nucleotides long were selected for analysis. To standardize the sequencing depth across samples, sequences were subsampled to 45,000 reads using Mothur v.1.35.1. Subsequently, USEARCH v8.1.1861 was used to generate operational taxonomic units (OTUs) with a 98% similarity cut-off. OTU generation included the removal of putative chimeras identified against the Gold reference database, in addition to the chimera removal inherent to the OTU clustering step in UPARSE. The resulting reads were assigned to different taxonomic levels from Phylum to Genus using a parallelized version of CLASSIFIER (rdp_classifier_v2.10.1) from the Ribosomal Database Project (RDP). Taxonomic assignment for the OTUs was obtained using the "Identify" function in EZbiocloud (307). Sequences whose identity was lower than 97% were classified using the Classifier and SeqMatch functions in Ribosomal Database Project webpage (308, 309).

The number of reads in each taxonomic bin was normalized to the proportion of the total number of reads per each sample for statistical analyses. To achieve normality for the microbiome data that were not normally distributed, values were subjected to $\log_{10}$ transformations. Diversity analyses were done using MacQIIME version 1.9.1 (310).

Identification of GM1-mimicking bacteria from ceca

Chicken cecal contents were resuspended in PBS to a concentration of 1 mg mL^{-1}. To address non-specific binding, the mixture was further diluted 1:5 with PBS-T containing 2% skim milk and incubated in a gravity flow column with 500 µL protein G agarose (Sigma) for 10–15 min at room temperature. Samples were mixed every 2–3 min, the flow-through was collected and incubated with 5 µL of α-GM1 antibody on ice for 15 min, mixing regularly. The suspension was then passed through a gravity flow column containing 500 µL of protein G agarose. After two washes with PBS-T, 2% skim milk and PBS-T and one final wash with PBS (5 mL each), protein G agarose beads were recovered with 1 mL PBS and 50 µL of a 5-fold serial dilution series were plated on either Brain Heart infusion (BHI), De Man, Rogosa and Sharpe (MRS), or Yeast, Casitone-Fatty Acid (YCFA) agar. Plates were incubated microaerobically or anaerobically at 37 °C for up to 72 h. Colonies were picked, isolated and tested for GM1 ganglioside antibody reactivity by whole cell ELISA followed by GM1 and CTB binding by fluorescence microscopy. One GM1 and CTB-reactive bacterial species was further identified by 16S rRNA gene sequencing with oligonucleotides 926R, 515F, 1068F, 1391R, and 519R (Table 2.3) after PCR-amplification of the 16S rRNA gene from extracted DNA with oligonucleotides 27F and 1492R (Table 2.3).

GM1 antibody and lysis solution spot assay

These spot assays were performed in the same way as the others with minor changes. For the GM1 ganglioside antibody spot assay, 2 μL of the antibody (Abcam) or 2 μg of CTB was spotted directly onto the cells prior to growth. For the lysis buffer spot assay, 2 μL of lysis buffer (undiluted from Thermo Scientific GeneJET Plasmid Miniprep Kit) or 2 μg of CTB was spotted onto cells after growth for 24 h.

Statistics

For the EtBr accumulation and *Galleria mellonella* data, two-tailed, unpaired t-tests were performed to compare the relative fluorescence upon addition of EtBr, and *C. jejuni* HS:19 infection with and without CTB respectively. For microbiome analyses, two-tailed Mann Whitney tests were performed for the CTB dataset comparisons, while two-tailed unpaired t-tests with Welch's correction or multiple t-tests were performed for the LTB comparisons using Graph Pad Prism version 7. The Adonis PERMANOVA test was performed on NMDS plots using the statistical software R version 3.3.1 (http://www.r-project.org/).

Data availability

All relevant data are available from the corresponding author. The source data underlying Figures 2.4a-b, 5a-b and 7, and Figures 2.8c-d, 2.10 and 2.11 are provided as a Source Data file. The 16S rRNA datasets generated and analyzed during these studies are available in the NCBI SRA repository under BioProject PRJNA522915; the BioSamples accession numbers are listed in table 2.4.

Acknowledgements

We would like to thank Brandi Davis and Yee Ying Lock for preparation of samples for 16S rRNA sequencing, Arlene Oatway for help with preparing cecal samples for electron microscopy, the Molecular Biology Services Unit at the University of Alberta for performing the Sanger sequencing reactions and Drs. James and Adrienne Paton for providing us with their E. coli CWG 308 wildtype and pGM1/pCst strains. We also thank Dr. Xiaoming Bian and Dr. Hanwen Huang for statistical advice, Dr. Xiaorong Lin for the use of her stereoscope, and Dr. Stefan Pukatzki and Dr. Michel Gilbert for helpful discussions. This study was funded in part by fellowships to RTP from the Natural Sciences and Engineering Research Council of Canada and Alberta Innovates Health Solutions. C.M.S. is an Alberta Innovates Strategic Chair in Bacterial Glycomics. J.W. is a CAIP Chair in Nutrition, Microbes, and Gastrointestinal Health. B.A.V. is the CH.I.L.D. Foundation Chair in Pediatric Gastroenterology.

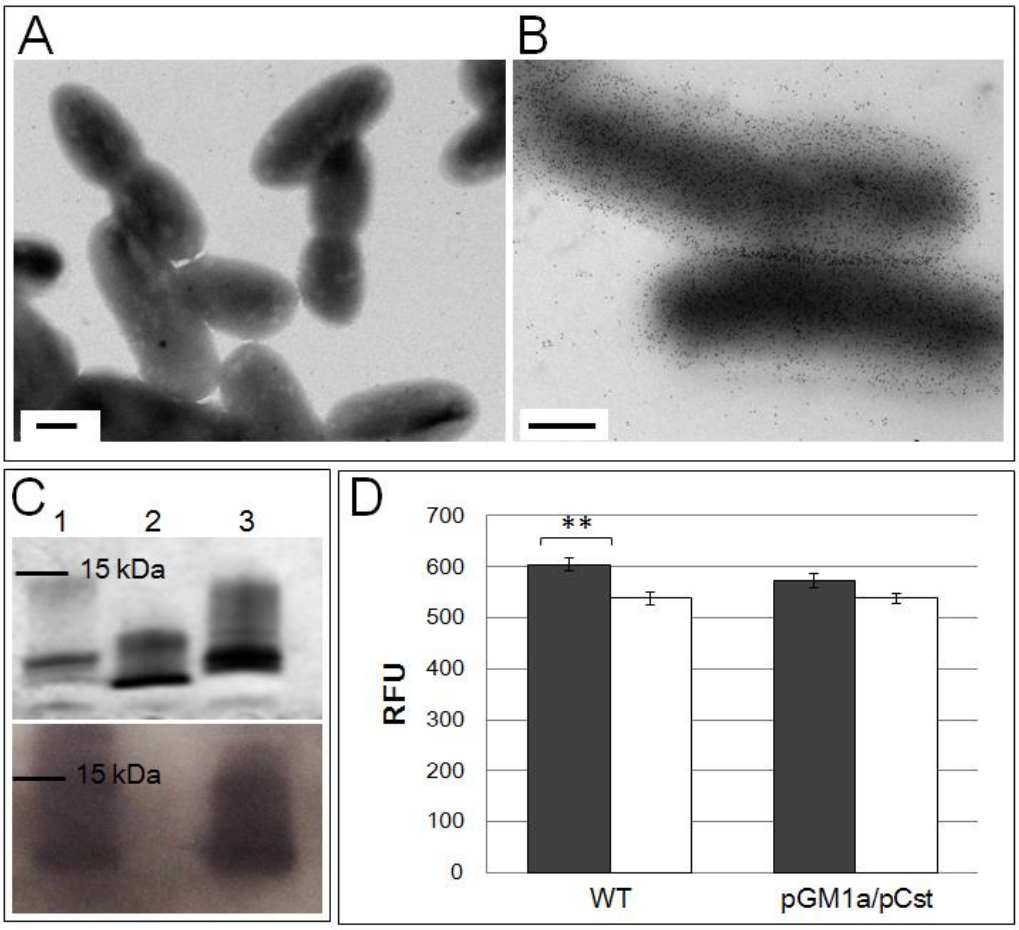

Figure 2.8. Cholera toxin B subunit (CTB) binds to *Escherichia coli* engineered to express GM1 ganglioside-mimicking lipooligosaccharides (LOS) but does not impact cell permeability. Transmission electron microscopy following immunogold labeling with CTB was performed on (A) wildtype *E. coli* CWG 308, and (B) *E. coli* CWG 308 expressing pGM1/pCst (scale bars are 0.5 μm). (C) Upper panel: Silver stain of LOS isolated from cells shown in A (lane 1), cells shown in B (lane 2), and from LOS isolated from *C. jejuni* HS:19 (lane 3); lower panel: far western blot of the same samples using CTB as a probe. (D) Each *E. coli* strain was incubated with ethidium bromide for 20 min following treatment with PBS (white) or CTB (grey) and their relative fluorescence was measured. Error bars represent standard error of the mean (**p=0.0015). Source data are provided as a Source Data file.

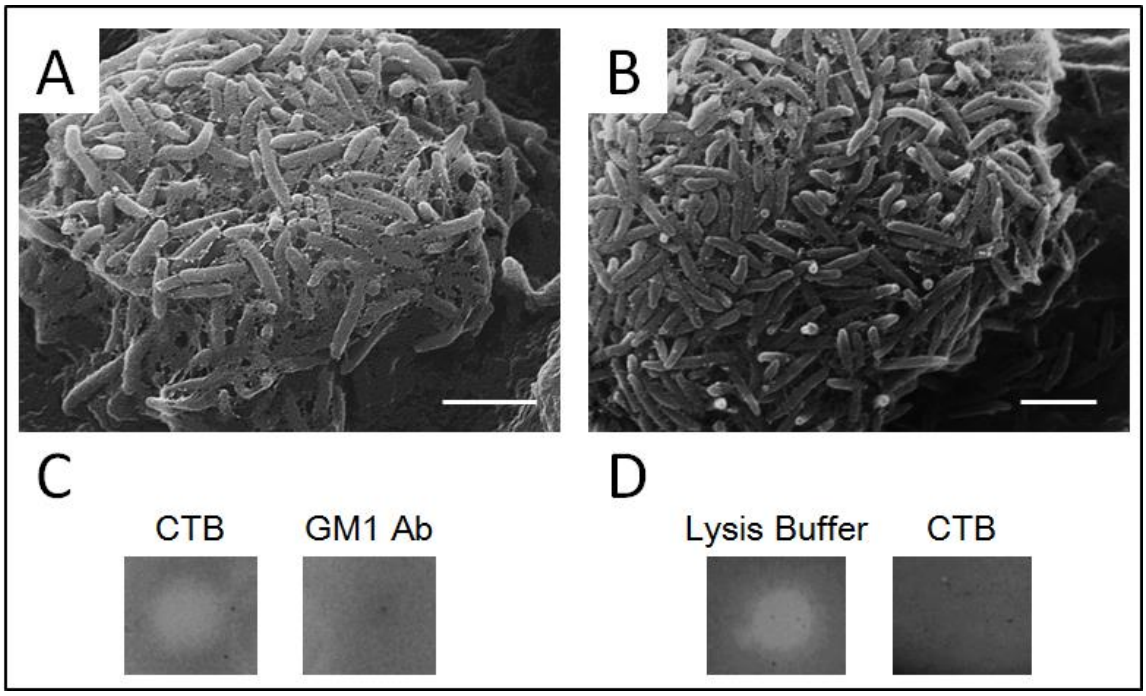

Figure 2.9. Cholera toxin B subunit (CTB) is bacteriostatic and not bactericidal to *C. jejuni* HS:19. Scanning electron micrographs show surface morphology of *C. jejuni* HS:19 within (A) or outside (B) of the CTB zone of clearance. Agar clearance assays show the effect of various agents spotted either before (C) or after overnight *C. jejuni* HS:19 growth in soft agar (D). Scale bars are 2 μm.

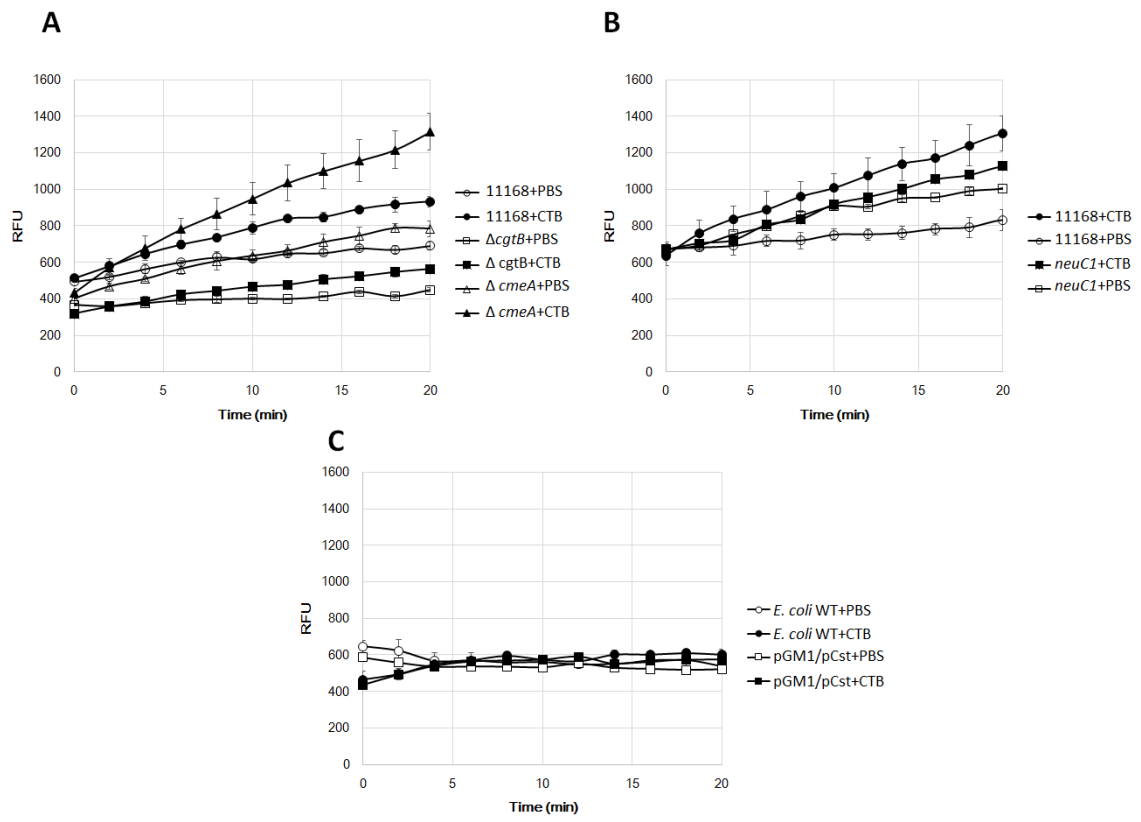

Figure 2.10. Graphs from representative experiments showing the relative fluorescence of bacterial strains following treatment with ethidium bromide. (A) *C. jejuni* 11168 wildtype, Δ*cgtB* and Δ*cmeA*, (B) *C. jejuni* 11168 and *ΔneuC1,* or (C) *E. coli* CWG 308 and *E. coli* CWG 308 expressing pGM1/pCst were incubated with ethidium bromide for 20 min following treatment with PBS (control) or CTB and the relative fluorescence was measured. Error bars represent standard deviation. Source data are provided as a Source Data file.

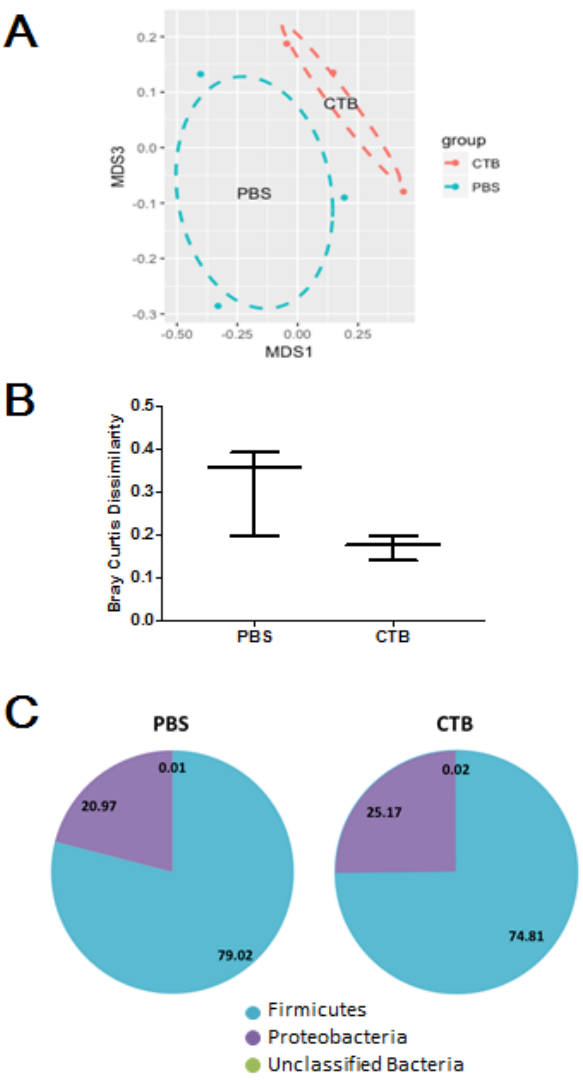

Figure 2.11. Administration of CTB toxin to chickens results in shifts in the intestinal microbiome resembling trends observed with LTB. A small scale chicken experiment was done introducing either CTB (n=3) or PBS (n=3) and monitoring the relative changes in microbiome composition. (A) NMDS plot based on Bray Curtis distances show that introduction of CTB causes a shift in the gut microbiome of chickens relative to chickens treated with PBS. (B) Similar to the effect of LTB in the chicken gut microbiome, LTB decreases β-diversity without affecting α-diversity. (C) The toxin causes decreases in the relative abundance of Firmicutes with parallel increases in Proteobacteria. Statistical analyses: Adonis PERMANOVA test for A, Mann-Whitney test for B and C. Source data are provided as a Source Data file.

Table 2.3. A list of primers used in this study

Primer name	Sequence (5'-3')	Use
cgtB-mut-F-XhoI	ATATCTCGAGGAGCTAAAATGAGTCAAATTTCCATC	*C. jejuni* 11168 Δ*cgtB*
cgtB-mut-R-SacI	ATATGAGCTCGTTATGAAATTTTTAATATCTTTACGG	
InvPCR-cgtB-F-BamHI	ATATGGATCCGGACAATGTGGGCTAAAATAATC	
InvPCR-cgtB-R-BamHI	ATATGGATCCGGATTTTTAGTTTTAAGTATTTGC	
neuC1F15	TTTTGTTAGCGGAACTAGAGCTGAT	*C. jejuni* 11168 *ΔneuC1*
neuC1R984	TAATACGACTCACTATAGGGATTTAAAATCGCTTCCAATATATCC	
CmeA-F	TTATTGTGCTCCAATTTCTTTAACTTC	*C. jejuni* 11168 *ΔcmeA*
CmeA-R	ATGAAATTATTTCAAAAAAATACTATTTTAG	
CmeA-os-R	TAGGAGGGGTTAAAGAAGGATATTG	
CmeA-os-F	TTTCTAAATGGAATCAATAGCT	
DL39	TTAAGAGCAAGATATGAAGGTG	*cgtB* gene sequencing
DL41	CCATTTGAATTGATATTTTTG	
primer 1139R	TTAGCCCACATTGTCCAAAA	
926F	AAACTYAAAKGAATWGRCGG	16S rRNA sequence analysis
1392R	ACGGGCGGTGWGTRC	
926R	ACCGCTTGTGCGGGCCC	
515F	GTGCCAGCMGCCGCGGTAA	
1068F	GCATGGCYGYCGTCAG	
1391R	GACGGGCGGTGTGTRCA	
519R	GWATTACCGCGGCKGCTG	
27F	AGAGTTTGATCCTGGCTCAG	
1492R	GGTTACCTTGTTACGACTT	

R=A or G, Y=C or T, W=A or T, K=G or T, M=A or C

Table 2.4. List of BioSample accession numbers for the 16S rRNA datasets.

Sample name	Accession number	Sample name	Accession number
454	SAMN10962775	467	SAMN10962788
455	SAMN10962776	468	SAMN10962789
456	SAMN10962777	469	SAMN10962790
457	SAMN10962778	470	SAMN10962791
458	SAMN10962779	471	SAMN10962792
459	SAMN10962780	472	SAMN10962793
460	SAMN10962781	301	SAMN10962794
461	SAMN10962782	302	SAMN10962795
462	SAMN10962783	303	SAMN10962796
463	SAMN10962784	304	SAMN10962797
464	SAMN10962785	305	SAMN10962798
465	SAMN10962786	306	SAMN10962799
466	SAMN10962787		

CHAPTER 3

LOW-DOSE EXPOSURE TO GANGLIOSIDE-MIMICKING BACTERIA TOLERIZES HUMAN MACROPHAGES TO GUILLAIN-BARRÉ SYNDROME-ASSOCIATED ANTIGENS.[7]

[7] **Robert T. Patry**, Lauren Essler, Frederick Quinn and Christine M. Szymanski. To be submitted to *PLOS Pathogens*.

Author Contributions: RTP and CMS designed the study with insight from LE. RTP screened infant cecal isolates for GM1 ganglioside mimicry. RTP and LE performed pro-inflammatory cytokine release assays. RTP purified LOS by hot water/phenol extraction and performed the silver stain and western blot on the product. LE prepared TLR2 and TR4 knock-down mutants using shRNA. RTP and LE generated THP-1 lysates and analyzed them by western blot. Paper was written by RTP and CMS with contributions from LE. FQ and CMS supervised the project.

Abstract

Early in life, commensal bacteria play a major role in the development of the immune system, helping to guide the host to respond to harmful stimuli, while tolerating harmless antigens, preventing autoimmunity. Guillain-Barré Syndrome (GBS) is an autoimmune disease where the body attacks ganglioside receptors on its own nerve cells, damaging them and resulting in paralysis. *Campylobacter jejuni* infections commonly precede GBS due to their ability to mimic human gangliosides with their lipooligosaccharide structures, stimulating the autoimmune response. In low and middle-income nations, young children are consistently exposed to *C. jejuni* and it is not known if this impacts their susceptibility to GBS later in life. In this study, we screened *Campylobacters* from 154 infant fecal samples for the ability to mimic GM1 ganglioside, finding that 23.4% were capable of mimicry and that these came from infants both symptomatic and asymptomatic for campylobacteriosis. Using a macrophage model, we then examined the effect of training with low doses of ganglioside-mimicking bacteria prior to challenge with GBS-associated antigens. This training caused decreased production of pro-inflammatory cytokines, suggesting tolerance induction. Short-hairpin RNA knock-downs of TLR2 and TLR4 suggested that these receptors are not involved in tolerance mediated by TNF-α or IL-6, but TLR4 appears to be involved in IL-1β-mediated tolerance. These results suggest that exposure to low-doses of ganglioside-mimicking bacteria could reduce susceptibility to GBS.

Introduction

Bacteria have been implicated in the development of proper immune function for decades. The original hygiene hypothesis proposed in 1989 suggested that as hygiene among the general population improved and families were having fewer children, the incidence of childhood infections would decline and children were no longer exposed to bacteria that prevent allergies (311). Since then, the importance that bacteria have in immune homeostasis has become increasingly apparent as these relationships are further explored. Humans are colonized by bacteria within moments of birth and the types of bacteria that they are exposed to during this stage of life have profound impacts on immune system development. The makeup of a child's intestinal microbiota is impacted by several factors including mode of birth (whether vaginal or by caesarean section), exposure to antibiotics, diet and dietary supplements, probiotics and environmental exposure (262). Disruptions in the composition of the microbiome early in development have clear consequences for future health (263-265). Healthy conditions influence a complex ecosystem of microbes that will help in programming the immune system to tolerate harmless antigens, preventing allergies and autoimmune diseases, while responding to markers associated with harmful infections (266). However, unhealthy conditions can lead to a dysbiotic microbiota, which later impacts susceptibility to infection (312) as well as many other conditions including: allergies (313, 314), asthma (314, 315), eczema (314), type I diabetes (316), type II diabetes (317), arthritis and other connective tissue diseases (318-320), inflammatory bowel disease (321, 322), immunodeficiencies (323), leukemia (324), and obesity (325).

An important example of how bacteria can induce tolerance of the host immune system is endotoxin tolerance. This phenomenon first reported by Watson and Kim 1963, describes that when immune cells are stimulated with lipopolysaccharide (LPS), they enter a temporary state where their immune responses are abrogated to subsequent challenges (326). In mice, it has been observed that when pups are delivered vaginally, their intestinal epithelial cells acquire endotoxin tolerance by being exposed to bacterial LPS immediately after birth (327). The same is not seen in pups delivered by caesarian section (327). It has long been noted that asthma incidence was lower in houses where dust contained increased amounts of LPS. This is the case for children that are raised on farms, who are shown to have reduced incidence of asthma and allergies inversely related to the level of LPS found in the dust, bedding and mattresses at their homes (328, 329). Bashir *et al*. 2004 also reported that mice which are TLR4 deficient are more susceptible to food allergy and a similar effect is observed for normal mice treated with broad-spectrum antibiotics shortly after birth, implicating TLR4 recognition of LPS as the likely cause of this phenomenon (330). These molecules can be responsible for preventing autoimmunity or the induction of autoimmune diseases, as is the case for *Campylobacter jejuni*-induced Guillain-Barré Syndrome (GBS).

GBS is reported as the most frequent cause of paralysis since the near-eradication of polio-myelitis and the disease is commonly associated with antecedent infections (35). The pathogen most commonly associated with the triggering of GBS is *C. jejuni*, implicated in at least 39% of cases (43, 46). *C. jejuni* induces the production of auto-reactive antibodies against ganglioside receptors abundantly found on peripheral motor neuron axons (41). These auto-reactive antibodies bind to these receptors and result in

complement activation, recruiting the membrane attack complex and subsequently damaging the neurons (41). *C. jejuni* possesses a lipooligosaccharide (LOS) that can mimic various human gangliosides, leading to the induction of this autoimmune reaction following infection (77). It is estimated that 60% of *C. jejuni* strains can produce these mimics (47) and that 0.1% of *C. jejuni* infections result in GBS (53, 54). One serotype commonly associated with this disease is HS:19, likely due to its ability to display two different GBS-associated ganglioside mimics on its surface simultaneously (GM1 and GD1a) (331). Previous studies have found that patients often produce antibodies that recognize ganglioside complexes in addition to individual gangliosides (332, 333). The ability of HS:19 to display both gangliosides simultaneously allows for production of autoreactive antibodies against both GM1 and GD1a antibodies as well as a combined complex of the two.

C. jejuni is among the primary causes of bacterial diarrhea in the world, impacting both developed and developing nations. However, in low- to middle-income countries (LMICs), the pathogen is associated with a high incidence of childhood mortality (183, 334). In these nations, the most common sources of *C. jejuni* are contaminated food and water, and those most susceptible to campylobacteriosis are children under the age of two (20). Importantly, it is also common for these children to be transiently exposed to *C. jejuni* and shed the bacterium, but not experience disease symptoms (20). The Global Enteric Multicenter Study (GEMS) was designed to investigate the causes and impact of diarrheal disease in LMICs for children up to five years of age (184). This study collected samples from four countries in sub-Saharan Africa (The Gambia, Kenya, Mali and Mozambique) and three in South Asia (Bangladesh, India and Pakistan) (184).

We received all *Campylobacter* isolates collected from the GEMS fecal samples collected from infants under the age of one that were either exclusively breastfed or not (193). In this study, we analyze these isolates of *C. jejuni* to determine the proportion of infants colonized with strains capable of mimicking GM1 ganglioside, which would result in exposure to this antigen during the life stage critical for development of immune tolerance to antigens. Following this analysis, we used a human macrophage model to show that it is possible to reduce the pro-inflammatory cytokine response to *C. jejuni* HS:19 whole cells by first exposing immune cells to lower doses of bacteria with similar lipooligosaccharide structures.

Results

Infant fecal *Campylobacter* GM1 ganglioside mimic screen

This screen involved isolates collected from the feces of 154 *Campylobacter*-infected infants under one year of age. The samples were collected from seven different nations (The Gambia, Kenya, Mali, Mozambique, Bangladesh, India and Pakistan) and came from infants that experienced symptomatic *Campylobacter* infections as well as those that were asymptomatic (i.e., positive for the pathogen without experiencing campylobacteriosis). More information regarding each sample is listed in Table 3.1. Of the 154 isolates, 86 were from symptomatic and 68 were from asymptomatic individuals. LOS was isolated from each of these samples and examined for GM1 ganglioside mimicry using the cholera toxin B subunit (CTB) as a probe for this structure (Figure 3.1C). We and others have used the toxin for this purpose due to its ability to bind the GM1 ganglioside mimics found in *Campylobacter* LOS as previously described (6). Microscopy with CTB was also used to confirm the binding in some of the samples (Figure 3.1D). For these experiments,

C. jejuni HS:19 was used as a positive control and HS:3 (cannot produce ganglioside mimics and does not bind CTB (6, 47)) as a negative control (Figure 3.2). In total, 36 of the 154 isolates (23.4%) were positive for GM1 ganglioside mimics and of these, 18 came from symptomatic and 18 were from asymptomatic infants (Figure 3.1A). It is also important to note that the GM1-positive isolates originated from all of the nations involved in the study showing that their presence was not concentrated at a particular site (Table 3.1). These data show that infants can be exposed to ganglioside-mimicking bacteria early in life and that bacterial presence may not be accompanied by gastroenteritis from an inflammatory response.

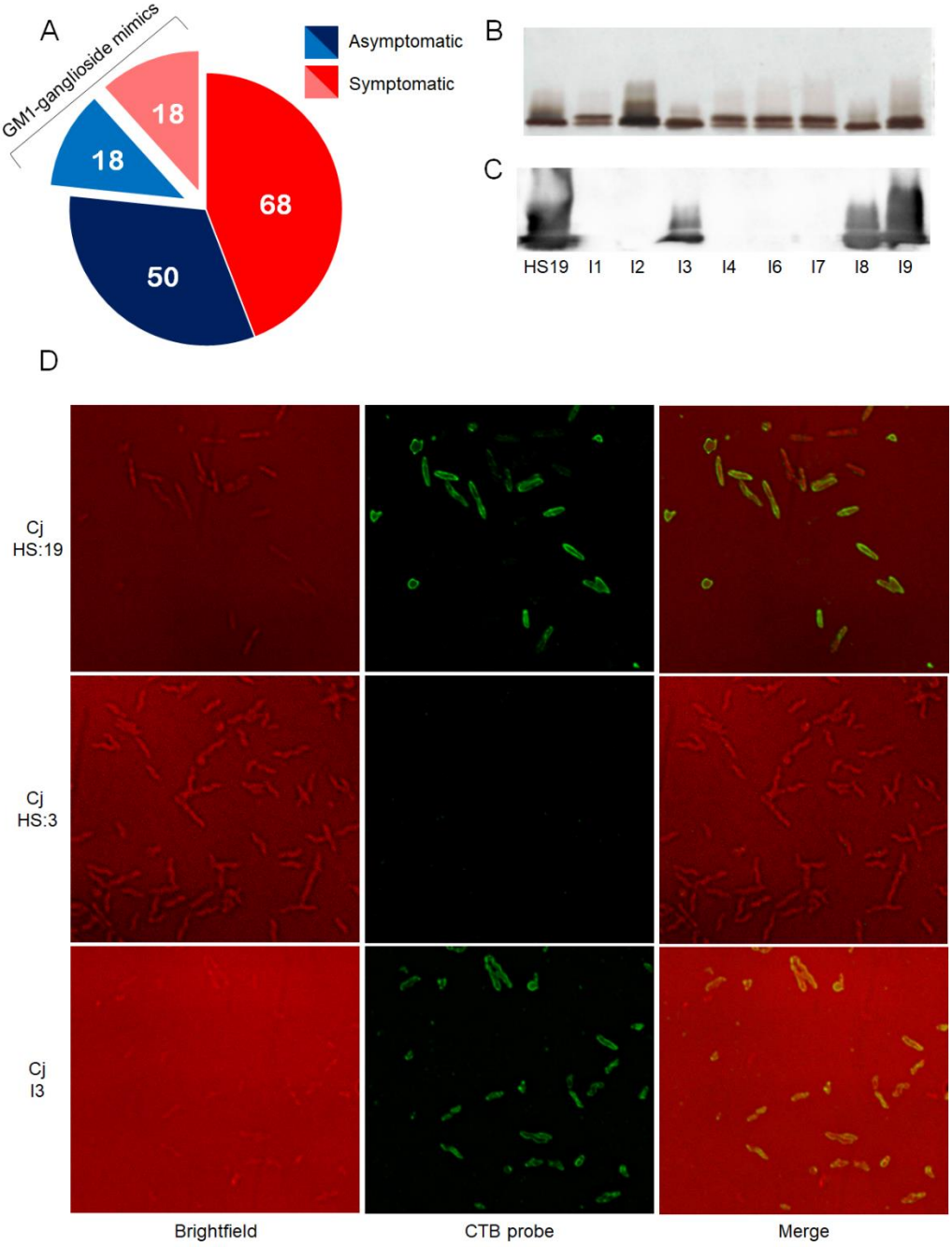

Figure 3.1. Infants in low and middle-income countries are exposed to GM1 ganglioside-mimicking *C. jejuni*. A) A pie chart of infant *Campylobacter* isolates separated by symptoms and highlighting GM1 ganglioside mimic positive samples. B) Example silver stain of LOS from *Campylobacter* isolates, C) corresponding western blot using cholera toxin B subunit as a probe, and D) an example of fluorescence microscopy done on GM1-positive isolate, *C. jejuni* I3, using a CTB probe with *C. jejuni* HS:19 as a positive control and *C. jejuni* HS:3 as a negative control. Images taken using a microscope set to 1000x magnification.

Training with GM1 ganglioside-mimicking bacteria induces tolerance to challenge with GBS-associated antigen in macrophages

In order to assess the influence of prior exposure to ganglioside-mimicking bacteria on subsequent challenge with bacteria displaying GBS-associated antigens, the human leukemia monocytic THP-1 cell line was differentiated into macrophages in the presence or absence of ganglioside-mimicking bacteria at several low multiplicities of infection (MOI) between 0.001 and 1.0. After this training stage, the macrophages were challenged with high doses of ganglioside-mimicking bacteria known to be capable of causing GBS (*C. jejuni* HS:19 at MOI 5). The bacteria used to train these cells were either *C. jejuni* HS:19, *E. coli* CWG308 pCst/pGM1a (*E. coli* GM1) that is engineered to display the same mimics as *C. jejuni* HS:19 on a truncated lipopolysaccharide (LPS) or *E. coli* CWG308 wildtype (*E. coli* WT), the parent strain of the engineered *E. coli* displaying a truncated LPS with no mimic present (Figure 3.2). After challenge, the extent of the inflammatory immune response was determined by measuring the concentration of several pro-inflammatory cytokines produced in the supernatant of the macrophage cell culture. As a proof of principle, this experiment was first attempted using purified LPS in place of intact bacteria at concentrations previously used for tolerance (335) and stimulation (336) of pro-inflammatory responses for both training and challenging respectively. A downward trend in production of IL-1β following training supported that endotoxin-based tolerance could be observed in this model using our conditions and allowed us to move forward using intact cells (Figure 3.5).

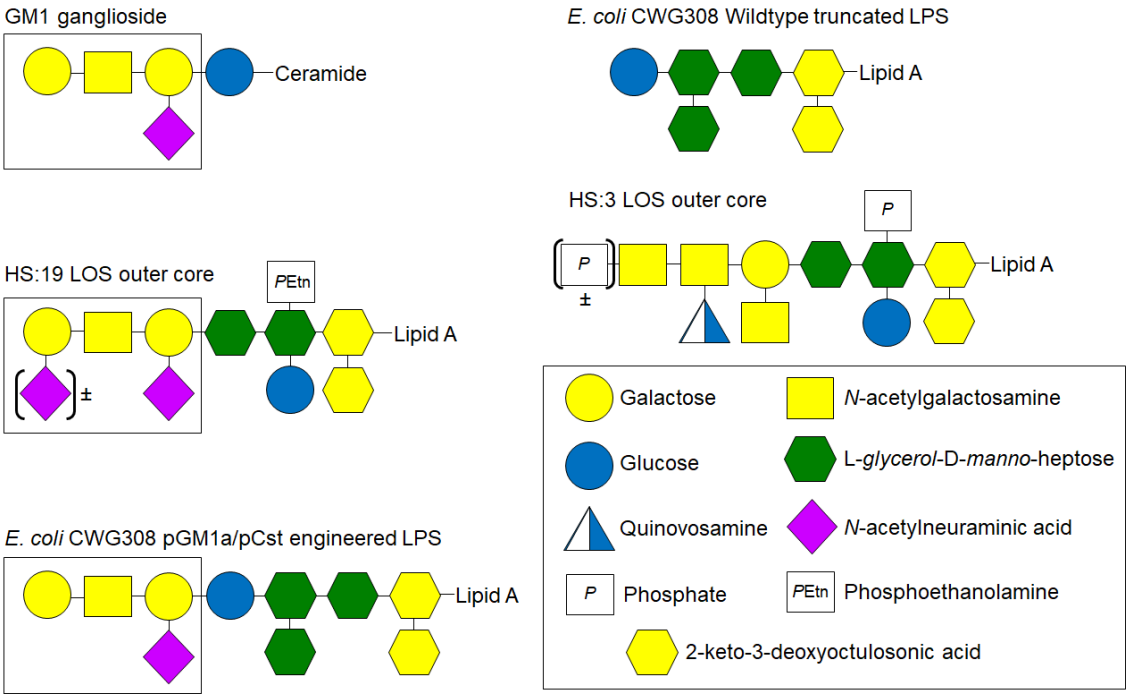

Figure 3.2. Lipooligosaccharide structures of strains described in this study. The portion of each molecule that mimics GM1 ganglioside is encompassed by a box in addition to the ganglioside itself.

When examining the impact of this training on the release of proinflammatory cytokines, it is shown that exposure to low MOI of both *C. jejuni* HS:19 and *E. coli* GM1 resulted in a decrease in TNF-α production when compared as a ratio with the untrained control (Figure 3.3A). This was true when the MOI of *C. jejuni* was 0.01 (p =0.0350), 0.1 (p =0.00590) or 1.0 (p =0.0296) and MOI of *E. coli* GM1 was 0.001 (p =0.00380) or 0.01 ($p < 0.0001$) (Figure 3.3A). The decrease in TNF-α production was even more pronounced in the *E. coli* GM1 group when accounting for the cytokine released in response to the training stimulus alone. This comparison was examined by measuring the cytokine production of macrophages that were trained in the same way but left unchallenged instead of receiving *C. jejuni* HS:19 at high dose (raw data shown in Figure 3.6). The resulting values were then subtracted from those obtained in the challenged groups, yielding statistically significant differences for *E. coli* GM1 at training MOIs of 0.001 (p =0.0001),

0.01 (p <0.0001) and 0.1 (p <0.0001) (Figure 3.3B). No statistically significant difference was observed in either case when the GM1 ganglioside mimic was absent using *E. coli* WT at the same MOI (Figure 3.3A and B).

Similar results were observed when examining two other pro-inflammatory cytokines IL-6 and IL-1β. For both cytokines, training with *C. jejuni* HS:19 or *E. coli* GM1 was accompanied by a downward trend compared to the untrained control (Figure 3.3C-F). However, for these experiments, not all these differences were significant. For fold change in IL-6 production, significant differences were seen for *C. jejuni* HS:19 at a MOI of 0.1 (p =0.0478) and *E. coli* GM1 at a MOI of 0.01 (p =0.0102) (Figure 3C). The same was observed when the background IL-6 produced against the training organism was subtracted, where *C. jejuni* HS:19 at a MOI of 0.1 (p =0.0485) and *E. coli* GM1 at a MOI of 0.01 (p =0.0025) were significant (Figure 3D). In the case of IL-1β, the downward trend in production was significant for *C. jejuni* HS:19 at a MOI of 1.0 (p = 0.0230) and *E. coli* GM1 at a MOI of 0.01 (p = 0.0017) (Figure 3E). When the IL-1β response by unchallenged macrophages was subtracted, this decrease was again significant for *C. jejuni* HS:19 at a MOI of 1.0 (p =0.0194) and the difference for *E. coli* GM1 were all statistically significant with MOIs of 0.001 (p =0.0039), 0.01 (p <0.0001) and 0.1 (p <0.0001) (Figure 3F). As with TNF-α, training with *E. coli* WT did not impact the amount of IL-6 or IL-1β released when compared to an untrained control (Figure 3C-F). Taken together, these results show that training of macrophages with low MOI of GM1 ganglioside-mimicking bacteria can cause a decrease in the magnitude of pro-inflammatory responses directed at that same antigen in subsequent exposures. It also suggests that this effect is even more pronounced

when training with *E. coli* GM1 than with the same bacteria that will be used for the challenge.

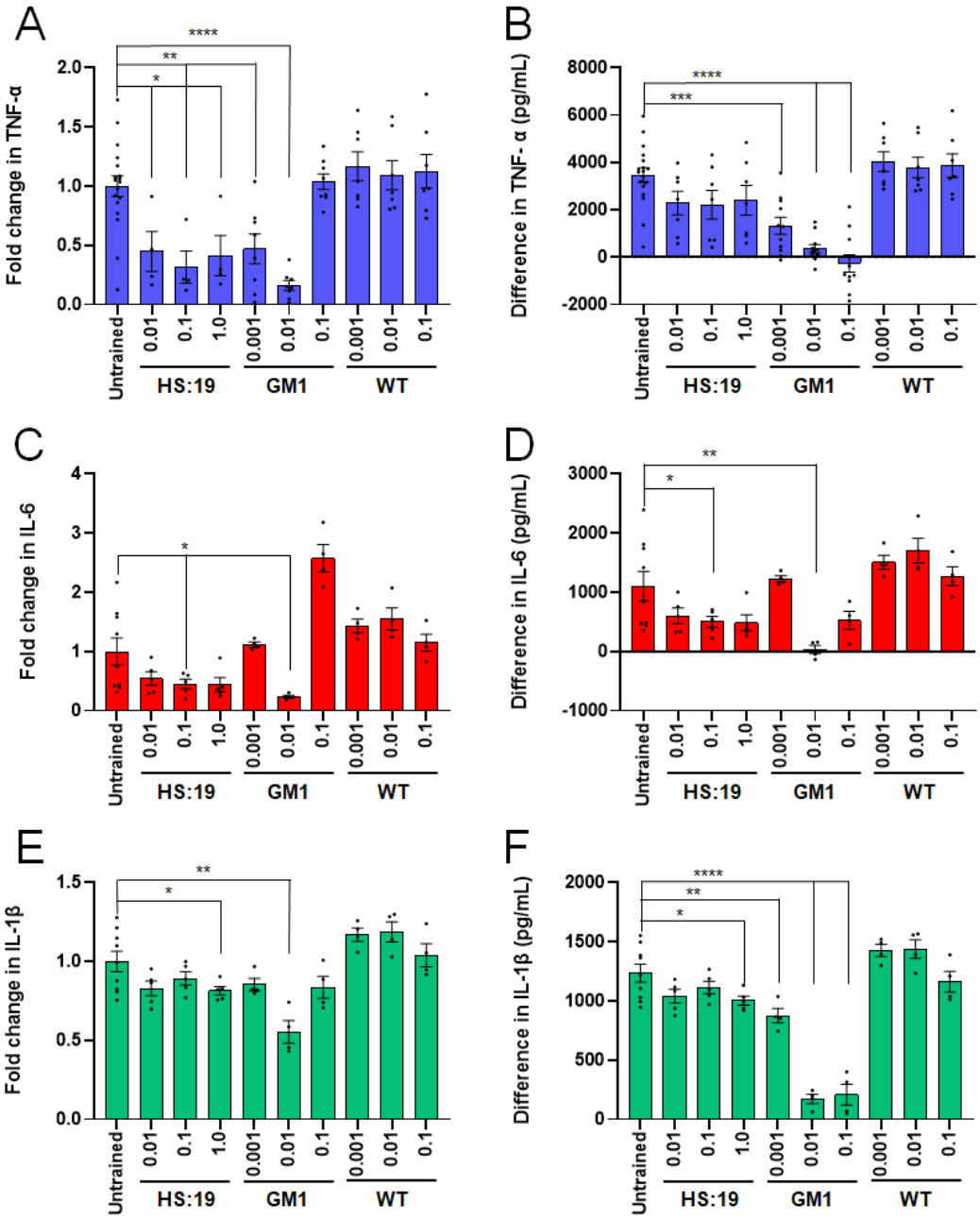

Figure 3.3. Training with *C. jejuni* HS:19 or *E. coli* GM1 prior to challenge with *C. jejuni* HS:19 causes reduction in macrophage pro-inflammatory cytokine responses. This effect is displayed in graphs representing release of pro-inflammatory cytokines after training macrophages with *C. jejuni* HS:19 (HS:19), *E. coli* GM1 (GM1) or *E. coli* WT (WT) at the indicated multiplicities of infection (MOI) and subsequently challenging with *C. jejuni* HS:19 at an MOI of 5. The graphs show fold changes in cytokine release compared to untrained controls (A, C, E) and the direct measurement of cytokines released after subtracting values for macrophages trained in parallel, but left unchallenged (B, D, F). The pro-inflammatory cytokines measured were TNF-α (A, B), IL-6 (C, D) and IL-1β (E, F). ****p-value < 0.0001, ***p-value ≤ 0.001, **p-value ≤ 0.01, *p-value ≤ 0.05 determined by two-tailed t-test from experiments repeated 4-18 times.

Tolerance experiments using Toll-like receptor 2 and Toll-like receptor 4 knockdowns suggest alternative signaling involved

Once we discovered that GM1-ganglioside mimicking bacteria can tolerize macrophages to subsequent challenge with high doses of *C. jejuni* HS:19, the next step was to determine the mechanism for this decrease in inflammatory response. To test this, the genes responsible for toll-like receptor (TLR) 2 and TLR4 in the macrophages were silenced using lentiviral short hairpin RNA (shRNA) specific to these genes and compared to non-specific scramble lentiviral shRNA as a negative control. When trained with *E. coli* GM1 or *E. coli* WT and challenged with *C. jejuni* HS:19, the cells treated with scramble shRNA (ShScram) again displayed a tolerance trend following *E. coli* GM1 training that was not seen with *E. coli* WT training. This was the case for TNF-α with an MOI of 0.01 (Figure 3.4A), IL-6 with an MOI of 0.001 (Figure 3.4B) and IL-1β with an MOI of 0.001 (Figure 3.4C). For the macrophages treated with TLR2-specific shRNA (ShTLR2), a similar pattern of tolerance was shown, replicating what was seen in the ShScram control for TNF-α, IL-6 and IL-1β. Interestingly however, production of all three cytokines in the ShTLR2 macrophages showed a lower trend than what was observed in the ShScram cells. Finally, for cells treated with shRNA specific to TLR4 (ShTLR4), the results for TNF-α and IL-6 were also similar to the ShScram cells, with tolerance trends seen in the same training MOIs of *E. coli* GM1. However, in the case of IL-1β, production of the cytokine showed no downward trend when trained with *E. coli* GM1 at any MOI, suggesting that TLR4 is involved in the tolerance observed by IL-1β production. It is important to note that there were not enough biological replicates of this experiment to detect small but

statistically significant effects, so more replicates may be required to make further well supported claims.

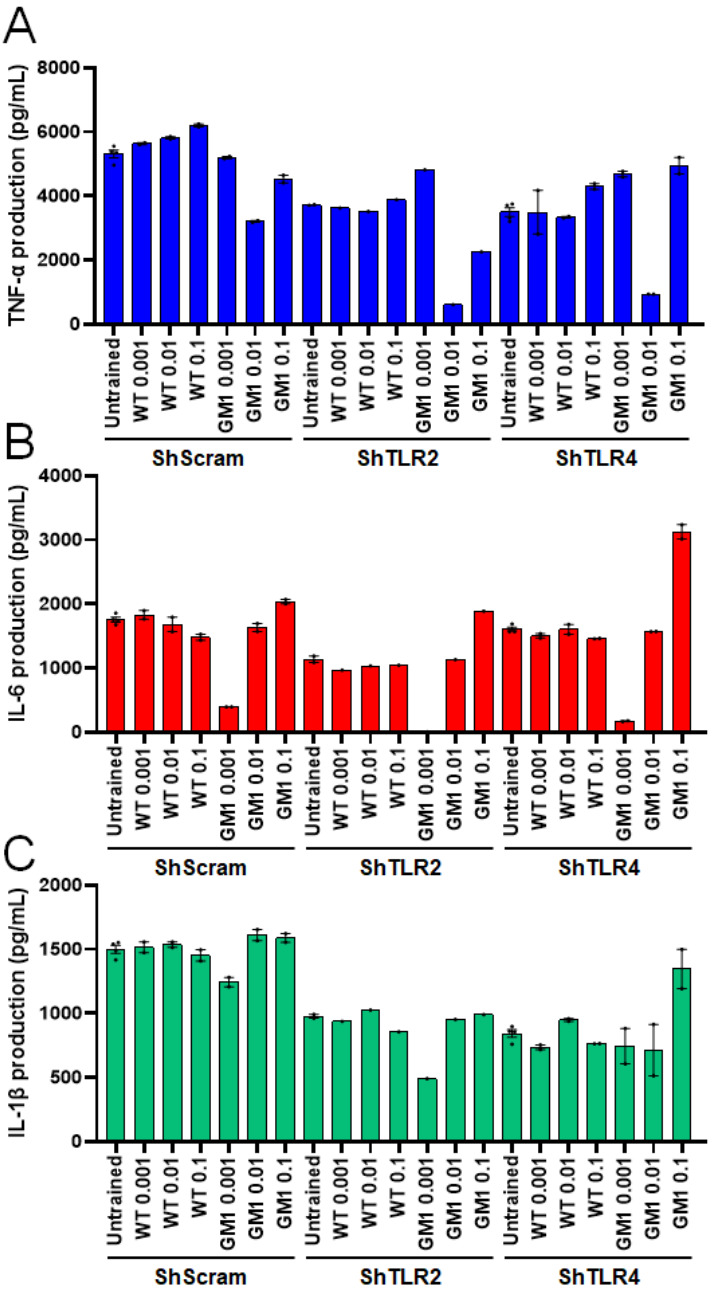

Figure 3.4. TLR4 appears to be involved in IL-1β-mediated tolerance. graphs representing release of TNF-α (A), IL-6 (B) and IL-1β (C) after training shRNA treated macrophages with *E. coli* GM1 (GM1) or *E. coli* WT (WT) at differing multiplicities of infection and subsequently challenging with *C. jejuni* HS:19 at a multiplicity of infection of 5. ShScram= scramble shRNA, ShTLR2= TLR2 shRNA and ShTLR4= TLR4 shRNA. This experiment was only done twice so there are insufficient biological replicates to report statistical significance.

Discussion

It has been well established that the bacteria humans are exposed to early in life help shape the human immune response later in life. This effect not only impacts the way that we respond to pathogens, but also our susceptibility to autoimmune diseases. In LMICs, it has been shown that *Campylobacter* species are regularly found in infants and young children during this development stage (184, 193). From an autoimmune disease perspective, this is significant because *C. jejuni* is known to illicit GBS by mimicking human ganglioside structures during infections. However, no one has examined whether being colonized with ganglioside-mimicking bacteria present at low levels in the gut during infancy can influence susceptibility to GBS.

In this study, we first hypothesized that infants in LMICs are exposed to ganglioside-mimicking *Campylobacter* strains during both symptomatic and asymptomatic infections. Our screen using CTB as a probe for GM1 gangliosides confirmed that these infants can be colonized with ganglioside-mimicking *Campylobacter* strains for an undetermined period of time. Interestingly, half of the mimicking isolates that we observed were from infants that did not show any signs of campylobacteriosis, suggesting that the presence of the mimic did not influence gastroenteritis and that many children are exposed to these ganglioside mimicking *Campylobacter* strains without taking notice.

Armed with the knowledge that people can be exposed to ganglioside mimics during infancy, we then sought to study whether presence of these bacteria impacts the immune system's tolerance of these antigens upon future exposure. It has been shown in multiple studies that *Campylobacter* infection leads to increased intestinal and systemic inflammation, which is believed to be associated with growth stunting in children (337). A

recent investigation called the Malnutrition and Enteric Disease Study (MAL-ED), examined 26,267 diarrheal and 7,601 non-diarrheal stool samples from 1,892 children across Brazil, Peru, South Africa, Tanzania, India, Pakistan, Bangladesh and Nepal (13). In this study, various fecal markers of intestinal inflammation were detected including neopterin (NEO), which can be used to estimate T-helper cell 1 activated cellular immunity (338). Their results showed that NEO concentration was actually lower during *Campylobacter* infection, hinting that the inflammation caused in *Campylobacter* may be driven by the innate rather than the adaptive immune system (13). Therefore, to investigate the impact of low-dose exposure of ganglioside-mimicking bacteria on subsequent immune response to ganglioside mimics, we measured the release of pro-inflammatory cytokines from human macrophages.

The human leukemia THP-1 monocytic cell line was treated with phorbol 12-myristate-13-acetate (PMA) to differentiate these cells into macrophages and is a widely used model to investigate cellular immunity. Our results suggest that when macrophages are exposed to low-doses of ganglioside-mimicking bacteria during differentiation, they become tolerized to the ganglioside antigen and pro-inflammatory cytokine release is reduced upon subsequent exposure. In addition to *C. jejuni* HS:19, the pair of *E. coli* GM1 and *E. coli* WT were used because they represent two strains that are isogenic and only differ in the structure of their LPS, where *E. coli* GM1 displays a ganglioside mimic and *E. coli* WT does not (Figure 3.2) (285). By using these strains, we could examine the impact of the ganglioside mimic itself, while controlling for other antigens on the cell surface. To further prove that the LOS is responsible for tolerance-induction, hot-phenol extractions were performed on all three strains to obtain purified LOS to use in future experiments

(Figure 3.7). However, our current data suggests that *E. coli* GM1 induces tolerance against *C. jejuni* HS:19 more effectively than *C. jejuni* HS:19 itself. It has been previously shown that the immunogenicity of LPS structures has a distinct impact on their ability to induce innate immune signaling and endotoxin tolerance (339). The more potent of an innate immune activator, the more capable a particular LPS is of endotoxin tolerance induction (339). In *C. jejuni*, the dehydrogenase GnnA and transaminase GnnB allow for modification of the lipid A molecule by mediating the replacement of an ester-linked acyl chain with an amide-linked acyl chain (340). This was shown to increase resistance to various antimicrobial peptides, but also reduces endotoxin activity and avoids activation of innate host defenses mediated through TLR4 when compared to *E. coli* lipid A (340). The difference is further supported by the higher pro-inflammatory cytokine secretion we observed in *E. coli* GM1 even when the cells were not challenged with *C. jejuni* HS:19, especially at an MOI of 0.1 (Figure 3.6). This increase in lipid A immunogenicity may explain why *E. coli* GM1 was better able to induce tolerance when compared to *C. jejuni* HS:19.

Once it was determined that ganglioside-mimicking bacteria could tolerize macrophages to a ganglioside antigen, we wanted to further investigate the signaling pathway responsible for this signaling. Tolerance induced by LPS and LOS results from changes in TLR signaling and primarily involves TLR4 (341). Cytokine production stimulated by LPS can also be reduced by cross-tolerance signaling when TLR2 is exposed to alternate ligands such as: lipopeptide (342), lipoarabinomannan (343), soluble tuberculosis factor (343), lipoteichoic acid (344), and zymosan (345, 346). *C. jejuni* has been previously shown to interact with the innate immune system via TLR2 (347) and

TLR4 (348) among other receptors (349). Though researchers have reported LPS signaling through TLR2 (350, 351), TLR4 is the receptor most commonly associated with LPS (352, 353). Both of these receptors are capable of inducing and suppressing the production of pro-inflammatory cytokines depending on the antigen they bind and the quantity (341, 353). Therefore, we targeted TLR2 and TLR4 for knockdown using shRNA to determine if either of these receptors was responsible for the tolerance signaling that we observed. After silencing these receptors and testing with the same macrophage molecule by training with *E. coli* GM1 or WT and challenging with *C. jejuni* HS:19 again, our results suggested that while TLR4 signaling is involved in the suppression of IL-1β secretion, the silencing of neither TLR2 or TLR4 impacted the decrease in TNF-α or IL-6 secretion associated with training using *E. coli* GM1. As mentioned previously, more biological replicates of this experiment are required to report statistical significance, and experiments are needed to verify the silencing of TLR2 and TLR4. This was attempted by performing a western blot to show a decrease in each receptor, however the antibodies used to detect for TLR2 (~89 kDa, Figure 3.8A) and TLR4 (~95 kDa, Figure 3.8B) were unable to detect the presence of either receptor, even for wildtype cell lysates. This result could be due to the loss of antibody binding capability resulting from reagent expiration. The negative result suggests that the experiment must be repeated using new antibodies, because the loading control used to show standard loading between lanes (Glyceraldehyde 3-phosphate dehydrogenase, GAPDH, ~37 kDa), was probed with new antibodies and was simultaneously detected on the same blots without any issues (Figure 3.8A and B).

To gain further insight into the tolerance mechanism we observed, an attempt was also made to measure the level of a diagnostic protein involved in LPS tolerance. Tumor necrosis factor, alpha-induced protein 3 (TNFAIP3, or A20) is a ubiquitin-editing enzyme that negatively impacts TLR-induced immune responses and induces LPS tolerance when upregulated (354-356). This enzyme was also shown to be involved in tolerance induction specifically in the THP-1 monocyte model used in this study (357, 358). Another western blot was performed using α-A20 antibody as a probe to determine if macrophage tolerance correlated with an increase in A20 production. However, we likely observed a similar issue as observed with the TLR western blots, the A20 antibody that was used did not detect an associated band (~90 kDa) in any of the lanes (Figure 3.8C) as was also beyond its expiration date. Once again, GAPDH was used as a loading control for this experiment and consistently had visible bands in the predicted range. Once new antibodies are obtained, this experiment will be repeated to determine if A20 is increased to correlate with the observed tolerance response.

In conclusion, this study has determined that infants in LMICs are exposed to ganglioside-mimicking *Campylobacter* early in life and that this does not always involve symptomatic infections. We also showed that ganglioside-mimicking intact bacteria induce innate immune tolerance to subsequent challenge with high doses of strains with GBS-associated antigen. Though more experiments are needed to investigate the mechanism for this tolerance, the differences we observed could indicate that ganglioside-mimicking bacteria present in the gut during immune development impact an individual's susceptibility to GBS. The *E. coli* strain used in this study was initially intended for use as a probiotic to bind to CT in the gut and treat/prevent cholera (285). The knowledge that

this strain can also induce tolerance to GBS-associated antigens suggests that in the future, probiotics could also have a role as a preventative to defend against GBS development.

Materials and Methods

Bacterial growth conditions

Campylobacter infant fecal isolates were streaked from frozen stocks onto Campy-Line agar (CLA) (359) plates and grown overnight at 37 °C in microaerobic conditions. Resulting growth was then re-streaked onto brain-heart infusion (BHI) agar and incubated overnight at 37 °C again in microaerobic conditions prior to use in experiments. *E. coli* cells were streaked from frozen stocks onto LB agar plates and grown overnight at 37 °C. Colonies from the resulting plates are used to inoculate overnight cultures in liquid LB medium that are grown overnight at 37 °C with agitation to be used in experiments. *E. coli* GM1 strains were grown in media supplemented with ampicillin (50 μg /mL) and kanamycin (25 μg/mL). *C. jejuni* wildtype cultures were streaked from frozen stocks onto NZCYM agar plates and grown overnight at 37 °C in microaerobic conditions. The resulting colonies are then re-streaked onto another NZCYM plate and grown overnight at 37 °C in microaerobic conditions prior to use in experiments.

Preparation of LOS from infant fecal isolates

LOS preparation was done as described previously with minor modifications (360). Briefly, the isolates were harvested into sterile PBS and adjusted to an optical density at 600 nm (OD_{600}) of 0.375. Then 1.5 mL of this suspension is transferred to a new tube and centrifuged for 4 min at 6200 ×g. The resulting pellet was then resuspended in 150 μL of lysing buffer (100 mM Tris-Cl (pH 8.0), 2% β-mercaptoethanol, 4% SDS, 0.2% bromophenol blue, 0.2% xylene cyanol, 20% glycerol). This mixture was boiled for 10 min

at 95 °C before being cooled to room temperature and adding an additional 150 µL of lysing buffer and proteinase K to a final concentration of 0.5 mg/mL. The samples were then incubated overnight at 37 °C before inactivating any remaining proteinase K by heating to 65 °C for 1h. These samples were directly loaded onto an SDS-PAGE gel or stored at -20 °C.

Hot phenol preparation of LOS

E. coli cells were streaked onto LB from frozen stocks and grown overnight at 37 °C in atmospheric conditions before a colony was picked, used to inoculate 5 mL of liquid LB medium and grown with agitation under the same conditions. This culture was used to inoculate 500 mL of LB medium and grown with agitation under the same conditions. *C. jejuni* HS:19 was grown from frozen stocks onto NZCYM agar and grown overnight at 37 °C in microaerobic conditions. They were then re-streaked onto more NZCYM agar plates, grown in the same conditions and this process was repeated until the resulting pellet resembled those obtained from *E. coli* cultures in quantity. To obtain pellets, *C. jejuni* cells were resuspended in PBS and both cultures were centrifuged at 7,649 ×g. From there, lipooligosaccharides were isolated using the hot water/phenol extraction method as previously described (361). The resulting pellet was lyophilized in a pre-weighed tube, then resuspended and analyzed for purity by silver stain and ability to bind CTB by western blot using methods previously described (6). Purified LOS was further quantified using the Pierce™ *Limulus* Amebocyte Lysate Endotoxin Quantification kit (Thermo Scientific) as directed by the manufacturer.

Far western blots of isolate and hot phenol purified LOS

Far western blots were performed as described previously with minor modifications (6). Briefly, samples were migrated using SDS-PAGE and the resulting gel was wet transferred to a nitrocellulose membrane for 1 h at 100 V at room temperature. Following this, the membrane was immersed in blocking solution (PBST+5% skim milk) overnight at 4 °C. The next day, the membrane was probed with CTB (1 mg/mL, Sigma, diluted 1:100,000 in blocking solution) for 1 h, rinsed 3 times and washed 3 times for 5 min in PBST. It was then probed with rabbit α-CT antibodies (1:6,500 in blocking solution) for 1 h, washed as before, probed with goat α-rabbit-HRP antibodies (1:20,000) for 1h and washed again as before. The membranes were developed using Clarity™ Western ECL Substrate (BioRad) and images were captured using the ChemiDoc XRS system (BioRad).

Fluorescent microscopy of infant fecal isolates

After growth as described above, the isolates were harvested from plates in PBS and their OD_{600} was adjusted to 0.05. Next, 2 mL of this suspension was mixed with 2 µL of CTB and incubated for 1 h at room temperature with agitation. The mixture was then centrifuged for 4 min at 6200 ×g and washed with PBS 3 times. Then 10 µL of the mixture was spotted onto a coverslip and left to air dry before heat fixing to the coverslip. The slips were then blocked for 1 h in blocking solution before being probed with rabbit α-CT antibodies (1:6,500 in blocking solution) for 1 h. They were then washed 3x with PBS for 5 min and probed with goat α-rabbit-Alexa 488 antibodies (Invitrogen, 1:500 in blocking solution) before being washed again as before. The coverslips were then rinsed in mQH_2O and allowed to dry before mounting with VectaShield antifade mounting medium (Vector Laboratories). Samples were imaged using an Olympus IX-71 inverted microscope with a CoolSnap HQ2 camera.

THP-1 human monocyte-like cell culturing

The human leukemia monocytic THP-1 cell line was obtained from the American Type Culture Collection (TIB-202) and maintained in RPMI with 2-mM L-glutamine and 10% fetal bovine serum (C-RPMI) at 3-8 × 10^5 cells/mL.

Preparation of paraformaldehyde-treated bacterial cells

C. jejuni and *E. coli* grown as described above were resuspended and washed in sterile PBS. The cells were then resuspended in PBS with 4% paraformaldehyde and incubated at room temperature for 30 min. Following this killing step, the paraformaldehyde was washed away three times with sterile PBS. The resulting killed bacterial suspensions were counted using a Petroff-Hausser counter and either used directly in monocyte assays or stored at 4 °C.

THP-1 human monocyte-like cell cytokine release assays

Experiments in THP-1 cells were based on methods previously described and expanded upon (362). After being grown to approximately 8 × 10^5 cells/mL in RPMI with 2-mM l-glutamine and 10% fetal bovine serum (C-RPMI), monocyte-like THP-1 cells were pelleted by centrifugation at 0.2×g for 5 minutes and resuspended in C-RPMI to a concentration of 1× 10^6 cells/mL. Phorbol 12-myristate-13-acetate (PMA) was then added to a final concentration of 50 nM and the cells were seeded in 48-well tissue culture plates at 4× 10^5 cells/well. Purified LPS (LPS-EB from E. coli O111:B4, InvivoGen) at 10 ng/mL or paraformaldehyde-treated bacteria at different multiplicities of infection (MOI) were added to the wells during this time for training. The cells were then incubated for approximately 24 h before the media was replaced and they were incubated for another 16 hours before being challenged with purified LPS at 500 ng/mL or *C. jejuni* HS19 at a MOI

of 5. The cells were incubated with the challenge for 24 h before the supernatants were removed and cytokine production is measured using TNF-α (BD-Biosciences), IL-6 (BD-Biosciences) or IL-1β (Invitrogen) ELISA kits. Cytokine production was measured in technical duplicates and each experiment was repeated in several biological replicates represented as dots on their respective bar graphs.

Silencing of TLR2 and TLR4 by lentiviral particle transduction

To begin, 1 mL of THP-1 cells at 4×10^5 cells/mL were pelleted in a 1.5 mL microfuge tube by centrifugation at 2000 rpm for 3 min and resuspended in C-RPMI + 5µg/mL polybrene. Next 2×10^4 cells were transferred to a 0.5 mL tube and Co-GFP scram CTR, TLR2-specific or TLR4-specific lentiviral particles were added to the tube at an MOI of 10 and the volume was adjusted to 100 µL with CRPMI + 5ug/ml polybrene. This mixture was then centrifuged for 30 min at 900×g at 20 °C, resuspended and transferred to a flat-bottom 96-well plate to be incubated overnight at 37 °C in 5% CO_2. The next morning, cells were transferred to a 0.5 mL tube and centrifuged at 2000 rpm for 3 min. The supernatant was discarded and the cells were resuspended in C-RPMI without polybrene and added to a clean flat-bottom 96-well plate and incubated for 72 h at 37 °C in 5% CO_2. Afterward, growth, cell morphology, and GFP expression was monitored by microscopy. Cells were then grown to 70-80% confluency in 96 well plate by replacing media every 2 to 3 days. Once this occurred, cells were transferred to a 48-well plate, volume was adjusted to 750 µL and they were grown for another 2-3 days while monitoring for GFP production in the Co-GFP control. Selection was then started by adding puromycin at 1 µg/mL and cells were monitored for growth and morphology, increase in Co-GFP expressing cells in the control group and death of untransduced cells. Cells are then

transferred to a 6-well plate with 5 mL of C-RPMI + 1ug/ml puromycin and left for multiple days continuing to check for selection. From there, transduced cells were expanded to make freezer stocks to be used in experiments. Attempts were made to verify these silence mutations by western blot, however, the antibodies used did not detect the receptors in the wildtype positive control, so the experiments must be repeated (Figure 3.8A and B).

Lysate preparation and western blotting for TLR and A20 experiments

For the A20 experiments, THP-1 cells were trained with *E. coli* WT or GM1 at a MOI of 0.1 and then challenged with *C. jejuni* HS:19 or left unchallenged as described above. To verify TLR silencing, ShScram, ShTLR2 and ShTLR4 were seeded in 12-well tissue-culture plates at 2×10^6 cells/well, differentiated and grown in the same conditions as THP-1 cells for the cytokine experiments. The exception being that they were not trained or challenged dring this time. Once finished, cells from both experiments were lysed using Pierce™ IP Lysis Buffer (Thermo Scientific) and a protease/phosphatase inhibitor (Cell Signaling Technology) as directed by the Pierce™ IP Lysis Buffer manufacturer's protocol. Protein concentration of the lysates was then standardized using the Pierce™ BCA Protein Assay Kit (Thermo Scientific) and boiled in lysing buffer for 10 min at 95 °C before being migrated by SDS-PAGE. The resulting gels were wet-transferred to nitrocellulose membrane as described earlier and the membrane was blocked in PBST+5%BSA (blocking solution) for 1 h. The membrane was then probed with mouse α-human A20 (BD Biosciences, 1:2000 in blocking solution), mouse α-TLR2 (Imgenex, 1:1000 in blocking solution) or mouse α-TLR4 (Imgenex, 1:1000 in blocking solution) that also contained mouse α-GAPDH (Thermo Scientific, 1:2000) as a loading control. This

was done overnight at 4 °C before washing 3 times in PBST for 5 min. The membrane was then probed with goat α-mouse-HRP (Invitrogen, 1:15000) for 1 h before washing as before and developing with Clarity™ Western ECL Substrate (BioRad) and capturing images using the ChemiDoc XRS system (BioRad).

Statistics

Statistics presented for the THP-1 monocyte experiments were performed using two-tailed unpaired t-tests with Welch's correction.

Acknowledgements

We would like Dr. Sharon Tennant and Jennifer Jones for providing us with the infant fecal *Campylobacter* isolates and Drs. James and Adrienne Paton for providing us with the *E. coli* CWG 308 wildtype and pGM1/pCst strains. Also, to Dr. Rodrigo Abreu for helpful discussions.

Supplementary information

Table 3.1. Information about infant fecal isolate samples. Describes information regarding CTB western blot results (CTB), strain isolation location, disease symptoms and other pathogens detected in each individual sample. Case and Ctrl represent infants with symptomatic campylobacteriosis and asymptomatic infants, respectively.

Stock Code	Isolate ID	CTB bound	Stool Consistency	Blood, Pus or Mucous?	Pathogens identified	Location	Type
1 A1	400956	Yes	Opaque watery	Mucus	*C. jejuni*	Kenya	Case
1 A3	203886	No	Thick liquid	None	*C. jejuni*, *E. coli* (ETEC), *E. coli estA* Pos	Mali	Case
1 A5	102878	No	Opaque watery	None	*C. jejuni*, *E coli* (ETEC), *E. coli eltB* Pos, *Cryptosporidium*	The Gambia	Case
1 A6	103067	Yes	Opaque watery	None	*C. jejuni*, *Rotavirus*	The Gambia	Case
1 A7	500680	No	Opaque watery	Mucus	*C. jejuni*, *Rotavirus*	India	Case
1 B1	500429	No	Formed	Blood, Mucus	*C. jejuni*	India	Case
1 B10	704058	No	Soft	None	*C. jejuni*, *Giardia*	Pakistan	Ctrl
1 B2	204462	No	Rice water-clear watery	Mucus	*C. jejuni*, *E coli (ETEC)*, *E. coli eltB* Pos	Mali	Case
1 B3	704064	No	Soft	None	*C. jejuni*	Pakistan	Ctrl
1 B4	703886	Yes	Rice water-clear watery	None	*C. jejuni*, *Rotavirus*	Pakistan	Case
1 B5	704012	No	Soft	None	*Aeromonas*, *C. jejuni*, *Salmonella* non-typhi, *E. coli* (EAEC), *E. coli aatA* Pos	Pakistan	Ctrl
1 B6	703934	No	Thick liquid	Blood, Mucus	*Aeromonas*, *C. jejuni*, *Rotavirus*, *Adenovirus*, *Adenovirus* 40/41, *Norovirus* GII	Pakistan	Case
1 B7	704017	No	Soft	None	*C. jejuni*, *Sapovirus*	Pakistan	Ctrl
1 B8	704138	No	Soft	Mucus	*C. jejuni*, *Cryptosporidium*, *Adenovirus*	Pakistan	Ctrl
1 B9	704137	No	Soft	None	*C. jejuni*, *E. coli* (EAEC), *E. coli aatA* Pos, *Cryptosporidium*, *Norovirus* GII	Pakistan	Ctrl
1 C10	700544	No	Rice water-clear watery	None	*Aeromonas*, *C. jejuni*	Pakistan	Case
1 C2	702567	Yes	Soft	Mucus	*C. jejuni*	Pakistan	Ctrl

1 C3	703207	Yes	Rice water-clear watery	None	*C. jejuni*, *Sapovirus*	Pakistan	Case
1 C4	703312	No	Thick liquid	None	*C. jejuni*, *Sapovirus*	Pakistan	Case
1 C5	702621	No	Thick liquid	None	*C. jejuni*, *E coli* (EAEC), *E. coli aatA* Pos, *Norovirus* GI	Pakistan	Ctrl
1 C6	702647	No	Thick liquid	Mucus	*C. jejuni*, *E. coli* (EAEC), *E. coli aatA* Pos	Pakistan	Ctrl
1 C7	702893	No	Opaque watery	None	*C. jejuni*, *E. coli* (EAEC), *E. coli aatA* Pos, *E. coli aaiC* Pos, *Norovirus* GII, *Sapovirus*	Pakistan	Case
1 C8	700541	No	Opaque watery	None	*Aeromonas, C. jejuni, V. cholerae, Rotavirus*	Pakistan	Case
1 C9	700006	No	Rice water-clear watery	None	*Aeromonas, C. jejuni, E. coli* (ETEC), *E. coli estA* Pos, *E. coli eltB* Pos	Pakistan	Case
1 D1	700690	No	Opaque watery	None	*C. jejuni, V. cholerae, E. coli* (tEPEC)	Pakistan	Case
1 D10	710352	No	Soft	None	*C. jejuni*, *E. coli* (EPECeae)	Pakistan	Ctrl
1 D2	702296	No	Thick liquid	None	*C. jejuni*, *E. coli* (aEPEC)	Pakistan	Case
1 D3 and J1	702519	No	Opaque watery	None	*C. jejuni*, *Norovirus* GII	Pakistan	Case
1 D4 and J3	703533	No	Rice water-clear watery	None	*C. jejuni*, *E coli* (tEPEC)	Pakistan	Case
1 D5	720383	No	Soft	None	*C. jejuni*, *E. coli* (EPEC, *eae*)	Pakistan	Ctrl
1 D6	720420	Yes	Opaque watery	None	*C. jejuni*, *E. coli* (EPEC, *eae*)	Pakistan	Case
1 D7	720390	Yes	Soft	None	*C. jejuni*, *E. coli* (EPEC, *eae, aaiC*)	Pakistan	Ctrl
1 D8	710444	No	Soft	None	*C. jejuni*, *E. coli (EPEC, eae)*	Pakistan	Ctrl
1 D9	710136	No	Soft	None	*C. jejuni*, *E coli* (EPEC, *eae, aatA, aaiC*)	Pakistan	Ctrl
1 E1	710351	Yes	Opaque watery	None	*C. jejuni*, *Giardia lamblia, Adenovirus, E. coli* (EPEC, *eae, aatA*)	Pakistan	Case
1 E10	720437	No	Thick liquid	None	*C. jejuni*, *Giardia lamblia, Rotavirus, Norovirus* GII, *S. boydii, E. coli* (EPEC, *eae*)	Pakistan	Case
1 E2	720296	No	Opaque watery	None	*C. jejuni*, *Astrovirus, B.fragilis, E. coli* (EPEC, *eae, aatA*)	Pakistan	Case

1 E3	720284	No	Soft	None	*C. jejuni*, *Adenovirus*, *B.fragilis*, *E coli* (EPEC, *eae*)	Pakistan	Ctrl
1 E4	710121	No	Rice water-clear watery	None	*C. jejuni*, *E. coli* (EPEC, *eae*)	Pakistan	Case
1 E5	710236	No	Opaque watery	None	*C. jejuni*, *V. cholerae*, *Vibrio* 132, *Astrovirus*, *E. coli* (EPEC, *eae*, *aaiC*)	Pakistan	Case
1 E6	720032	No	Opaque watery	None	*C. jejuni*, *Helicobacter pylori*, *E. coli* (EPEC, *eae*)	Pakistan	Case
1 E7	610396	Yes				Bangladesh	Case
1 E8	620425	No	Formed	None	*C. jejuni*, *Clostridium difficile* (GDH, Ag), *E. coli* (EPEC, *eae*)	Bangladesh	Ctrl
1 E9	720607	No	Thick liquid	None	*C. jejuni*, *E. coli* (EPEC, *eae*, *aaiC*)	Pakistan	Ctrl
1 F1	320435	Yes	Formed	None	*C. jejuni*, *Giardia lamblia*, *E coli* (EPEC, *eae*, *bfpA*)	Mozambique	Ctrl
1 F10	603060	Yes	Formed	None	*Aeromonas*, *C. jejuni*, *Salmonella* non-typhi, *E. coli* (ETEC), *E. coli eltB* Pos, *Giardia*	Bangladesh	Ctrl
1 F2	710293	No	Soft	None	*C. jejuni*, *Helicobacter pylori*, *Norovirus* GII, *E coli* (EPEC, *eae*, *bfpA*)	Pakistan	Ctrl
1 F3	720075	No	Opaque watery	Mucus	*C. jejuni*, *E. coli* (EPEC, *eae*)	Pakistan	Case
1 F4	720005	No	Thick liquid	Pus, Mucus	*C. jejuni*, *E. coli* (EPEC, *eae*, *aatA*)	Pakistan	Case
1 F5	603771	No	Formed	None	*Aeromonas*, *C. jejuni*	Bangladesh	Ctrl
1 F6	600099	No	Opaque watery	None	*C. jejuni*, *E. coli* (EAEC), *E. coli aaiC* Pos, *Cryptosporidium*, *Rotavirus*	Bangladesh	Case
1 F7	600021	No	Soft	Blood, Mucus	*C. jejuni*	Bangladesh	Case
1 F8	604419	No	Soft	Blood, Mucus	*Aeromonas*, *C. jejuni*, *Salmonella* non-typhi, *E. coli* (tEPEC), *E. coli bfpA* Pos	Bangladesh	Case
1 F9	603180	No	Thick liquid	Mucus	*Aeromonas*, *C. jejuni*, *Rotavirus*	Bangladesh	Case
1 G1	710087	No	Soft	None	*C. jejuni*, *Giardia lamblia*, *Helicobacter pylori*,	Pakistan	Ctrl

					*Sapovirus, E. coli (*EPEC, *eae, aaiC*)		
1 G10	403459	No	Thick liquid	Mucus	*C. jejuni*	Kenya	Case
1 G2	720255	No	Thick liquid	None	*C. jejuni, E. coli* (EPEC, *eae, aaiC*)	Pakistan	Case
1 G3	720147	No	Soft	None	*C. jejuni, Clostridium difficile* (GDH *Ag*) *E. coli* (EPEC, *eae*)	Pakistan	Ctrl
1 G4	600978	No	Soft	Blood, Mucus	*Aeromonas, C. jejuni, E. coli* (EAEC), *E. coli aatA* Pos, *Rotavirus*	Bangladesh	Case
1 G5	600883	No	Thick liquid	Mucus	*C. jejuni*	Bangladesh	Case
1 G6	601037	Yes	Thick liquid	Mucus	*C. jejuni*	Bangladesh	Case
1 G7	704231	No	Soft	None	*C. jejuni, Cryptosporidium*	Pakistan	Case
1 G8	400738	No	Thick liquid	Mucus	*C. jejuni, E. coli* (tEPEC), *E. coli bfpA* Pos, *E. coli eae* Pos, *Adenovirus*	Kenya	Case
1 G9	400526	No	Opaque watery	Mucus	*C. jejuni, E. coli* (aEPEC), *E coli eae* Pos	Kenya	Case
1 H1	403205	No	Opaque watery	None	*C. jejuni, Cryptosporidium*	Kenya	Case
1 H10	703664	No	Opaque watery	None	*C. jejuni, E. coli* (ETEC), *E. coli estA* Pos, *E. coli eltB* Pos	Pakistan	Case
1 H2	401022	No	Formed	None	*C. jejuni, E. coli* (EAEC), *E. coli aaiC* Pos	Kenya	Ctrl
1 H3	402870	No	Opaque watery	None	*C. jejuni, E. coli* (aEPEC)	Kenya	Case
1 H4	401051	No	Soft	None	*C. jejuni*	Kenya	Ctrl
1 H5	403385	No	Opaque watery	Mucus	*C. jejuni*	Kenya	Case
1 H6	320256	No	Formed	None	*C. jejuni, E coli* (EPEC, *eae*)	Mozambique	Ctrl
1 H7	403257	No	Soft	None	*C. jejuni, Entamoeba*	Kenya	Ctrl
1 H8	703672	No	Soft	None	*C. jejuni, E. coli* (EAEC), *E. coli aatA* Pos, *E. coli aaiC* Pos, *Norovirus* GI	Pakistan	Ctrl
1 H9	703637	Yes	Soft	None	*C. jejuni, Salmonella non-typhi, E. coli* (EAEC), *E. coli* (tEPEC), *E. coli* (aEPEC), *E. coli aaiC* Pos, *E. coli eae* Pos, *Astrovirus*	Pakistan	Case
1 I1	703882	No	Soft	None	*C. jejuni, Norovirus* GII	Pakistan	Ctrl

1 I10	721262	No	Opaque watery	None	*C. jejuni*, *Rotavirus*, *Norovirus* GII, *E. coli* (EPEC *eae*, *bfpA*)	Pakistan	Case
1 I2	703779	No	Rice water-clear watery	None	*C. jejuni*, *Cryptosporidium*, *Rotavirus*	Pakistan	Case
1 I3	703871	Yes	Soft	Mucus	*Aeromonas*, *C. jejuni*, *Salmonella* non-typhi, *Norovirus* GI	Pakistan	Ctrl
1 I4	720906	No	Soft	None	*Aeromonas*, *C. jejuni*, *Sapovirus*, *E. coli* (EPEC *eae*, *eltB*)	Pakistan	Ctrl
1 I6	710603	No	Rice water-clear watery	None	*C. jejuni*, *E. coli* (EPEC, *eae*, *aaiC*)	Pakistan	Case
1 I7	720839	No	Soft	Mucus	*C. jejuni*, *S. flexneri* 4a, *E. coli* (EPEC, *eae*)	Pakistan	Case
1 I8	110498	Yes	Opaque watery	Mucus	*C. jejuni*	The Gambia	Case
1 I9	721314	Yes	Soft	None	*C. jejuni*, *Clostridium difficile* (GDH Ag*) E. coli* (EPEC, *eae*, *aatA*, *aaiC*)	Pakistan	Case
1 J10	520188	No	Formed	Pus, Mucus	*C. jejuni*, *Clostridium difficile* GDH Ag, *E coli* (EPEC, *eae*)	India	Ctrl
1 J2	120617	Yes	Thick liquid	None	*C. jejuni*, *Clostridium difficile* GDH Ag, *B.fragilis*, *E coli* (EPEC, *eae*, *aatA*)	The Gambia	Ctrl
1 J4	721311	No	Soft	None	*C. jejuni*, *E coli* (EPEC, *eae*, *aatA*)	Pakistan	Ctrl
1 J5	103169	Yes	Thick liquid	None	*C. jejuni*	The Gambia	Ctrl
1 J6	503818	No	Opaque watery	Pus, Mucus	*C. jejuni*, *E. coli* (EAEC), *E. coli* (tEPEC), *E. coli bfpA* Pos, *E coli aaiC* Pos, *E coli eae* Pos, *Giardia*, *Cryptosporidium*	India	Case
1 J7	504021	Yes	Opaque watery	None	*C. jejuni*	India	Case
1 J8	504343	Yes	Soft	Mucus	*C. jejuni*	India	Ctrl
1 J9	520016	Yes	Soft	Pus, Mucus	*C. jejuni*, *E coli* (EPEC, *eae*, *aatA*)	India	Case
2 A1	504076	No	Thick liquid	Mucus	*C. jejuni*, *Cryptosporidium*	India	Case
2 A10	510831	No	Thick liquid	Pus, Mucus	*C. jejuni*, *Adenovirus*,	India	Case

					Adenovirus 40/41, *E. coli* (EPEC, *eae*)		
2 A2	504764	No	Formed	None	*C. jejuni*, *E coli* (EAEC), *E coli aaiC* Pos, *Giardia*, *Cryptosporidium*	India	Ctrl
2 A3	504611	No	Opaque watery	Mucus	*C. jejuni*	India	Case
2 A4	504977	No	Soft	Pus, Mucus	*C. jejuni*, *E. coli* (EAEC), *E. coli aatA* Pos, *E. coli aaiC* Pos	India	Ctrl
2 A5	505394	Yes	Soft	Mucus	*C. jejuni*	India	Ctrl
2 A6	504196	Yes	Formed	None	*C. jejuni*, *E. coli* (EAEC), *E. coli aatA* Pos	India	Ctrl
2 A7	503610	No	Soft	Mucus	*C. jejuni*, *Cryptosporidium*, *Rotavirus*	India	Case
2 A8	503674	No	Opaque watery	None	*C. jejuni*, *Cryptosporidium*, *Rotavirus*	India	Case
2 A9	504730	No	Soft	None	*C. jejuni*, *Adenovirus*	India	Ctrl
2 B1	510942	Yes	Soft	Pus, Mucus	*C. jejuni*, *Salmonella* non-typhi, *Clostridium difficile* GDH Ag, *E. coli* (EPEC*eae*)	India	Ctrl
2 B10	703833	Yes	Soft	None	*Aeromonas*, *C. jejuni*	Pakistan	Case
2 B2	511171	No	Soft	Mucus	*C. jejuni*, *Clostridium difficile* GDH Ag, *E. coli* (EPEC, *eae*)	India	Ctrl
2 B3	520190	No	Soft	Pus, Mucus	*C. jejuni*, *E. coli (EPEC, eae*)	India	Ctrl
2 B4	520430	No	Thick liquid	Pus, Mucus	*C. jejuni*, *E. coli* (EPEC, *eae*)	India	Case
2 B5	521136	Yes	Soft	Mucus	*C. jejuni*, *Clostridium difficile* GDH Ag, *E. coli* (EPEC, *eae*, *estA*)	India	Ctrl
2 B6	521162	No	Soft	Mucus	*C. jejuni*, *E coli* (EPEC, *eae*)	India	Ctrl
2 B7	703493	No	Soft	None	*C. jejuni*, *Cryptosporidium*	Pakistan	Ctrl
2 B8	703438	No	Thick liquid	Mucus	*C. jejuni*	Pakistan	Case
2 B9	703777	No	Opaque watery	None	*C. jejuni*, *Cryptosporidium*	Pakistan	Case
2 C1	710652	Yes	Opaque watery	None	*Aeromonas*, *C. jejuni*, *Salmonella* non-typhi, *V. cholerae*, *Vibrio* 13V inaba ogawa, *E. coli* (EPEC, *eae*)	Pakistan	Case

2 C2	720972	No	Thick liquid	None	*C. jejuni*, *Cryptosporidium spp.*, *Norovirus* GI, *E. coli* (EPEC, *eae*, *bfpA*)	Pakistan	Case
2 C3	721225	No	Soft	Mucus	*C. jejuni*, *Norovirus* GII, *E. coli* (EPEC, *eae*, *aatA*, *aaiC*)	Pakistan	Ctrl
2 C4	721253	No	Soft	None	*C. jejuni*, *Clostridium difficile* GDH Ag, *E. coli* (EPEC, *eae*)	Pakistan	Case
2 C5	721319	No	Soft	None	*C. jejuni*, *Giardia lamblia*, *E. coli* (EPEC, *eae*, *aatA*)	Pakistan	Ctrl
3 1	201666	No				Mali	Ctrl
3 5	203084	No	Soft	None	*Campylobacter* nonspec, *E. coli* (EAEC), *E coli aatA* Pos, *E coli aaiC* Pos, *Giardia*, *Sapovirus*	Mali	Ctrl
3 6	203106	No	Thick liquid	Mucus	*Campylobacter* nonspec	Mali	Case
3 8	203460	No	Soft	None	*Campylobacter* nonspec	Mali	Ctrl
3 9	203524	No	Thick liquid	None	*Campylobacter* nonspec, *E. coli* (EAEC), *E. coli aaiC Pos*	Mali	Case
3 10	204409	Yes	Opaque watery	None	*C. jejuni*, *Rotavirus*	Mali	Ctrl
3 11	310356	No				Mozambique	Case
3 12	310457	Yes	Formed	None	*C. jejuni*, *Entamoeba histolytica*, *E. coli* (EPEC, *eae*)	Mozambique	Ctrl
3 13	320061	Yes	Opaque watery	None	*C. jejuni*, *E. coli* (EPEC, *eae*, *bfpA*)	Mozambique	Case
3 14	320644	No	Opaque watery	None	*C. jejuni*, *Rotavirus*, *E. coli* (EPEC, *eae*)	Mozambique	Case
3 15	500963	No	Formed	None	*C. jejuni*	India	Ctrl
3 16	503093	No	Opaque watery	None	*C. jejuni*	India	Case
3 17	503603	No	Opaque watery	None	*C. jejuni*, *E. coli* (aEPEC), *E. coli eae* Pos, *Cryptosporidium*	India	Case
3 18	504361	Yes	Soft	None	*C. jejuni*	India	Ctrl
3 19	600035	Yes	Soft	Mucus	*C. jejuni*, *E. coli* (ETEC), *E. coli eltB* Pos, *Cryptosporidium*	Bangladesh	Case
3 20	703317	No	Soft	None	*Aeromonas*, *C. jejuni*, *E. coli* (aEPEC)	Pakistan	Ctrl

3 21	710670	No	Soft	None	*C. jejuni*, *Giardia lamblia*, *Norovirus* GII, *E. coli* (*EPEC, eae, aatA, aaiC*)	Pakistan	Ctrl
3 22	710796	No	Opaque watery	None	*C. jejuni*, *Cryptosporidium spp.*, *S. flexneri* 3a, *E. coli* (EPEC, *eae, bfpA,* Stx2, Stx1)	Pakistan	Case
3 23	710963	No	Soft	None		Pakistan	Ctrl
3 41	100801	Yes	Thick liquid	None	*C. coli*, *E. coli* (EAEC), *E. coli aaiC* Pos	The Gambia	Ctrl
3 42	121307	No	Opaque watery	Mucus	*C. coli*, *E. coli* (EPEC, *eae*)	The Gambia	Case
3 43	202388	No	Opaque watery	Mucus	*Campylobacter* nonspec	Mali	Case
3 44	204304	No	Thick liquid	Mucus	*Campylobacter* nonspec, *Giardia*	Mali	Case
3 45	400679	No	Thick liquid	Mucus	*C. coli*, *E. coli* (aEPEC), *E. coli eae* Pos	Kenya	Case
3 46	400879	No	Thick liquid	Blood, Pus, Mucus	*C. coli*, *Cryptosporidium*	Kenya	Case
3 47	403965	No	Thick liquid	Mucus	*C. coli*, *Rotavirus*	Kenya	Case
3 48	500573	Yes	Soft	None	*C. coli*, *E. coli* (EAEC), *E. coli aatA* Pos	India	Ctrl
3 49 & 50	403362	Yes	Opaque watery	Mucus	*C. coli*, *E. coli* (tEPEC), *E. coli bfpA* Pos, *E. coli eae* Pos, *Norovirus* GI	Kenya	Case
3 51	505506	No	Soft	Mucus	*C. coli*, *E. coli* (ETEC), *E. coli estA* Pos	India	Ctrl
3 52	505965	No	Soft	Pus, Mucus	*C. coli*, *V. cholerae*	India	Ctrl
3 53	510333	No	Soft	None	*C. coli*, *Clostridium difficile* GDH Ag, *E. coli* (EPEC, *eae*)	India	Ctrl
3 54 & 55	601035	No	Formed	None	*C. coli*, *E. coli* (ETEC), *E. coli eltB* Pos	Bangladesh	Ctrl
3 56	602330	Yes	Formed	None	*Aeromonas*, *C. coli*	Bangladesh	Ctrl
3 57	602497	No	Thick liquid	Blood, Mucus	*Aeromonas*, *C. coli*, *E. coli* (ETEC), *E. coli eltB* Pos	Bangladesh	Case
3 58	602723	No	Formed	None	*C. coli*, *V. cholerae*, *E. coli* (EAEC), *E. coli aaiC* Pos	Bangladesh	Ctrl
3 59	603567	No	Formed	None	*C. coli*, *Astrovirus*	Bangladesh	Ctrl
3 60	610001	No	Thick liquid	Mucus	*Aeromonas*, *C. coli*, *Giardia lamblia*,	Bangladesh	Case

					Clostridium difficile GDH Ag, *E. coli* (EPEC, *eae*)		
3 61	610647	No	Thick liquid	Mucus	*C. coli, V. cholerae, Vibrio* non, *S. sonnei, E coli* (EPEC, *eae*)	Bangladesh	Case

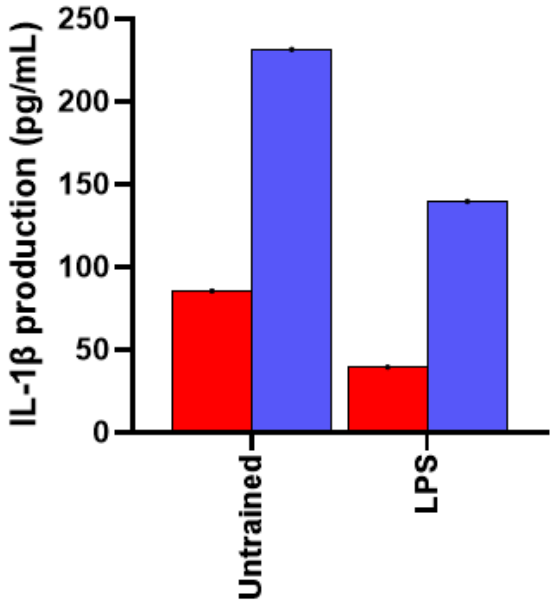

Figure 3.5. Direct measurement of cytokine production levels in THP-1 macrophage experiments with commercial LPS. IL-1β production from macrophages trained with 10 ng/mL LPS prior to being challenged with LPS at 500 ng/mL (blue) or left unchallenged (red).

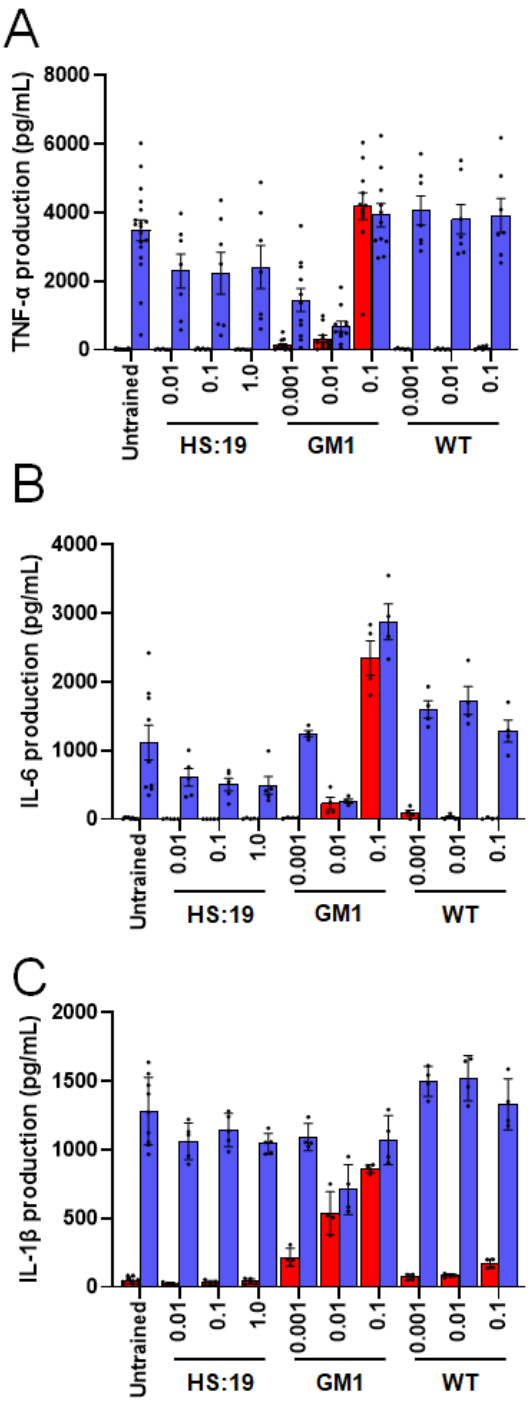

Figure 3.6. Direct measurement of cytokine production in THP-1 macrophage experiments with intact bacteria. TNF-α, IL-6 and IL-1β production from macrophages trained with *C. jejuni* HS:19, *E. coli* GM1 or *E. coli* WT at the indicated MOI values prior to challenge with *C. jejuni* HS:19 at MOI 5 (blue) or left unchallenged (red).

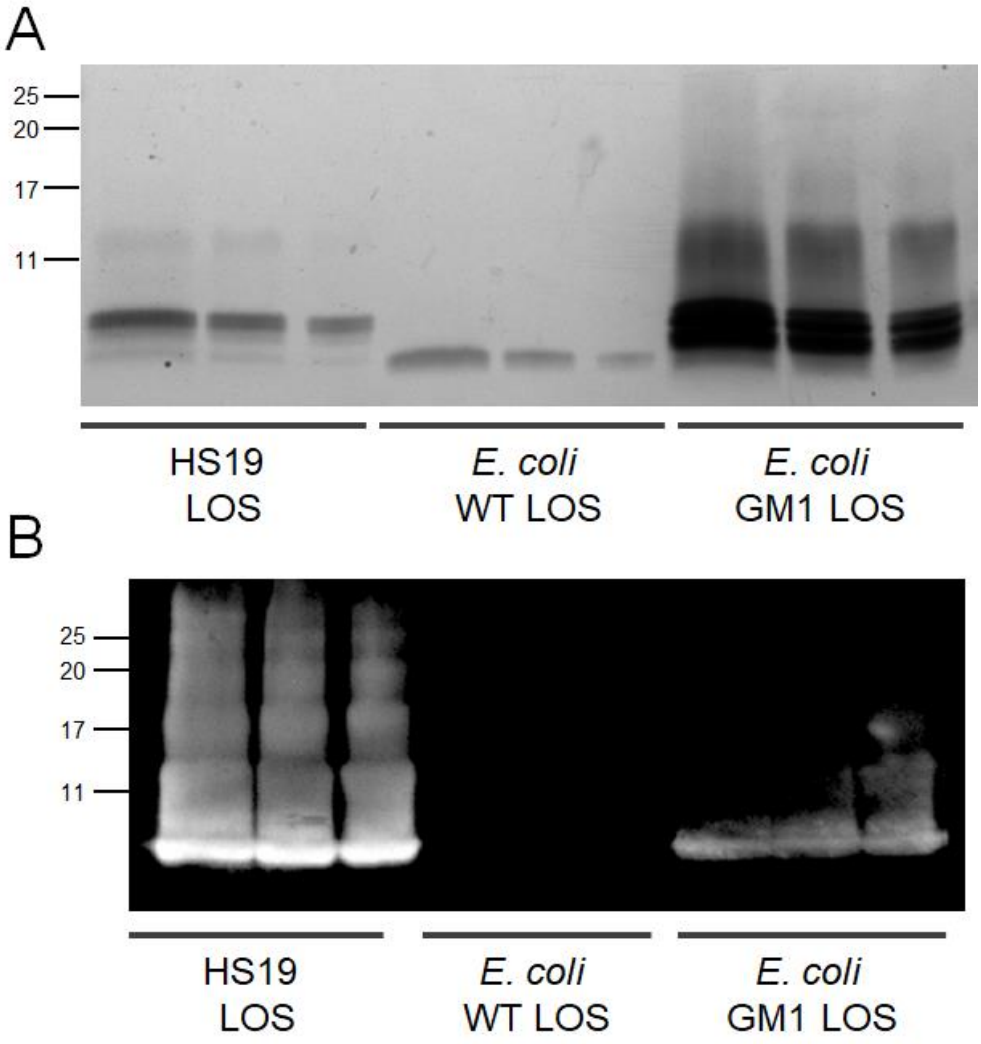

Figure 3.7. Phenol-purified LOS from *C. jejuni* HS:19, *E. coli* WT and *E. coli* GM1. Images demonstrate purity by silver stain (A) and ability to bind CTB probe by western blot (B). Samples were loaded in triplicate in decreasing concentrations. Molecular weight markers are shown in kDa.

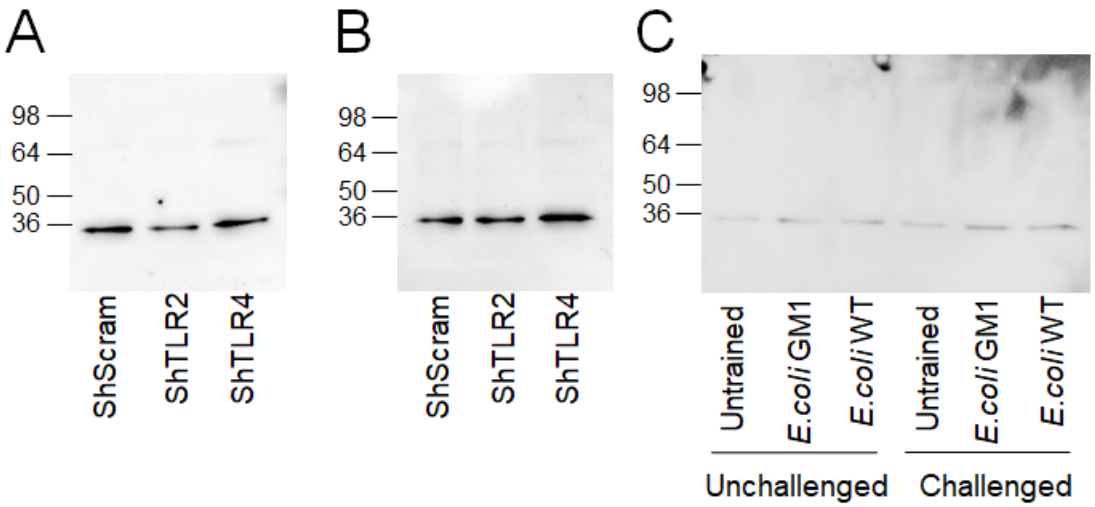

Figure 3.8. Confirmation of TLR silencing and investigation of A20 production. Western blots performed to confirm silencing of TLR2 (A) and TLR4 (B), or measure differential A20 production in untrained compared to *E. coli* GM1 or WT-trained macrophages (C). Training MOI for (C) was 0.01 and macrophages were challenged with *C. jejuni* HS:19 at a MOI of 5 where indicated.

CHAPTER 4

CHARACTERIZATION OF GANGLIOSIDE-MIMICKING ENTEROCOCCI.[8]

[8] **Robert T. Patry,** Harald Nothaft, Robert Bridger, Asif Shajahan, Kerry K. Cooper, Steven Huynh, Susan Sanchez, Parastoo Azadi, William G. Miller, Craig T. Parker, Lance Wells and Christine M. Szymanski. To be submitted to *Glycobiology*.

Author Contributions: Project concept was designed by RTP, HN and CMS. *Enterococcus* species were isolated from the chicken ceca by RTP and HN. Separation and identification of mixed cultures was done by RTP, HN and SS. Lysate generation and analysis by western blot was done by RTP. Sample preparation for mass spectrometry of glycoproteins excised from SDS-PAGE gels was done by RTP. LC MS/MS analysis of these samples was performed by AS. Preparation of genomic DNA for genome sequencing was done by RTP and SH. Full-genomic sequencing, assembly and annotation was done by SH, WGM and CTP. Analysis of core genes shared between *Enterococcus* strains was performed by KKC. Acetone precipitation of proteins was done by RTP and mass spectrometry of these samples to generate glycoproteomic data was done by RB. Glycoproteomic data was analyzed by RTP, RB, LW and CMS. Paper was written by RTP and CMS with contributions from all other authors. SS, PS, WGM, CTP, LW and CMS supervised the project.

Abstract

Ganglioside-mimicking bacteria are a precipitating agent of the autoimmune disease Guillain-Barré Syndrome (GBS). The most well-known example of this phenomenon involves *Campylobacter jejuni* strains using their lipooligosaccharide structures to mimic human gangliosides. This stimulates the immune system to produce autoreactive antibodies that target gangliosides on host nerve cells, resulting in paralysis. Despite the importance of ganglioside-mimicry in this disease, the extent of ganglioside-mimicking bacteria that interact with the host is largely unknown. Previous reports of ganglioside mimicry have primarily focused on infectious agents, and for bacteria, Gram-negative organisms are over-represented. This may be due to the comparative lack of knowledge about the glycosylation systems of Gram-positive bacteria in general. This chapter details the identification of three *Enterococcus* strains that were isolated from the chicken cecum: *E. gallinarum* EGM181, *E. casseliflavus* EGM182 and *E. faecalis* EGM183. These strains were selected based on their reactivity with α-ganglioside antibodies and subsequent demonstration that the reactive components were sensitive to proteinase K digestion, suggesting that the glycans are part of glycoproteins. The full genomes of these three *Enterococcus* strains were sequenced and are reported here. Whole genome sequences were compared with 12 other strains representing different *Enterococcus* species to better understand carbohydrate metabolism and glycoconjugate biosysnthesis within this genus and to provide clues into which genes could encode enzymes involved in ganglioside mimicry. Glycoproteomic analysis was also performed to identify ganglioside-mimicking glycoproteins to target for purification and further glycan analysis. In addition, *E. casseliflavus* EGM182 was

tested in a macrophage model, showing that exposure to the organism in low-doses can increase pro-inflammatory cytokine production upon subsequent exposure to GBS-associated antigens. This work expands the knowledge of ganglioside-mimicry as well as protein glycosylation in Gram-positive bacteria, by suggesting that these commensal organisms of the chicken microbiome have a general protein glycosylation system and can produce ganglioside mimics that could potentially impact GBS development.

Introduction

In order to thrive in the diverse and complex system of the human microbiome, bacteria have developed intricate strategies to evade host defenses and compete with other microbes that occupy the community. One primary mechanism that microbes use to evade the host immune response is through the vast diversity of glycan structures that they can display on their surface. Many bacteria are also capable of using these structures to mimic host glycans, disguising themselves to appear like the host. This is the case for *Campylobacter jejuni*, which can use its lipooligosaccharides to mimic human ganglioside receptors (47, 258, 363). *C. jejuni* is a common foodborne pathogen that naturally resides in the chicken gut and is among the world's most common causes of gastroenteritis primarily from the consumption of contaminated poultry products (1, 13, 184, 194). Infection by this organism can also lead to paralysis through the development of Guillain-Barré Syndrome (GBS), where cross-reactive antibodies are generated against bacterial ganglioside mimics that subsequently react with human nerve cells (35, 268, 364). There have been many studies showing other infective agents that can cause GBS or are at least correlated with the disease. These include bacteria such as: *Campylobacter coli* (100), *Mycoplasma pneumoniae* (46, 101), *Brucella melitensis* (102), *Haemophilus influenzae*

(103, 104), and multiple viruses including: cytomegalovirus (106-108) and Epstein barr virus (108-110). Recently Zika virus has also been associated with GBS and this link has been observed all over South America (111-116) and in French Polynesia (117). While all of these infectious agents have been linked with GBS, none have been proven to mimic gangliosides by complete structure characterization of the glycans components, as for *C. jejuni*.

Through our investigation of *C. jejuni* GM1-ganglioside mimicry in its natural chicken host, we discovered other resident gut microbes seemingly capable of this mimicry (6). The ganglioside-mimicking bacteria were purified from chicken cecal contents and identified by 16S rRNA gene sequencing as *Enterococcus gallinarum/casseliflavus* (6). Further investigation has led us to show that both the *E. gallinarum* and *E. casseliflavus* strains possess these ganglioside-mimics, in addition to another *Enterococcus* strain from the *faecalis* spp. It is known that bacteria have a profound impact on how our body learns to tolerate harmless antigens and respond strongly to harmful antigens (266), especially early on in life (262-265). As a result, the microbiome is heavily linked to the susceptibility of individuals to a variety of different autoimmune diseases (262). Recently, *Enterococcus gallinarum* has also been linked to systemic lupus erythematosus (SLE) in mice and humans following infection, showing that this organism in particular can potentiate autoimmunity in the human host (206).

Enterococci are commercially and medically important bacteria commonly part of the normal intestinal microbiota of humans and animals. Their large colonization range is enabled through their enormous genome plasticity, diverse range of stress tolerance capabilities and extensive metabolic capacity (365, 366). Enterococci also frequently cause

infection opportunistically when they gain access to privileged areas of the body such as the blood, urinary and biliary tracts, and wounds (203). They are thought to be the second most common cause of wound and urinary tract infection and the third most common cause of bacteremia (199). It has been reported that they cause about 12% of hospital-acquired infections in the United States (199) and about 30% of these infections are vancomycin resistant (204), causing the CDC to declare vancomycin resistant enterococci a "serious threat" (204). While *E. faecalis* most commonly causes infections associated with the genus, *E. faecium* is more likely to be antibiotic resistant and over 70% are thought to be vancomycin resistant (204). Besides *E. faecalis* and *E. faecium*, *E. gallinarum* can also result in infection, usually causing similar disease outcomes to the other *Enterococcus* species, but studies have suggested that it is increasingly involved in meningitis due to hospital-acquired infections (205). *E. gallinarum*, *E. casseliflavus*, and *E. flavescens* naturally possess the *vanC* gene, which makes them unique among the enterococci due to their intrinsic ability to resist this last-line antibiotic (199, 207). Non-*faecium*, Non-*faecalis* Vancomycin resistant *Enterococcus* infections are only reported in 1-2% of cases, but this is likely underestimated due to limits of detection (207).

This study describes the identification of three ganglioside-mimicking *Enterococcus* isolates from the chicken gut and the identification of multiple glycosylated proteins likely related to a generalized protein glycosylation system in these *Enterococcus* species. We report the genomic sequences of all three isolates along with a detailed glycoproteome analysis for each.

Results

Identification of chicken cecal isolates

Though the isolation of the *E. gallinarum* and *E. casseliflavus* used in this study was previously described (Figure 4.1A) (6), this isolation was previously thought to be a pure culture, but subsequently separated and further identified in this study. To determine the identity of the Enterococcus isolates, universal primers were employed to sequence the 16S rRNA gene. The resulting sequence revealed that the isolated organisms belonged to the *Enterococcus* genus, but we were unable to differentiate between *gallinarum* and *casseliflavus* at the species level (6). This was not surprising given that these two species are highly related genetically and are frequently difficult to differentiate based on 16S rRNA sequencing given that they differ only by a few base pairs (367) .

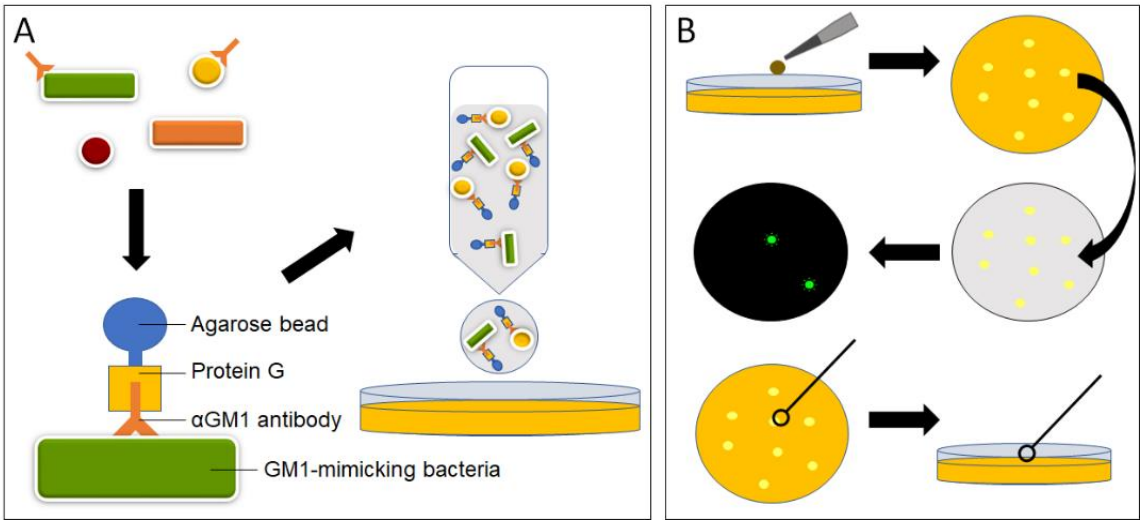

Figure 4.1. Schematic depicting the methods used to isolate the three strains described in this study. A) *E. gallinarum* and *E. faecalis* were isolated by incubating chicken cecal mucin with α-GM1 ganglioside antibodies and binding these complexes to a protein G resin in a gravity flow column. The column was then washed thoroughly, beads bound to GM1 ganglioside-mimicking bacteria were collected, diluted and plated to yield isolated colonies. B) *E. faecalis* was isolated by dilution-plating chicken cecal samples onto rich media and growing in permissive conditions. Plates with isolated colonies were transferred to a nitrocellulose membrane and blotted using cholera toxin B subunit as a probe for GM1 ganglioside mimicry. Once positive colonies were identified by fluorescence, they were selected from the original plate and characterized.

Upon further study, it became clear that the isolate consisted of a mixed culture, due to the presence of differing colony morphologies. Specifically, colonies were either white or yellow colored when grown on agar plates (Figure 4.2A and B). These two newly independent isolates were confirmed to be distinct by PCR amplification of the *vanC-1*, *vanC-2* and *vanC-3* regions (Figure 4.2C and D), a method previously shown to differentiate between these species (368). These gene products are expected to be 796, 484 and 224 base pairs in length respectively. Notably, *E. casseliflavus* encodes for *vanC-3* and *E. gallinarum* does not (368). We observed that the *vanC-3* band is absent for the white colonies (Figure 4.2C), but present for the yellow (Figure 4.2D), suggesting that the former is *E. gallinarum* and the latter is *E. casseliflavus*. This observation was

further verified using MALDI-TOF mass spectrometry of whole cells from each colony type, which confirmed the identification. The new strains have been named *E. gallinarum* EGM181 and *E. casseliflavus* EGM182. A third ganglioside-mimicking *Enterococcus* isolate was discovered by plating chicken cecal contents and performing a colony lift using cholera toxin B-subunit (CTB) as a probe (Figure 4.1B). The colony lift isolate was subsequently identified using MALDI-TOF mass spectrometry to be *E. faecalis* and named EGM183.

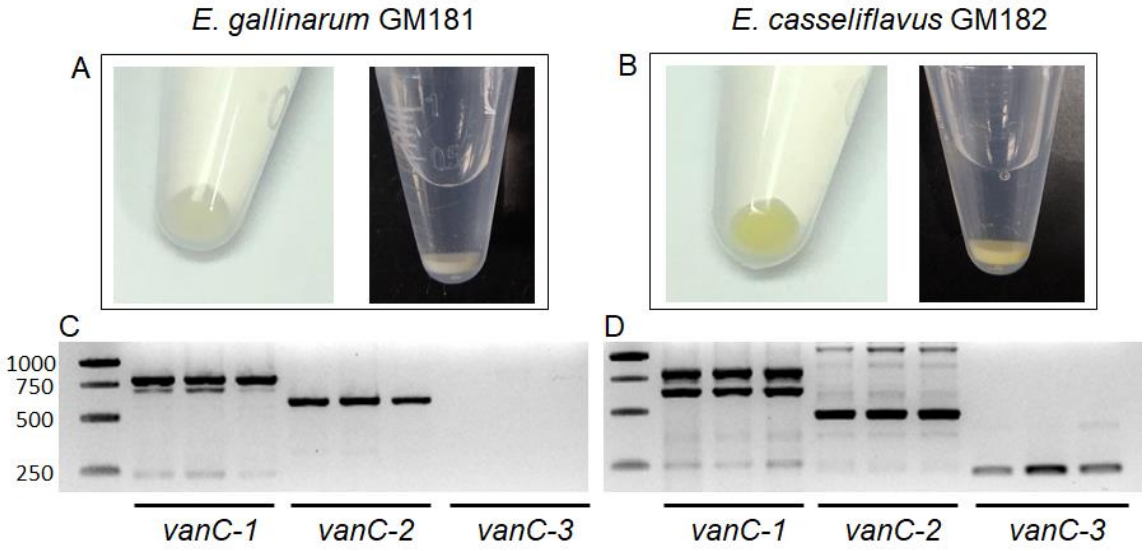

Figure 4.2. Separation of chicken cecal isolates. A and B) Images highlighting the difference in color between (A) *E. gallinarum* EGM181 and (B) *E. casseliflavus* EGM182. C and D) Agarose DNA gels showing colony PCR reactions in triplicate amplifying the *van-C1*, *van-C2* and *van-C3* regions for distinction between *E. gallinarum* EGM181 (C) and *E. casseliflavus* EGM182 (D). Numbers indicate size in base pairs.

Enterococcus lysate analysis reveals potential ganglioside-mimicking glycoproteins

Cell lysates were generated for each of the *Enterococcus* species and examined for GM1-ganglioside binding by western blot after treating with proteinase K or being left untreated. As shown by the Coomassie stained gel (Figure 4.3A), when the lysates were incubated with proteinase K, there were no remaining bands in those lanes,

suggesting that the proteins had been significantly degraded. The blots showed several prominent bands binding to α-GM1-ganglisoide antibodies; however, these were not present in the proteinase K lanes, suggesting that the antibody is binding to glycoproteins (Figure 4.3B). Several bands from each isolate were excised from corresponding coomassie-stained gels, destained, digested with trypsin and analyzed by LC-MS/MS. These results identified the presence of Hex, HexNAc and HexNAc-Hex (Figures 4.8-4.15) as part of glycoproteins in all three isolates but did not yield any data to support the presence of a sialic acid. Due to background binding found naturally in the rabbit, the manufacturer of the α-GM1 ganglioside antibody states that there is consistent cross-reactivity of the commercial antibody with asialo-GM1 ganglioside structures (Abcam, personal communication). Knowing this, the lysates were examined again using α-asialo-GM1 ganglioside which reacts with the GM1 structure lacking the sialic acid branch. Once again, the antibody bound to proteins in the lanes untreated with proteinase K and the reactive bands showed some similarities to those recognized by the α-GM1 ganglioside antibody (Figure 4.3C). After seeing evidence of multiple glycoproteins reacting with these antibodies, we decided to sequence the genomes of these three strains and investigate their glycoproteome to determine the identity of the glycoproteins responsible for ganglioside mimicry and to characterize this general glycosylation system in the *Enterococcus* genus.

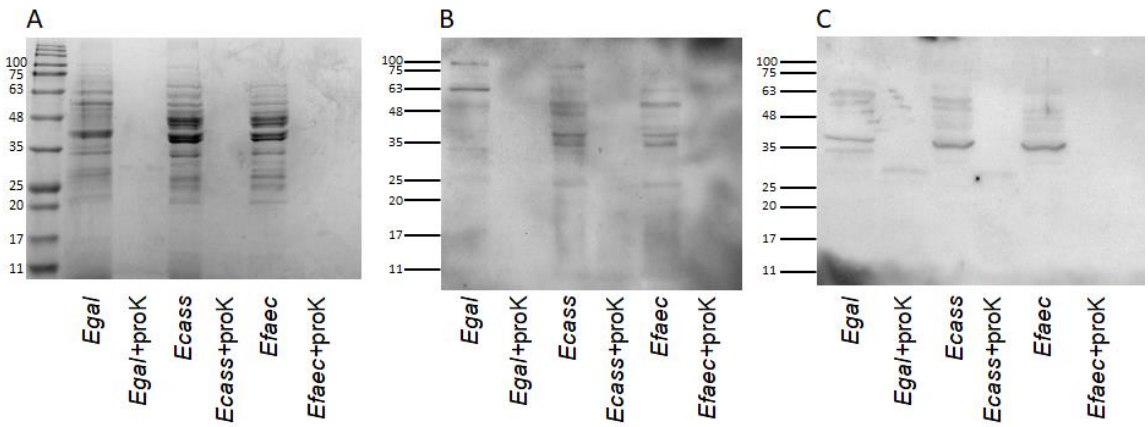

Figure 4.3. All three *Enterococcus* isolates produce glycoproteins that mimic gangliosides. Lysates of *E. gallinarum* EGM181, *E. casseliflavus* EGM182 and *E. faecalis* EGM 183 were treated with proteinase K or left untreated before separation by SDS-PAGE and Coomassie stained or western blotted using α-GM1 or α-asialo GM1-ganglioside antibodies. Molecular weights are shown in kDa.

Genome sequencing of *E. gallinarum* EGM181, *E. casseliflavus* EGM182 and *E. faecalis* EGM183.

The PacBio RSII next generation sequencing platform was used to sequence the full genome of *E. gallinarum* EGM181 and *E. casseliflavus* EGM182. For *E. gallinarum* EGM181, the strain has a circular genome of 3,726,057 bp with an average GC-content of 40.1%. In addition, the strain possesses two plasmids, pEGM181-1 (24,463 nt) and pEGM181-2 (24,463 nt). The circular genome for *E. casseliflavus* EGM182 is 3,450,044 bp in length, with an average GC-content of 42.6%. This strain contains three plasmids, pEGM182-1 (75,933 nt), pEGM182-2 (73,709 nt) and pEGM182-3 (20,183 nt). For *E. faecalis* EGM183, Oxford Nanopore Technologies libraries were assembled to reveal a circular genome of 2,693,441 bp with an average GC-content of 37.8%. This strain possesses one plasmid called pEGM183 (73,653 nt). The genomes were annotated using the NCBI Prokaryotic Genome Annotation Pipeline (PGAP) and generally confirmed by

RAST (Rapid Annotation using Subsystem Technology; v. 2.0, http://rast.nmpdr.org/) comparisons (369). The resulting analysis is summarized in Table 4.1.

Table 4.1. Genome statistics of *Enterococcus* strains

	E. gallinarum **EGM181**	***E. casseliflavus*** **EGM182**	***E. faecalis*** **EGM183**
Accession numbers of chromosomes and plasmids	CP050485 CP050484 CP050486	CP050490 CP050488 CP050489 CP050487	CP050491 CP050492
Chromosome size	3,726,057	3,450,044	2,693,441
GC-content	40.1%	42.6%	37.8%
Plasmids/size	pEGM181-1: 24,463 nt pEGM181-2: 42,043 nt	pEGM182-1:75,933 nt pEGM182-2:73,709 nt pEGM182-3:20,183 nt	pEGM183:73,653 nt
Protein-coding sequences	3,520	3,330	2,534
Pseudogenes	86	109	29
Complete rRNA	5	5	4
tRNAs	64	61	60

Analysis was also done to determine the core (present in 99% of strains) and shell genes between the three isolated *Enterococcus* strains (present in > 0 but ≤ 2 strains) at varying protein identity cutoffs in order to identify common genes between the strains that could be involved in protein glycosylation and ganglioside-mimicry (Table 4.2). A comparison was also made with other *Enterococcus* strains to determine the extent to which

these genes could be shared among other species in the genus. This separated core (present in 99% of strains) from shell (present in ≥ 2 but < 14 strains) and cloud (present in > 2 strains) genes among 15 different *Enterococcus* strains (Table 4.2). These results are also represented in a ring image using *E. gallinarum* EGM181 as a reference strain to compare to the other 14 *Enterococcus* strains including the other two ganglioside-mimicking isolates (Figure 4.4). In addition to a wide array of carbohydrate degrading enzymes, these organisms possess many genes related to the generation of sugar structures. For our isolates, this includes proteins involved in the synthesis of wall teichoic and lipoteichoic acids, poly-*N*-acetyl glucosamine and possibly extracellular polysaccharide. Enzymes were present for the synthesis of hexoses and *N*-acetylhexosamines; however, none of the genome comparisons suggested evidence for sialic acid biosynthesis. Other interesting proteins found in at least one of the strains included: an ESAT-6 secretion system, hemolysin, bacteriocin, several antibiotic resistance mechanisms including multi-drug efflux pumps and a CRISPR system.

Table 4.2. Number of core genes shared among *Enterococcus* strains

		95% Identity	**90% Identity**	**85% Identity**	**80% Identity**	**75% Identity**	**70% Identity**	**65% Identity**
Three ganglioside mimicking *Enterococcus* isolates	**Number of core genes (99% strains)**	28	92	225	404	556	730	870
	Number of shell genes (0 < strains =>2)	9,038	8,542	7,928	7,227	6,619	6,016	5,554
Total 15 *Enterococcus* sp. strains	**Number of core genes (99% strains)**	19	98	215	364	512	656	778
	Number of shell genes (2 <= strains <14)	5,423	5,321	5,111	4,816	4,548	4,269	4,024
	Number of cloud genes (<2 strains)	10,480	9,235	8,415	7,634	6,959	6,346	5,814

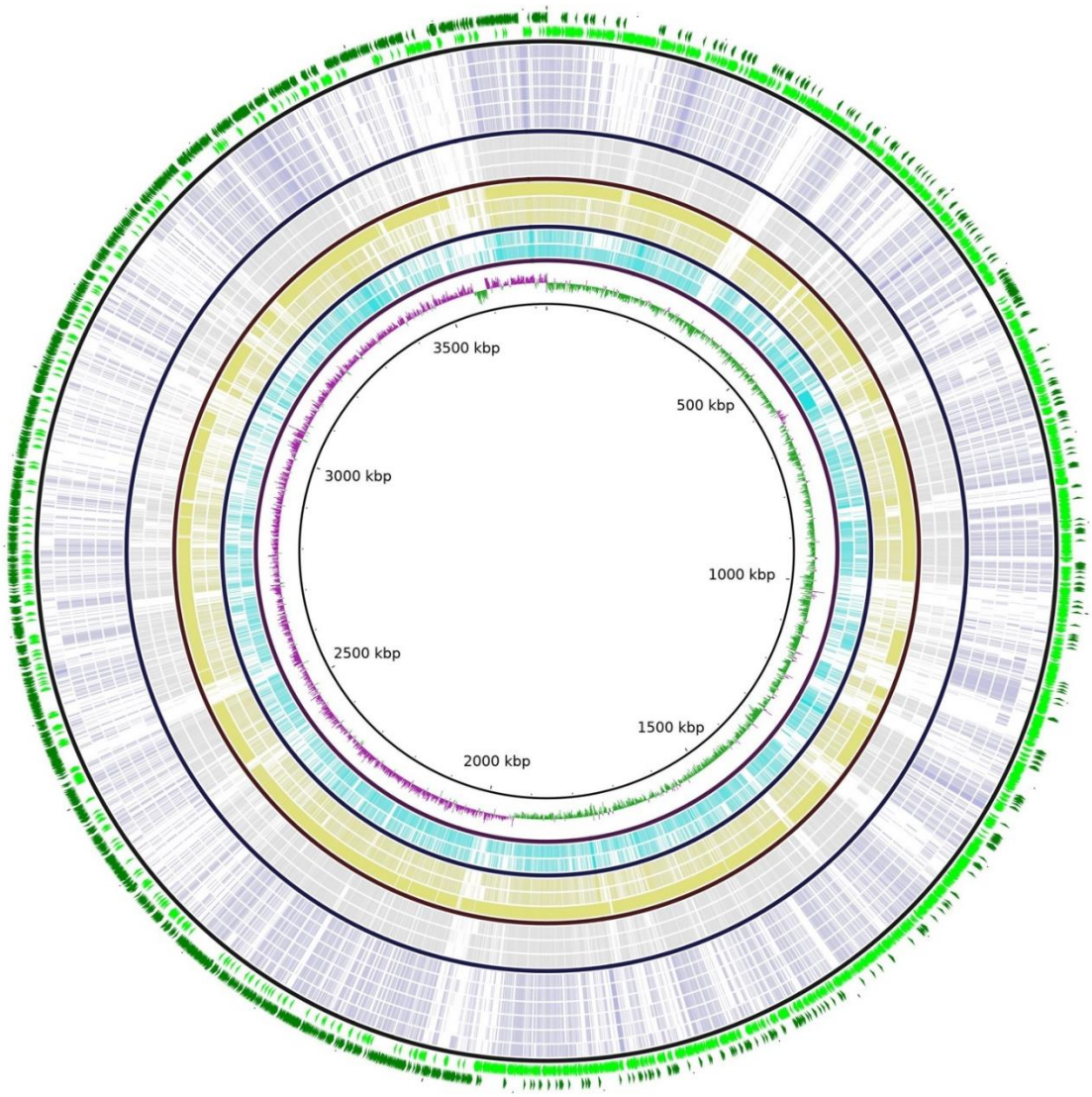

Figure 4.4. BLAST Atlas comparing *Enterococcus gallinarum* str. EGM181 against the other two *Enterococcus* strains that mimic gangliosides and strains of *Enterococcus* species using blastn with an upper identity threshold of 75% and lower identity threshold of 50%. Inner to outer ring: (1) GC skew; (2) *E. casseliflavus* str. EGM182; (3) *E. faecalis* str. EGM183; (4) *E. gallinarum* str. FDAARGOS_163; (5) *Enterococcus* sp. str FDAARGOS_375; (6) *Enterococcus* sp. str. M190262; (7) *E. casseliflavus* str. 4928STDY387870; (8) *E. casseliflavus* str. EC-369; (9) *E. casseliflavus* str. EC20; (10) *E. faecalis* str. C25; (11) *E. faecalis* str. CVM_N60443; (12) *E. faecalis* str. DM01; (13) *E. faecalis* str. C54; (14) *E. faecalis* str. H25; (15) *E. faecium* str. FA3; (16) *E. gallinarum* str. EGM181 Forward CDSs; (17) *E. gallinarum* str. EGM181 Reverse CDSs. Solid black rings represent breakage between different *Enterococcus* species groups, based on color differences: light blue – *Enterococcus* strains sequenced for this study; light yellow – *E. gallinarum* and unidentified species; grey – *E. casseliflavus* strains; light purple – *E. faecalis* and *E. faecium* strains. Image generated with BRIG program.

Glycoproteomic analysis reveals general O-linked protein glycosylation system

With the genomes of each strain sequenced, glycoproteomic analysis could now be performed for both *E. gallinarum* EGM181 (Table 4.3) and *E. casseliflavus* EGM182 (Table 4.4) specifically looking for peptides that contain Hex, HexNAc or HexNAc-Hex modifications that were previously observed by LC-MS/MS. Candidate glycoproteins identified for *E. gallinarum* EGM181 and *E. casseliflavus* EGM182 are listed in Tables 4.3 and 4.4 respectively including the protein name, the peptide that was modified, and the type of modification observed. The criteria inclusion in this list were proteins that were detected using more than one dissociation method, or more than one protein identification software. Among the resulting peptides, increased interest was given to proteins that were modified with a HexNAc-Hex, as this is would closely resemble asialo-GM1 ganglioside, since the glycan is predicted to be Gal-GalNAc-S/T. There were 3 HexNAc-Hex modified proteins from *E. gallinarum* EGM181 that were of particular interest. Protein >fig|1353.30.peg.11, annotated as an LSU ribosomal protein L9p, had one peptide that Byonic detected 6 times from CID and EThcD and a peptide-spectrum match score (PSMs) of 39. Protein >fig|1353.30.peg.1234 (example spectrum shown in Figure 4.5), annotated as a 6-phosphogluconate dehydrogenase, had 3 peptides detected by Byonic 6 times from CID and EThcD and a PSMs of 77. Finally, protein >fig|1353.30.peg.3571, annotated as DNA-directed RNA polymerase beta 39; subunit, had one peptide detected 6 times in Byonic by all three dissociation methods and a PSMs of 196. There were also 3 distinctive HexNAc-Hex-modified proteins listed for *E. casseliflavus* EGM182. Protein >fig|37734.44.peg.1236, annotated as “tyrosine-protein kinase EpsD”, having peptides detected by both Byonic and PD with a PSMs of 53.

Protein >fig|37734.44.peg.2283, annotated as an “ABC-transporter (ATP-binding protein) possibly involved in cell wall localization and side chain formation of rhamnose-glucose polysaccharide”, with 5 different peptides detected by Byonic from all three different dissociation methods and a PSMs of 38. Lastly, protein >fig|37734.44.peg.3362 (example spectrum shown in Figure 4.6), annotated as "DNA-directed RNA polymerase beta' subunit", where Byonic detected a peptide that was modified with 2 HexNAc-Hex glycans 11 different times from all three dissociation methods and a PSMs of 303. These glycoproteins in addition to the others listed in Tables 4.3 and 4.4 point to the presence of a general O-linked protein glycosylation pathway that may be common between *Enterococcus* species.

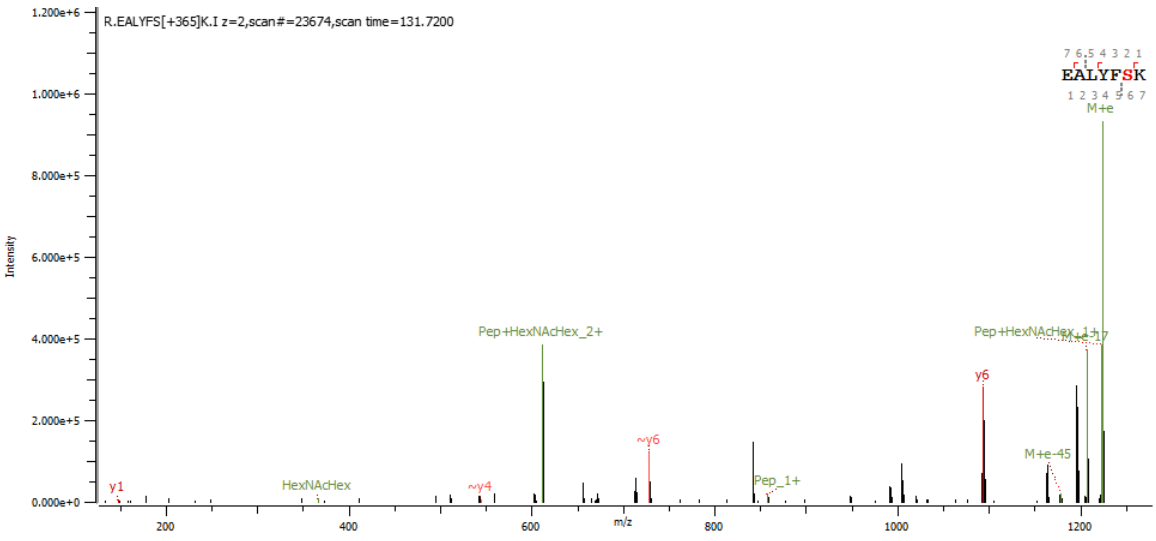

Figure 4.5. Glycopeptide spectrum of a peptide modified with HexNAc-Hex from *E. gallinarum* EGM181. The spectrum displayed is of protein >fig|1353.30.peg.1234.

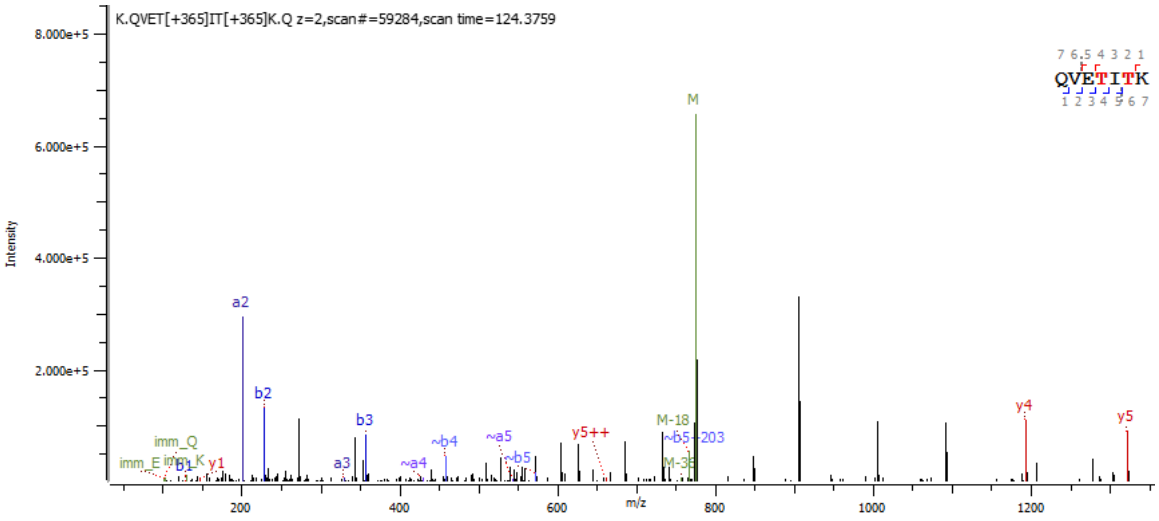

Figure 4.6. Glycopeptide spectrum of a peptide modified with HexNAc-Hex from *E. casseliflavus* EGM182. The spectrum displayed is of protein >fig|37734.44.peg.3362.

Table 4.3. A list of proposed glycoproteins, identified by mass spectrometry from *E. gallinarum* EGM181 lysate. This table includes the protein annotation, total protein coverage (Cov), peptide spectrum match score (PSMs), modified peptide, type of glycan modification and number of instances each peptide was found with Byonic (B) and PD (P).

ID	Protein annotation	Cov	PSMs	Modified peptide	Mass shift	Glycan	B	P
5	DNA gyrase subunit B	21	35	K.GALEISNLPGK.L	S[+162]	1xHex	2	0
				R.TVTDR.L	T[+162]*2	2xHex	1	0
11	LSU ribosomal protein L9p	34	39	R.ALGYTK.V	T[+365]	1x HexNac-Hex	6	0
42	RecA protein	22	32	R.GRIVEVYGPESSGK.T	S[+203]	1xHexNAc	0	7
191	Foldase protein PrsA precursor @ Foldase clustered with pyrimidine conversion	39	78	K.QYGDSDKFESALEASGLTK.K	S[+162]; T[+162]	2xHex	4	4
231	GTP pyrophosphokinase, (p)ppGpp synthetase I	10	25	K.LVATSK.A	T[+162]	1xHex	8	0
				R.ITVSIQNLTHLK.S	S[+203]; T[+365]*2	1xHexNAc; 2xHexNAc-Hex	0	1
437	Histidyl-tRNA synthetase	19	32	K.QLGLSQLR.L	S[+365]	1HexNAc-Hex	2	0
503	4-hydroxy-tetrahydrodipicolinate synthase	8	15	K.AAVSLLGK.S	S[+162]	1xHex	5	0
				K.SDLHYR.L	S[+203]	1xHexNAc	1	0
790	Lysine-arginine-ornithine-binding periplasmic protein precursor	39	40	K.EISEK.Y	S[+203]	1xHexNAc	1	0
				K.AKEDNSLSRVQESK.E	S[+162]	1xHex	0	9
869	Branched-chain amino acid ABC transporter, amino acid-binding protein	13	6	K.SAVVLGLTEGK.E	S[+203]	1xHexNAc	0	4
945	Signal recognition particle, subunit Ffh SRP54	24	56	R.IAAGSGNSVVEVNRMIK.Q	S[+162]	1xHex	0	1
				R.GGAALSIR.Q	S[+162]	1xHex	2	0
				R.GGAALSIR.Q	S[+162]	1xHexNAc	1	0
1234		52	77	R.EALYFSK.I	S[+365]	1x HexNac-Hex	3	0

	6-phosphogluconate dehydrogenase, decarboxylating			R.KDDLGTGK.P	T[+365]	1x HexNac-Hex	2	0
				R.TGSKTEEVVK.E	S[+365], T[+162]*2	1xHexNAc-Hex; 2xHex	1	0
1257	Methionine ABC transporter ATP-binding protein	21	8	K.EISRVFQDPRMGTAVR.L	S[+203]; T[+203]	2xHexNAc	0	6
1485	tRNA:m(5)U-54 MTase gid	10	18	K.SRYDK.G	S[+365]	1xHexNAc-Hex	9	0
1492	LacX protein, plasmid	8	20	K.NDALIYETKGLNSFSIR.S	S[+162]; S[+162]	1xHex	0	3
				K.TGIQR.L	T[+162]	1xHex	4	0
				R.LTHEMFK.N	T[+203]	1HexNAc	15	0
				R.LTHEMFKNDALIYETK.G	T[+365]	1xHexNAc-Hex	1	0
				R.TLGQTNTDLR.L	T[+365]	1xHexNAc-Hex	1	0
1571	Branched-chain amino acid aminotransferase	15	7	R.ALYDELTGIQFGER.K	T[+203]	1xHexNAc	1	0
				R.LNRSAR.R	S[+203]	1xHexNAc	1	0
2016	ClpB protein	25	44	R.VEMNSMPTELDQVTR.R	T[+365]	1xHexNAc-Hex	1	0
				K.AIDLIDEASATIR.V	T[+203]	1xHexNAc	0	2
2028	Ribonucleotide reductase transcriptional regulator NrdR	27	18	R.FTTFER.I	T[+365]	1xHexNAc-Hex	1	0
				R.PVTMEQMEK.I	M[+16]; T[+365]	1xOxidation; 1xHexNAc-Hex	1	0
2040	Transcription accessory protein (S1 RNA-binding domain)	10	23	R.NELTEK.A	T[+203]	1xHexNAc	4	0
				R.YGVQMIAIGNGTASR.E	M[+16]; T[+162]; S[+162]	1xOxidation; 2xHex	0	1
2060	ATP-dependent DNA helicase UvrD/PcrA	15	35	K.GAAASFQPKVFK.P	S[+162]	1xHex	3	0
				K.GAAASFQPK.V	S[+203]	1xHexNAc	3	0
2090	Excinuclease ABC subunit B	17	20	R.SLVQTIGRAARNSDGK.V	S[+203]*2; T[+203]	3xHexNAc	0	4
2119	Translation initiation factor 2	21	41	R.SSAK.P	S[+365]	1xHexNAc-Hex	3	0

2197	Phosphate starvation-inducible protein PhoH, predicted ATPase	13	7	R.GINISTPDVITALNMANK.G	M[+16]; S[+162]; T[+162]	1xOxidation; 2xHex	0	4
2221	ABC transporter, ATP-binding protein			K.SLLIIK.T	S[+162]	1xHex	2	0
				K.TYSLGMR.Q	S[+203]	1xHexNAc	3	0
				R.MIVGLMKHNKGSITIMGNSLETSFK.A	M[+16]; S[+162]; S/T[+162]	1xOxidation; 2xHex	0	2
2237	conserved hypothetical protein	19	13	R.HVTTER.Y	T[+203]	1xHexNAc	2	0
				K.FLAFLGTSSFTGPVNAAAK.G	T[+162]; T[+203]	1xHex; 1xHexNAc	0	1
3173	Nucleoside-diphosphate-sugar epimerases	18	4	K.ITTNVIKACIESHSK.L	C[+57]; S[+162]; T[+203]*2	1xCarbamidomethyl; 1xHex; 2xHexNAc	0	1
				R.YEQDNIFLSDKFKQAFPDFSITTLEEGIS.R	S[+162]; S[+203]	1xHex; 1xHexNAc	0	3
3268	Chromosome partition protein smc	13	32	K.TVSVR.L	S[+365]	1HexNAc-Hex	2	0
				R.SLQDIQENYAGFYQGVR.L	S[+203]	1xHexNAc	1	0
3308	SSU ribosomal protein S19p (S15e)	30	24	K.LGEFAPTRTYRGHAADDK.K	T[+203]	1xHexNAc	1	14
3571	DNA-directed RNA polymerase beta 39; subunit	42	196	K.QLLTEREYR.E	T[+162]	1xHex	1	0
				K.QVETITK.Q	T[+365]*2	2xHexNac-Hex	6	0
3572	DNA-directed RNA polymerase beta subunit	34	185	K.DISYVR.I	S[+365]	1xHexNAc-Hex	1	0
				R.EIEQQAQTEAK.N	T[+162]	1xHex	2	0
				R.LSALGPGGLTR.D	T[+203]	1xHexNAc	1	0
3632	Peptidoglycan N-acetylglucosamine deacetylase	30	63	K.VTLK.Y	T[+365]	1xHexNAc-Hex	2	0

Table 4.4. A list of proposed glycoproteins, identified by mass spectrometry from *E. casseliflavus* EGM182 lysate. This table includes the protein annotation, total protein coverage (Cov), peptide spectrum match score (PSMs), modified peptide, type of glycan modification and number of instances each peptide was found with Byonic (B) and PD (P).

ID	Protein annotation	Cov	PSMs	Modified peptide	Mass shift	Glycan	B	P
269	SSU ribosomal protein S19p (S15e)	52	50	K.LGEFAPTRTYRGHAADDK.K	T[+203]	1xHexNAc	0	17
448	Pyrroline-5-carboxylate reductase	21	22	K.LADVTEK.A	T[+203]	1x HexNAc	1	0
				K.LADVTEK.A	T[+365]	1x HexNAc-Hex	1	0
490	Iron-sulfur cluster assembly protein SufB	32	70	K.LGIVFTDTDSALK.K	T[+365]	1x HexNAc-Hex	1	0
				K.LVPPTDNK.L	T[+162]	1x Hex	1	0
661	5'-nucleotidase family protein in cluster with NagD-like phosphatase	5	8	R.TVVGDYLSQKYPIQ	S[+162]	1xHex	0	7
1104	Cation-transporting ATPase	6	9	R.DPNAGIFTGK.T	T[+365]	1x HexNAc-Hex	1	0
				R.GLDSFSKK.L	S[+203]	1x HexNAc	1	0
1236	Tyrosine-protein kinase EpsD	72	53	K.ADGTLLVVR.E	T[+365]	1x HexNAc-Hex	1	0
				K.NLYDVVIFDMPPVVAVTDAQIMASK.A	M[+16]; T[+162]; S[+162]	1xOxidation; 2xHex	0	1
				K.TVIDNLSVLTSGPKPPNPSELLGSAR.M	S[+203]*2	2xHexNAc	0	1
1289	ABC transporter, substrate-binding protein (cluster 5, nickel/peptides/opines)	7	11	K.SLRQAMGYAMDNNAIGER.F	M[+16], S[+162]	1xOxidation; 1xHex	0	8
1430	Endonuclease IV	30	20	M.LIGSHVSMSGK.K	S[+203]	1xHexNAc	1	0
				K.GLNEVLEKNQTAQIALETMAGK.G	M[+16]; T[162]	1xOxidation; 1xHex	0	2
1593	Glutamine--fructose-6-phosphate aminotransferase [isomerizing]	27	67	K.GTYPYYMLK.E	T[+162]	1x Hex	1	0
				R.GYDSAGLYVADR.T	S[+162]	1x Hex	1	0
1774	Hypothetical protein	23	9	K.VEDYDTVDGK.N	T[+203]	1xHexNAc	4	0
1783	3-phosphoshikimate 1-carboxyvinyltransferase	30	23	K.ETSR.N	S[+162], T[+162]	1x Hex, 1x Hex	1	0

				K.SISHRSIMFGALAEGTTTVR.N	S[+162]	1xHex	0	1
2040	hypothetical protein	35	19	K.VELLTESEETAQYLDLR.V	T[+162]	1xHex	1	3
2222	GTP-sensing transcriptional pleiotropic repressor codY	52	31	K.VLNSR.F	S[+365]	1xHexNAc-Hex	1	0
				R.ELYPNGLTTIVPIYGAGER.L	T[+203]	1xHexNAc	0	1
2229	DNA topoisomerase I	29	52	K.LPNAESIKEVTDR.L	T[+203]	1xHexNAc	1	0
				R.LIWSR.F	S[+162]	1xHex	1	0
				R.LIWSR.F	S[+203]	1xHexNAc	1	0
				K.QGTVGLITYMRTDSTRIADTAK.G	M[+16]; S[+203]; T[+203]	1xOxidation; 2xHexNAc	0	1
2283	ABC-transporter (ATP-binding protein) -possibly involved in cell wall localization and side chain formation of rhamnose-glucose polysaccharide	33	38	K.IISQIYTPEK.G	S[+365], T[+162]	1x HexNAc-Hex; 1x Hex	1	0
				K.KTFK.Y	T[+365]	1x HexNAc-Hex	1	0
				K.TFK.Y	T[+365]	1x HexNAc-Hex	2	0
				R.LAFSVAIQAK.S	S[+365]	1x HexNAc-Hex	1	0
				R.VEFLISYEVLK.D	S[+365]	1x HexNAc-Hex	1	0
2511	3-dehydroquinate dehydratase I	22	11	K.ELLFTFR.T	T[+365]	1x HexNAc-Hex	1	0
				R.LMGIITK.A	M[+16], T[+203]	1x Oxidation, 1x HexNAc	1	0
2513	Lipoteichoic acid synthase LtaS Type IIc	5	7	R.LQQPFYSK.F	S[+203]	1x HexNAc	2	0
2554	FIG00632534: hypothetical protein	70	55	K.VTETKGK.L	T[+203]	1xHexNAc	1	0
				K.LTGDDSEELKGKTQNK.Y	T[+365]	1xHexNAc-Hex	0	1
2642	UDP-N-acetylglucosamine 1-carboxyvinyltransferase	22	39	K.LQQLGASVER.V	S[+203]	1x HexNAc	14	0
				K.LIEMGAEVTEVAEGIR.V	T[+162]	1xHex	0	1
2726	Redox-sensing transcriptional repressor Rex	31	23	R.ITAPK.G	T[+365]	1x HexNAc-Hex	3	0

3125	Guanosine-3',5'-bis(diphosphate) 3'-pyrophosphohydrolase / GTP pyrophosphokinase, (p)ppGpp synthetase II	17	47	K.LVATSK.A	T[+162]	1x Hex	8	0
3184	Cell division protein FtsH	47	145	R.IVGEYNEEQTVSNDNSLSVLGNTQASSTR.F	S[+162]	1xHex	1	5
3194	ErfK/YbiS/YcfS/YnhG family protein, putative	14	10	K.SADATLEK.G	T[+162]	1x Hex	1	0
				K.TEIDGIDISNK.T	S[+162]	1xHex	0	2
3362	DNA-directed RNA polymerase beta' subunit	57	303	K.QVETITK.Q	T[+365]*2	2x HexNAc-Hex	11	0
				R.GAPLTEGSIDPK.Q	S[+162], T[+162]	2x Hex	1	0

Training with whole cell *E. casseliflavus* EGM182 increases macrophages proinflammatory response to GBS-associated antigen

In chapter 3, we examined the impact of ganglioside-mimicking bacteria on pro-inflammatory cytokine release using the THP-1 human macrophage cell line as a model (370). We discovered that macrophages trained with bacteria expressing ganglioside-mimicking LOS at low multiplicity of infection (MOI) induce tolerance toward GBS-causing antigens. Due to these results, we decided to test one of the ganglioside-mimicking *Enterococcus* isolates using this same system. Macrophages were exposed to *E. casseliflavus* EGM182 at differing low MOI levels prior to being challenged with *C. jejuni* HS:19, at an MOI of 5, to determine how this training would impact the inflammatory response directed toward a known GBS-causing pathogen (331). When trained with *E. casseliflavus* EGM182, the macrophages showed a trend of heightened pro-inflammatory cytokine production when compared to the untrained control (Figure 4.7). This treatment resulted in statistically significant increases in TNF-α when the training MOI was 1.0 (p =0.0199) (Figure 4.7A), in all three training MOIs for IL-6 (p =0.0154, p =0.0059 and p =0.0035 for MOI 0.01, 0.1 and 1.0 respectively) (Figure 4.7B) and when the training MOI was 0.1 for IL-1β (p =0.0249) (Figure 4.7C). These results suggest that *E. casseliflavus* EGM182 exposure stimulates the immune response against subsequent GBS antigen challenge.

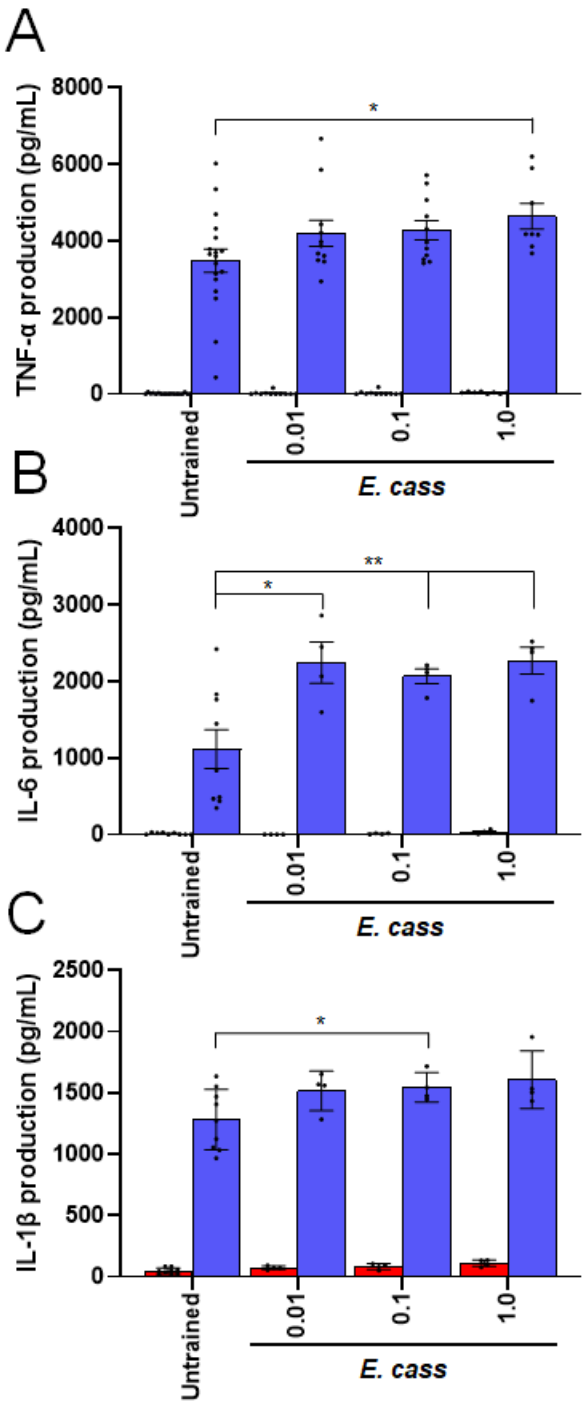

Figure 4.7. Direct measurement of TNF-α, IL-6 and IL-1β from THP-1 macrophages. Macrophages were trained with *E. casseliflavus* EGM182 at the MOI values indicated prior to challenge with *C. jejuni* HS:19 at MOI 5 (blue) or left unchallenged (red).

Discussion

Besides *C. jejuni*, the evidence for ganglioside-mimicry in other bacteria does not generally include definitive structural characterization. For those organisms, ganglioside-mimicry is often reported due to reactivity with CT or antibodies directed against gangliosides (100-102). This was also the basis behind our isolation of *E. gallinarum* EGM181, *E. casseliflavus* EGM182 and *E. faecalis* EGM183. The two former isolates were obtained by a method described previously (6), but at that time they were together in a mixed culture. Once separated, it was clear that both isolates were capable of binding to α-GM1 ganglioside antibodies and likely display some form of ganglioside mimic. The same was true for *E. faecalis* EGM183, which was identified by a different method, but similar patterns to the other isolates when lysate binding to α-GM1 was compared by western blot. These reactive bands disappeared when treated with proteinase K, suggesting that the ganglioside-mimicking glycans were part of several glycoproteins. The presence of glycoproteins in *E. faecalis* has been reported before via lectin binding (239), and this species has also been found to O-glycosylate a bacteriocin with N-acetylglucosamine residues (240). Despite these studies supporting the presence of glycoproteins in *Enterococcus,* there has not been a study that fully explored the glycoproteome of these organisms. In our study, the presence of glycoproteins in all three isolates was further confirmed by performing LC-MS/MS on excised gel slices corresponding to α-GM1 positive bands (Figures 4.8-4.15). The results from these experiments suggested the presence of Hex, HexNAc and HexNAc-Hex, but did not show any evidence of Neu5Ac to point toward GM1 ganglioside mimicry. Given the sensitivity of sialic acid modifications to both heat and acid during sample

preparations and analysis (371), it is possible that this modification was lost during processing of the sample. Alternatively, the glycan could instead be mimicking asialo-GM1 ganglioside, which is an alternate binding ligand for the α-GM1 antibody that is listed by the manufacturer. The latter explanation was supported by western blots showing the binding of α-asialo-GM1 to bands in the lysates for each of the three *Enterococcus* isolates. We also found no evidence of sialic acid biosynthesis genes annotated in the sequenced genomes. In either case, it was clear that these isolates produced multiple glycoproteins and glycoproteomic analysis was warranted.

Full genome sequencing of all three isolates allowed for the comparison of the core genomes between the strains. This analysis showcased the tremendous capacity that these bacteria have for transporting, synthesizing and catabolizing carbohydrates. In order to produce ganglioside mimics, an organism galactose and N-acetylgalactosamine as these monosaccharides are predicted to be part of the structure. There were enzymes present for the biosynthesis of these sugars, including GalE, a 4-epimerase capable of converting UDP-glucose to UDP-galactose (372), and N-acetylgalactosamine 4-epimerase for conversion of UDP-N-acetylglucosamine to N-acetylgalactosamine. The enterococci also possessed multiple annotated glycosyltransferases (GTase), including Gtf, a GTase responsible for O-linked modification of serine-rich repeat proteins in *Streptococcus* species (373). Glycoproteomic analysis suggested numerous glycoproteins are produced by *E. gallinarum* EGM181 and *E. casseliflavus* EGM182. Among them were proteins modified by Hex, HexNAc and HexNAc-Hex residues. We were particularly interested in the HexNAc-Hex residues as those could represent ganglioside-like structures if the HexNAc and Hex residues are confirmed to be GalNAc

and Gal. Several prominent proteins emerged as the most likely to be modified with HexNAc-Hex, and these will be the target for future analysis to investigate the glycan structure. In the coming months, the glycoproteome analysis of *E faecalis* EGM183 will be completed and the prominent glycoproteins will also be identified for this strain. The isolation of these proteins in high amounts will allow for further characterization of their glycans using NMR spectroscopy and more concrete proof of ganglioside mimicry. All the information taken together from genome sequencing these strains and analyzing their glycoproteomes suggests that there may be a common protein glycosylation system among enterococci.

Given that these organisms represent potential ganglioside-mimicking commensal bacteria, we also wanted to test the strains for their potential impact on the host immune system following challenge with a ganglioside-mimicking pathogen. In Chapter 3, we discovered that low-dose exposure to bacteria displaying GM1-ganglioside receptors on their lipooligosaccharides could help tolerize the immune response against subsequent challenge with a *C. jejuni* strain displaying a GBS-associated antigen (370). The macrophage experiments performed here expand upon that study by examining the effect of *E. casseliflavus* EGM182 using the same protocol. This isolate represents a vastly different bacterium than those that were studied in our previous work. *E. casseliflavus* EGM182 is a Gram-positive bacterium with ganglioside-mimicking structures present on glycoproteins rather than being displayed on lipooligosaccharides. From the results of this experiment, it was concluded that the presence of *E. casseliflavus* EGM182 stimulates macrophages to produce more inflammatory cytokines upon subsequent exposure to bacteria displaying GBS-

associated antigen. This suggests that if this organism were a part of the natural microbiome, its host may have an increased susceptibility to GBS. However, since the macrophages were treated with intact *E. casseliflavus* cells, we cannot conclude that this result was related to ganglioside-mimicking glycoproteins or other antigens from the cell surface. To rectify this issue, purification and characterization of these glycoproteins is again necessary. By repeating the experiment with exposure to the purified glycoprotein, we can re-evaluate if the stimulation response was due to ganglioside-mimicry or alternate surface antigens.

In conclusion, this study presents the full genome sequences of three *Enterococcus* species isolated from chicken ceca that mimic ganglioside structures using glycoproteins. The glycoproteome of *E. gallinarum* EGM181 and *E. casseliflavus* EGM182 are also reported, revealing numerous glycoproteins modified with different glycan structures. These results suggest a general protein glycosylation system that may be common across the *Enterococcus* genus.

Methods

CTB probe colony lift of chicken cecal bacteria

Serial dilutions of chicken cecal contents were made using PBS and 30 µL of each dilution was spread on a brain heart infusion agar plate, then incubated at 37 ^{o}C in anaerobic conditions. Those plates with single isolated colonies were then chosen for use in a colony lift. Nitrocellulose membranes were cut to the size of an agar plate, briefly soaked in PBS, dried and then laid on each plate to absorb colonies. The plates were then incubated as before in order for the colonies to regrow. The resulting membranes were blocked in Odyssey Blocking Buffer (Li-Cor) overnight at 4^{o}C. The membranes were then incubated

with CTB (1:100 000 in blocking buffer) for 1 h, then rinsed 3 times with PBST followed by 3 PBST washes for 5 min, 10 min and 5 min respectively. The membranes were then incubated with rabbit anti-CTB (1:6500 in blocking buffer) for 1 h, washed as before, then incubated with IRDye® 800CW Goat anti-rabbit IgG (Li-Cor) antibody (1:15 000 in blocking buffer) and washed again as before. Membranes were imaged using the Li-Cor Odyssey for positive colonies. Those colonies were then grown from the original plate and made into frozen stocks.

PCR amplification of *van-C1*, *van-C2* and *van-C3*

Colony PCR was employed in order to differentiate between *E. gallinarum* and *E. casseliflavus.* After being streaked from freezer stocks, three independent single colonies for each gene were selected from plates containing *E. gallinarum* EGM181 or *E. casseliflavus* EGM182 and used in PCR reactions. The *vanC1*, *vanC2* and *vanC3* genes were amplified by PCR using the following primers: vanC-1-1 (5'-GAAAGACAACAGGAAGACCGC-3') and vanC-1-2 (5'-ATCGCATCACAAGCACCAATC-3'), vanC-2-1 (5'- CGGGGAAGATGGCAGTAT-3') and vanC-2-2 (5'- CGCAGGGACGGTGATTTT-3'), vanC-3-1 (5'-GCCTTTACTTATTGTTCC-3') and vanC-3-2 (5'- GCTTGTTCTTTGACCTTA-3'). The cycle used annealing temperatures of 54 ºC, 52 ºC, and 45ºC for *van-C1*, *van-C2* and *van-C3* respectively and the resulting products were migrated on a 1.5% agarose gel at 100V.

Generation of *Enterococcus* lysates

E. gallinarum, E. casseliflavus and *E. faecalis* were streaked from frozen onto brain-heart infusion (BHI) agar, grown overnight at 37 ºC and then used to inoculate 5 mL BHI overnight cultures. These overnight cultures were then used to inoculate larger 500

mL BHI cultures of each species and left to grow over 2 days. The resulting cultures were centrifuged for 30 min at 4420xg and after removing the supernatant, the pellet was washed three times with 30 mL of PBS before being resuspended in either PBS (for Western blots) or 40 mM tris (pH 8.0, for acetone precipitation) and lysed using the Emulsiflex C5 homogenizer (Avestin).

Coomassie staining and anti-ganglioside western blots

Cell lysates were first mixed with Laemmli buffer (100 mM Tris-Cl (pH 8.0), 2% β-mercaptoethanol, 4% SDS, 0.2% bromophenol blue, 0.2% xylene cyanol, 20% glycerol) and boiled at 95 °C before being migrated on 12.5% SDS-PAGE gels, first at 110V for 10 minutes to pre-stack followed by 170V until the dye-front reached the bottom of the gel (approx. 45 min). Once migration was finished, the gels were either stained using Coomassie brilliant blue for 1 hour, de-stained overnight and imaged using the ChemiDoc XRS System (BioRad) or transferred to a nitrocellulose membrane via wet transfer. Following western transfer, membranes were blocked in blocking buffer (5% skim milk in PBS with 0.05% Tween-20) for 1 hour, then incubated overnight with rabbit α-GM1-ganglioside antibody (Abcam) or rabbit α-asialo-GM1-ganglioside antibody (Abcam) (1:5000 in blocking buffer) at 4 °C. The membrane was then quickly rinsed with PBST (PBS with 0.05% Tween-20) 3 times and washed with PBST 3 times for 5 min. Next, the membrane was incubated with goat α-rabbit IgG conjugated to HRP (1:20 000 in blocking buffer) for 1 hour and washed afterward as done above. The membranes were developed using Clarity Western ECL Substrate (BioRad) as directed by the manufacturer. The stained gels and membranes were imaged using the ChemiDoc XRS System (BioRad).

LC MS/MS of excised lysate proteins

Following excision of αGM1-ganglioside antibody-reactive proteins from Coomassie-stained gels, destaining and tryptic digest were performed using the following protocol. Gel pieces were initially cut into small cubes (approximately 1mm) and 100 µL of acetonitrile:NH_4HCO_3 (1:1) was added and incubated for 30 min at room temperature to remove the stain. The supernatant was removed and 100 µL of acetonitrile was added and incubated for another 20-30 min. These first two steps were repeated until the stain was fully removed from the gel pieces. The supernatant was removed and enough DTT (25 mM) was added to cover the gel pieces, then incubated at 56 °C for 30 min. Once cooled to room temperature, the supernatant was discarded and 200-500 µL of acetonitrile was added and incubated at room temperature for 10 min. The acetonitrile was then removed and 100 µL of 90 mM iodoacetamide was added to incubate for 20 min at room temperature in the dark. The supernatant was discarded and 200-500 µL of acetonitrile was added and incubated at room temperature for 10 min. Enough trypsin digest buffer (NH_4HCO_3) was then added along with trypsin (Promega, 1:20) to cover the gel pieces and left for 30 min at room temperature before incubating for 16-18 h at 37 °C. Once finished, 500 µL of 1 part H_2O and 2 parts 66% acetonitrile, 5% formic acid solution was added and kept at room temperature for 15 min. The supernatant was then collected and this was repeated 1-2 more times before combining the supernatants and filtering through a 2 µm filter. The released peptides were dried by speed vac (no heat), then trypsin digestion buffer was added and heated to 100 °C for 5 min to deactivate remaining trypsin before analysis by LC MS/MS.

The glycoprotein digest was analyzed using an Orbitrap Fusion Tribrid mass spectrometer (ThermoScientific) that is equipped with a nanospray ion source and connected to a Dionex binary solvent system. Chromatographic separation of samples was achieved using pre-packed nano-LC columns (15 cm length, 75 µm internal diameter), that were filled with 3 µm C18 packing material (reverse phase). Precursor ion scanning was acquired at 120000 resolution using an Orbitrap analyzer and subsequent MS/MS fragmentation was done on precursors detected at a time frame of 3 secs using the Orbitrap analyzer at 15000 resolution or in ion trap. The counts needed to trigger an MS/MS event set to 1000 and this was done using HCD (Higher-energy Collisional Dissociation) product triggered CID (Collision-Induced Dissociation) (HCDpdCID). Charge state screening was enabled, and precursors were excluded if they had a charge state of +1, or the charge state was unknown (positive-ion mode). Dynamic exclusion was also enabled (exclusion duration of 30 secs). Data analysis was performed by with Xcalibur 4.2.

Genomic DNA extraction and sequencing

Genomic DNA was extracted by sucrose-tris w/ phenol/chloroform cleanup extractions. Briefly, bacteria were harvested and resuspended in 1.5 mL of 10% (w/v) sucrose, 50 mM Tris (pH 8.0). A 250-µL aliquot of a 10 mg/mL lysozyme solution (in 250 mM Tris, pH 8.0) and 600 µL of 0.1 M EDTA were then added to the suspension. The suspension was incubated for 10 min on ice, then 300 µL of a 5% (w/v) SDS solution was added, and the mixture was vortexed briefly to clarify the solution. The lysates were incubated sequentially with RNAase (10 mg/mL) and proteinase K (10 mg/mL), and the DNA was spooled following addition of sodium acetate (1/10 volume) and ethanol (2 volumes). DNA was resuspended in 10mM Tris Hcl (pH 8.0), extracted once with

phenol/chloroform (1:1 v/v), once with chloroform, concentrated by ethanol precipitation (2.5:1 v/v) and resuspended in 10mM Tris Hcl (pH 8.0).

Sequencing of *E. gallinarum* str. EGM181 and *E. casseliflavus* str. EGM182 were performed using Pacific Biosciences (PacBio) RSII with 20-kb SMRTbell libraries (374). The PacBio reads were assembled using the hierarchical genome assembly process (HGAP) version 3.0 in single-molecule real-time (SMRT) analysis version 2.3.0 (Pacific Biosciences). The chromosomes and plasmids for each strain were circularized from one contig with overlapping ends. For *E. faecalis* str. EGM183, Oxford Nanopore Technologies (ONT) libraries were prepared with Ligation Sequencing Kit (SQK-LSK109) and Native Barcoding Expansions 1-12 (EXP-NBD104) following standard protocols (1d-native-barcoding-genomic-dna-NBE_9065_v109_revH_23May2018) with the following exceptions: DNA repair and end-prep was for 30 minutes at both 20 °C and 65 °C; all ampure binding on tube rotator was 20min; all elutions were 10min on rotator. Two libraries were made: NB01 library used 1 µg unsheared gDNA. NB02 library used 130ng gDNA (recovered from 5 µg gDNA that was sheared using Covaris g-tubes (D-Mark Biosystems, Woburn, USA) by centrifuging twice at 7,300 rpm for 1 min to approximately 15kb in an Eppendorf minispin, and then size selected by Circulomics Short Read Eliminator SS-100-101-01 (Circulomics, MD, USA) following "Shortreadeliminator5518db_218e8d6a2be74d62a536240ddbf5c9e7" handbook v2). Large library fragments were enriched with L Fragment Buffer. 45fmol of NB01 and 9.5 fmol of NB02 library were pooled before ligation. Fifty fmol of libraries were loaded onto R9.4 flowcells (FLO-MIN 106) on a MinION sequencer (MIN-101B) for a 48 hour run. MinKNOW v2.0 and Guppy v3.3.0 were used for local base calling on a MinIT with

accuracy high basecalling and default Q-score ≥7. De novo assembly was conducted using a genome size of 2.9Mb in Canu.v1.8 on Debian v1.1.8.0 OS w/ 6 cpu's and 16GB memory using a total of 326,776 long reads (mean 12,731bp) totaling 4.1Gbp (1102x coverage).

Additional sequencing for all strains was performed using Illumina MiSeq platform and the KAPA LTP library preparation kit (KAPA Biosystems, Wilmington, MA). The pooled libraries were loaded into a MiSeq system and sequenced using a MiSeq reagent kit v2 with 2 × 250 cycles for *E. gallinarum* str. EGM181 and *E. faecalis* str. EGM183 or 1 x 150 cycles for *E. casseliflavus* str. EGM182 (Illumina, Inc.). A final base call validation of the PacBio contigs was performed using MiSeq reads trimmed using a quality score threshold of 30 or higher (Q30) and the reference assembler within Geneious software v 2020.0.1 (Biomatters, Ltd., Auckland, New Zealand). Error-correction for the ONT/Canu contigs of *E. faecalis* str. EGM183 required identification and correction of several 4-22 nt deletions within the contigs followed by additional rounds of Geneious reference assembly. The final coverage for each strain was >100X. Protein-, rRNA-, and tRNA-coding genes were annotated using the NCBI Prokaryotic Genomes Automatic Annotation Pipeline (PGAAP) (**http://www.ncbi.nlm.nih.gov/genomes/static/Pipeline.html**).

Identification of core and shell genes

The following data analysis pipeline was utilized to determine the core (present in 99% of strains) or shell (0 < strains =>2) genes of the three *Enterococcus* sp. strains (1) *E. casseliflavus* str. EGM182; (2) *E. faecalis* str. EGM183; (3) *Enterococcus gallinarum* str. EGM181] sequenced in this study. First, each genome was annotated with Prokka software (375) using the default parameters with the annotation option --kingdom Bacteria. The output GFF file from Prokka for each of the genomes was used as input files for the

program Roary (376) to calculate the number of core and shell genes between the strains at different protein identity cutoffs (95%, 90%, 85%, 80%, 75%, 70% and 65%). The analysis was run with the following options -e (multiFASTA alignment of core genes using PRANK), -n (fast core gene alignment with MAFFT), and -v (verbose output to STDOUT). A newick file was generated for the three strains by determining the core genome phylogeny of the three strains using the program Parsnp (377). The number of core and shell genes at each of the different protein identity cutoffs were then tabulated using the python script, roary_plots.py with the newick file generated from ParSNP software. The core (present in 99% of strains), shell (2 <= strains <14) and cloud (strains >2) genes of the fifteen *Enterococcus* sp. strains [(1) *E. casseliflavus* str. EGM182; (2) *E. faecalis* str. EGM183; (3) *Enterococcus gallinarum* str. EGM181; (4) *E. gallinarum* str. FDAARGOS_163; (5) *Enterococcus* sp. str FDAARGOS_375; (6) *Enterococcus* sp. str. M190262; (7) *E. casseliflavus* str. 4928STDY387870; (8) *E. casseliflavus* str. EC-369; (9) *E. casseliflavus* str. EC20; (10) *E. faecalis* str. C25; (11) *E. faecalis* str. CVM_N60443; (12) *E. faecalis* str. DM01; (13) *E. faecalis* str. C54; (14) *E. faecalis* str. H25; (15) *E. faecium* str. FA3] were determined as described above.

BLAST Atlas

Visualization of the total genomic differences between all fifteen strains used for genomic comparisons in this study were accomplished by generating a BLAST atlas with the software BLAST Ring Image Generator (BRIG) (378). *Enterococcus gallinarum* str. EGM181 was set as the reference genome for the analysis, and each of the other 14 *Enterococcus* sp. strains were compared using blastn with an upper identity of 75% and a lower identity of 50%. Each group of *Enterococcus* species were color coordinated: light

blue – *Enterococcus* strains sequenced for this study; light yellow – *E. gallinarum* and unidentified species; grey – *E. casseliflavus* strains; light purple – *E. faecalis* and *E. faecium* strains, and each group was separated by a solid black ring.

Acetone precipitation of lysate proteins

E. gallinarum, E. casseliflavus and *E. faecalis* were streaked from frozen onto brain-heart infusion (BHI) agar, grown overnight at 37 °C and then used to inoculate 5 mL BHI overnight cultures. These overnight cultures were then used to inoculate larger 500 mL BHI cultures of each species and left to grow over 2 days. The resulting cultures were centrifuged for 30 min at 4420 x g and after removing the supernatant, the pellet was washed three times with 30 mL of PBS before resuspending in 40 mM tris (pH 8.0) and lysing using the Emulsiflex C5 homogenizer (Avestin). The lysate was then centrifuged at 10 000 x g, then the supernatant was transferred to an acetone-compatible container. At this time, protein concentration was determined using a Bicinchoninic acid (BCA) assay. Four times the sample volume of cold acetone (-20 °C) was added to the samples, vortexed and incubated overnight at -20 °C. The samples were then centrifuged at 10 000xg in a pre-cooled centrifuge (0 °C) and the supernatant was discarded. Milli-Q water was then added to the pellet to create a sample that was approximately 50 mg/mL total protein based on the BCA assays done previously. Four times the sample volume of cold acetone (-20 °C) was added to the samples, vortexed and incubated for 4 hours at -20 °C. Samples were then centrifuged at 27 410xg for 10 min in a pre-chilled centrifuge (0 °C), the supernatant was discarded, and the pellet was dried by heating to 40 °C for 4 min or until the acetone odor was not detectable. The pellet was cooled to room temperature and stored at -20 °C until analysis.

Glycoproteomic analysis

For each sample to be analyzed, roughly 1mg of protein powder was collected in an individual tube in preparation for an in-solution digest. Each sample was reconstituted with freshly made 40mM ammonium bicarbonate, pH 8.1. Samples were reduced for one hour in 10 mM dithiothreitol at 56 °C. Denatured proteins were then alkylated by 55mM iodoacetamide in the dark for 45 minutes with intermittent vortexing. Sequencing grade trypsin (Promega, V5111) was then utilized to digest proteins overnight at 37 °C with gentle vortexing. Resulting peptides were desalted via reverse-phase cleanup using C18 spin columns (The Nest Group, SMM SS18V). Following elution from the C18 spin columns, peptides were dried down and then reconstituted in 0.1% formic acid in 5% acetonitrile. Approximately 12 µg of each sample was passed through a 0.2 µm bio-inert membrane tube (PALL, ODM02C35) to remove any residual particulate before prior to being loaded into the autosampler vials. Each sample was injected independently into an Orbitrap Fusion Lumos Tribrid mass spectrometer (Thermo Fisher Scientific) interfaced with an UltiMate 3000 RSLCnano HPLC system (Thermo Scientific). Peptides were resolved on an Acclai PepMap RSLC C18 analytical column (75um ID x 15cm; 2µm particle size) at a flow rate of 200nL/min using a gradient of increasing buffer B (80% acetonitrile in 0.1% formic acid) over 180 minutes. Three separate methods were used for three separate injections of each sample. Data dependent acquisition was carried out using the Orbitrap mass analyzer collecting full scans every three seconds (300–2000 m/z range at 60,000 resolution). The most intense ions that met mono-isotopic precursor selection requirements were selected, isolated, and fragmented based on the three different methods. Precursors were fragmented using either 38% collision-induced dissociation (CID), 25-30-

35% stepped high-energy collision dissociation (sHCD), or they were subject to electron transfer dissociation (EThcD) with calibrated reaction times and 15% supplemental HCD energy. Each precursor selected for fragmentation was added to the dynamic exclusion list and precursors selected twice within 10 seconds were excluded for the following 20 seconds. Fragment ions were detected using the Orbitrap to increase the mass accuracy of each fragment ion present in the ms/ms scans. Raw data for each method was searched separately against the appropriate databases, *Enterococcus casseliflavus*, *Enterococcus gallinarum*, using the Sequest HT search algorithm in Proteome Discoverer 2.2 (Thermo Fisher Scientific) as well as the Byonic search algorithm. Search parameters for both algorithms were set to allow for two missed tryptic cleavages, 20 ppm mass tolerance for precursor ions, and 20 ppm mass tolerance for fragment ions. A fixed modification of carbamidomethylation on cysteine residues and a variable modification of oxidation on methionine residues were enabled to accurately match fragment ions. Additional variable post-translational modifications were added to the search settings to allow for up to two instances of Hex, HexNAc, or HexNAc-Hex per peptide. For each algorithm, the programs create a decoy database, by reversing each sequence in the target database, used to generate known false-positive spectral matches. For Sequest, results are shown to be medium confidence (meaning less than a 5% false discovery rate) or high confidence (less than a 1% false discovery rate). For Byonic, a straight cut at less than 2% false discovery rate was used. For glycopeptide matches, we filtered the data even further to require all precursor masses to be within 10ppm and implemented score requirements. For Sequest, all glycopeptides must have an Xcorr greater than 2.5, 3.0, 4.0 for charge states 2, 3, 4+. All glycopeptides generated by Byonic were required to have a score greater than 50.

THP-1 human monocyte-like cell culturing

The human leukemia monocytic THP-1 cell line was obtained from the American Type Culture Collection (TIB-202) and maintained in RPMI with 2-mM L-glutamine and 10% fetal bovine serum (C-RPMI) at 3-8 × 10^5 cells/mL.

Preparation of paraformaldehyde-treated bacterial cells

C. jejuni HS:19 and *E. casseliflavus* EGM182 were streaked from frozen onto NZCYM and BHI agar plates respectively. *C. jejuni* HS:19 was then incubated in microaerobic conditions at 37 °C for 24 h before being re-streaked and grown again in the same manner. *E. casseliflavus* EGM182 was incubated in atmospheric conditions for 24 h at 37 °C and a colony from the resulting plate was used to inoculate an overnight culture in liquid BHI to be incubated in the same conditions. The resulting growth was then washed in sterile PBS before being resuspended in PBS with 4% paraformaldehyde and incubated at room temperature for 30 min. Following this killing step, the paraformaldehyde was washed away three times with sterile PBS. The killed bacterial suspensions were then counted by Petroff-Hausser and used directly or stored at 4 °C.

THP-1 human monocyte-like cell cytokine release assay

Experiments in THP-1 cells were done as previously described (370). Briefly, monocyte-like THP-1 cells were grown to approximately 8 × 10^5 cells/mL in RPMI with 2-mM l-glutamine and 10% fetal bovine serum (C-RPMI), centrifuged at 0.2 × g for 5 minutes and resuspended in C-RPMI to a concentration of 1× 10^6 cells/mL. Phorbol 12-myristate-13-acetate (PMA) was added to the cells (final concentration 50 nM) for differentiation and the cells were seeded in 48-well tissue culture plates at 4× 10^5 cells/well. Next, the paraformaldehyde-treated *E. casseliflavus* EGM182 intact cells were added to

the wells at varying low multiplicities of infection (MOI). The cells were then incubated for approximately 24 h, their media was then replaced before incubation for 16 more hours. At this point the macrophages were challenged with *C. jejuni* HS19 at a MOI of 5. This mixture was incubated for 24 h, the supernatants were removed and cytokine production was measured using TNF-α (BD-Biosciences), IL-6 (BD-Biosciences) or IL-1β (Invitrogen) ELISA kits.

Acknowledgements

We would like to thank the Veterinary Diagnostics Facility at the University of Georgia for their help with identification of the mixed culture isolates by MALDI-TOF mass spectrometry.

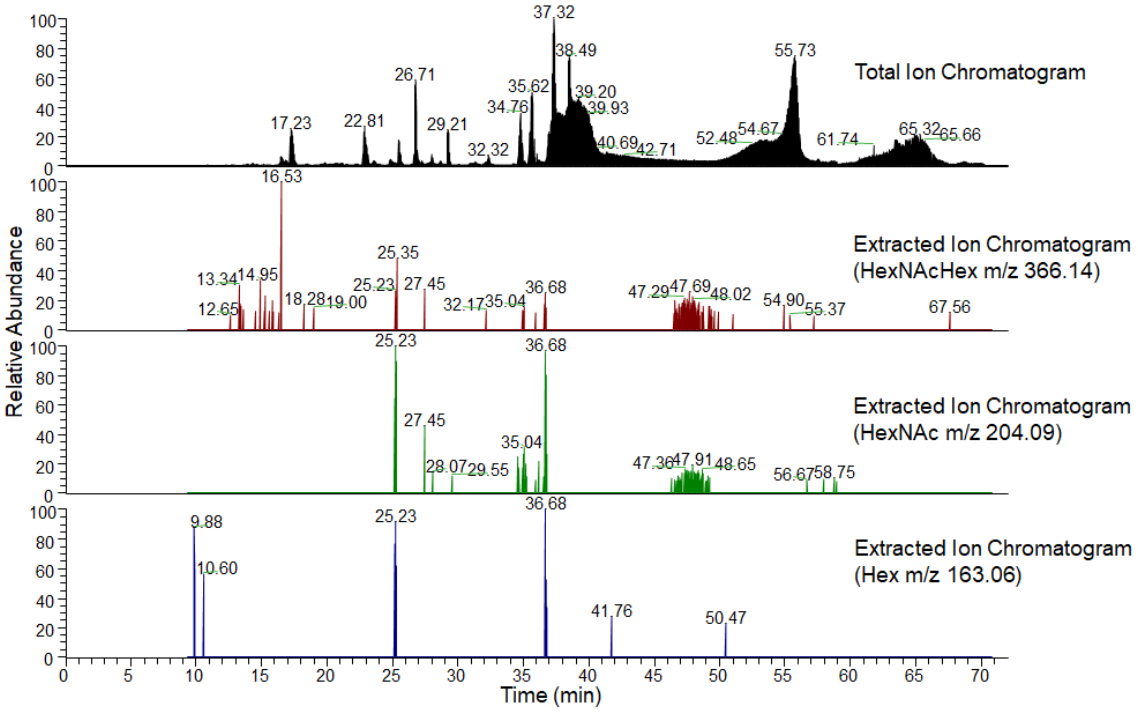

Figure 4.8: Mass spectra of *E. gallinarum* EGM181 lysate proteins excised from an SDS-PAGE gel corresponding to the 55 kDa band. The upper panel shows the total ion chromatogram and the lower panels are extracted ion chromatograms of HexNAc (m/z 204.09), HexNAcHex (m/z 366.14) and Hex (m/z 163.06).

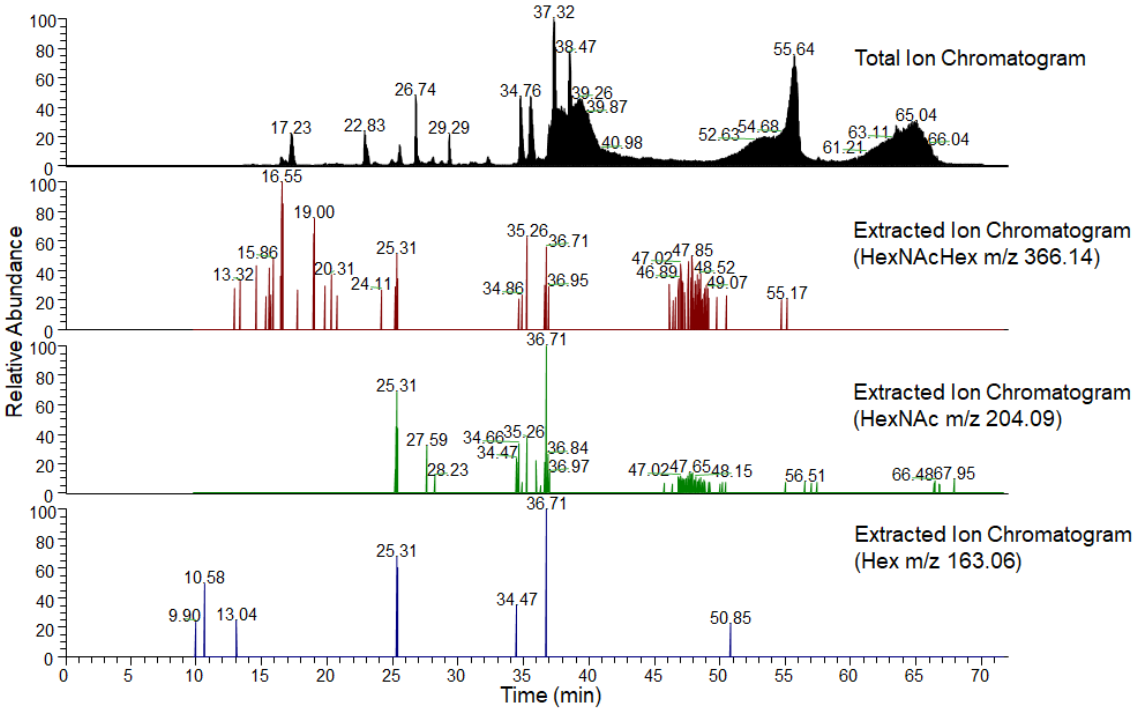

Figure 4.9: Mass spectra of *E. gallinarum* EGM181 lysate proteins excised from an SDS-PAGE gel corresponding to the 75 kDa band. The upper panel shows the total ion chromatogram and the lower panels are extracted ion chromatograms of HexNAc (m/z 204.09), HexNAcHex (m/z 366.14) and Hex (m/z 163.06).

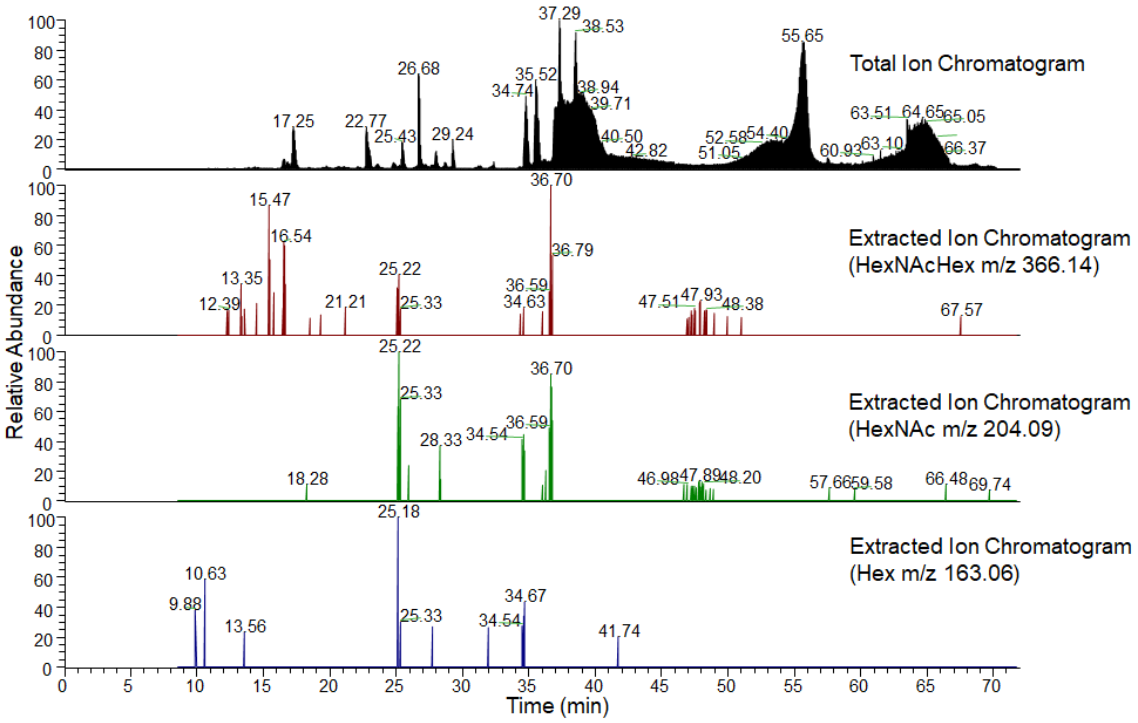

Figure 4.10: Mass spectra of *E. gallinarum* EGM181 lysate proteins excised from an SDS-PAGE gel corresponding to the 100 kDa band. The upper panel shows the total ion chromatogram and the lower panels are extracted ion chromatograms of HexNAc (m/z 204.09), HexNAcHex (m/z 366.14) and Hex (m/z 163.06).

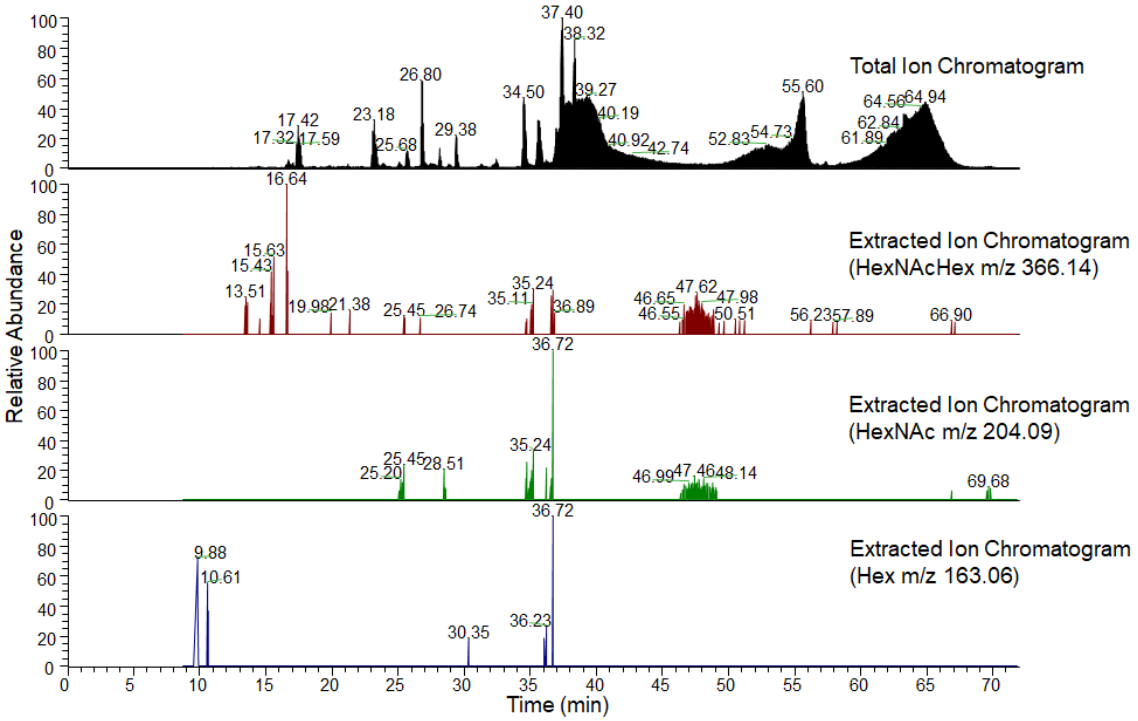

Figure 4.11: Mass spectra of *E. casseliflavus* EGM182 lysate proteins excised from an SDS-PAGE gel corresponding to the 55 kDa band. The upper panel shows the total ion chromatogram and the lower panels are extracted ion chromatograms of HexNAc (m/z 204.09), HexNAcHex (m/z 366.14) and Hex (m/z 163.06).

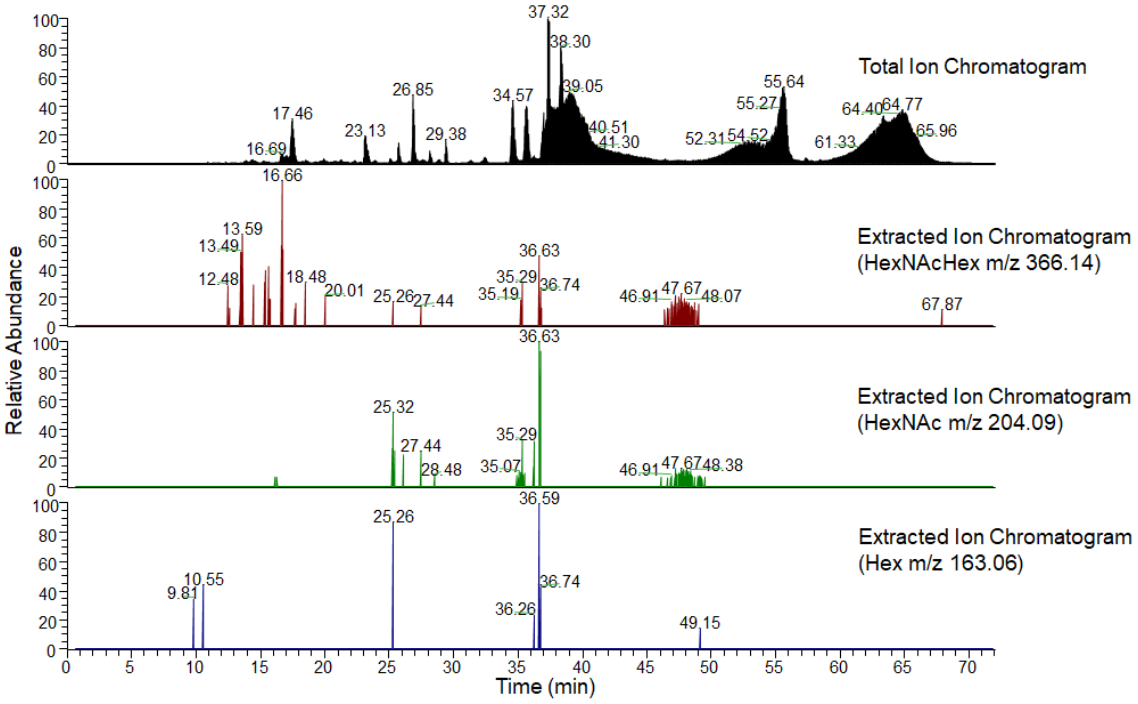

Figure 4.12: Mass spectra of *E. casseliflavus* EGM182 lysate proteins excised from an SDS-PAGE gel corresponding to the 75 kDa band. The upper panel shows the total ion chromatogram and the lower panels are extracted ion chromatograms of HexNAc (m/z 204.09), HexNAcHex (m/z 366.14) and Hex (m/z 163.06).

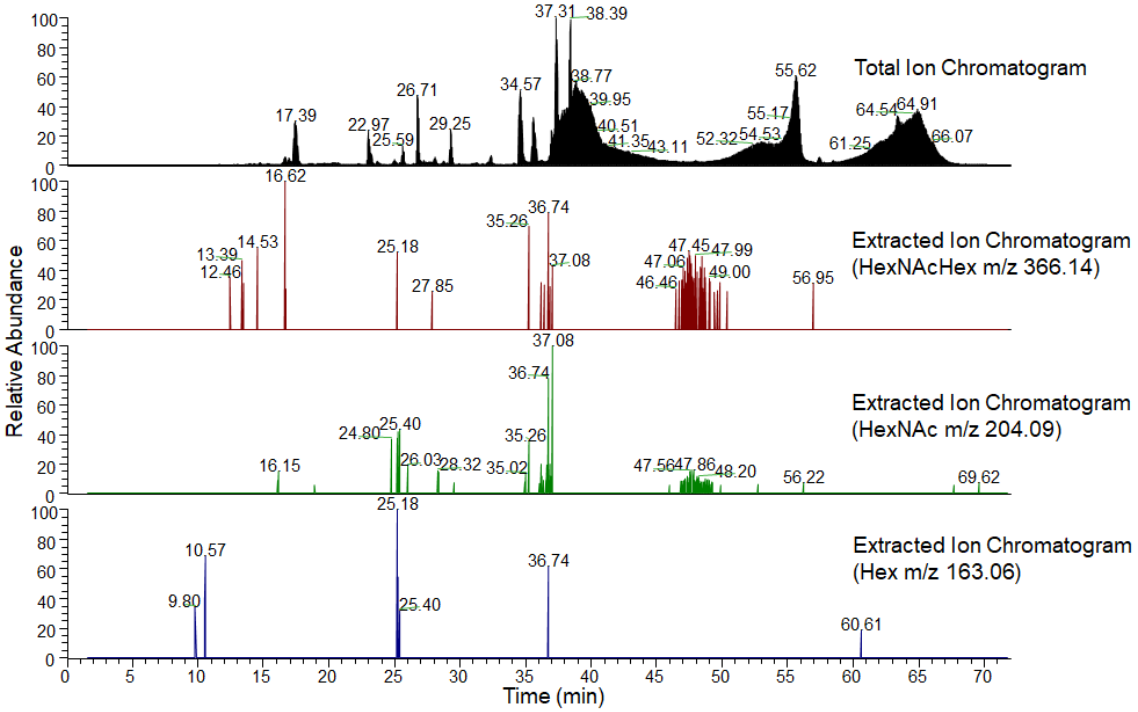

Figure 4.13: Mass spectra of *E. casseliflavus* EGM182 lysate proteins excised from an SDS-PAGE gel corresponding to the 100 kDa band. The upper panel shows the total ion chromatogram and the lower panels are extracted ion chromatograms of HexNAc (m/z 204.09), HexNAcHex (m/z 366.14) and Hex (m/z 163.06).

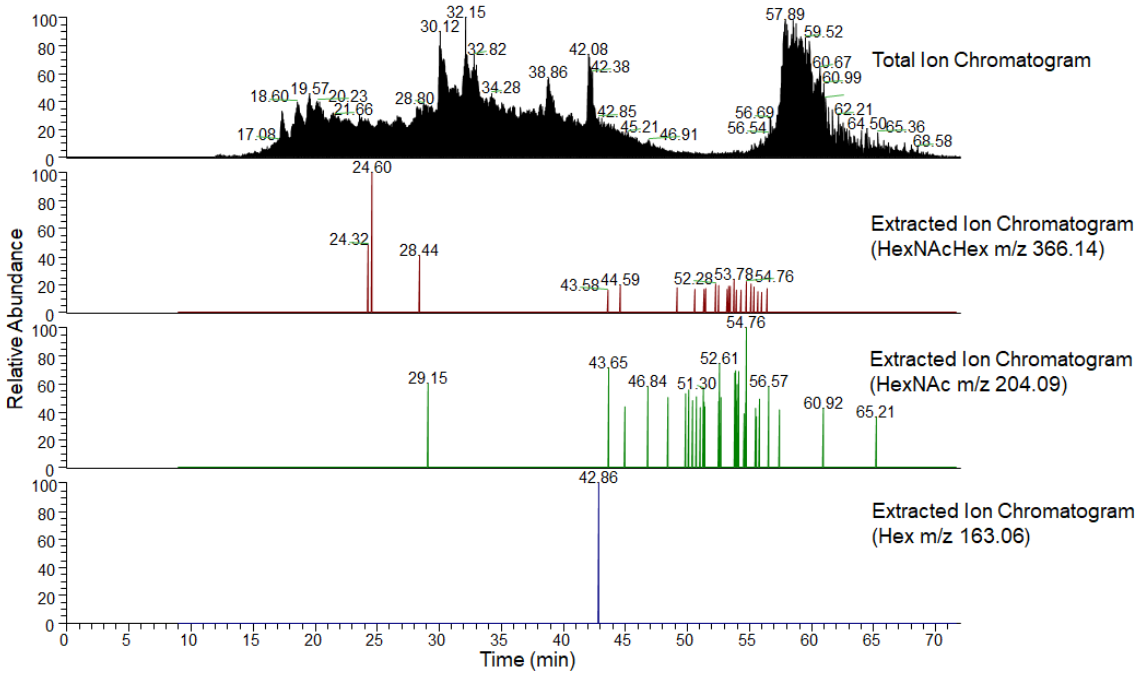

Figure 4.14: Mass spectra of *E. faecalis* EGM183 lysate proteins excised from an SDS-PAGE gel corresponding to the 75 kDa band. The upper panel shows the total ion chromatogram and the lower panels are extracted ion chromatograms of HexNAc (m/z 204.09), HexNAcHex (m/z 366.14) and Hex (m/z 163.06).

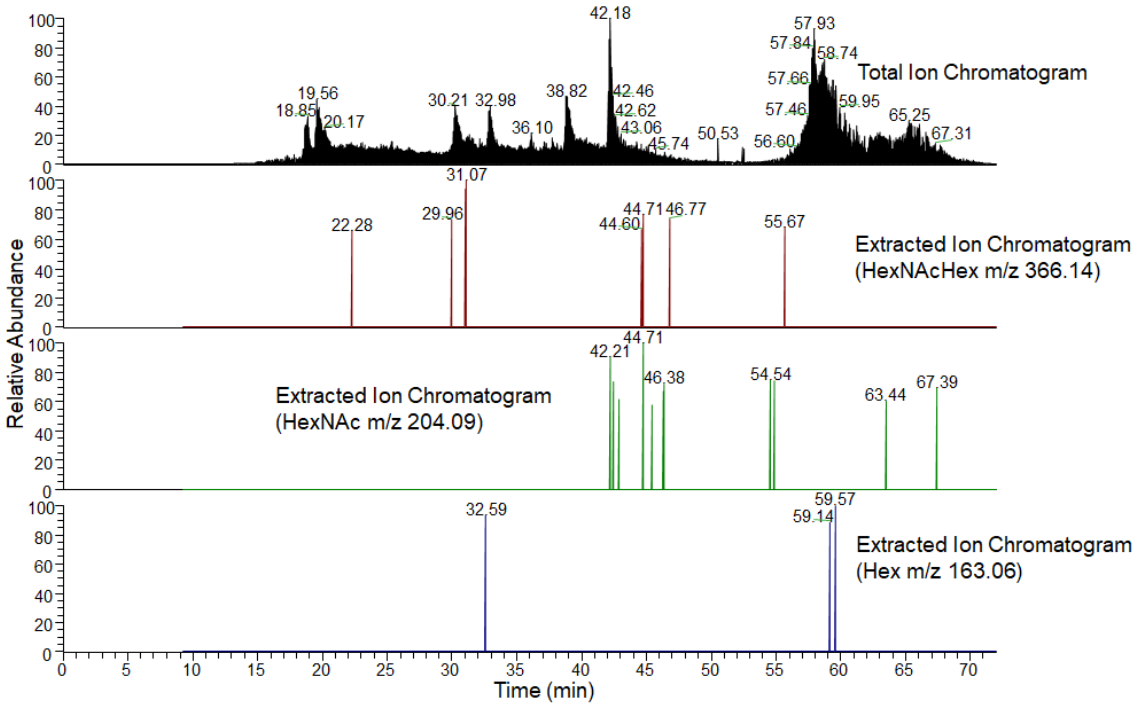

Figure 4.15: Mass spectra of *E. faecalis* EGM183 lysate proteins excised from an SDS-PAGE gel corresponding to the 100 kDa band. The upper panel shows the total ion chromatogram and the lower panels are extracted ion chromatograms of HexNAc (m/z 204.09), HexNAcHex (m/z 366.14) and Hex (m/z 163.06).

CHAPTER 4

CONCLUSIONS AND FUTURE DIRECTIONS

Ganglioside-mimicking bacteria and microbiome interactions

A central theme throughout this dissertation has been the various impacts of ganglioside-mimicking bacteria on host immunity and competing microbes. This pursuit began by investigating the interaction between the GM1 ganglioside-mimicking *C. jejuni* and AB_5 toxins that can bind to the bacterial surface. Through this work, we discovered that these toxins have a deleterious effect on *C. jejuni* related to an increase in cell permeability caused by toxin binding. Interestingly, this mechanism occurs independently from the enzymatic portion of the AB_5 toxins and suggests that the cross-linking ability of the toxin's binding subunit alone could be harmful to these bacterial cells. However, further investigation is needed to determine the biomechanical properties of this interaction as well as potential alternative factors involved in the phenomenon to fully understand the mechanism. The pentameric structure of AB_5 toxins provides avidity that is important to the immense strength of its binding interaction with gangliosides. It would be interesting to keep the B-subunits in their monomeric form to determine if the pentameric avidity is necessary for the deleterious effect that we see. RNA sequencing would also be an invaluable tool to determine what proteins are upregulated and downregulated in the presence of the toxins to shed light on possible signaling changes that occur during this interaction. It was also discovered that the negative influence of AB_5 toxins on *C. jejuni* can result in a selective pressure for phase-variable strains to favor display of LOS

structures that cannot be bound by the toxin. Taken together, these discoveries suggest that there could be competition between these pathogens in the host during co-infection and that *Campylobacter* phase-variation could play a key role in this relationship. In the case of CT, *V. cholerae* acquired the toxin genes from the CTX bacteriophage, but the true origin of the toxin remains unknown (148). It is speculated that the CTX phage obtained these genes from a more ancient bacterial source since the GC content in the *ctxAB* genes differs from the rest of the phage genome (148). The genome of the deep-sea γ-proteobacterium *Idiomarina loihiensis* contains enzymes capable of sialic acid biosynthesis and sialylation of glycans on the cell surface (379, 380). This organism is found in deep-sea hydrothermal vents, which are believed to be the most ancient ecosystems occupied by life on this planet(381). Given that bacteria have produced sialic acid-containing structures long before their animal hosts, the interaction we observed between *C. jejuni* and these AB_5 toxins could suggest a more ancient alternative mechanism for both the production of the toxins as well as phase-variability in *C. jejuni* LOS structures. This alternative function for AB_5 toxins in bacterial competition is further supported by the observation of a shift in microbiome diversity following oral gavage of chickens with these toxins. However, to support this theory, the isolation of other ganglioside-mimicking bacteria that are similarly impacted by these toxins is necessary.

In a related finding, our investigations also revealed the presence of unknown ganglioside-mimicking bacteria present within the chicken gut microbiome. This dissertation has outlined previous studies suggesting other bacteria may mimic ganglioside structures; however, none have been fully characterized by glycan analysis as has been done for *C. jejuni.* Additionally, research on this topic has primarily focused on the study

of infectious agents thought to cause GBS and not much effort has gone toward the study of commensal ganglioside-mimicking bacteria that could be transiently introduced into our bodies through our diet. We were able to isolate ganglioside-mimicking *Enterococci* from the chicken gut, but to determine if these types of bacteria are present in humans, additional efforts must be directed at sampling the human microbiome. Future experiments in our lab will expand upon our findings by examining the human fecal microbiome of GBS patients in comparison to healthy matched controls. One of our goals is to isolate and identify commensal ganglioside-mimicking bacteria with the hypothesis that they could have a significant impact on GBS susceptibility or development. To investigate this possibility, part of the grant also plans to use the isolated organisms to humanize the microbiome of GBS-model mice (260) and test their susceptibility to autoimmune disease development.

Effect of ganglioside-mimicking bacteria on the immune system

While we do not yet have access to the human fecal samples from our upcoming study, our lab had previously received samples from the GEMS study to examine the *Campylobacter* strains isolated from breastfed infants in LMICs (193). Since these infant populations are exposed to *Campylobacter* at a significantly higher rate than those in developed nations, they represent a group that is also potentially exposed to ganglioside-mimicking bacterial antigens consistently throughout life. The microbiome of infants and young children still has an immense impact on how the immune system will respond to foreign and self-antigens. As expected, our screen confirmed that these infants are exposed to ganglioside-mimicking *Campylobacter* early in life, which can both be accompanied by disease symptoms or occur without any outward signs of illness. This was the case across all the nations involved in the study, revalidating that *Campylobacter* ganglioside-mimicry

is wide-spread and that many people's immune systems have been exposed to them. Even though exposure to these antigens transiently could be enough to impact the immune system, we currently do not have information regarding how long the *Campylobacter* strains were carried by the infants since the GEMS study was not intended to be a longitudinal analysis. In future studies, it would be interesting to determine the time span which *Campylobacter* is carried by reducing subsequent exposure to the organism and monitoring the presence of the original strain over time. By limiting exposure, the individuals would no longer be constantly infected by *Campylobacter* and it could be determined whether the organism is only present transiently by ingestion, or if it is able to colonize and grow in the host as a part of the microbiome. It has been shown previously that *C. jejuni* contains several variable genes that can allow for persistent infection and even cause relapse after treatment by enabling the organism to occupy a new niche and avoid being shed from the human gut (382). Although these large case-control studies are massive endeavors taking extensive planning and resources to undertake, they are currently underway and funded through organizations such as the Bill and Melinda Gates Foundation. In the meanwhile, the use of model systems to investigate the influence of ganglioside-mimicking bacteria on immunity is also important to obtain a better understanding of the detailed mechanisms at play in studies looking at populations with broad strokes.

Our work pursued this idea using the leukocyte THP-1 monocyte cell line to study the impact of ganglioside-mimicking bacteria on human macrophages. This model allowed us to train macrophages with low-dose exposure to GM1 ganglioside-mimicking bacteria prior to challenge with GM1-mimicking bacteria and observe changes in pro-inflammatory

cytokine production. These results suggested that ganglioside-mimicking bacteria present in low-doses can induce tolerance to subsequent exposure of pathogens with ganglioside antigens. Our experiments using TLR2 and TLR4 knock-down mutants suggest that there is more involved in this tolerance effect than signaling through these two TLR receptors, but that TLR4 does have an influence on the decrease in IL-1β. Importantly, verification of these two lentiviral transduction mutants was not successfully completed and is absolutely necessary to claim these results as valid. An attempt was also made to monitor the production of the tolerance protein, A20 in the macrophages but that was unfortunately unsuccessful amidst the haste to end experiments for the University closure for COVID-19. This experiment is important to repeat, since A20 has been implicated in endotoxin tolerance induction for the THP-1 model and this information would tell us more about the mechanism behind the tolerance (357, 358). Future experiments regarding this project will include additional approaches to determine the signaling pathway involved in this tolerance induction. Also, if other ganglioside-mimicking commensal bacteria are isolated from humans feces or other sources, they should be tested using this model as was done with our isolate from chicken cecal mucus, *E. casseliflavus* EGM182.

Ganglioside-mimicking enterococci isolated from chickens

Three ganglioside-mimicking bacteria were already isolated from chicken ceca all belonging to the *Enterococcus* genus. These isolates were named *E. gallinarum* EGM181, *E. casseliflavus* EGM182 and *E. faecalis* EGM183. After these bacteria were isolated and pure cultures were obtained, we determined that each of them possessed glycoproteins that bound to α-GM1 ganglioside antibodies. This led us to obtain the full genome sequence of each organism along with glycoproteomic analysis of *E. gallinarum* and *E. casseliflavus*

to identify potential glycoproteins. Analysis of the three genomes revealed many genes encoding proteins involved in the transport, synthesis and catalysis of sugars. This included some major enzymes that could be involved in protein glycosylation and ganglioside-mimicry. Mutation of these genes will help in answering some key questions regarding the *Enterococcus* protein glycosylation pathway and how ganglioside-mimics are generated in these strains. Numerous glycopeptides were also discovered through the glycoproteome analysis and the most intriguing, in relation to ganglioside mimicry, were those modified with a HexNAc-Hex residue. These modifications could be revealing the generation of ganglioside-mimicking glycoproteins. In the coming months, the glycoproteome of *E. faecalis* will also be performed and the results added to our list of potential glycoproteins to target. Additionally, the glycoproteins most likely to be modified with ganglioside mimics will be enriched and isolated based on their predicted characteristics. Once the purified protein is obtained in larger concentrations, NMR analysis will be performed to characterize the glycan structure responsible for ganglioside mimicry and the protein will also be used in macrophage tolerance assays. The latter will determine if the presence of these commensal bacteria and their surface glycoproteins could have an impact on the susceptibility for GBS development.

Summary

In conclusion, the work described within this dissertation was directed at better understanding ganglioside-mimicking bacteria and their impact on their environment in the host gut. This included the study of inter-bacterial competition between GM1 ganglioside-mimicking *C. jejuni* and gut pathogens producing ganglioside-binding AB_5 toxins. In addition, we discovered additional bacteria in the chicken gut that mimic ganglioside

structures and determined that ganglioside-mimicking bacteria could tolerize the innate immune system to GBS-associated antigens. This information was paired with a screen to show that infants in LMICs harbor GM1-mimicking *C. jejuni* during a crucial stage in the development of oral tolerance. We further pursued commensal ganglioside-mimicking bacteria by isolating and identifying three *Enterococcus* species using α-GM1 antibodies. It was proven that these species contain glycoproteins that are likely part of a general protein glycosylation system in *Enterococcus* that has not been previously described. This work presents new information regarding ganglioside-mimicking bacteria and may lead to new preventative strategies for GBS as well as new information for glycosylation in enterococci and Gram-positive bacteria in general.

REFERENCES

1. Butzler JP. 2004. *Campylobacter*, from obscurity to celebrity. Clinical Microbiology and Infection 10:868-876.

2. Escherich T. 1886. Beitrage zur Kenntniss der Darmbacterien. III. Ueber das Vorkommen von Vibrionen im Darmcanal und den Stuhlgangen der Sauglinge. Münchener Med Wochenschrift 33:815-817.

3. Skirrow MB. 2006. John McFadyean and the centenary of the first isolation of *Campylobacter* species. Clinical Infectious Diseases 43:1213-1217.

4. McFadyean J, Stockman S. 1913. Report of the Departmental Committee appointed by the Board of Agriculture and Fisheries to inquire into Epizootic Abortion. III. Abortion in Sheep. London: HMSO.

5. Dekeyser P, Butzler JP, Sternon J, Gossuind.M. 1972. Acute Enteritis due to Related *Vibrio* - First Positive Stool Cultures. Journal of Infectious Diseases 125:390-392.

6. Patry RT, Stahl M, Perez-Munoz ME, Nothaft H, Wenzel CQ, Sacher JC, Coros C, Walter J, Vallance BA, Szymanski CM. 2019. Bacterial AB_5 toxins inhibit the growth of gut bacteria by targeting ganglioside-like glycoconjugates. Nature Communications 10:1390.

7. Sheppard SK, Maiden MC. 2015. The evolution of *Campylobacter jejuni* and *Campylobacter coli*. Cold Spring Harb Perspect Biol 7:a018119.

8. Bohaychuk VM, Gensler GE, King RK, Manninen KI, Sorensen O, Wu JT, Stiles ME, McMullen LM. 2006. Occurrence of pathogens in raw and ready-to-eat meat and poultry products collected from the retail marketplace in Edmonton, Alberta, Canada. Journal of food protection 69:2176-2182.

9. Clark CG, Price L, Ahmed R, Woodward DL, Melito PL, Rodgers FG, Jamieson F, Ciebin B, Li A, Ellis A. 2003. Characterization of Waterborne Outbreak-associated *Campylobacter jejuni*, Walkerton, Ontario. Emerging Infectious Diseases 9:1232-1241.

10. Blaser MJ, Engberg J. 2008. Clinical Aspects of *Campylobacter jejuni* and *Campylobacter coli* Infections. *Campylobacter*, 3rd Edition:99-121.

11. Marshall JK, Thabane M, Garg AX, Clark WF, Salvadori M, Collins SM, Walkerton Health Study I. 2006. Incidence and epidemiology of irritable bowel syndrome after a large waterborne outbreak of bacterial dysentery. Gastroenterology 131:445-50; quiz 660.

12. García Rodríguez LA, Ruigómez A, Panés J. 2006. Acute gastroenteritis is followed by an increased risk of inflammatory bowel disease. Gastroenterol 130:1588-1594.

13. Amour C, Gratz J, Mduma E, Svensen E, Rogawski ET, McGrath M, Seidman JC, McCormick BJJ, Shrestha S, Samie A, Mahfuz M, Qureshi S, Hotwani A, Babji S, Trigoso DR, Lima AAM, Bodhidatta L, Bessong P, Ahmed T, Shakoor S, Kang G, Kosek M, Guerrant RL, Lang D, Gottlieb M, Houpt ER, Platts-Mills JA, Etiology Risk Factors I. 2016. Epidemiology and Impact of *Campylobacter* Infection in Children in 8 Low-Resource Settings: Results From the MAL-ED Study. Clinical Infectious Diseases 63:1171-1179.

14. Lee G, Pan W, Penataro Yori P, Paredes Olortegui M, Tilley D, Gregory M, Oberhelman R, Burga R, Chavez CB, Kosek M. 2013. Symptomatic and asymptomatic *Campylobacter* infections associated with reduced growth in Peruvian children. PLoS Negl Trop Dis 7:e2036.

15. Rogawski ET, Liu J, Platts-Mills JA, Kabir F, Lertsethtakarn P, Siguas M, Khan SS, Praharaj I, Murei A, Nshama R, Mujaga B, Havt A, Maciel IA, Operario DJ, Taniuchi M, Gratz J, Stroup SE, Roberts JH, Kalam A, Aziz F, Qureshi S, Islam MO, Sakpaisal P, Silapong S, Yori PP, Rajendiran R, Benny B, McGrath M, Seidman JC, Lang D, Gottlieb M, Guerrant RL, Lima AAM, Leite JP, Samie A, Bessong PO, Page N, Bodhidatta L, Mason C, Shrestha S, Kiwelu I, Mduma ER, Iqbal NT, Bhutta ZA, Ahmed T, Haque R, Kang G, Kosek MN, Houpt ER, Investigators M-EN. 2018. Use of quantitative molecular diagnostic methods to investigate the effect of enteropathogen infections on linear growth in children in low-resource settings: longitudinal analysis of results from the MAL-ED cohort study. Lancet Glob Health 6:e1319-e1328.

16. Skirrow MB, Jones DM, Sutcliffe E, Benjamin J. 1993. *Campylobacter* Bacteremia in England and Wales, 1981-91. Epidemiology and infection 110:567-573.

17. Smith GS, Blaser MJ. 1985. Fatalities Associated with *Campylobacter jejuni* Infections. Journal of the American Medical Association 253:2873-2875.

18. Prevention CfDCa. 2017. Foodborne Diseases Active Surveillance Network (FoodNet): FoodNet 2015 Surveillance Report (Final Data). U.S. Department of Health and Human Services, CDC., Atlanta, Georgia.

19. Centers for Disease Control and Prevention N, DFWED. December 23, 2019. *Campylobacter* (Campylobacteriosis). https://www.cdc.gov/campylobacter/index.html. Accessed February 5, 2020.

20. Coker AO, Isokpehi RD, Thomas BN, Amisu KO, Obi CL. 2002. Human campylobacteriosis in developing countries. Emerging Infectious Diseases 8:237-243.

21. Blaser MJ, Taylor DN, Echeverria P. 1986. Immune-Response to *Campylobacter jejuni* in a Rural-Community in Thailand. Journal of Infectious Diseases 153:249-254.

22. Butzler JP, Dekeyser P, Lafontai.T. 1974. Susceptibility of Related Vibrios and *Vibrio fetus* to 12 Antibiotics. Antimicrobial Agents and Chemotherapy 5:86-89.

23. Ge B, Wang F, Sjolund-Karlsson M, McDermott PF. 2013. Antimicrobial resistance in *Campylobacter*: susceptibility testing methods and resistance trends. J Microbiol Methods 95:57-67.

24. Gillespie IA, O'Brien SJ, Frost JA, Adak GK, Horby P, Swan AV, Painter MJ, Neal KR, Campylobacter Sentinel S. 2002. A case-case comparison of *Campylobacter coli* and *Campylobacter jejuni* infection: A tool for generating hypotheses. Emerging Infectious Diseases 8:937-942.

25. Robinson DA. 1981. Infective Dose of *Campylobacter jejuni* in Milk. British medical journal 282:1584-1584.

26. Poly F, Guerry P. 2008. Pathogenesis of *Campylobacter*. Current opinion in gastroenterology 24:27-31.

27. Hu L, Kopecko DJ. 2008. Cell Biology of Human Host Cell Entry by *Campylobacter jejuni*. *Campylobacter*, 3rd Edition:297-313.

28. Szymanski CM, Burr DH, Guerry P. 2002. *Campylobacter* protein glycosylation affects host cell interactions. Infection and immunity 70:2242-2244.

29. Guerry P, Ewing CP, Schirm M, Lorenzo M, Kelly J, Pattarini D, Majam G, Thibault P, Logan S. 2006. Changes in flagellin glycosylation affect *Campylobacter* autoagglutination and virulence. Molecular microbiology 60:299-311.

30. Hu L, Kopecko DJ. 1999. *Campylobacter jejuni* 81-176 associates with microtubules and dynein during invasion of human intestinal cells. Infection and immunity 67:4171-4182.

31. Oelschlaeger TA, Guerry P, Kopecko DJ. 1993. Unusual Microtubule-Dependent Endocytosis Mechanisms Triggered by *Campylobacter jejuni* and *Citrobacter freundii*. Proceedings of the National Academy of Sciences of the United States of America 90:6884-6888.

32. Biswas D, Itoh K, Sasakawa C. 2003. Role of microfilaments and microtubules in the invasion of INT-407 cells by *Campylobacter jejuni*. Microbiology and immunology 47:469-473.

33. Watson RO, Galan JE. 2008. *Campylobacter jejuni* survives within epithelial cells by avoiding delivery to lysosomes. PLoS pathogens 4:e14-e14.

34. Lindmark B, Rompikuntal PK, Vaitkevicius K, Song T, Mizunoe Y, Uhlin BE, Guerry P, Wai SN. 2009. Outer membrane vesicle-mediated release of cytolethal distending toxin (CDT) from *Campylobacter jejuni*. BMC Microbiol 9:220.

35. Yuki N. 2001. Infectious origins of, and molecular mimicry in, Guillain-Barré and Fisher syndromes. The Lancet Infectious diseases 1:29-37.

36. Wijdicks EF, Klein CJ. 2017. Guillain-Barré Syndrome. Mayo Clin Proc 92:467-479.

37. Goodfellow JA, Willison HJ. 2016. Guillain-Barré syndrome: a century of progress. Nat Rev Neurol 12:723-731.

38. Jackson BR, Zegarra JA, Lopez-Gatell H, Sejvar J, Arzate F, Waterman S, Nunez AS, Lopez B, Weiss J, Cruz RQ, Murrieta DY, Luna-Gierke R, Heiman K, Vieira AR, Fitzgerald C, Kwan P, Zarate-Bermudez M, Talkington D, Hill VR, Mahon B, Team GBSOI. 2014. Binational outbreak of Guillain-Barré syndrome associated with *Campylobacter jejuni* infection, Mexico and USA, 2011. Epidemiol Infect 142:1089-99.

39. Diaz-Soto S, Chavez K, Chaca A, Alanya J, Tirado-Hurtado I. 2019. Outbreak of Guillain-Barré Syndrome in Peru. eNeurologicalSci 14:89-90.

40. Asbury AK, Cornblath DR. 1990. Assessment of Current Diagnostic-Criteria for Guillain-Barré Syndrome. Annals of Neurology 27:S21-S24.

41. Shahrizaila N, Yuki N. 2011. Guillain-Barré Syndrome Animal Model: The First Proof of Molecular Mimicry in Human Autoimmune Disorder. Journal of Biomedicine and Biotechnology doi:10.1155/2011/829129:829129-829129.

42. Yuki N, Susuki K, Koga M, Nishimoto Y, Odaka M, Hirata K, Taguchi K, Miyatake T, Furukawa K, Kobata T, Yamada M. 2004. Carbohydrate mimicry between human ganglioside GM1 and *Campylobacter jejuni* lipooligosaccharide causes Guillain-Barré syndrome. Proceedings of the National Academy of Sciences of the United States of America 101:11404-11409.

43. Dimachkie MM, Barohn RJ. 2013. Guillain-Barré Syndrome and Variants. Neurologic clinics 31:491-510.

44. Rhodes KM, Tattersfield AE. 1982. Guillain-Barré syndrome associated with *Campylobacter* infection. Br Med J (Clin Res Ed) 285:173-4.

45. Nachamkin I, Allos BM, Ho T. 1998. *Campylobacter* species and Guillain-Barré syndrome. Clinical microbiology reviews 11:555-567.

46. Yu RK, Usuki S, Ariga T. 2006. Ganglioside molecular mimicry and its pathological roles in Guillain-Barré syndrome and related diseases. Infection and immunity 74:6517-6527.

47. Parker CT, Horn ST, Gilbert M, Miller WG, Woodward DL, Mandrell RE. 2005. Comparison of *Campylobacter jejuni* lipooligosaccharide biosynthesis loci from a variety of sources. Journal of clinical microbiology 43:2771-2781.

48. Ang CW, Laman JD, Willison HJ, Wagner ER, Endtz HP, De Klerk MA, Tio-Gillen AP, Van den Braak N, Jacobs BC, Van Doorn PA. 2002. Structure of *Campylobacter jejuni* lipopolysaccharides determines antiganglioside specificity and clinical features of Guillain-Barré, and Miller Fisher patients. Infection and immunity 70:1202-1208.

49. Moran AP. 1997. Structure and conserved characteristics of *Campylobacter jejuni* lipopolysaccharides. J Infect Dis 176 Suppl 2:S115-21.

50. Jacobs BC, Endtz H, van der Meche FG, Hazenberg MP, Achtereekte HA, van Doorn PA. 1995. Serum anti-GQ1b IgG antibodies recognize surface epitopes on *Campylobacter jejuni* from patients with Miller Fisher syndrome. Ann Neurol 37:260-4.

51. Endtz HP, Ang CW, van Den Braak N, Duim B, Rigter A, Price LJ, Woodward DL, Rodgers FG, Johnson WM, Wagenaar JA, Jacobs BC, Verbrugh HA, van Belkum A. 2000. Molecular characterization of *Campylobacter jejuni* from patients with Guillain-Barré and Miller Fisher syndromes. J Clin Microbiol 38:2297-301.

52. Nachamkin I, Allos BM, Ho T. 1998. *Campylobacter* species and Guillain-Barré syndrome. Clinical microbiology reviews 11:555-567.

53. Allos BM. 1997. Association between *Campylobacter* infection and Guillain-Barré syndrome. Journal of Infectious Diseases 176:S125-S128.

54. Jacobs BC, Rothbarth PH, van der Meche FGA, Herbrink P, Schmitz PIM, de Klerk MA, van Doorn PA. 1998. The spectrum of antecedent infections in Guillain-Barré syndrome - A case-control study. Neurology 51:1110-1115.

55. van den Berg B, Bunschoten C, van Doorn PA, Jacobs BC. 2013. Mortality in Guillain-Barré syndrome. Neurology 80:1650-1654.

56. Bhagat SK, Sidhant S, Bhatta M, Ghimire A, Shah B. 2019. Clinical Profile, Functional Outcome, and Mortality of Guillain-Barré Syndrome: A Five-Year Tertiary Care Experience from Nepal. Neurol Res Int 2019:3867946.

57. Nothaft H, Szymanski CM. 2010. Protein glycosylation in bacteria: sweeter than ever. Nature Reviews Microbiology 8:765-778.

58. Cain JA, Dale AL, Niewold P, Klare WP, Man L, White MY, Scott NE, Cordwell SJ. 2019. Proteomics Reveals Multiple Phenotypes Associated with *N*-linked Glycosylation in *Campylobacter jejuni*. Mol Cell Proteomics 18:715-734.

59. Nothaft H, Szymanski CM. 2019. New discoveries in bacterial *N*-glycosylation to expand the synthetic biology toolbox. Curr Opin Chem Biol 53:16-24.

60. Szymanski CM, Yao RJ, Ewing CP, Trust TJ, Guerry P. 1999. Evidence for a system of general protein glycosylation in *Campylobacter jejuni*. Molecular microbiology 32:1022-1030.

61. Karlyshev AV, Everest P, Linton D, Cawthraw S, Newell DG, Wren BW. 2004. The *Campylobacter jejuni* general glycosylation system is important for attachment to human epithelial cells and in the colonization of chicks. Microbiology-Sgm 150:1957-1964.

62. Logan SM, Schoenhofen IC, Guerry P. 2008. *O*-Linked Flagellar Glycosylation in *Campylobacter*. *Campylobacter*, 3rd Edition:471-481.

63. Roberts IS. 1996. The biochemistry and genetics of capsular polysaccharide production in bacteria. Annual Review of Microbiology 50:285-315.

64. Bacon DJ, Szymanski CM, Burr DH, Silver RP, Alm RA, Guerry P. 2001. A phase-variable capsule is involved in virulence of *Campylobacter jejuni* 81-176. Molecular microbiology 40:769-777.

65. Guerry P, Poly F, Riddle M, Maue AC, Chen Y-H, Monteiro MA. 2012. *Campylobacter* polysaccharide capsules: virulence and vaccines. Frontiers in Cellular and Infection Microbiology 2:7-7.

66. Moran AP, Annuk H. 2003. Recent advances in understanding biofilms of mucosae. Reviews in Environmental Science and Bio/Technology 2:121-140.

67. Otto M. 2006. Bacterial evasion of antimicrobial peptides by biofilm formation. Current Topics in Microbiology and Immunology 306:251-258.

68. Bachtiar BM, Coloe PJ, Fry BN. 2007. Knockout mutagenesis of the kpsE gene of *Campylobacter jejuni* 81116 and its involvement in bacterium-host interactions. FEMS immunology and medical microbiology 49:149-154.

69. Sorensen MCH, van Alphen LB, Harboe A, Li J, Christensen BB, Szymanski CM, Brondsted L. 2011. Bacteriophage F336 Recognizes the Capsular Phosphoramidate Modification of *Campylobacter jejuni* NCTC11168. Journal of Bacteriology 193:6742-6749.

70. Sorensen MCH, Van Alphen LB, Fodor C, Crowley SM, Christensen BB, Szymanski CM, Brondsted L. 2012. Phase variable expression of capsular polysaccharide modifications allows *Campylobacter jejuni* to avoid bacteriophage infection in chickens. Frontiers in Cellular and Infection Microbiology 2:11-11.

71. Sorensen MC, Gencay YE, Birk T, Baldvinsson SB, Jackel C, Hammerl JA, Vegge CS, Neve H, Brondsted L. 2015. Primary isolation strain determines both phage type and receptors recognised by *Campylobacter jejuni* bacteriophages. PLoS One 10:e0116287.

72. Maue AC, Mohawk KL, Giles DK, Poly F, Ewing CP, Jiao Y, Lee G, Ma Z, Monteiro MA, Hill CL, Ferderber JS, Porter CK, Trent MS, Guerry P. 2013. The polysaccharide capsule of *Campylobacter jejuni* modulates the host immune response. Infect Immun 81:665-72.

73. Monteiro MA, Baqar S, Hall ER, Chen YH, Porter CK, Bentzel DE, Applebee L, Guerry P. 2009. Capsule polysaccharide conjugate vaccine against diarrheal disease caused by *Campylobacter jejuni*. Infect Immun 77:1128-36.

74. Rose A, Kay E, Wren BW, Dallman MJ. 2012. The *Campylobacter jejuni* NCTC11168 capsule prevents excessive cytokine production by dendritic cells. Med Microbiol Immunol 201:137-44.

75. Moran AP, Zahringer U, Seydel U, Scholz D, Stutz P, Rietschel ET. 1991. Structural-Analysis of the Lipid-a Component of *Campylobacter jejuni* Ccug 10936 (Serotype O-2) Lipopolysaccharide - Description of a Lipid-a Containing a Hybrid Backbone of 2-Amino-2-Deoxy-D-Glucose and 2,3-Diamino-2,3-Dideoxy-D-Glucose. European Journal of Biochemistry 198:459-469.

76. Moran AP. 2010. The Role of Endotoxin in Infection: *Helicobacter pylori* and *Campylobacter jejuni*. Subcellular Biochemistry 53:209-240.

77. Gilbert M, Parker CT, Moran AP. 2008. *Campylobacter jejuni* Lipooligosaccharides: Structures and Biosynthesis. *Campylobacter*, 3rd Edition:483-504.

78. Guerry P, Szymanski CM. 2008. *Campylobacter* sugars sticking out. Trends in microbiology 16:428-435.

79. Moran AP, Rietschel ET, Kosunen TU, Zahringer U. 1991. Chemical Characterization of *Campylobacter jejuni* Lipopolysaccharides Containing *N*-Acetylneuraminic Acid and 2,3-Diamino-2,3-Dideoxy-D-Glucose. Journal of Bacteriology 173:618-626.

80. Yu RK, Tsai YT, Ariga T, Yanagisawa M. 2011. Structures, biosynthesis, and functions of gangliosides--an overview. Journal of oleo science 60:537-544.

81. Schnaar RL, Gerardy-Schahn R, Hildebrandt H. 2014. Sialic acids in the brain: gangliosides and polysialic acid in nervous system development, stability, disease, and regeneration. Physiol Rev 94:461-518.

82. Sheikh KA, Sun J, Liu YJ, Kawai H, Crawford TO, Proia RL, Griffin JW, Schnaar RL. 1999. Mice lacking complex gangliosides develop Wallerian degeneration and myelination defects. Proceedings of the National Academy of Sciences of the United States of America 96:7532-7537.

83. Yamashita T, Wu YP, Sandhoff R, Werth N, Mizukami H, Ellis JM, Dupree JL, Geyer R, Sandhoff K, Proia RL. 2005. Interruption of ganglioside synthesis produces central nervous system degeneration and altered axon-glial interactions. Proceedings of the National Academy of Sciences of the United States of America 102:2725-2730.

84. Lopez PH. 2014. Role of myelin-associated glycoprotein (siglec-4a) in the nervous system. Adv Neurobiol 9:245-62.

85. Sandhoff K, Harzer K. 2013. Gangliosides and Gangliosidoses: Principles of Molecular and Metabolic Pathogenesis. Journal of Neuroscience 33:10195-10208.

86. Schneider JS. 2014. Gangliosides and glycolipids in neurodegenerative disorders, p 449-461. *In* Yu RK, Schengrund C-L (ed), Glycobiology of the Nervous System doi:- 10.1007/978-1-4939-1154-7_20. Springer New York.

87. Parker CT, Gilbert M, Yuki N, Endtz HP, Mandrell RE. 2008. Characterization of lipooligosaccharide-biosynthetic loci of *Campylobacter jejuni* reveals new lipooligosaccharide classes: Evidence of mosaic organizations. Journal of Bacteriology 190:5681-5689.

88. Kuziemko GM, Stroh M, Stevens RC. 1996. Cholera toxin binding affinity and specificity for gangliosides determined by surface plasmon resonance. Biochemistry 35:6375-6384.

89. MacKenzie CR, Hirama T, Lee KK, Altman E, Young NM. 1997. Quantitative analysis of bacterial toxin affinity and specificity for glycolipid receptors by surface plasmon resonance. Journal of Biological Chemistry 272:5533-5538.

90. Chinnapen DJF, Chinnapen H, Saslowsky D, Lencer WI. 2007. Rafting with cholera toxin: endocytosis and trafficking from plasma membrane to ER. FEMS microbiology letters 266:129-137.

91. Guerry P, Szymanski CM, Prendergast MM, Hickey TE, Ewing CP, Pattarini DL, Moran AP. 2002. Phase variation of *Campylobacter jejuni* 81-176 lipooligosaccharide affects ganglioside mimicry and invasiveness in vitro. Infection and immunity 70:787-793.

92. Prendergast MM, Tribble DR, Baqar S, Scott DA, Ferris JA, Walker RI, Moran AP. 2004. In vivo phase variation and serologic response to lipooligosaccharide of *Campylobacter jejuni* in experimental human infection. Infection and immunity 72:916-922.

93. Kuroki S, Saida T, Nukina M, Haruta T, Yoshioka M, Kobayashi Y, Nakanishi H. 1993. Campylobacter jejuni strains from patients with Guillain-Barré syndrome belong mostly to Penner serogroup 19 and contain beta-*N*-acetylglucosamine residues. Annals of Neurology 33:243-247.

94. Parker CT, Huynh S, Heikema AP. 2016. Complete Genomic Sequence of *Campylobacter jejuni* subsp. jejuni HS:19 Strain RM1285 Isolated from Packaged Chicken. Genome Announc 4.

95. Parker CT, Huynh S, Heikema AP. 2017. Genomic Sequence of *Campylobacter jejuni* subsp. jejuni HS:19 Penner Serotype Reference Strain RM3420. Genome Announc 5.

96. Aspinall GO, McDonald AG, Pang H, Kurjanczyk LA, Penner JL. 1994. Lipopolysaccharides of *Campylobacter jejuni* serotype O:19: Structures of core oligosaccharide regions from the serostrain and two bacterial isolates from patients with the Guillain-Barré syndrome. Biochemistry 33:241-249.

97. Linton D, Gilbert M, Hitchen PG, Dell A, Morris HR, Wakarchuk WW, Gregson NA, Wren BW. 2000. Phase variation of a beta-1,3 galactosyltransferase involved in generation of the ganglioside GM(1)-like lipo-oligosaccharide of *Campylobacter jejuni*. Molecular microbiology 37:501-514.

98. Aspinall GO, McDonald AG, Pang H, Kurjanczyk LA, Penner JL. 1993. Lipopolysaccharide of *Campylobacter coli* Serotype-O-30 - Fractionation and Structure of Liberated Core Oligosaccharide. Journal of Biological Chemistry 268:6263-6268.

99. Ang CW, Jacobs BC, Laman JD. 2004. The Guillain-Barré syndrome: a true case of molecular mimicry. Trends Immunol 25:61-6.

100. Bersudsky M, Rosenberg P, Rudensky B, Wirguin I. 2000. Lipopolysaccharides of a *Campylobacter coli* isolate from a patient with Guillain-Barré syndrome display ganglioside mimicry. Neuromuscul Disord 10:182-6.

101. Yoshino H, Inuzuka T, Miyatake T. 1992. IgG antibody against GM1, GD1b and asialo-GM1 in chronic polyneuropathy following *Mycoplasma pneumoniae* infection. Eur Neurol 32:28-31.

102. Watanabe K, Kim S, Nishiguchi M, Suzuki H, Watarai M. 2005. Brucella melitensis infection associated with Guillain-Barré syndrome through molecular mimicry of host structures. FEMS immunology and medical microbiology 45:121-127.

103. Mori M, Kuwabara S, Miyake M, Noda M, Kuroki H, Kanno H, Ogawara K, Hattori T. 2000. Haemophilus influenzae infection and Guillain-Barré syndrome. Brain 123 (Pt 10):2171-8.

104. Tagami S, Susuki K, Takeda M, Koga M. 2008. Fulminant case of Guillain-Barré syndrome with poor recovery and depression following *Haemophilus influenzae* infection. Psychiatry Clin Neurosci 62:486.

105. Koga M, Koike S, Hirata K, Yuki N. 2005. Ambiguous value of *Haemophilus influenzae* isolation in Guillain-Barré and Fisher syndromes. J Neurol Neurosurg Psychiatry 76:1736-8.

106. Irie S, Saito T, Nakamura K, Kanazawa N, Ogino M, Nukazawa T, Ito H, Tamai Y, Kowa H. 1996. Association of anti-GM2 antibodies in Guillain-Barré syndrome with acute cytomegalovirus infection. J Neuroimmunol 68:19-26.

107. Jacobs BC, van Doorn PA, Groeneveld JH, Tio-Gillen AP, van der Meche FG. 1997. Cytomegalovirus infections and anti-GM2 antibodies in Guillain-Barré syndrome. J Neurol Neurosurg Psychiatry 62:641-3.

108. Nafissi S, Vahabi Z, Sadeghi Ghahar M, Amirzargar AA, Naderi S. 2013. The role of cytomegalovirus, *Haemophilus influenzae* and Epstein Barr virus in Guillain Barré syndrome. Acta Med Iran 51:372-6.

109. Glaser R, Brennan R, Berlin CM. 1979. Guillain-Barré syndrome associated with Epstein-Barr virus in a cytomegalovirus-negative patient. Dev Med Child Neurol 21:787-90.

110. Grose C, Feorino PM. 1972. Epstein-Barr virus and Guillain-Barré syndrome. Lancet 2:1285-7.

111. Parra B, Lizarazo J, Jimenez-Arango JA, Zea-Vera AF, Gonzalez-Manrique G, Vargas J, Angarita JA, Zuniga G, Lopez-Gonzalez R, Beltran CL, Rizcala KH, Morales MT, Pacheco O, Ospina ML, Kumar A, Cornblath DR, Munoz LS, Osorio L, Barreras P, Pardo CA. 2016. Guillain-Barré Syndrome Associated with Zika Virus Infection in Colombia. N Engl J Med 375:1513-1523.

112. Araujo LM, Ferreira ML, Nascimento OJ. 2016. Guillain-Barré syndrome associated with the Zika virus outbreak in Brazil. Arq Neuropsiquiatr 74:253-5.

113. Mendez N, Oviedo-Pastrana M, Mattar S, Caicedo-Castro I, Arrieta G. 2017. Zika virus disease, microcephaly and Guillain-Barré syndrome in Colombia: epidemiological situation during 21 months of the Zika virus outbreak, 2015-2017. Archives of Public Health 75:65-65.

114. Salinas JL, Walteros DM, Styczynski A, Garzon F, Quijada H, Bravo E, Chaparro P, Madero J, Acosta-Reyes J, Ledermann J, Arteta Z, Borland E, Burns P, Gonzalez M, Powers AM, Mercado M, Solano A, Sejvar JJ, Ospina ML. 2017. Zika virus disease-associated Guillain-Barré syndrome-Barranquilla, Colombia 2015-2016. Journal of the neurological sciences 381:272-277.

115. Styczynski AR, Malta J, Krow-Lucal ER, Percio J, Nobrega ME, Vargas A, Lanzieri TM, Leite PL, Staples JE, Fischer MX, Powers AM, Chang GJ, Burns PL, Borland EM, Ledermann JP, Mossel EC, Schonberger LB, Belay EB, Salinas JL, Badaro RD, Sejvar JJ, Coelho GE. 2017. Increased rates of Guillain-Barré syndrome associated with Zika virus outbreak in the Salvador metropolitan area, Brazil. PLoS Negl Trop Dis 11:e0005869.

116. Uncini A, Gonzalez-Bravo DC, Acosta-Ampudia YY, Ojeda EC, Rodriguez Y, Monsalve DM, Ramirez-Santana C, Vega DA, Paipilla D, Torres L, Molano-Gonzalez N, Osorio JE, Anaya JM. 2018. Clinical and nerve conduction features in Guillain-Barré syndrome associated with Zika virus infection in Cucuta, Colombia. Eur J Neurol 25:644-650.

117. Cao-Lormeau VM, Blake A, Mons S, Lastere S, Roche C, Vanhomwegen J, Dub T, Baudouin L, Teissier A, Larre P, Vial AL, Decam C, Choumet V, Halstead SK, Willison HJ, Musset L, Manuguerra JC, Despres P, Fournier E, Mallet HP, Musso D, Fontanet A, Neil J, Ghawche F. 2016. Guillain-Barré Syndrome outbreak associated with Zika virus infection in French Polynesia: a case-control study. Lancet 387:1531-1539.

118. Rivera-Correa J, de Siqueira IC, Mota S, do Rosario MS, Pereira de Jesus PA, Alcantara LCJ, Ernst JD, Rodriguez A. 2019. Anti-ganglioside antibodies in patients with Zika virus infection-associated Guillain-Barré Syndrome in Brazil. PLoS Negl Trop Dis 13:e0007695.

119. Saad T, PennaeCosta AA, de Goes FV, de Freitas M, de Almeida JV, de Santa Ignez LJ, Amancio AP, Alvim RJ, Antunes Kramberger LA. 2018. Neurological manifestations of congenital Zika virus infection. Childs Nerv Syst 34:73-78.

120. Kirn TJ, Jude BA, Taylor RK. 2005. A colonization factor links *Vibrio cholerae* environmental survival and human infection. Nature 438:863-866.

121. Meibom KL, Blokesch M, Dolganov NA, Wu CY, Schoolnik GK. 2005. Chitin induces natural competence in *Vibrio cholerae*. Science 310:1824-1827.

122. Colwell RR. 1996. Global climate and infectious disease: The cholera paradigm. Science 274:2025-2031.

123. Deen JL, von Seidlein L, Sur D, Agtini M, Lucas MES, Lopez AL, Kim DR, Ali M, Clemens JD. 2008. The High Burden of Cholera in Children: Comparison of Incidence from Endemic Areas in Asia and Africa. Plos Neglected Tropical Diseases 2:e173-e173.

124. Harris JB, LaRocque RC, Charles RC, Mazumder RN, Khan AI, Bardhan PK. 2010. Cholera's western front. Lancet 376:1961-1965.

125. Harris JB, LaRocque RC, Qadri F, Ryan ET, Calderwood SB. 2012. Cholera. Lancet 379:2466-2476.

126. Centers for Disease C, Prevention. 2010. Update: cholera outbreak --- Haiti, 2010. MMWRMorbidity and mortality weekly report 59:1473-9.

127. Lindenba.J, Greenoug.Wb, Islam MR. 1967. Antibiotic Therapy of Cholera in Children. Bulletin of the World Health Organization 37:529-538.

128. Merrell DS, Butler SM, Qadri F, Dolganov NA, Alam A, Cohen MB, Calderwood SB, Schoolnik GK, Camilli A. 2002. Host-induced epidemic spread of the cholera bacterium. Nature 417:642-645.

129. Siddique AK, Cash R. 2014. Cholera Outbreaks in the Classical Biotype Era. Current Topics in Microbiology and Immunology 379:1-16.

130. Lippi D, Gotuzzo E. 2014. The greatest steps towards the discovery of *Vibrio cholerae*. Clinical Microbiology and Infection 20:191-195.

131. Morris JG. 2003. Cholera and other types of vibriosis: A story of human pandemics and oysters on the half shell. Clinical Infectious Diseases 37:272-280.

132. Bart KJ, Huq Z, Khan M, Mosley WH. 1970. Seroepidemiologic Studies during a Simultaneous Epidemic of Infection with El Tor Ogawa and Classical Inaba *Vibrio cholerae*. Journal of Infectious Diseases 121:S17-S24.

133. Stroeher UH, Karageorgos LE, Morona R, Manning PA. 1992. Serotype Conversion in *Vibrio cholerae* O1. Proceedings of the National Academy of Sciences of the United States of America 89:2566-2570.

134. Ramamurthy T, Garg S, Sharma R, Bhattacharya SK, Nair GB, Shimada T, Takeda T, Karasawa T, Kurazano H, Pal A, Takeda Y. 1993. Emergence of Novel Strain of *Vibrio cholerae* with Epidemic Potential in Southern and Eastern India. Lancet 341:703-704.

135. Albert MJ, Siddique AK, Islam MS, Faruque ASG, Ansaruzzaman M, Faruque SM, Sack RB. 1993. Large Outbreak of Clinical Cholera due to *Vibrio cholerae* Non-01 in Bangladesh. Lancet 341:704-704.

136. Mukhopadhyay AK, Takeda Y, Nair GB. 2014. Cholera Outbreaks in the El Tor Biotype Era and the Impact of the New El Tor Variants. Current Topics in Microbiology and Immunology 379:17-47.

137. Publication WHO. 2010. Cholera vaccines: WHO position paper-Recommendations. Vaccine 28:4687-4688.

138. Samson JE, Magadan AH, Sabri M, Moineau S. 2013. Revenge of the phages: defeating bacterial defences. Nature Reviews Microbiology 11:675-687.

139. Deresinski S. 2009. Bacteriophage Therapy: Exploiting Smaller Fleas. Clinical Infectious Diseases 48:1096-1101.

140. Catalao MJ, Gil F, Moniz-Pereira J, Sao-Jose C, Pimentel M. 2013. Diversity in bacterial lysis systems: bacteriophages show the way. FEMS Microbiol Rev 37:554-71.

141. Abedon ST, Thomas-Abedon C, Thomas A, Mazure H. 2011. Bacteriophage prehistory: Is or is not Hankin, 1896, a phage reference? Bacteriophage 1:174-178.

142. Hankin ME. 1896. L'action bactéricide des eaux de la Jumna et du Gange sur le vibrion du choléra. Annales de l'Institut Pasteur 10:511-523.

143. Faruque SM, Islam MJ, Ahmad QS, Faruque ASG, Sack DA, Nair GB, Mekalanos JJ. 2005. Self-limiting nature of seasonal cholera epidemics: Role of host-mediated amplification of phage. Proceedings of the National Academy of Sciences of the United States of America 102:6119-6124.

144. Waldor MK, Mekalanos JJ. 1996. Lysogenic conversion by a filamentous phage encoding cholera toxin. Science 272:1910-1914.

145. Faruque SM, Mekalanos JJ. 2003. Pathogenicity islands and phages in *Vibrio cholerae* evolution. Trends in microbiology 11:505-510.

146. Kovach ME, Shaffer MD, Peterson KM. 1996. A putative integrase gene defines the distal end of a large cluster of ToxR-regulated colonization genes in *Vibrio cholerae*. Microbiology-Sgm 142:2165-2174.

147. Karaolis DKR, Somara S, Maneval DR, Johnson JA, Kaper JB. 1999. A bacteriophage encoding a pathogenicity island, a type-IV pilus and a phage receptor in cholera bacteria. Nature 399:375-379.

148. Faruque SM, Mekalanos JJ. 2012. Phage-bacterial interactions in the evolution of toxigenic *Vibrio cholerae*. Virulence 3:556-565.

149. Krebs SJ, Taylor RK. 2011. Protection and Attachment of *Vibrio cholerae* Mediated by the Toxin-Coregulated Pilus in the Infant Mouse Model. Journal of Bacteriology 193:5260-5270.

150. Davis BM, Lawson EH, Sandkvist M, Ali A, Sozhamannan S, Waldor MK. 2000. Convergence of the secretory pathways for cholera toxin and the filamentous phage, CTX phi. Science 288:333-335.

151. Johnson TL, Abendroth J, Hol WGJ, Sandkvist M. 2006. Type II secretion: from structure to function. FEMS microbiology letters 255:175-186.

152. Beddoe T, Paton AW, Le Nours J, Rossjohn J, Paton JC. 2010. Structure, biological functions and applications of the AB_5 toxins. Trends in biochemical sciences 35:411-418.

153. Sanchez J, Holmgren J. 2008. Cholera toxin structure, gene regulation and pathophysiological and immunological aspects. Cellular and Molecular Life Sciences 65:1347-1360.

154. Zhang RG, Scott DL, Westbrook ML, Nance S, Spangler BD, Shipley GG, Westbrook EM. 1995. The 3-Dimensional Crystal-Structure of Cholera-Toxin. Journal of Molecular Biology 251:563-573.

155. Lencer WI, Tsai B. 2003. The intracellular voyage of cholera toxin: going retro. Trends in biochemical sciences 28:639-645.

156. Spangler BD. 1992. Structure and Function of Cholera-Toxin and the Related *Escherichia coli* Heat-Labile Enterotoxin. Microbiological reviews 56:622-647.

157. Simons K, Ikonen E. 1997. Functional rafts in cell membranes. Nature 387:569-572.

158. London E, Brown DA. 2000. Insolubility of lipids in Triton X-100: physical origin and relationship to sphingolipid/cholesterol membrane domains (rafts). Biochimica Et Biophysica Acta-Biomembranes 1508:182-195.

159. Wands AM, Huang H, Zhang Y, Sampson NS, Kohler JJ. 2016. Structure-activity relationship (SAR) study on the role of L-fucose in cholera toxin binding to intestinal epithelial cells. Glycobiology 26:1405-1405.

160. Wands A, Fujita A, McCombs J, Rodriguez A, Kohler J. 2014. Discovery of novel glycan-mediated binding partners for cholera toxin. Abstracts of Papers of the American Chemical Society 247.

161. Wands AM, Cervin J, Huang H, Zhang Y, Youn G, Brautigam CA, Matson Dzebo M, Bjorklund P, Wallenius V, Bright DK, Bennett CS, Wittung-Stafshede P, Sampson NS, Yrlid U, Kohler JJ. 2018. Fucosylated Molecules Competitively Interfere with Cholera Toxin Binding to Host Cells. ACS Infect Dis 4:758-770.

162. Heim JB, Hodnik V, Heggelund JE, Anderluh G, Krengel U. 2019. Crystal structures of cholera toxin in complex with fucosylated receptors point to importance of secondary binding site. Sci Rep 9:12243.

163. Wands AM, Fujita A, McCombs JE, Cervin J, Dedic B, Rodriguez AC, Nischan N, Bond MR, Mettlen M, Trudgian DC, Lemoff A, Quiding-Jarbrink M, Gustavsson B, Steentoft C, Clausen H, Mirzaei H, Teneberg S, Yrlid U, Kohler JJ. 2015. Fucosylation and protein glycosylation create functional receptors for cholera toxin. eLife 4.

164. Sethi A, Wands A, Mettlen M, Kohler JJ. 2016. Fucosylation contributes to Cholera toxin intoxication, even in the presence of GM1. Glycobiology 26:1410-1410.

165. Sandvig K, Garred O, Prydz K, Kozlov JV, Hansen SH, Vandeurs B. 1992. Retrograde Transport of Endocytosed Shiga Toxin to the Endoplasmic-Reticulum. Nature 358:510-512.

166. Fujinaga Y, Wolf AA, Rodighiero C, Wheeler H, Tsai B, Allen L, Jobling MG, Rapoport T, Holmes RK, Lencer WI. 2003. Gangliosides that associate with lipid rafts mediate transport of cholera and related toxins from the plasma membrane to endoplasmic reticulm. Molecular biology of the cell 14:4783-4793.

167. Lencer WI, Constable C, Moe S, Jobling MG, Webb HM, Ruston S, Madara JL, Hirst TR, Holmes RK. 1995. Targeting of Cholera-Toxin and *Escherichia coli* Heat-Labile Toxin in Polarized Epithelia - Role of Cooh-Terminal Kdel. Journal of Cell Biology 131:951-962.

168. Saslowsky DE, te Welscher YM, Chinnapen DJF, Wagner JS, Wan J, Kern E, Lencer WI. 2013. Ganglioside GM1-mediated Transcytosis of Cholera Toxin Bypasses the Retrograde Pathway and Depends on the Structure of the Ceramide Domain. Journal of Biological Chemistry 288:25804-25809.

169. Lencer WI, Moe S, Rufo PA, Madara JL. 1995. Transcytosis of Cholera-Toxin Subunits Across Model Human Intestinal Epithelia. Proceedings of the National Academy of Sciences of the United States of America 92:10094-10098.

170. Hazes B, Read RJ. 1997. Accumulating evidence suggests that several AB-toxins subvert the endoplasmic reticulum-associated protein degradation pathway to enter target cells. Biochemistry 36:11051-11054.

171. Sixma TK, Kalk KH, Vanzanten BAM, Dauter Z, Kingma J, Witholt B, Hol WGJ. 1993. Refined Structure of *Escherichia coli* Heat-Labile Enterotoxin, a Close Relative of Cholera-Toxin. Journal of Molecular Biology 230:890-918.

172. Rodighiero C, Tsai B, Rapoport TA, Lencer WI. 2002. Role of ubiquitination in retro-translocation of cholera toxin and escape of cytosolic degradation. EMBO reports 3:1222-1227.

173. Bharati K, Ganguly NK. 2011. Cholera toxin: A paradigm of a multifunctional protein. Indian Journal of Medical Research 133:179-187.

174. Hudault S, Guignot J, Servin AL. 2001. *Escherichia coli* strains colonising the gastrointestinal tract protect germfree mice against Salmonella typhimurium infection. Gut 49:47-55.

175. Bentley R, Meganathan R. 1982. Biosynthesis of vitamin K (menaquinone) in bacteria. Microbiol Rev 46:241-80.

176. Lawrence JG, Roth JR. 1996. Evolution of coenzyme B12 synthesis among enteric bacteria: evidence for loss and acquisition of a multigene complex. Genetics 143:11-24.

177. Blount ZD. 2015. The unexhausted potential of *E. coli*. eLife 4:e05826.

178. Kaper JB, Nataro JP, Mobley HLT. 2004. Pathogenic *Escherichia coli*. Nature Reviews Microbiology 2:123-140.

179. Yamamoto T, Gojobori T, Yokota T. 1987. Evolutionary origin of pathogenic determinants in enterotoxigenic *Escherichia coli* and *Vibrio cholerae* O1. J Bacteriol 169:1352-7.

180. Sanchez-Villamil J, Navarro-Garcia F. 2015. Role of virulence factors on host inflammatory response induced by diarrheagenic *Escherichia coli* pathotypes. Future Microbiology 10:1009-1033.

181. Mudrak B, Kuehn MJ. 2010. Heat-Labile Enterotoxin: Beyond G(M1) Binding. Toxins 2:1445-1470.

182. Gupta SK, Keck J, Ram PK, Crump JA, Miller MA, Mintz ED. 2008. Part III. Analysis of data gaps pertaining to enterotoxigenic *Escherichia coli* infections in low and medium human development index countries, 1984–2005. Epidemiol Infect 136:721-738.

183. Lozano R, Naghavi M, Foreman K, Lim S, Shibuya K, Aboyans V, Abraham J, Adair T, Aggarwal R, Ahn SY, Alvarado M, Anderson HR, Anderson LM, Andrews KG, Atkinson C, Baddour LM, Barker-Collo S, Bartels DH, Bell ML, Benjamin EJ, Bennett D, Bhalla K, Bikbov B, Bin Abdulhak A, Birbeck G, Blyth F, Bolliger I, Boufous S, Bucello C, Burch M, Burney P, Carapetis J, Chen H, Chou D, Chugh SS, Coffeng LE, Colan SD, Colquhoun S, Colson KE, Condon J, Connor MD, Cooper LT, Corriere M, Cortinovis M, de Vaccaro KC, Couser W, Cowie BC, Criqui MH, Cross M, Dabhadkar KC, et al. 2012. Global and regional mortality from 235 causes of death for 20 age groups in 1990 and 2010: a systematic analysis for the Global Burden of Disease Study 2010. Lancet 380:2095-128.

184. Kotloff KL, Nataro JP, Blackwelder WC, Nasrin D, Farag TH, Panchalingam S, Wu Y, Sow SO, Sur D, Breiman RF, Faruque AS, Zaidi AK, Saha D, Alonso PL, Tamboura B, Sanogo D, Onwuchekwa U, Manna B, Ramamurthy T, Kanungo S, Ochieng JB, Omore R, Oundo JO, Hossain A, Das SK, Ahmed S, Qureshi S, Quadri F, Adegbola RA, Antonio M, Hossain MJ, Akinsola A, Mandomando I, Nhampossa T, Acacio S, Biswas K, O'Reilly CE, Mintz ED, Berkeley LY, Muhsen K, Sommerfelt H, Robins-Browne RM, Levine MM. 2013. Burden and aetiology of diarrhoeal disease in infants and young children in developing countries (the Global Enteric Multicenter Study, GEMS): a prospective, case-control study. Lancet 382:209-22.

185. Leder K. 2015. Advising travellers about management of travellers' diarrhoea. Australian Family Physician 44:34-37.

186. Mirhoseini A, Amani J, Nazarian S. 2018. Review on pathogenicity mechanism of enterotoxigenic *Escherichia coli* and vaccines against it. Microb Pathog 117:162-169.

187. Turnbull WB, Precious BL, Homans SW. 2004. Dissecting the cholera toxin-ganglioside GM1 interaction by isothermal titration calorimetry. Journal of the American Chemical Society 126:1047-1054.

188. Sanchez J, Holmgren J. 2011. Cholera toxin - A foe & a friend. Indian Journal of Medical Research 133:153-163.

189. Linton D, Karlyshev AV, Hitchen PG, Morris HR, Dell A, Gregson NA, Wren BW. 2000. Multiple N-acetyl neuraminic acid synthetase (*neuB*) genes in *Campylobacter jejuni*: identification and characterization of the gene involved in sialylation of lipo-oligosaccharide. Molecular microbiology 35:1120-1134.

190. Pukin AV, Weijers CAGM, van Lagen B, Wechselberger R, Sun B, Gilbert M, Karwaski M-F, Florack DEA, Jacobs BC, Tio-Gillen AP, van Belkum A, Endtz HP, Visser GM, Zuilhof H. 2008. GM3, GM2 and GM1 mimics designed for biosensing: chemoenzymatic synthesis, target affinities and 900 MHz NMR analysis. Carbohydrate research 343:636-650.

191. Moyo SJ, Kommedal O, Blomberg B, Hanevik K, Tellevik MG, Maselle SY, Langeland N. 2017. Comprehensive Analysis of Prevalence, Epidemiologic Characteristics, and Clinical Characteristics of Monoinfection and Coinfection in Diarrheal Diseases in Children in Tanzania. Am J Epidemiol 186:1074-1083.

192. Winter SE, Baumler AJ. 2014. Why related bacterial species bloom simultaneously in the gut: principles underlying the 'Like will to like' concept. Cell Microbiol 16:179-84.

193. Bian X, Garber JM, Cooper KK, Huynh S, Jones J, Mills MK, Rafala D, Nasrin D, Kotloff KL, Parker CT, Tennant SM, Miller WG, Szymanski CM. 2020. *Campylobacter* Abundance in Breastfed Infants and Identification of a New Species in the Global Enterics Multicenter Study. mSphere 5: e00735-19.

194. Platts-Mills JA, Babji S, Bodhidatta L, Gratz J, Haque R, Havt A, McCormick BJ, McGrath M, Olortegui MP, Samie A, Shakoor S, Mondal D, Lima IF, Hariraju D, Rayamajhi BB, Qureshi S, Kabir F, Yori PP, Mufamadi B, Amour C, Carreon JD, Richard SA, Lang D, Bessong P, Mduma E, Ahmed T, Lima AA, Mason CJ, Zaidi AK, Bhutta ZA, Kosek M, Guerrant RL, Gottlieb M, Miller M, Kang G, Houpt ER, Investigators M-EN. 2015. Pathogen-specific burdens of community diarrhoea in developing countries: a multisite birth cohort study (MAL-ED). Lancet Glob Health 3:e564-75.

195. Akond MA, Alam S, Hasan SMR, Shirin M. 2009. Distribution of *Vibrio cholerae* and its antibiotic resistance in the samples from poultry and poultry environment of Bangladesh. Advances in Environmental Biology 3:25-32.

196. Oh J-Y, Kang M-S, An B-K, Shin E-G, Kim M-J, Kwon J-H, Kwon Y-K. 2012. Isolation and epidemiological characterization of heat-labile enterotoxin-producing *Escherichia fergusonii* from healthy chickens. Veterinary microbiology 160:170-175.

197. Hyun CS, Kimmich GA. 1984. Interaction of Cholera-Toxin and *Escherichia coli* Entero-Toxin with Isolated Intestinal Epithelial-Cells. American Journal of Physiology 247:G623-G631.

198. Byappanahalli MN, Nevers MB, Korajkic A, Staley ZR, Harwood VJ. 2012. Enterococci in the environment. Microbiol Mol Biol Rev 76:685-706.

199. Fisher K, Phillips C. 2009. The ecology, epidemiology and virulence of *Enterococcus*. Microbiology 155:1749-1757.

200. Foulquie Moreno MR, Sarantinopoulos P, Tsakalidou E, De Vuyst L. 2006. The role and application of enterococci in food and health. Int J Food Microbiol 106:1-24.

201. Scheleifer KH, Kilpper-Balz R. 1984. Transfer of *Streptococcus faecalis* and *Streptococcus faecium* to the genus *Enterococcus* nom. rev. as *Enterococcus faecalis* comb. nov. and *Enterococcus faecium* comb. nov. International Journal of Systematic and Evolutionary Microbiology 34:31-34.

202. Van den Berghe E, De Winter T, De Vuyst L. 2006. Enterocin A production by *Enterococcus faecium* FAIR-E 406 is characterised by a temperature- and pH-dependent switch-off mechanism when growth is limited due to nutrient depletion. International journal of food microbiology 107:159-170.

203. Poh CH, Oh HM, Tan AL. 2006. Epidemiology and clinical outcome of enterococcal bacteraemia in an acute care hospital. J Infect 52:383-6.

204. CDC. 2019. Antibiotic resistance threats in the United States, 2019. CDC, Atlanta, GA.

205. Zhao B, Ye MS, Zheng R. 2018. *Enterococcus gallinarum* meningitis: a case report and literature review. BMC Infect Dis 18:231.

206. Vieira SM, Hiltensperger M, Kumar V, Zegarra-Ruiz D, Dehner C, Khan N, Costa FRC, Tiniakou E, Greiling T, Ruff W, Barbieri A, Kriegel C, Mehta SS, Knight JR, Jain D, Goodman AL, Kriegel MA. 2018. Translocation of a gut pathobiont drives autoimmunity in mice and humans. Science 359:1156-1160.

207. Britt NS, Potter EM. 2016. Clinical epidemiology of vancomycin-resistant *Enterococcus gallinarum* and *Enterococcus casseliflavus* bloodstream infections. J Glob Antimicrob Resist 5:57-61.

208. Brown S, Santa Maria JP, Jr., Walker S. 2013. Wall teichoic acids of gram-positive bacteria. Annu Rev Microbiol 67:313-36.

209. Neuhaus FC, Baddiley J. 2003. A continuum of anionic charge: structures and functions of *D*-alanyl-teichoic acids in gram-positive bacteria. Microbiol Mol Biol Rev 67:686-723.

210. Swoboda JG, Campbell J, Meredith TC, Walker S. 2010. Wall teichoic acid function, biosynthesis, and inhibition. Chembiochem 11:35-45.

211. Reichmann NT, Grundling A. 2011. Location, synthesis and function of glycolipids and polyglycerolphosphate lipoteichoic acid in Gram-positive bacteria of the phylum Firmicutes. FEMS Microbiol Lett 319:97-105.

212. Warshakoon HJ, Burns MR, David SA. 2009. Structure-activity relationships of antimicrobial and lipoteichoic acid-sequestering properties in polyamine sulfonamides. Antimicrob Agents Chemother 53:57-62.

213. Weidenmaier C, Peschel A. 2008. Teichoic acids and related cell-wall glycopolymers in Gram-positive physiology and host interactions. Nat Rev Microbiol 6:276-87.

214. Gross M, Cramton SE, Gotz F, Peschel A. 2001. Key role of teichoic acid net charge in *Staphylococcus aureus* colonization of artificial surfaces. Infect Immun 69:3423-6.

215. Schaffer C, Messner P. 2017. Emerging facets of prokaryotic glycosylation. FEMS Microbiol Rev 41:49-91.

216. Dell A, Galadari A, Sastre F, Hitchen P. 2010. Similarities and differences in the glycosylation mechanisms in prokaryotes and eukaryotes. Int J Microbiol 2010:148178.

217. Mescher MF, Strominger JL. 1976. Purification and characterization of a prokaryotic glucoprotein from the cell envelope of *Halobacterium salinarium*. J Biol Chem 251:2005-2014.

218. Sleytr UB, Thorne KJ. 1976. Chemical characterization of the regularly arranged surface layers of Clostridium thermosaccharolyticum and *Clostridium thermohydrosulfuricum*. J Bacteriol 126:377-83.

219. Schaffer C, Messner P. 2004. Surface-layer glycoproteins: an example for the diversity of bacterial glycosylation with promising impacts on nanobiotechnology. Glycobiology 14:31R-42R.

220. Twine SM, Paul CJ, Vinogradov E, McNally DJ, Brisson JR, Mullen JA, McMullin DR, Jarrell HC, Austin JW, Kelly JF, Logan SM. 2008. Flagellar glycosylation in *Clostridium botulinum*. FEBS J 275:4428-44.

221. Twine SM, Reid CW, Aubry A, McMullin DR, Fulton KM, Austin J, Logan SM. 2009. Motility and flagellar glycosylation in *Clostridium difficile*. J Bacteriol 191:7050-62.

222. Schirm M, Kalmokoff M, Aubry A, Thibault P, Sandoz M, Logan SM. 2004. Flagellin from *Listeria monocytogenes* is glycosylated with beta-O-linked N-acetylglucosamine. J Bacteriol 186:6721-7.

223. Janesch B, Schirmeister F, Maresch D, Altmann F, Messner P, Kolarich D, Schaffer C. 2016. Flagellin glycosylation in *Paenibacillus alvei* CCM 2051T. Glycobiology 26:74-87.

224. Bensing BA, Gibson BW, Sullam PM. 2004. The *Streptococcus gordonii* platelet binding protein GspB undergoes glycosylation independently of export. J Bacteriol 186:638-45.

225. Zhou M, Wu H. 2009. Glycosylation and biogenesis of a family of serine-rich bacterial adhesins. Microbiology 155:317-327.

226. Xiong YQ, Bensing BA, Bayer AS, Chambers HF, Sullam PM. 2008. Role of the serine-rich surface glycoprotein GspB of *Streptococcus gordonii* in the pathogenesis of infective endocarditis. Microb Pathog 45:297-301.

227. Yang Y, Jiang Y, Zhang J, Wang L, Bai X, Zhang S, Ren Y, Li N, Zhang Y, Zhang Z, Gong Q, Mei Y, Xue T, Zhang J, Chen Y, Zhou C. 2014. Structural Insights into SraP-Mediated *Staphylococcus aureus* Adhesion to Host Cells. PLoS pathogens 10.

228. Lu Q, Li S, Shao F. 2015. Sweet Talk: Protein Glycosylation in Bacterial Interaction With the Host. Trends Microbiol 23:630-641.

229. Shivshankar P, Sanchez C, Rose LF, Orihuela CJ. 2009. The *Streptococcus pneumoniae* adhesin PsrP binds to Keratin 10 on lung cells. Mol Microbiol 73:663-79.

230. Dong S, McPherson SA, Tan L, Chesnokova ON, Turnbough CL, Jr., Pritchard DG. 2008. Anthrose biosynthetic operon of *Bacillus anthracis*. J Bacteriol 190:2350-9.

231. Daubenspeck JM, Zeng H, Chen P, Dong S, Steichen CT, Krishna NR, Pritchard DG, Turnbough CL, Jr. 2004. Novel oligosaccharide side chains of the collagen-like region of BclA, the major glycoprotein of the *Bacillus anthracis* exosporium. J Biol Chem 279:30945-53.

232. Maes E, Krzewinski F, Garenaux E, Lequette Y, Coddeville B, Trivelli X, Ronse A, Faille C, Guerardel Y. 2016. Glycosylation of BclA Glycoprotein from *Bacillus cereus* and *Bacillus anthracis* Exosporium Is Domain-specific. J Biol Chem 291:9666-9677.

233. Strong PC, Fulton KM, Aubry A, Foote S, Twine SM, Logan SM. 2014. Identification and characterization of glycoproteins on the spore surface of *Clostridium difficile*. J Bacteriol 196:2627-37.

234. Yang H, Singh M, Kim SJ, Schaefer J. 2017. Characterization of the tertiary structure of the peptidoglycan of *Enterococcus faecalis*. Biochim Biophys Acta Biomembr 1859:2171-2180.

235. Geiss-Liebisch S, Rooijakkers SH, Beczala A, Sanchez-Carballo P, Kruszynska K, Repp C, Sakinc T, Vinogradov E, Holst O, Huebner J, Theilacker C. 2012. Secondary cell wall polymers of *Enterococcus faecalis* are critical for resistance to complement activation via mannose-binding lectin. J Biol Chem 287:37769-77.

236. Fabretti F, Theilacker C, Baldassarri L, Kaczynski Z, Kropec A, Holst O, Huebner J. 2006. Alanine esters of enterococcal lipoteichoic acid play a role in biofilm formation and resistance to antimicrobial peptides. Infect Immun 74:4164-71.

237. Im J, Baik JE, Kim KW, Kang SS, Jeon JH, Park OJ, Kim HY, Kum KY, Yun CH, Han SH. 2015. *Enterococcus faecalis* lipoteichoic acid suppresses Aggregatibacter actinomycetemcomitans lipopolysaccharide-induced IL-8 expression in human periodontal ligament cells. Int Immunol 27:381-91.

238. Wobser D, Ali L, Grohmann E, Huebner J, Sakinc T. 2014. A novel role for D-alanylation of lipoteichoic acid of *Enterococcus faecalis* in urinary tract infection. PLoS One 9:e107827.

239. Uysal H, Ciftci G, Ciftci A. 2013. Determination of antigenic glycoproteins of *Enterococcus faecalis* strains distinguished with aggregation substance, gelatinase and cytolysine. Revue Med Vet 164:374-381.

240. Maky MA, Ishibashi N, Zendo T, Perez RH, Doud JR, Karmi M, Sonomoto K. 2015. Enterocin F4-9, a Novel O-Linked Glycosylated Bacteriocin. Applied and Environmental Microbiology 81:4819-4826.

241. Pabst O, Mowat AM. 2012. Oral tolerance to food protein. Mucosal Immunol 5:232-9.

242. Tsai F, Coyle WJ. 2009. The microbiome and obesity: is obesity linked to our gut flora? Curr Gastroenterol Rep 11:307-313.

243. Chistiakov DA, Bobryshev YV, Kozarov E, Sobenin IA, Orekhov AN. 2015. Intestinal mucosal tolerance and impact of gut microbiota to mucosal tolerance. Frontiers in Microbiology 5:UNSP 781-UNSP 781.

244. Sorini C, Cardoso RF, Gagliani N, Villablanca EJ. 2018. Commensal Bacteria-Specific CD4(+) T Cell Responses in Health and Disease. Front Immunol 9:2667.

245. Lathrop SK, Bloom SM, Rao SM, Nutsch K, Lio CW, Santacruz N, Peterson DA, Stappenbeck TS, Hsieh CS. 2011. Peripheral education of the immune system by colonic commensal microbiota. Nature 478:250-4.

246. Niess JH, Leithauser F, Adler G, Reimann J. 2008. Commensal gut flora drives the expansion of proinflammatory CD4 T cells in the colonic lamina propria under normal and inflammatory conditions. J Immunol 180:559-68.

247. Asseman C, Read S, Powrie F. 2003. Colitogenic Th1 cells are present in the antigen-experienced T cell pool in normal mice: control by CD4+ regulatory T cells and IL-10. J Immunol 171:971-8.

248. Cebula A, Seweryn M, Rempala GA, Pabla SS, McIndoe RA, Denning TL, Bry L, Kraj P, Kisielow P, Ignatowicz L. 2013. Thymus-derived regulatory T cells contribute to tolerance to commensal microbiota. Nature 497:258-62.

249. Round JL, Mazmanian SK. 2010. Inducible Foxp3+ regulatory T-cell development by a commensal bacterium of the intestinal microbiota. Proc Natl Acad Sci U S A 107:12204-9.

250. Hrncir T, Stepankova R, Kozakova H, Hudcovic T, Tlaskalova-Hogenova H. 2008. Gut microbiota and lipopolysaccharide content of the diet influence development of regulatory T cells: studies in germ-free mice. BMC Immunol 9:65.

251. Chamaillard M, Hashimoto M, Horie Y, Masumoto J, Qiu S, Saab L, Ogura Y, Kawasaki A, Fukase K, Kusumoto S, Valvano MA, Foster SJ, Mak TW, Nunez G, Inohara N. 2003. An essential role for NOD1 in host recognition of bacterial peptidoglycan containing diaminopimelic acid. Nat Immunol 4:702-7.

252. Abreu MT. 2010. Toll-like receptor signalling in the intestinal epithelium: how bacterial recognition shapes intestinal function. Nat Rev Immunol 10:131-144.

253. Gewirtz AT, Navas TA, Lyons S, Godowski PJ, Madara JL. 2001. Cutting edge: bacterial flagellin activates basolaterally expressed TLR5 to induce epithelial proinflammatory gene expression. J Immunol 167:1882-5.

254. Wen L, Ley RE, Volchkov PY, Stranges PB, Avanesyan L, Stonebraker AC, Hu C, Wong FS, Szot GL, Bluestone JA, Gordon JI, Chervonsky AV. 2008. Innate immunity and intestinal microbiota in the development of Type 1 diabetes. Nature 455:1109-13.

255. Maassen CB, Claassen E. 2008. Strain-dependent effects of probiotic lactobacilli on EAE autoimmunity. Vaccine 26:2056-7.

256. Ochoa-Repáraz J, Mielcarz DW, Ditrio LE, Burroughs AR, Foureau DM, Haque-Begum S, Kasper LH. 2009. Role of gut commensal microflora in the development of experimental autoimmune encephalomyelitis. J Immunol 183:6041-6050.

257. Ochoa-Reparaz J, Mielcarz DW, Wang Y, Begum-Haque S, Dasgupta S, Kasper DL, Kasper LH. 2010. A polysaccharide from the human commensal *Bacteroides fragilis* protects against CNS demyelinating disease. Mucosal Immunol 3:487-95.

258. Moran AP. 1997. Structure of conserved characteristics of *Campylobacter jejuni* lipopolysaccharides. Journal of Infectious Diseases 176:S115-S121.

259. Yuki N, Yamada M, Koga M, Odaka M, Susuki K, Tagawa Y, Ueda S, Kasama T, Ohnishi A, Hayashi S, Takahashi H, Kamijo M, Hirata K. 2001. Animal model of axonal Guillain-Barré syndrome induced by sensitization with GM1 ganglioside. Ann Neurol 49:712-20.

260. St Charles JL, Bell JA, Gadsden BJ, Malik A, Cooke H, Van de Grift LK, Kim HY, Smith EJ, Mansfield LS. 2017. Guillain Barré Syndrome is induced in Non-Obese Diabetic (NOD) mice following *Campylobacter jejuni* infection and is exacerbated by antibiotics. Journal of Autoimmunity 77:11-38.

261. Brooks PT, Brakel KA, Bell JA, Bejcek CE, Gilpin T, Brudvig JM, Mansfield LS. 2017. Transplanted human fecal microbiota enhanced Guillain Barré syndrome autoantibody responses after *Campylobacter jejuni* infection in C57BL/6 mice. Microbiome 5:10.1186/s40168-017-0284-4.

262. Tamburini S, Shen N, Wu HC, Clemente JC. 2016. The microbiome in early life: implications for health outcomes. Nat Med 22:713-22.

263. Bunyavanich S, Shen N, Grishin A, Wood R, Burks W, Dawson P, Jones SM, Leung DYM, Sampson H, Sicherer S, Clemente JC. 2016. Early-life gut microbiome composition and milk allergy resolution. J Allergy Clin Immunol 138:1122-1130.

264. Arrieta MC, Stiemsma LT, Dimitriu PA, Thorson L, Russell S, Yurist-Doutsch S, Kuzeljevic B, Gold MJ, Britton HM, Lefebvre DL, Subbarao P, Mandhane P, Becker A, McNagny KM, Sears MR, Kollmann T, Investigators CS, Mohn WW, Turvey SE, Finlay BB. 2015. Early infancy microbial and metabolic alterations affect risk of childhood asthma. Sci Transl Med 7:307ra152.

265. Cox LM, Yamanishi S, Sohn J, Alekseyenko AV, Leung JM, Cho I, Kim SG, Li H, Gao Z, Mahana D, Zarate Rodriguez JG, Rogers AB, Robine N, Loke P, Blaser MJ. 2014. Altering the intestinal microbiota during a critical developmental window has lasting metabolic consequences. Cell 158:705-721.

266. Honda K, Littman DR. 2016. The microbiota in adaptive immune homeostasis and disease. Nature 535:75-84.

267. Krinos CM, Coyne MJ, Weinacht KG, Tzianabos AO, Kasper DL, Comstock LE. 2001. Extensive surface diversity of a commensal microorganism by multiple DNA inversions. Nature 414:555-558.

268. Moran AP, O'Malley DT. 1995. Potential role of lipopolysaccharides of Campylobacter jejuni in the development of Guillain-Barré syndrome. Journal of Endotoxin Research 2:233-235.

269. Yuki N, Taki T, Inagaki F, Kasama T, Takahashi M, Saito K, Handa S, Miyatake T. 1993. A Bacterium Lipopolysaccharide that Elicits Guillain-Barré-Syndrome has a GM1 Ganglioside-Like Structure. Journal of Experimental Medicine 178:1771-1775.

270. Comstock LE, Kasper DL. 2006. Bacterial glycans: Key mediators of diverse host immune responses. Cell 126:847-850.

271. Yi W, Shao J, Zhu L, Li M, Singh M, Lu Y, Lin S, Li H, Ryu K, Shen J, Guo H, Yao Q, Bush CA, Wang PG. 2005. Escherichia coli O86 O-antigen biosynthetic gene cluster and stepwise enzymatic synthesis of human blood group B antigen tetrasaccharide. Journal of the American Chemical Society 127:2040-2041.

272. Chang Y-C, Nizet V. 2014. The interplay between Siglecs and sialylated pathogens. Glycobiology 24:818-825.

273. Stowell SR, Arthur CM, Dias-Baruffi M, Rodrigues LC, Gourdine J-P, Heimburg-Molinaro J, Ju T, Molinaro RJ, Rivera-Marrero C, Xia B, Smith DF, Cummings RD. 2010. Innate immune lectins kill bacteria expressing blood group antigen. Nature medicine 16:295-U90.

274. Wesener DA, Wangkanont K, McBride R, Song X, Kraft MB, Hodges HL, Zarling LC, Splain RA, Smith DF, Cummings RD, Paulson JC, Forest KT, Kiessling LL. 2015. Recognition of microbial glycans by human intelectin-1. Nature Structural & Molecular Biology 22:603-610.

275. Propheter DC, Chara AL, Harris TA, Ruhn KA, Hooper LV. 2017. Resistin-like molecule beta is a bactericidal protein that promotes spatial segregation of the microbiota and the colonic epithelium. Proceedings of the National Academy of Sciences of the United States of America 114:11027-11033.

276. Ali M, Nelson AR, Lopez AL, Sack DA. 2015. Updated Global Burden of Cholera in Endemic Countries. Plos Neglected Tropical Diseases 9:e0003832-e0003832.

277. Holmgren J, Lonnroth I, Mansson JE, Svennerholm L. 1975. Interaction of Cholera Toxin and Membrane GM1 Ganglioside of Small-Intestine. Proceedings of the National Academy of Sciences of the United States of America 72:2520-2524.

278. El-Hawiet A, Kitova EN, Klassen JS. 2015. Recognition of human milk oligosaccharides by bacterial exotoxins. Glycobiology 25:845-854.

279. Heggelund JE, Burschowsky D, Bjornestad VA, Hodnik V, Anderluh G, Krengel U. 2016. High-Resolution Crystal Structures Elucidate the Molecular Basis of Cholera Blood Group Dependence. Plos Pathogens 12:e1005567-e1005567.

280. Lin J, Michel LO, Zhang QJ. 2002. CmeABC functions as a multidrug efflux system in *Campylobacter jejuni*. Antimicrobial Agents and Chemotherapy 46:2124-2131.

281. Storek KM, Auerbach MR, Shi H, Garcia NK, Sun D, Nickerson NN, Vij R, Lin Z, Chiang N, Schneider K, Wecksler AT, Skippington E, Nakamura G, Seshasayee D, Koerber JT, Payandeh J, Smith PA, Rutherford ST. 2018. Monoclonal antibody targeting the β-barrel assembly machine of *Escherichia coli* is bactericidal. Proceedings of the National Academy of Sciences doi:10.1073/pnas.1800043115.

282. Penner JL, Hennessy JN, Congi RV. 1983. Serotyping of *Campylobacter jejuni* and *Campylobacter coli* on the Basis of Thermostable Antigens. European Journal of Clinical Microbiology & Infectious Diseases 2:378-383.

283. Thibault P, Logan SM, Kelly JF, Brisson J-R, Ewing CP, Trust TJ, Guerry P. 2001. Identification of the carbohydrate moieties and glycosylation motifs in *Campylobacter jejuni* flagellin. Journal of Biological Chemistry 276:34862-34870.

284. Heinrichs DE, Yethon JA, Amor PA, Whitfield C. 1998. The assembly system for the outer core portion of R1- and R4-type lipopolysaccharides of *Escherichia coli* - The R1 core-specific beta-glucosyltransferase provides a novel attachment site for O-polysaccharides. Journal of Biological Chemistry 273:29497-29505.

285. Focareta A, Paton JC, Morona R, Cook J, Paton AW. 2006. A recombinant probiotic for treatment and prevention of cholera. Gastroenterology 130:1688-1695.

286. Senior NJ, Bagnall MC, Champion OL, Reynolds SE, La Ragione RM, Woodward MJ, Salguero FJ, Titball RW. 2011. *Galleria mellonella* as an infection model for *Campylobacter jejuni* virulence. Journal of medical microbiology 60:661-669.

287. Akashi N, Hitotsubashi S, Yamanaka H, Fujii Y, Tsuji T, Miyama A, Joya JE, Okamoto K. 1993. Production of heat-stable enterotoxin II by chicken clinical isolates of *Escherichia coli*. FEMS (Federation of European Microbiological Societies) Microbiology Letters 109:311-316.

288. Tsuji T, Joya JE, Honda T, Miwatani T. 1990. A Heat-Labile Enterotoxin (Lt) Purified from Chicken Enterotoxigenic *Escherichia coli* is Identical to Porcine Lt. FEMS microbiology letters 67:329-332.

289. Wilson BA, Salyers AA, Whitt DD, Winkler ME. 2011. Chapter 12: Toxins and Other Toxic Virulence Factors, p 225-253, Bacterial Pathogenesis: A Molecular Approach, Third ed. ASM Press, Washington, DC.

290. Guerry P, Ewing CP, Hickey TE, Prendergast MM, Moran AP. 2000. Sialylation of lipooligosaccharide cores affects immunogenicity and serum resistance of *Campylobacter jejuni*. Infection and immunity 68:6656-6662.

291. Albert MJ, Faruque ASG, Faruque SM, Sack RB, Mahalanabis D. 1999. Case-control study of enteropathogens associated with childhood diarrhea in Dhaka, Bangladesh. Journal of clinical microbiology 37:3458-3464.

292. Lertsethtakarn P, Silapong S, Sakpaisal P, Serichantalergs O, Ruamsap N, Lurchachaiwong W, Anuras S, Platts-Mills JA, Liu J, Houpt ER, Bodhidatta L, Swierczewski BE, Mason CJ. 2018. Travelers' Diarrhea in Thailand: A Quantitative Analysis Using TaqMan (R) Array Card. Clinical Infectious Diseases 67:120-127.

293. Holmgren J, Czerkinsky C, Lycke N, Svennerholm AM. 1994. Strategies for the Induction of Immune-Responses at Mucosal Surfaces Making use of Cholera-Toxin-B Subunit as Immunogen, Carrier, and Adjuvant. American Journal of Tropical Medicine and Hygiene 50:42-54.

294. Cordero RJB, Pontes B, Frases S, Nakouzi AS, Nimrichter L, Rodrigues ML, Viana NB, Casadevall A. 2013. Antibody Binding to *Cryptococcus neoformans* Impairs Budding by Altering Capsular Mechanical Properties. Journal of Immunology 190:317-323.

295. Nikaido H. 2003. Molecular basis of bacterial outer membrane permeability revisited. Microbiology and Molecular Biology Reviews 67:593-656.

296. Stahl M, Friis LM, Nothaft H, Liu X, Li J, Szymanski CM, Stintzi A. 2011. L-Fucose utilization provides *Campylobacter jejuni* with a competitive advantage. Proceedings of the National Academy of Sciences of the United States of America 108:7194-7199.

297. Hsiao A, Ahmed AMS, Subramanian S, Griffin NW, Drewry LL, Petri WA, Jr., Haque R, Ahmed T, Gordon JI. 2014. Members of the human gut microbiota involved in recovery from *Vibrio cholerae* infection. Nature 515:423-426.

298. Monira S, Nakamura S, Gotoh K, Izutsu K, Watanabe H, Alam NH, Nakaya T, Horii T, Ali SI, Iida T, Alam M. 2013. Metagenomic profile of gut microbiota in children during cholera and recovery. Gut Pathogens 5:1-1.

299. Albert MJ, Mustafa AS, Islam A, Haridas S. 2013. Oral Immunization with Cholera Toxin Provides Protection against *Campylobacter jejuni* in an Adult Mouse Intestinal Colonization Model. Mbio 4:e00246-13-e00246-13.

300. Baldauf KJ, Royal JM, Hamorsky KT, Matoba N. 2015. Cholera Toxin B: One Subunit with Many Pharmaceutical Applications. Toxins 7:974-996.

301. Javed MA, Sacher JC, van Alphen LB, Patry RT, Szymanski CM. 2015. A Flagellar Glycan-Specific Protein Encoded by *Campylobacter* Phages Inhibits Host Cell Growth. Viruses-Basel 7:6661-6674.

302. Javed MA, van Alphen LB, Sacher J, Ding W, Kelly J, Nargang C, Smith DF, Cummings RD, Szymanski CM. 2015. A receptor-binding protein of *Campylobacter jejuni* bacteriophage NCTC 12673 recognizes flagellin glycosylated with acetamidino-modified pseudaminic acid. Molecular microbiology 95:101-115.

303. Tsai CM, Frasch CE. 1982. A Sensitive Silver Stain for Detecting Lipopolysaccharides in Polyacrylamide Gels. Analytical Biochemistry 119:115-119.

304. van Alphen LB, Wenzel CQ, Richards MR, Fodor C, Ashmus RA, Stahl M, Karlyshev AV, Wren BW, Stintzi A, Miller WG, Lowary TL, Szymanski CM. 2014. Biological Roles of the O-Methyl Phosphoramidate Capsule Modification in *Campylobacter jejuni*. Plos One 9:e87051-e87051.

305. Stahl M, Ries J, Vermeulen J, Yang H, Sham HP, Crowley SM, Badayeva Y, Turvey SE, Gaynor EC, Li X, Vallance BA. 2014. A Novel Mouse Model of *Campylobacter jejuni* Gastroenteritis Reveals Key Pro-inflammatory and Tissue Protective Roles for Toll-like Receptor Signaling during Infection. Plos Pathogens 10:e1004264-e1004264.

306. Nothaft H, Davis B, Lock YY, Perez-Munoz ME, Vinogradov E, Walter J, Coros C, Szymanski CM. 2016. Engineering the *Campylobacter jejuni N*-glycan to create an effective chicken vaccine. Scientific Reports 6:26511-26511.

307. Yoon S-H, Ha S-M, Kwon S, Lim J, Kim Y, Seo H, Chun J. 2017. Introducing EzBioCloud: a taxonomically united database of 16S rRNA gene sequences and whole-genome assemblies. International Journal of Systematic and Evolutionary Microbiology 67:1613-1617.

308. Wang Q, Garrity GM, Tiedje JM, Cole JR. 2007. Naive Bayesian classifier for rapid assignment of rRNA sequences into the new bacterial taxonomy. Applied and Environmental Microbiology 73:5261-5267.

309. Cole JR, Wang Q, Fish JA, Chai B, McGarrell DM, Sun Y, Brown CT, Porras-Alfaro A, Kuske CR, Tiedje JM. 2014. Ribosomal Database Project: data and tools for high throughput rRNA analysis. Nucleic acids research 42:D633-D642.

310. Caporaso JG, Kuczynski J, Stombaugh J, Bittinger K, Bushman FD, Costello EK, Fierer N, Pena AG, Goodrich JK, Gordon JI, Huttley GA, Kelley ST, Knights D, Koenig HE, Ley RE, Lozupone CA, McDonald D, Muegge BD, Pirrung M, Reeder J, Sevinsky JR, Turnbaugh PJ, Walters WW, Widmann J, Yatsunenko T, Jesse Z, Knight R. 2010. QIIME allows analysis of high-throughput community sequencing data. Nat Methods 7: 335-336.

311. Strachan DP. 1989. Hay fever, hygiene, and household size. BMJ 299:1259-60.

312. Libertucci J, Young VB. 2019. The role of the microbiota in infectious diseases. Nat Microbiol 4:35-45.

313. Iweala OI, Nagler CR. 2019. The Microbiome and Food Allergy. Annu Rev Immunol 37:377-403.

314. Zimmermann P, Messina N, Mohn WW, Finlay BB, Curtis N. 2019. Association between the intestinal microbiota and allergic sensitization, eczema, and asthma: A systematic review. J Allergy Clin Immunol 143:467-485.

315. Sokolowska M, Frei R, Lunjani N, Akdis CA, O'Mahony L. 2018. Microbiome and asthma. Asthma Res Pract 4:1.

316. Zheng P, Li Z, Zhou Z. 2018. Gut microbiome in type 1 diabetes: A comprehensive review. Diabetes Metab Res Rev 34:e3043.

317. Gurung M, Li Z, You H, Rodrigues R, Jump DB, Morgun A, Shulzhenko N. 2020. Role of gut microbiota in type 2 diabetes pathophysiology. EBioMedicine 51:102590.

318. De Filippo C, Di Paola M, Giani T, Tirelli F, Cimaz R. 2019. Gut microbiota in children and altered profiles in juvenile idiopathic arthritis. J Autoimmun 98:1-12.

319. van Dijkhuizen EHP, Del Chierico F, Malattia C, Russo A, Pires Marafon D, Ter Haar NM, Magni-Manzoni S, Vastert SJ, Dallapiccola B, Prakken B, Martini A, De Benedetti F, Putignani L, Model Driven Paediatric European Digital Repository C. 2019. Microbiome Analytics of the Gut Microbiota in Patients With Juvenile Idiopathic Arthritis: A Longitudinal Observational Cohort Study. Arthritis Rheumatol 71:1000-1010.

320. Talotta R, Atzeni F, Ditto MC, Gerardi MC, Sarzi-Puttini P. 2017. The Microbiome in Connective Tissue Diseases and Vasculitides: An Updated Narrative Review. J Immunol Res 2017:6836498.

321. Glassner KL, Abraham BP, Quigley EMM. 2020. The microbiome and inflammatory bowel disease. J Allergy Clin Immunol 145:16-27.

322. Franzosa EA, Sirota-Madi A, Avila-Pacheco J, Fornelos N, Haiser HJ, Reinker S, Vatanen T, Hall AB, Mallick H, McIver LJ, Sauk JS, Wilson RG, Stevens BW, Scott JM, Pierce K, Deik AA, Bullock K, Imhann F, Porter JA, Zhernakova A, Fu J, Weersma RK, Wijmenga C, Clish CB, Vlamakis H, Huttenhower C, Xavier RJ. 2019. Gut microbiome structure and metabolic activity in inflammatory bowel disease. Nat Microbiol 4:293-305.

323. Pellicciotta M, Rigoni R, Falcone EL, Holland SM, Villa A, Cassani B. 2019. The microbiome and immunodeficiencies: Lessons from rare diseases. J Autoimmun 98:132-148.

324. Wen Y, Jin R, Chen H. 2019. Interactions Between Gut Microbiota and Acute Childhood Leukemia. Front Microbiol 10:1300.

325. Davis CD. 2016. The Gut Microbiome and Its Role in Obesity. Nutr Today 51:167-174.

326. Watson DW, Kim YB. 1963. Modification of Host Responses to Bacterial Endotoxins. I. Specificity of Pyrogenic Tolerance and the Role of Hypersensitivity in Pyrogenicity, Lethality, and Skin Reactivity. J Exp Med 118:425-46.

327. Lotz M, Gutle D, Walther S, Menard S, Bogdan C, Hornef MW. 2006. Postnatal acquisition of endotoxin tolerance in intestinal epithelial cells. J Exp Med 203:973-84.

328. Braun-Fahrlander C, Riedler J, Herz U, Eder W, Waser M, Grize L, Maisch S, Carr D, Gerlach F, Bufe A, Lauener RP, Schierl R, Renz H, Nowak D, von Mutius E, Allergy, Endotoxin Study T. 2002. Environmental exposure to endotoxin and its relation to asthma in school-age children. N Engl J Med 347:869-77.

329. von Mutius E, Vercelli D. 2010. Farm living: effects on childhood asthma and allergy. Nat Rev Immunol 10:861-868.

330. Bashir ME, Louie S, Shi HN, Nagler-Anderson C. 2004. Toll-like receptor 4 signaling by intestinal microbes influences susceptibility to food allergy. J Immunol 172:6978-87.

331. Nachamkin I, Liu J, Li M, Ung H, Moran AP, Prendergast MM, Sheikh K. 2002. *Campylobacter jejuni* from patients with Guillain-Barré syndrome preferentially expresses a GD1a-like epitope. Infect Immun 70:5299-303.

332. Willison HJ. 2005. Ganglioside complexes: new autoantibody targets in Guillain-Barré syndromes. Nat Clin Pract Neurol 1:2-3.

333. Halstead SK, Kalna G, Islam MB, Jahan I, Mohammad QD, Jacobs BC, Endtz HP, Islam Z, Willison HJ. 2016. Microarray screening of Guillain-Barré Syndrome sera for antibodies to glycolipid complexes. NeurologyÂ® Neuroimmunology & Neuroinflammation 3:e284. doi:10.1212/NXI.0000000000000284.

334. Liu J, Platts-Mills JA, Juma J, Kabir F, Nkeze J, Okoi C, Operario DJ, Uddin J, Ahmed S, Alonso PL, Antonio M, Becker SM, Blackwelder WC, Breiman RF, Faruque AS, Fields B, Gratz J, Haque R, Hossain A, Hossain MJ, Jarju S, Qamar F, Iqbal NT, Kwambana B, Mandomando I, McMurry TL, Ochieng C, Ochieng JB, Ochieng M, Onyango C, Panchalingam S, Kalam A, Aziz F, Qureshi S, Ramamurthy T, Roberts JH, Saha D, Sow SO, Stroup SE, Sur D, Tamboura B, Taniuchi M, Tennant SM, Toema D, Wu Y, Zaidi A, Nataro JP, Kotloff KL, Levine MM, Houpt ER. 2016. Use of quantitative molecular diagnostic methods to identify causes of diarrhoea in children: a reanalysis of the GEMS case-control study. Lancet 388:1291-301.

335. Deng H, Maitra U, Morris M, Li L. 2013. Molecular mechanism responsible for the priming of macrophage activation. J Biol Chem 288:3897-906.

336. Ceccarelli S, Panera N, Mina M, Gnani D, De Stefanis C, Crudele A, Rychlicki C, Petrini S, Bruscalupi G, Agostinelli L, Stronati L, Cucchiara S, Musso G, Furlanello C, Svegliati-Baroni G, Nobili V, Alisi A. 2015. LPS-induced TNF-alpha factor mediates pro-inflammatory and pro-fibrogenic pattern in non-alcoholic fatty liver disease. Oncotarget 6:41434-52.

337. Mbuya MN, Humphrey JH. 2016. Preventing environmental enteric dysfunction through improved water, sanitation and hygiene: an opportunity for stunting reduction in developing countries. Matern Child Nutr 12 Suppl 1:106-20.

338. Murr C, Widner B, Wirleitner B, Fuchs D. 2002. Neopterin as a marker for immune system activation. Curr Drug Metab 3:175-87.

339. Vatanen T, Kostic AD, d'Hennezel E, Siljander H, Franzosa EA, Yassour M, Kolde R, Vlamakis H, Arthur TD, Hamalainen AM, Peet A, Tillmann V, Uibo R, Mokurov S, Dorshakova N, Ilonen J, Virtanen SM, Szabo SJ, Porter JA, Lahdesmaki H, Huttenhower C, Gevers D, Cullen TW, Knip M, Group DS, Xavier RJ. 2016. Variation in Microbiome LPS Immunogenicity Contributes to Autoimmunity in Humans. Cell 165:842-53.

340. van Mourik A, Steeghs L, van Laar J, Meiring HD, Hamstra H-J, van Putten JPM, Wosten MMSM. 2010. Altered Linkage of Hydroxyacyl Chains in Lipid A of *Campylobacter jejuni* Reduces TLR4 Activation and Antimicrobial Resistance. Journal of Biological Chemistry 285:15828-15836.

341. Seeley JJ, Ghosh S. 2017. Molecular mechanisms of innate memory and tolerance to LPS. Journal of leukocyte biology 101:107-119.

342. Sato S, Nomura F, Kawai T, Takeuchi O, Muhlradt PF, Takeda K, Akira S. 2000. Synergy and cross-tolerance between toll-like receptor (TLR) 2- and TLR4-mediated signaling pathways. J Immunol 165:7096-101.

343. Medvedev AE, Henneke P, Schromm A, Lien E, Ingalls R, Fenton MJ, Golenbock DT, Vogel SN. 2001. Induction of tolerance to lipopolysaccharide and mycobacterial components in Chinese hamster ovary/CD14 cells is not affected by overexpression of Toll-like receptors 2 or 4. J Immunol 167:2257-67.

344. Lehner MD, Morath S, Michelsen KS, Schumann RR, Hartung T. 2001. Induction of cross-tolerance by lipopolysaccharide and highly purified lipoteichoic acid via different Toll-like receptors independent of paracrine mediators. J Immunol 166:5161-7.

345. Cavaillon JM, Pitton C, Fitting C. 1994. Endotoxin tolerance is not a LPS-specific phenomenon: partial mimicry with IL-1, IL-10 and TGFβ. Journal of Endotoxin Research 1:21-29.

346. Zuckerman SH, Evans GF, Snyder YM, Roeder WD. 1989. Endotoxin-macrophage interaction: post-translational regulation of tumor necrosis factor expression. J Immunol 143:1223-7.

347. Friis LM, Keelan M, Taylor DE. 2009. *Campylobacter jejuni* drives MyD88-independent interleukin-6 secretion via Toll-like receptor 2. Infect Immun 77:1553-60.

348. Rathinam VA, Appledorn DM, Hoag KA, Amalfitano A, Mansfield LS. 2009. *Campylobacter jejuni*-induced activation of dendritic cells involves cooperative signaling through Toll-like receptor 4 (TLR4)-MyD88 and TLR4-TRIF axes. Infect Immun 77:2499-507.

349. Schnee AE, Petri WA, Jr. 2017. *Campylobacter jejuni* and associated immune mechanisms: short-term effects and long-term implications for infants in low-income countries. Curr Opin Infect Dis 30:322-328.

350. Yang RB, Mark MR, Gray A, Huang A, Xie MH, Zhang M, Goddard A, Wood WI, Gurney AL, Godowski PJ. 1998. Toll-like receptor-2 mediates lipopolysaccharide-induced cellular signalling. Nature 395:284-8.

351. McIsaac SM, Stadnyk AW, Lin TJ. 2012. Toll-like receptors in the host defense against *Pseudomonas aeruginosa* respiratory infection and cystic fibrosis. J Leukoc Biol 92:977-85.

352. Muroi M, Ohnishi T, Azumi-Mayuzumi S, Tanamoto K. 2003. Lipopolysaccharide-mimetic activities of a Toll-like receptor 2-stimulatory substance(s) in enterobacterial lipopolysaccharide preparations. Infect Immun 71:3221-6.

353. Mukherjee S, Karmakar S, Babu SP. 2016. TLR2 and TLR4 mediated host immune responses in major infectious diseases: a review. Braz J Infect Dis 20:193-204.

354. Wang J, Ouyang Y, Guner Y, Ford HR, Grishin AV. 2009. Ubiquitin-editing enzyme A20 promotes tolerance to lipopolysaccharide in enterocytes. J Immunol 183:1384-92.

355. Xiong Y, Medvedev AE. 2011. Induction of endotoxin tolerance in vivo inhibits activation of IRAK4 and increases negative regulators IRAK-M, SHIP-1, and A20. J Leukoc Biol 90:1141-8.

356. Xiong Y, Qiu F, Piao W, Song C, Wahl LM, Medvedev AE. 2011. Endotoxin tolerance impairs IL-1 receptor-associated kinase (IRAK) 4 and TGF-beta-activated kinase 1 activation, K63-linked polyubiquitination and assembly of IRAK1, TNF receptor-associated factor 6, and IkappaB kinase gamma and increases A20 expression. J Biol Chem 286:7905-16.

357. Gunther J, Vogt N, Hampel K, Bikker R, Page S, Muller B, Kandemir J, Kracht M, Dittrich-Breiholz O, Huber R, Brand K. 2014. Identification of two forms of TNF tolerance in human monocytes: differential inhibition of NF-kappaB/AP-1- and PP1-associated signaling. J Immunol 192:3143-55.

358. Hu J, Wang G, Liu X, Zhou L, Jiang M, Yang L. 2014. A20 is critical for the induction of Pam3CSK4-tolerance in monocytic THP-1 cells. PLoS One 9:e87528.

359. Line JE. 2001. Development of a selective differential agar for isolation and enumeration of *Campylobacter* spp. J Food Prot 64:1711-5.

360. Salloway S, Mermel LA, Seamans M, Aspinall GO, Nam Shin JE, Kurjanczyk LA, Penner JL. 1996. Miller-Fisher syndrome associated with *Campylobacter jejuni* bearing lipopolysaccharide molecules that mimic human ganglioside GD3. Infect Immun 64:2945-9.

361. Westphal O, Jann K. 1965. Bacterial Lipopolysaccharides Extraction with Phenol-Water and Further Applications of the Procedure. Methods in Carbohydrate Chemistry 5:83-91.

362. Abreu R, Essler L, Loy A, Quinn F, Giri P. 2018. Heparin inhibits intracellular *Mycobacterium tuberculosis* bacterial replication by reducing iron levels in human macrophages. Sci Rep 8:7296.

363. Gilbert M, Karwaski M-F, Bernatchez S, Young NM, Taboada E, Michniewicz J, Cunningham A-M, Wakarchuk WW. 2002. The genetic bases for the variation in the lipo-oligosaccharide of the mucosal pathogen, *Campylobacter jejuni*: Biosynthesis of sialylated ganglioside mimics in the core oligosaccharide. Journal of Biological Chemistry 277:327-337.

364. Jacobs BC, van Belkum A, Endtz HP. 2008. Guillain-Barré Syndrome and *Campylobacter* Infection. Campylobacter, 3rd Edition:245-261.

365. Yamanaka H, Takagi T, Ohsawa M, Yamamoto N, Kubo N, Takemoto T, Sasano S, Masuyama R, Ohsawa K. 2014. Identification and Characterization of Vancomycin-resistant *Enterococcus* species Frequently Isolated from Laboratory Mice. Experimental Animals 63:297-304.

366. Ramsey M, Hartke A, Huycke M. 2014. The Physiology and Metabolism of Enterococci. *In* Gilmore MS, Clewell DB, Ike Y, Shankar N (ed), Enterococci: From Commensals to Leading Causes of Drug Resistant Infection, Boston.

367. Moore DF, Zhowandai MH, Ferguson DM, McGee C, Mott JB, Stewart JC. 2006. Comparison of 16S rRNA sequencing with conventional and commercial phenotypic techniques for identification of enterococci from the marine environment. J Appl Microbiol 100:1272-81.

368. Clark NC, Teixeira LM, Facklam RR, Tenover FC. 1998. Detection and differentiation of vanC-1, vanC-2, and vanC-3 glycopeptide resistance genes in enterococci. Journal of clinical microbiology 36:2294-2297.

369. Aziz RK, Bartels D, Best AA, DeJongh M, Disz T, Edwards RA, Formsma K, Gerdes S, Glass EM, Kubal M, Meyer F, Olsen GJ, Olson R, Osterman AL, Overbeek RA, McNeil LK, Paarmann D, Paczian T, Parrello B, Pusch GD, Reich C, Stevens R, Vassieva O, Vonstein V, Wilke A, Zagnitko O. 2008. The RAST Server: rapid annotations using subsystems technology. BMC Genomics 9:75.

370. Patry RT, Essler L, Quinn F, Szymanski CM. 2020. Low-dose exposure to ganglioside-mimicking bacteria tolerizes macrophages to Guillain Barré Syndrome-associated antigens. In preparation.

371. Thaysen-Andersen M, Larsen MR, Packer NH, Palmisano G. 2013. Structural analysis of glycoprotein sialylation – Part I: pre-LC-MS analytical strategies. RSC Adv 3:22683-22705.

372. Holden HM, Rayment I, Thoden JB. 2003. Structure and function of enzymes of the Leloir pathway for galactose metabolism. J Biol Chem 278:43885-8.

373. Latousakis D, MacKenzie DA, Telatin A, Juge N. 2020. Serine-rich repeat proteins from gut microbes. Gut Microbes 11:102-117.

374. Parker CT, Cooper KK, Huynh S, Smith TP, Bono JL, Cooley M. 2018. Genome Sequences of Eight Shiga Toxin-Producing *Escherichia coli* Strains Isolated from a Produce-Growing Region in California. Microbiology Resource Announcements 7:e00807-18

375. Seemann T. 2014. Prokka: rapid prokaryotic genome annotation. Bioinformatics 30:2068-9.

376. Page AJ, Cummins CA, Hunt M, Wong VK, Reuter S, Holden MT, Fookes M, Falush D, Keane JA, Parkhill J. 2015. Roary: rapid large-scale prokaryote pan genome analysis. Bioinformatics 31:3691-3.

377. Treangen TJ, Ondov BD, Koren S, Phillippy AM. 2014. The Harvest suite for rapid core-genome alignment and visualization of thousands of intraspecific microbial genomes. Genome Biol 15:524.

378. Alikhan NF, Petty NK, Ben Zakour NL, Beatson SA. 2011. BLAST Ring Image Generator (BRIG): simple prokaryote genome comparisons. BMC Genomics 12:402.

379. Hou S, Saw JH, Lee KS, Freitas TA, Belisle C, Kawarabayasi Y, Donachie SP, Pikina A, Galperin MY, Koonin EV, Makarova KS, Omelchenko MV, Sorokin A, Wolf YI, Li QX, Keum YS, Campbell S, Denery J, Aizawa S, Shibata S, Malahoff A, Alam M. 2004. Genome sequence of the deep-sea gamma-proteobacterium *Idiomarina loihiensis* reveals amino acid fermentation as a source of carbon and energy. Proc Natl Acad Sci U S A 101:18036-41.

380. Garcia Garcia MI, Lau K, von Itzstein M, Garcia Carmona F, Sanchez Ferrer A. 2015. Molecular characterization of a new *N*-acetylneuraminate synthase (NeuB1) from *Idiomarina loihiensis*. Glycobiology 25:115-23.

381. Reysenbach AL, Shock E. 2002. Merging genomes with geochemistry in hydrothermal ecosystems. Science 296:1077-82.

382. Crofts AA, Poly FM, Ewing CP, Kuroiwa JM, Rimmer JE, Harro C, Sack D, Talaat KR, Porter CK, Gutierrez RL, DeNearing B, Brubaker J, Laird RM, Maue AC, Jaep K, Alcala A, Tribble DR, Riddle MS, Ramakrishnan A, McCoy AJ, Davies BW, Guerry P, Trent MS. 2018. *Campylobacter jejuni* transcriptional and genetic adaptation during human infection. Nat Microbiol 3:494-502.